ANALYTICA CHIMICA ACTA

International monthly devoted to all branches of analytical chemistry
Revue mensuelle internationale consacrée à tous les domaines de la chimie analytique
Internationale Monatsschrift für alle Gebiete der analytischen Chemie

ELSEVIER PUBLISHING COMPANY
AMSTERDAM

Anal. Chim. Acta, Vol. 55, No. 1, 1–284, June 1971
Published monthly

Publication Schedule for 1971

In the interests of rapid publication it has been found necessary to schedule 5 volumes for appearance in 1971. Since monthly publication will be maintained, this implies that 2 of the volumes will each consist of three issues, while 3 of the volumes will each consist of only 2 issues. The following provisional schedule applies:

Vol. **53**, No. **1**	January 1971	
Vol. **53**, No. **2**	February 1971	**(completing Vol. 53)**
Vol. **54**, No. **1**	March 1971	
Vol. **54**, No. **2**	April 1971	
Vol. **54**, No. **3**	May 1971	**(completing Vol. 54)**
Vol. **55**, No. **1**	June 1971	
Vol. **55**, No. **2**	July 1971	**(completing Vol. 55)**
Vol. **56**, No. **1**	August 1971	
Vol. **56**, No. **2**	September 1971	
Vol. **56**, No. **3**	October 1971	**(completing Vol. 56)**
Vol. **57**, No. **1**	November 1971	
Vol. **57**, No. **2**	December 1971	**(completing Vol. 57)**

Subscription price: $17.50 or Dfl. 63.— per volume plus postage. Total subscription price for 1971: $87.50 or Dfl. 315.— plus postage. Additional cost for copies by airmail available on request. For subscribers in the U.S.A. and Canada, 2nd class postage paid at New York, N.Y. For advertising rates apply to the publishers.

Subscriptions should be sent to:

ELSEVIER PUBLISHING COMPANY P.O. Box 211, Amsterdam, The Netherlands

GENERAL INFORMATION

Languages

Papers will be published in English, French or German.

Submission of papers

Papers should be sent to:

PROF. PHILIP W. WEST,
Coates Chemical Laboratories,
College of Chemistry and Physics,
Louisiana State University,
Baton Rouge 3,
La. 70803 (U.S.A.)

or to:

DR. A. M. G. MACDONALD,
Department of Chemistry,
The University,
P.O. Box 363
Birmingham B15 2TT (Great Britain)

Reprints

Fifty reprints will be supplied free of charge. Additional reprints (minimum 100) can be ordered at quoted prices. They must be ordered on order forms which are sent together with the proofs.

P.P.B. Sensitivity for $1925 with PAR Model 174 Polarographic Analyzer

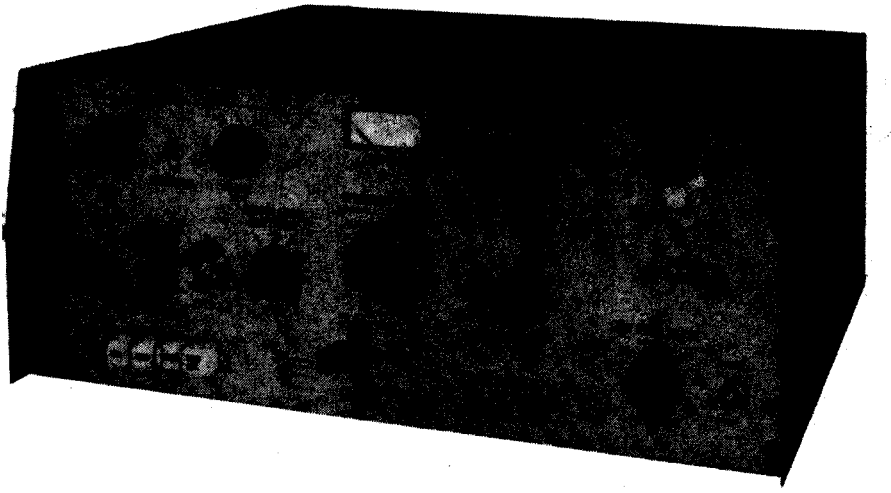

ANALYZE

- **Organics**
- **Pharmaceuticals**
- **Pollutants**
- **Metals**

BY

- **Differential Pulse**
- **Pulse**
- **Tast**
- **DC Polarography**

The PAR™ Model 174 Polarographic Analyzer complete with drop timer costs just $1925. Its part-per-billion sensitivity could heretofore only be found in units costing five times as much. The Model 174 brings all the analytical applications of ultra-sensitive polarographic techniques within the reach of any lab. For complete information, call or write Princeton Applied Research Corporation, Box 565, Princeton, New Jersey 08540; telephone (609) 452-2111.

PRINCETON APPLIED RESEARCH CORPORATION

Export price approximately 5% higher

REPRINTS BY AIR

Elsevier now provides a special service to the author in mailing reprints of articles by air at no extra charge.*

*Outside Europe and N. America only 10% extra will be charged, if airmail is required

Place stamp here

ELSEVIER PUBLISHING COMPANY
Journal Division

P.O. Box 211

AMSTERDAM
The Netherlands

ANALYTICA CHIMICA ACTA

Vol. 55 (1971)

ANALYTICA CHIMICA ACTA

International monthly devoted to all branches of analytical chemistry
Revue mensuelle internationale consacrée à tous les domaines de la chimie analytique
Internationale Monatsschrift für alle Gebiete der analytischen Chemie

ELSEVIER PUBLISHING COMPANY
AMSTERDAM

Anal. Chim. Acta, Vol. 55 (1971)

Analytica Chimica Acta
Elsevier Publishing Company, Amsterdam
Printed in The Netherlands

A NEUTRON ACTIVATION METHOD FOR THE DETERMINATION OF THORIUM IN ROCKS AND MINERALS USING THE 22-MINUTE ^{233}Th ACTIVITY*

ELINOR F. NORTON AND R. W. STOENNER
Chemistry Department, Brookhaven National Laboratory, Upton, N.Y. 11973 (U.S.A.)
(Received 22nd December 1970)

The technique of neutron activation has been widely used for the trace determination of thorium as evidenced by the more than one hundred entries in the Activation Analysis Bibliography recently published by the U.S. National Bureau of Standards[1]. Because of the great sensitivity attainable with the neutron fluxes now available, the method does not require the large samples necessary for other trace methods such as γ-ray spectrometry or spectrophotometric methods.

Thorium-232 in a thermal neutron flux undergoes neutron capture to form thorium-233 which decays with a 22-min half-life to protactinium-233. Most investigators have chosen to measure the protactinium-233 daughter of thorium-233 because of its convenient 27-day half-life. Some of these methods have involved chemical separations after the addition of protactinium-231 tracer for the determination of the chemical yield[2-5]. Others have relied on a quantitative separation of protactinium[6-8] or on a standard addition technique[9] which does not require complete recovery of protactinium-233. Recently, with the development of germanium detectors and their capability of resolving complex γ-spectra, the trend has been toward instrumental neutron activation analysis, whereby a large number of elements are determined in a sample either non-destructively[10,11] or with the use of group separations[12,13].

The determination of thorium by measurement of the 22-min thorium-233 activity has been little used although it is capable of yielding a sensitivity equal to the protactinium-233 measurement with a much shorter irradiation time, provided a fast radiochemical procedure can be worked out. Jenkins[14] has determined thorium at the 10 p.p.m. level and higher in dunite and monazite–dunite mixtures using a separation of thorium-233 based on oxalate precipitations and a chromatographic purification on an aluminum oxide–cellulose column. Travesi *et al.*[15] use an anion-exchange separation, a mesityl oxide extraction, and fluoride and oxalate precipitation for the separation of thorium-233 from uranium ores in which thorium is present to the extent of 9 p.p.m. While fast, this separation scheme lacks general applicability in that it does not yield radiochemically pure thorium-233 for samples containing one of the most common elements, calcium. Stärk and Turkowsky[16] use resonance neutrons to produce thorium-233 in rocks and minerals and a radiochemical separation based on anion exchange. In each of the above the sample was dissolved by a basic fusion or

* Research performed under the auspices of the U.S. Atomic Energy Commission.

sinter using sodium peroxide[14,15] or sodium potassium carbonate[16]. In contrast to the above methods in which β-radiation was measured, a recent paper by Twitty and Boback[17] described a determination of thorium in urine in which the 87 keV γ-ray of thorium-233 was used.

This paper presents a method for the determination of thorium at the 10-p.p.b. level or higher in rocks, ores, and minerals of diverse nature. The radiochemical separation consists of two anion-exchange separations, a thenoyltrifluoroacetone extraction and several precipitations which can be performed in approximately one hour and which result in a high degree of decontamination from interfering radionuclides. Results are presented for the thorium content of the USGS standard rocks; these results agree well with determinations by other methods.

A common method of attacking silicate rocks and rendering them acid soluble is the sodium peroxide sinter or fusion[18]. It was found while determining thorium in the USGS standard rocks that use of the sodium peroxide sinter can result in the formation of some acid-insoluble thorium. Evidence of incomplete recovery of thorium has also been observed by Arnfelt and Edmundsson[19] and by Abbey[20] when using the sodium peroxide sinter to decompose rocks and ores before a spectrophotometric determination of thorium. An important part of any neutron activation procedure in which inactive carrier is used is a step in which exchange equilibrium is established with the irradiated material. A sodium peroxide sinter which results in acid-insoluble material containing thorium allows for no such exchange and its use can result in serious errors.

A fast decomposition method adapted from the potassium fluoride–pyrosulfate fusion of Sill[21] was found to be the most reliable in obtaining complete recovery of thorium from a diversity of materials.

EXPERIMENTAL

Reagents

Thorium nitrate. Solid thorium nitrate tetrahydrate was used as a standard in the irradiation and a solution of the same thorium nitrate was used as the carrier. The thorium nitrate was analyzed for thorium by precipitation with hydrogen peroxide and ignition to thorium dioxide[22]. The thorium content of the thorium nitrate used in this work was 41.71%.

Potassium fluoride. Reagent-grade anhydrous potassium fluoride was used in the sample dissolution. The potassium fluoride was stored in a drying oven at 110° until needed.

Aluminum nitrate solution. Aluminum nitrate nonahydrate (454 g) was dissolved in enough water to give 400 ml of solution. The pH was adjusted to 1.0–1.2 with concentrated ammonium hydroxide.

TTA solution. A 0.25 *M* solution of thenoyltrifluoroacetone in benzene was used.

Chemicals. Reagent grade acids and ammonia were used throughout.

Ion-exchange columns. 25-ml burets of 9 mm i.d. were used for columns. A glass wool plug contained the resin. The columns were filled to a height of about 12 cm with Dowex 1-X8, 50–100 mesh in the chloride form. To convert to the nitrate form, 8 *M* nitric acid was poured through the column until the eluate no longer gave a silver

chloride precipitate when several drops of silver nitrate solution were added.

Sample preparation and irradiation

Finely powdered samples ($\leq$ 100 mg) were weighed into quartz ampoules of 3–4 mm i.d. and the ampoules were sealed. A standard of 10–15 mg of thorium nitrate tetrahydrate was weighed into an ampoule and sealed. The ampoules used were made from 6 mm quartz tubing and were scored 2–3 cm from the bottom so that a minimum of handling would be required in opening them after the irradiation. The samples and standard were wrapped together in polyethylene and placed in a plastic snap-top bottle.

The sample packages were irradiated in the pneumatic tube facilities of the Brookhaven Graphite Research Reactor or the Brookhaven Medical Research Reactor in a thermal neutron flux of 10^{13} n cm^{-2} sec^{-1} for twenty minutes. The samples were removed without delay to the laboratory where the initial steps in the chemical processing were performed behind lead shielding.

RECOMMENDED PROCEDURE

Sample dissolution

Open the sample ampoule and transfer the contents to a 100-ml platinum dish in which 8 mg of thorium carrier has been evaporated to dryness. Rinsing of the ampoule is not feasible when the potassium fluoride–pyrosulfate fusion is used as the means of dissolution. However, if the sample is dry and weighs at least 20 mg, the amount left in the ampoule will be negligible (less than 1 %). Add 1.0 g of anhydrous potassium fluoride for each 50 mg of sample, mix with a platinum wire and heat in a burner flame with gentle swirling until completely molten. A clear melt will result only for samples of very low iron content. Cool the dish and add 1.0 ml of concentrated sulfuric acid for each 1.0 g of potassium fluoride. Heat, gently at first to prevent excessive spattering, and finally strongly in the burner flame until a clear pyrosulfate fusion is obtained. There should be no undissolved material present at this stage. Cool the melt, dissolve it in 1 *M* nitric acid and transfer the solution to a 40-ml centrifuge tube.

Radiochemical separation

1. *Hydroxide precipitation.* Add an excess of concentrated ammonium hydroxide. Centrifuge and rinse the hydroxides once with water. Dissolve the precipitate in 5 ml of 8 *M* nitric acid.

2. *Nitrate column separation.* Load the nitric acid solution onto an ion-exchange column in the nitrate form. Rinse with 4–5 more 5-ml portions of 8 *M* nitric acid. Control the flow rate of the column at about one drop per second with the stopcock. Thorium is adsorbed on the resin. Elute the thorium with 20 ml of 2 *M* hydrochloric acid, receiving the eluate in a 40-ml centrifuge tube.

3. *Hydroxide precipitation.* Add an excess of concentrated ammonium hydroxide. Centrifuge and rinse the hydroxides once with water. Dissolve in 5 ml of concentrated hydrochloric acid.

4. *Chloride column separation.* Load the hydrochloric acid solution onto an ion-exchange column in the chloride form and elute the thorium with a total of 20 ml

of concentrated hydrochloric acid. Receive the eluate in a 40-ml polyethylene centrifuge tube.

5. *Fluoride precipitation.* Add 3–4 ml of 40% hydrofluoric acid. Centrifuge and rinse the fluoride precipitate once with water. Dissolve the precipitate in 10 ml of aluminum nitrate solution and transfer the solution to a 60-ml separatory funnel.

6. *TTA extraction.* Add 10 ml of TTA in benzene. Stopper and shake for one minute. Rinse the benzene phase once with 10 ml of 0.1 *M* nitric acid. Back-extract the thorium with 10 ml of 6 *M* nitric acid, shaking the funnel for 30 sec. Drain the nitric acid into a 40-ml centrifuge tube.

7. *Iodate precipitation.* Add 5 ml of 0.5 *M* iodic acid. Centrifuge and discard the supernate. Slurry the precipitate with several ml of 0.1 *M* nitric acid, heat briefly to coagulate the precipitate and filter onto a small filter paper circle. Wash the precipitate with ethanol, dry under a heat lamp and mount on an aluminum counting card.

Treatment of the standard

Since the thorium standard does not require radiochemical purification, a single iodate precipitation is used to prepare the counting sample. Dissolve the thorium nitrate standard in dilute nitric acid and make dilutions until an aliquot containing 0.5 to 1 μg of thorium can be taken into a 40-ml centrifuge tube. Add 4 mg of thorium carrier and nitric acid to give 10 ml of 5 to 6 *M* nitric acid. Precipitate thorium iodate as described in step 7 of the radiochemical separation above.

Counting

The activity (β) of the samples and standard was measured in gas-flow proportional counters. Several 1–6 min counts were recorded over a period of about three thorium-233 half-lives. If the samples appeared to be radiochemically pure, counting was discontinued for about three hours at which time a background count was made. The residual activity which amounts to several hundred counts per minute for a sample, or several thousand counts a minute for the standard, is activity from the

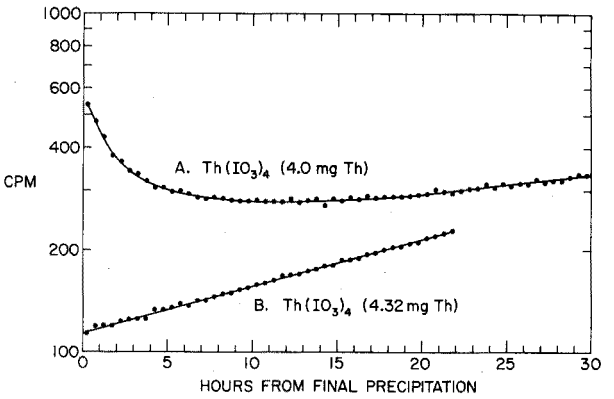

Fig. 1. Thorium carrier background. (A) Iodate precipitation only. (B) Through dissolution and radiochemical separation.

thorium-232 added as carrier plus, in the case of the standard, activity of the protactinium-233 daughter ($t_{\frac{1}{2}} = 27$ d). The background due to the thorium-232 carrier depends on the chemistry performed on the sample or standard. Typical carrier backgrounds are illustrated in Fig. 1. For the standard, the background determined after four hours in 100–200 c.p.m. lower than the true background at the time the standard was counted, because of the decay of bismuth-212 which was not separated in the single iodate precipitation used to prepare the counting sample of the standard. However, since the counting rate of a typical standard is of the order of 10^5 c.p.m. and never lower than 10^4 c.p.m., the difference between the true and approximated background causes no error. For a sample which has been taken through the complete radiochemical procedure, the background counting rate after four hours will be slightly high (10 to 15 c.p.m.) because of growth of the thorium-232 daughter chain, but again the difference is too small to cause any error except for samples of very low thorium content, *i.e.* with thorium-233 counting rates of less than 200 c.p.m.

Yield determination

After counting, the thorium iodate precipitates were dissolved in hydrochloric acid and the chemical yields determined spectrophotometrically by means of the arsenazo III complex in 5 *M* perchloric acid[20,23]. Typical yields for samples were 30 to 50%; for the standard 80–90%.

Calculations

The counting data were corrected for background, for decay of 22.1-min thorium-233, and for chemical yield. In addition, a correction was applied for the self

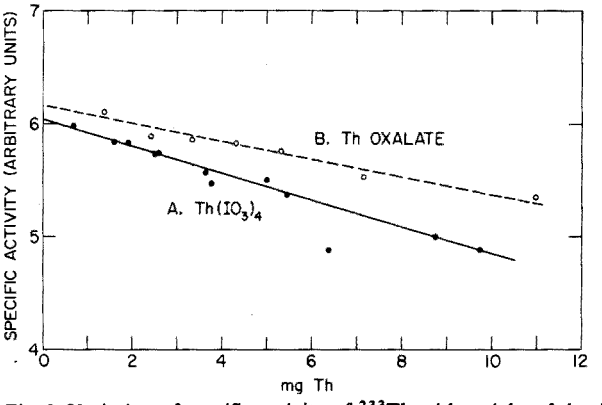

Fig. 2. Variation of specific activity of ^{233}Th with weight of thorium.

absorption of activity by the thorium iodate precipitate, using an experimentally determined curve (Fig. 2). Then

$$\text{p.p.m. Th} = \frac{\text{c.p.m. (sample)} \cdot \text{weight of Th in standard } (\mu\text{g})}{\text{c.p.m. (standard)} \cdot \text{sample weight (g)}} .$$

RESULTS

The thorium contents of the USGS standard rocks as determined by this method are presented in Table I. The results for G-1 and W-1 are in excellent agreement with Fleischer's recommended values[24]. The literature values[25] for the thorium content of the newer USGS rocks cover a wide range; however, the results by this method agree well with the γ-ray spectrometric and neutron activation results.

TABLE I

THORIUM IN THE USGS STANDARD ROCKS

Rock	*Th (p.p.m.)*		
	KF–pyrosulfate fusion	*Literature value*[25]	*HF–$HClO_4$ dissolution*
GSP-1	103, 105 } 104	99–125	104, 99 } 102
G-2	25.2, 25.0, 25.2, 24.8 } 25.0	21.5–26.6	25.8, 25.0 } 25.4
AGV-1	6.20, 6.19 } 6.20	6.1–8.1	6.35, 6.49 } 6.42
BCR-1	6.21, 6.19 } 6.20	5.8–7.6	6.23, 6.06 } 6.14
DTS-1	0.0100, 0.0099 } 0.0100	0.0092	
PCC-1	0.0114, 0.0101 } 0.0108	0.0108	
		Recommended value[24]	
W-1	2.35, 2.21 } 2.28	2.4	2.36, 2.40 } 2.38
G-1	50.8, 51.0, 51.7, 56.1 } 52.4	52	38.6, 59.1, 38.9, 48.6, 46.2, 45.2

The maximum error for samples containing more than 0.1 p.p.m. thorium is estimated as 4%; for samples in the 10–100 p.p.b. thorium range the error is estimated to be about 10%. The limit of detection with a 0.1-g sample is about 2 p.p.b.

With the irradiation conditions used in this work (20 min in a flux of 10^{13} n cm^{-2} sec^{-1}) a thorium-233 activity of $5 \cdot 10^5$ c.p.m. per μg of thorium was found 60 min after end of bombardment. Usually, when a sample, in duplicate, and a standard are taken through the procedure described here, the earliest that counting can be begun is 80 min after end of bombardment; hence an activity of $2–3 \cdot 10^5$ c.p.m. per μg of thorium can be expected.

DISCUSSION

Dissolution

The importance of the proper choice of method of dissolution was emphasized during the development of this procedure. Because of the short half-life of the radionuclide, the first requirement was that the dissolution be rapid. Initially an acid dissolution was employed using hydrofluoric and perchloric acids in the presence of thorium carrier and fast evaporations in a sand bath on a hot, hot-plate. This technique gave satisfactory results for a number of the standard rocks (Table I). However, the results for G-1 were consistently low, as if a thorium-bearing mineral in this rock were being incompletely attacked. The inefficiency of hydrofluoric–perchloric acid for the decomposition of certain minerals has been observed by others[20,26].

The sodium peroxide sinter or fusion is a widely used technique for the decomposition of silicate rocks. When a sodium peroxide sinter was used on G-1 and the sinter cake was decomposed in the presence of thorium carrier, the results were low. If thorium carrier was present before the sinter was performed, the results were scattered. A study was made to determine if thorium was being lost in the sodium peroxide sinter. Aliquots of thorium carrier were evaporated to dryness in platinum crucibles. To each was added a weighed amount of a standard rock sample plus two grams of powdered sodium peroxide. The sample and peroxide were mixed and the mixture was sintered at 470° for about 20 min. The sinter cake was decomposed with water and the precipitate was removed by centrifuging. Nitric acid was used to dissolve the precipitate plus any thorium carrier remaining in the crucible. Thorium was determined colorimetrically with arsenazo III in an aliquot of the nitric acid solution. The amounts of thorium, zirconium, and uranium (all of which form colored complexes with arsenazo III in 5 *M* $HClO_4$) present in the samples are too small to interfere. Other components of the samples have either been removed when the sodium hydroxide solution from the decomposition of the sinter was discarded or do not interfere with the arsenazo III determination. The recovery of thorium carrier is

TABLE II

RECOVERY OF CARRIER THORIUM AFTER Na_2O_2 SINTER AND KF–PYROSULFATE FUSION OF SILICATE ROCKS

Sample	*Weight (mg)*	*Th added (mg)*	*Th recovered (%)*
Na_2O_2 sinter			
G-1	63	7.92	82
AGV-1	66	7.92	83
PCC-1	131	7.92	66
SiO_2	54	7.92	93
—	—	11.8	96–98
KF–pyrosulfate fusion			
G-1	100	7.92	99
AGV-1	73	7.92	99
PCC-1	104	7.92	100
SiO_2	61	7.92	100
—	—	11.8	100

shown in Table II and is compared with the recovery, also determined with arsenazo III, after a potassium fluoride–pyrosulfate fusion as recommended in this paper.

The explanation of the thorium loss is difficult. Clearly an acid-insoluble thorium compound is formed in the sinter when sample and carrier are present. In another experiment, 0.1 g of thorium nitrate tetrahydrate was mixed with 0.5 g of PCC-1 and sintered with 10 g of sodium peroxide. The sinter cake was decomposed with water as before and the hydroxides removed by centrifuging. The hydroxides were dissolved in nitric acid and filtered. The filter paper was burned and ignited to 900° and the residue was fused with potassium fluoride–pyrosulfate as in the procedure finally adopted. Thorium was determined in all fractions. The nitric acid solution of the hydroxide precipitate was found to contain 84.1 % of the added thorium, the nitric acid insoluble residue contained 12.8 % and 0.4 % was found in the sodium hydroxide solution from which the hydroxide precipitate had been removed.

If the sodium peroxide sinter method of dissolution results in the formation of some acid-insoluble thorium when used with milligram amounts of thorium, it is reasonable to assume that the same might occur with the microgram amounts present in rock samples. The short half-life of thorium-233 precludes any extensive treatment to recover that portion lost in the nitric acid insoluble residue, and thus the potassium fluoride–pyrosulfate fusion becomes the preferred method of dissolution of rocks and minerals.

Radiochemical separation

The various steps of the radiochemical separation were put together to achieve maximum decontamination from a wide variety of radionuclides.

The dissolution results in the removal of silicon by volatilization. The nitrate column separation, although time consuming, is highly effective in removing a variety of interferences, including all of the major components of silicate rocks and also the rare earths and scandium. Besides thorium, only about ten elements, including uranium, are adsorbed by an anion-exchange resin from 8 *M* nitric acid[27]. However, because of time considerations the volumes of eluant which can be used in the separation must be kept minimal and the best decontamination from any one activity which can be expected from this step is a factor of 10^3. The adsorption of thorium from 8 *M* nitric acid is quantitative while the subsequent elution with 2 *M* hydrochloric acid results in about 90 % recovery of the thorium.

The chloride column step is essential for the removal of uranium. While uranium is normally not as abundant in rocks and minerals as thorium and the cross section for neutron capture is smaller (2.7 *vs.* 7.4 barns), the product of the n, γ reaction, uranium-239, has a half-life which is indistinguishable from that of thorium-233. In a spectrophotometric study with milligram amounts of uranium it was found that 15 to 20 % of the uranium accompanies thorium through the nitrate column separation and more than 50 % through the TTA extraction. That the decontamination from uranium-239 is adequate can be seen from Table III; most of this decontamination comes from the adsorption of uranium on the anion-exchange resin from 12 *M* hydrochloric acid. In addition the chloride column separates several other elements (zirconium, gold, and neptunium) which would not be removed in the nitrate column step. The recovery of thorium is 97–98%.

The TTA extraction was added to the procedure to give additional decontami-

TABLE III

DECONTAMINATION FROM SELECTED RADIONUCLIDES

Element irradiated	*Amount*	*Nuclear reaction*	*$T_{\frac{1}{2}}$ of product*	*c.p.m.$_{t_0}$ formed*	*c.p.m.$_{t_0}$ found*	*Decontamination*
Dy	107 μg	$^{164}Dy(n,\gamma)^{165}Dy$	2.35 h	$3.23 \cdot 10^9$	127	$2.5 \cdot 10^7$
Mn	1.77 mg	$^{55}Mn(n,\gamma)^{56}Mn$	2.58 h	$2.53 \cdot 10^9$	Not detected	$> 2.5 \cdot 10^9$
U	0.83 mg	$^{238}U(n,\gamma)^{239}U$	23.5 min	$6.2 \cdot 10^7$ [a]	105	$6 \cdot 10^5$
Ca	46.3 mg	$^{48}Ca(n,\gamma)^{49}Ca \xrightarrow{9\ min} {}^{49}Sc$	57.5 min	$3.75 \cdot 10^7$	720	$5 \cdot 10^4$
Ca[b]	42.8 mg			$4.4 \cdot 10^7$	< 20	$> 10^6$

[a] Calculated assuming 50% counting efficiency and $t_0 = 85$ min after end of bombardment.
[b] Reprecipitation of $Th(IO_3)_4$ added to radiochemical separation.

nation from rare earth activities. Initially the mesityl oxide extraction used by Travesi *et al.*[15] in their method and studied by Levine and Grimaldi[28] was used. However, contrary to the reports of others, we found that the rare earths, as represented by dysprosium, are appreciably extracted by mesityl oxide. In an experiment with dysprosium-165, 13% of the dysprosium activity was found with the thorium carrier after a mesityl oxide extraction. In contrast the TTA extraction gave a decontamination from dysprosium of 10^3. The recovery of thorium is 80–85%.

Several elements which might be expected to give troublesome activities were selected for testing the total efficiency of the radiochemical separation. These were dysprosium, manganese, uranium, and calcium, because of its radioactive scandium daughters. The uranium was purified from thorium by anion exchange. Samples containing known amounts of the test elements were prepared by evaporating solutions onto Matthey "specpure" silicon dioxide. The dried silica was ground to a powder in a mortar and pestle and the concentration of the test element was determined by specific colorimetric methods. Samples were irradiated and dissolved in the presence of thorium carrier. To determine the total activity produced from dysprosium, manganese and calcium, small aliquots were evaporated onto platinum discs and counted. Uranium was not treated in this manner since the 23.5-min uranium-239 was of primary concern, and measurement of this isotope in the manner described would be confused by the activity of all the fission products. Therefore the amount of uranium-239 activity was calculated from the capture cross-section and the neutron flux. The remainder of the solution in each case was taken through the separation procedure described above. The results of the decontamination experiments are shown in Table III.

The decontamination from rare earths and from manganese is excellent and probably sufficient for any sample likely to be encountered. The presence of small amounts of dysprosium-165 in a thorium-233 counting sample is not in itself a cause for concern since the decay curve can be resolved easily. However, the detection of dysprosium-165 serves as a warning of the possible presence of other rare earth activities such as 22-min samarium-155. Likewise, the absence of dysprosium-165 is an indication that no other rare earth activities are present.

The radionuclide most likely to be present as an impurity in the thorium-233 counting sample is the 57.5-min scandium-49 daughter of calcium-49. Scandium is chemically very similar to thorium and follows thorium through most steps of the radiochemical separation; only the nitrate column separation and the iodate precipitation separate thorium from scandium. In addition, the calcium-49 precursor is so short-lived (9 min) that early steps in the procedure which separate calcium do little to reduce the scandium activity. A calculation was made to determine the maximum permissible amount of calcium in a 0.1-g sample which would add no more than 2% to the counting rate of thorium-233, assuming a decontamination factor of $5 \cdot 10^4$ and an initial counting time (t_0) 90 min after end of bombardment. At the 10 p.p.b. thorium level 0.1 mg of calcium (or 0.1%) is permissible, at the 0.1 p.p.m. level, 1 mg of calcium (1%) and at the 1 p.p.m. level, 10 mg of calcium (10%). If the final thorium iodate precipitate is dissolved in a minimum of hydrochloric acid and the thorium iodate reprecipitated, the amounts of permissible calcium are raised 20–50 times. Such a reprecipitation is accompanied by a large reduction in the thorium yield and is time consuming and should be used only when necessary.

Thorium iodate was chosen as the counting form over the more commonly used thorium oxalate because of its specificity, in particular in the separation from scandium. In addition, the precipitation was found to be faster and more nearly quantitative especially when little time is available for complete precipitation. The self absorption of the iodate is greater than that of the oxalate, but is reproducible enough, so that a correction derived from an experimentally determined curve (Fig. 2) is adequate for adjustment of the counting data if the weights of carrier in the sample and standard are kept as nearly equal as possible. Thus only half as much carrier was added in the preparation of the standard since the single iodate precipitation used to prepare the standard results in a yield loss of only 10%–15%, while the complete radiochemical procedure results in yield losses of 50% or more.

SUMMARY

A method is described for the determination of thorium in rocks and minerals which utilizes neutron activation, a radiochemical separation scheme and counting of the thorium-233 β-activity. A discussion is presented of various dissolution procedures used for silicate rocks with the conclusion that a potassium fluoride–pyrosulfate fusion is preferable to acid dissolution or sodium peroxide fusion or sinter. The sensitivity of the method is 10 p.p.b. with a 100-mg sample. Results are given for the USGS standard rocks.

RÉSUMÉ

Une méthode est décrite pour le dosage du thorium dans les roches et les minerais utilisant activation neutronique, séparation radiochimique et comptage de l'activité bèta du thorium-233. On examine les possibilités de dissolution des silicates, en donnant la préférence à la fusion fluorure–pyrosulfate. La sensibilité de la méthode est 10 p.p.b. avec des échantillons de 100 mg. Des résultats sont donnés pour des roches standards USGS.

ZUSAMMENFASSUNG

Es wird eine Methode für die Bestimmung von Thorium in Gesteinen und Mineralen beschrieben. Sie beruht auf Neutronenaktivierung, einem radiochemischen Trennungsgang und der Messung der β-Aktivität von Thorium-233. Verschiedene Auflösungsverfahren für Silicatgesteine werden diskutiert mit dem Ergebnis, dass ein Kaliumfluorid–Pyrosulfat-Aufschluss einer Säurebehandlung sowie dem Schmelzen oder Sintern mit Natriumperoxid vorzuziehen ist. Die Methode hat eine Empfindlichkeit von 10 p.p.b. bei einer Probe von 100 mg. Die Ergebnisse von USGS-Standardgesteinen werden vorgelegt.

REFERENCES

1 G. J. Lutz, R. J. Boreni, R. S. Maddock and W. W. Meinke, *Nat. Bur. Std. (U.S.), Tech. Note 467*, Revision 1, Dec. 1969, p. II-27.
2 G. L. Bate, J. R. Huizenga and H. A. Potratz, *Geochim. Cosmochim. Acta*, 16 (1959) 88.
3 J. W. Morgan and J. F. Lovering, *Anal. Chim. Acta*, 28 (1963) 405.
4 M. Osawa, O. Tokunaga, M. Itani and M. Sakanoue, *J. Nucl. Sci. Technol.*, 3 (1966) 333.
5 H. Wakita, H. Nagasawa, S. Uyeda and H. Kuno, *Geochem. J.*, 1 (1967) 183.
6 D. N. Edgington, *Int. J. Appl. Radiat. Isotop.*, 18 (1967) 11.
7 E. V. Gangadharam and P. P. Parekh, *Radiochim. Acta*, 10 (1968) 65.
8 J. Op de Beeck, *Anal. Chim. Acta*, 40 (1968) 221.
9 A. Alian and R. Shabana, *Microchem. J.*, 12 (1967) 427.
10 J. C. Cobb, *Anal. Chem.*, 39 (1967) 127.
11 G. E. Gordon, K. Randle, G. G. Goles, J. B. Corliss, M. H. Beeson and S. S. Oxley, *Geochim. Cosmochim. Acta*, 32 (1968) 369.
12 K. Samsahl, P. O. Wester and O. Landström, *Anal. Chem.*, 40 (1968) 181.
13 G. H. Morrison, J. T. Gerard, A. Travesi, R. L. Currie, S. F. Peterson and N. M. Potter, *Anal. Chem.*, 41 (1969) 1633.
14 E. N. Jenkins, *Analyst*, 80 (1955) 301.
15 A. Travesi, J. Palomares and G. Dominguez, *Anal. Chim. Acta*, 35 (1966) 421.
16 H. Stärk and C. Turkowsky, *Radiochim. Acta*, 5 (1966) 16.
17 B. L. Twitty and M. W. Boback, *Anal. Chim. Acta*, 49 (1970) 19.
18 J. Dolezal, P. Povondra and Z. Sulcek, *Decomposition Techniques in Inorganic Analysis*, Elsevier, New York, 1968, pp. 111–120, 161–164.
19 A. L. Arnfelt and I. Edmundsson, *Talanta*, 8 (1961) 473.
20 S. Abbey, *Anal. Chim. Acta*, 30 (1964) 176.
21 C. W. Sill, *Anal. Chem.*, 33 (1961) 1684.
22 I. M. Kolthoff and P. J. Elving (Editors), *Treatise on Analytical Chemistry, Part II, Vol. 5*, Interscience, 1961, p. 203.
23 R. G. Bryan and G. R. Waterbury, *U.S. At. Energy Comm., Report no. LA-3468*, 1966.
24 M. Fleischer, *Geochim. Cosmochim. Acta*, 33 (1969) 65.
25 F. J. Flanagan, *Geochim. Cosmochim. Acta*, 33 (1969) 81.
26 F. J. Langmyhr and S. Sveen, *Anal. Chim. Acta*, 32 (1965) 1.
27 P. C. Stevenson and W. E. Nervik, *NAS-NS 3020*, 1961, pp. 159–161.
28 H. Levine and F. S. Grimaldi, *U. S. At. Energy Comm., Report no. AECD-3186*, 1950.

Analytica Chimica Acta
Elsevier Publishing Company, Amsterdam
Printed in The Netherlands

THE DETERMINATION OF ANTIMONY IN STANDARD ROCKS BY INSTRUMENTAL NEUTRON ACTIVATION ANALYSIS

S. M. LOMBARD AND K. W. MARLOW
Naval Research Laboratory, Washington, D. C. 20390 (U.S.A.)
AND
JAMES T. TANNER
Food and Drug Administration, Washington, D. C. 20204 (U.S.A.)
(Received 28th December 1970)

The application of neutron activation analysis (n.a.a.) to the determination of antimony in geological materials has been demonstrated several times[1-12]. There remain, however, some data on the abundance of antimony in the standard rocks that are incomplete or conflicting. Further analysis of these materials should provide better definition of their composition and thereby render them more useful as geological standars. With the large, high-resolution lithium-drifted germanium [Ge(Li)] γ-ray detectors currently available it is possible to determine antimony non-destructively. It is the intent of this work to determine antimony in this manner and to compare the data thus obtained with previously published results so that reliable antimony abundances may be established for several standard rocks.

Fleischer[1] has summarized available data on the two original rock standards, G-1 and W-1, issued by the United States Geological Survey (USGS); Webber[2] assembled available data on the standards SYE-1 and SUL-1 issued by the Nonmetallic Standards Committee of the Canadian Association for Applied Spectroscopy (CAAS); and Flanagan[3] compiled data on the six standards (G-2, GSP-1, AGV-1, PCC-1, DTS-1 and BCR-1) issued in 1964 by USGS.

Since these compilations were published, Tanner and Ehmann[4], Brunfelt and Steinnes[5,6], Hamaguchi *et al.*[7] and Morrison *et al.*[8] have reported antimony abundances in one or more of these standard rocks by n.a.a. with post-irradiation chemical separations. Gordon *et al.*[9] and Filby and Haller[10] have analyzed some of the rock standards non-destructively by n.a.a. using a high-resolution Ge(Li) detector. Recently Brunfelt and Steinness[11] determined antimony abundance in four standard rocks after activation with epi-cadmium neutrons in a nuclear reactor.

In the present work the abundances of antimony in the ten standard rocks mentioned above plus the basalt BCR-2 and the French granite GR are determined by instrumental neutron activation analysis and the data obtained are compared with previously reported results.

EXPERIMENTAL

The twelve standard rocks analyzed in this work are listed in Table I. With the exception of GR, three samples of each rock, weighing between 153 and 308 mg each,

TABLE I

STANDARD ROCKS ANALYZED IN THIS WORK

Code	*Rock type*	*Material*	*Location*	*Source*[b]
G-1	Acid	Granite	—	1
G-2	Acid	Granite	Westerly, R.I. (88/23)[a]	1
GR	Acid	Granite	Senones, Vosges, France	4
GSP-1	Intermediate	Granodiorite	Silver Plume, Colo. (45/30)[a]	1
AGV-1	Intermediate	Andesite	Guano Valley, Oreg. (57/9)[a]	1
SYE-1	Intermediate	Syenite	Bancroft Area, Ont.	2
W-1	Basic	Diabase	—	1
BCR-1	Basic	Basalt	Columbia River, Oreg. (75/14)[a]	1
BCR-2	Basic	Basalt	—	3
PCC-1	Ultrabasic	Peridotite	Sonoma Co., Calif. (33/28)[a]	1
DTS-1	Ultrabasic	Dunite	Twin Sisters, Wash. (37/24)[a]	1
SUL-1	Ore	Sulphide Ore	Falcon Bridge, Ont.	2

[a] Split/Position identification for new USGS rock standards.
[b] (1) U.S. Geological Survey, Washington, D.C.; (2) G. R. Weber, McGill University, Montreal, Canada; (3) University of California, Berkeley, Calif.; (4) Centre de Recherches Pétrographiques et Géochimiques, Nancy, France.

were sealed in vials of high-purity quartz (Thermal American Fused Quartz Co., Montville, N.J., Spectrosil Grade) for irradiation. Owing to the small quantity of GR available for analysis, only one sample, weighing ≈ 73 mg, was taken. The powdered rocks were mixed thoroughly before each sample was taken in an effort to obtain three samples representative of the lot. An empty quartz vial was included as a blank

The four antimony standards each consisted of 25 μl of a standard solution (2.532 μg Sb) absorbed on SiO_2 powder (99.9999% SiO_2) (Spex Industries, Inc., Metuchen, N.J.) in a quartz vial. The standards were dried at 90° for three days and

TABLE II

ANTIMONY ABUNDANCES FOR 12 STANDARD ROCKS (p.p.m.)

Sample	*This work*	*Previous work*	*Reference*
DTS-1	0.50 ± 0.05[a]	0.40, 0.53	4
		0.50 ± 0.05	5
		0.405–0.571 (0.502)[c]	6
BCR-1	0.67 ± 0.19[b]	0.32, 0.69	4
		0.534–0.619 (0.579)[c]	6
		0.68	8
		1.1 ± 0.4	9
		0.41–0.62	11

TABLE II (*continued*)

Sample	*This work*	*Previous work*	*Reference*
GSP-1	3.35 ± 0.09^a	1.38, 3.26	4
		2.86–3.37 (3.09)[c]	6
		4.1 ± 0.6	9
		3.0 ± 0.2	10
		2.64–3.27	11
PCC-1	1.37 ± 0.08^b	0.005, 1.59	4
		1.20–1.51 (1.39)[c]	6
AGV-1	4.6 ± 1.2^b	2.21, 5.42	4
		4.35 ± 0.13	5
		4.18–4.52 (4.35)[c]	6
		4.3	8
		5.2 ± 1.0	9
		3.98–4.35	11
G-2	0.040 ± 0.005^a	0.015, 0.10	4
		0.050–0.070 (0.063)[c]	6
		0.055	8
		0.2 ± 0.1	10
W-1	1.12 ± 0.18^b	1.2, 1.1, 0.96	1
		0.13, 0.15	4
		0.90 ± 0.02	5
		1.2	7
		0.8 ± 0.2	10
		0.75–1.06	11
		0.89–1.2 (1.03)[c]	12
G-1	0.37 ± 0.12^b	0.6, 0.4, 0.25	1
		0.42, 0.26	4
		0.231–0.338 (0.298)[c]	6
		0.29, 0.24	7
		0.24–0.38 (0.30)[c]	12
SUL-1	0.88 ± 0.13^a	2.09	4
SYE-1	1.34 ± 0.35^b	2.18	4
GR	0.24 ± 0.02^a	0.34	4
		0.261–0.275 (0.268)[c]	6
BCR-2	0.32 ± 0.08^a	—	

[a] Standard deviation based on counting statistics.
[b] Maximum deviation of the mean.
[c] Mean value.

then sealed with an oxygen–methane torch. The standard antimony solution was prepared by dissolving a weighed quantity of reagent-grade antimony powder in *aqua regia* and diluting to volume. The blank for these standards consisted of a quartz vial containing SiO_2 powder.

The three samples of each standard rock were wrapped in aluminum foil, then all the packages were wrapped together in aluminum foil with the standards and blanks uniformly distributed among them. The package was rotated in a high-flux position of the Naval Research Laboratory Nuclear Reactor for 28 h at a thermal neutron flux $\approx 6 \cdot 10^{12}$ n cm^{-2} sec^{-1}.

Analysis of the samples was started 39 days after termination of the irradiation to allow short-lived activities to decay. Each of the rock samples was counted initially for 160 live minutes with a large coaxial Ge(Li) detector coupled to a 4096-channel analyzer (resolution 2.1 keV; efficiency 6% *vs.* NaI(Tl) at 1332 keV and source-to-detector distance of 25 cm). The antimony standards and their blank were counted for 40 live minutes and the empty vial for nearly three days. The nuclide ^{124}Sb ($T_{\frac{1}{2}} = 60.2$ days), which emits prominent γ-rays at 603 and 1691 keV, was used for this determination. The areas under the photopeaks at 603 and 1691 keV were determined by numerical integration.

RESULTS AND DISCUSSION

The ratio of the area under the photopeak at 603 keV to that under the peak at 1691 keV ranged from 4.9 to 370 for the 34 rock samples indicating an interference with the 603 keV peak. This is due primarily to the 604.6 keV peak of ^{134}Cs with perhaps a slight contribution from the 604.4 keV peak of ^{192}Ir. Accordingly, the antimony abundance was calculated from the area under the 1691 keV photopeak only.

The four antimony standards were distributed throughout the package of samples during irradiation as a check on the homogeneity of the neutron flux. The deviations from the mean of the individual results for these standards were consistent with counting statistics indicating that the neutron flux was indeed homogeneous.

Table II gives antimony abundances in parts per million for the 12 standard rocks. The error limits given for the results of this work are the larger of two values—the standard deviation (σ) based on counting statistics or the maximum deviation of the mean of the individual results (δ). The value of δ was less than σ for five of the standard rocks and less than 2σ for four others.

The rather large deviations from the mean in the results for SYE-1, G-1 and AGV-1 suggest the possibility that the samples themselves may not be homogeneous.

In comparing all results for the 12 standard rocks it appears that the antimony abundance in DTS-1 is known most accurately. The mean of four values for DTS-1 is 0.51 with $\delta = 0.02$. More data are needed for SUL-1, GR and BCR-2.

The authors wish to thank the following for providing the samples of standard rocks used in this work: Prof. W. D. Ehmann, University of Kentucky, Lexington, Ky.; Prof. T. P. Kohman, Carnegie-Mellon University, Pittsburgh, Pa.; F. J. Flanagan, U.S. Geological Survey, Washington, D.C.; and Dr. E. F. Hodge, Mellon Institute, Pittsburgh, Pa. The cooperation of the operations staff of the Naval Research Laboratory Nuclear Reactor in performing the irradiation is gratefully acknowledged.

SUMMARY

The abundance of antimony in the standard rocks G-1, W-1, G-2, BCR-1, AGV-1, PCC-1, DTS-1, GSP-1, SUL-1, SYE-1, BCR-2 and GR has been determined

by instrumental neutron activation analysis. Comparison of the results of this work with those previously reported indicate that DTS-1 is the best choice as an antimony standard. Results for SYE-1, G-1 and AGV-1 indicate that these standards may not be sufficiently homogeneous.

RÉSUMÉ

L'abondance de l'antimoine dans les roches standards G-1, W-1, G-2, BCR-1, AGV-1, PCC-1, DTS-1, GSP-1, SUL-1, SYE-1, BCR-2 et GR a pu être déterminée grâce à l'analyse par activation neutronique. Par comparaison de ces résultats avec ceux indiqués au préalable, on constate que le DTS-1 constitue le meilleur choix comme étalon antimoine. Les résultats obtenus pour SYE-1, G-1 et AGV-1 montrent que ces étalons ne sont pas suffisamment homogènes.

ZUSAMMENFASSUNG

Der Gehalt an Antimon in den Standardgesteinen G-1, W-1, G-2, BCR-1, AGV-1, PCC-1, DTS-1, GSP-1, SUL-1, SYE-1, BCR-2 und GR wurde durch instrumentelle Neutronenaktivierungsanalyse bestimmt. Der Vergleich der Ergebnisse dieser Arbeit mit den früher vorgelegten ergibt, dass sich DTS-1 als Antimonstandard am besten eignet. Die Ergebnisse von SYE-1, G-1 und AGV-1 zeigen, dass diese Standardgesteine nicht genügend homogen sein können.

REFERENCES

1 M. Fleischer, *Geochim. Cosmochim. Acta*, 29 (1965) 1263.
2 G. R. Webber, *Geochim. Cosmochim. Acta*, 29 (1965) 229.
3 F. J. Flanagan, *Geochim. Cosmochim. Acta*, 33 (1969) 81.
4 J. T. Tanner and W. D. Ehmann, *Geochim. Cosmochim. Acta*, 31 (1967) 2007.
5 A. O. Brunfelt and E. Steinnes, *Analyst*, 93 (1968) 286.
6 A. O. Brunfelt and E. Steinnes, *Earth Planet. Sci. Lett.*, 5 (1969) 282.
7 H. Hamaguchi, N. Onuma, Y. Hirao, H. Yokoyama, S. Bando and M. Furukawa, *Geochim. Cosmochim. Acta*, 33 (1969) 507.
8 G. H. Morrison, J. T. Gerard, A. Travesi, R. L. Currie, S. F. Peterson and N. M. Potter, *Anal. Chem.*, 41 (1969) 1633.
9 G. E. Gordon, K. Randle, G. G. Goles, J. B. Corliss, M. H. Beeson and S. S. Oxley, *Geochim. Cosmochim. Acta*, 32 (1968) 369.
10 R. M. Filby and W. A. Haller, in J. R. DeVoe (Editor), *Modern Trends in Activation Analysis*, U. S. Government Printing Office, Washington, D. C., 1969, p. 399.
11 A. O. Brunfelt and E. Steinnes, *Anal. Chim. Acta*, 48 (1969) 13.
12 J. Esson, R. H. Stevens and E. A. Vincent, *Mineral. Mag.*, 35 (1965) 88.

Analytica Chimica Acta
Elsevier Publishing Company, Amsterdam
Printed in The Netherlands

DETERMINATION OF OXYGEN IN ALUMINUM ELECTROLYTIC BATHS BY A FAST-NEUTRON ACTIVATION METHOD

K. TAKADA*, I. FUJII, M. ISHIHARA* AND H. MUTO
Toshiba Research and Development Center, Tokyo Shibaura Electric Co., Ltd., Kangawa (Japan)
(Received 30th November 1970)

It is commonly known that oxygen in several substances[1-6] can be determined by a fast-neutron activation method based on the $^{16}O(n,p)^{16}N$ reaction, but when fluorine and oxygen are present in the same sample, it is also known that direct interference can be provided by the simultaneous $^{19}F(n,\alpha)^{16}N$ reaction.

The alumina content of aluminum electrolytic baths (referred to as bath in the following description) is a very important parameter in maintaining the optimal conditions for aluminum production; therefore, a rapid determination of alumina or oxygen content in baths is very desirable. However, the use of the simple fast-neutron activation method based on the $^{16}O(n,p)^{16}N$ reaction may be impossible for oxygen in bath samples which mainly comprise cryolite (Na_3AlF_6), because the fluorine content is as high as about 50%, whereas the oxygen content is only 1–5% (2–10%, as alumina).

Accordingly, in bath samples irradiated by fast neutrons, the induced radioactivities through the $^{16}O(n,p)^{16}N$ reaction may be heavily overlapped by those through the $^{19}F(n,\alpha)^{16}N$ reaction. A method of minimizing the error caused by the large subtraction due to the above-mentioned reaction was therefore investigated, and it was shown that a reasonable precision in the determination of oxygen in bath samples can be achieved by utilizing a functional property of the ^{16}N total activities based on the oxygen/fluorine ratio in the samples.

TABLE I

NUCLEAR DATA OF ELEMENTS CONTAINED IN ALUMINUM ELECTROLYTIC BATHS

Element	*Nuclear reaction*	*Half-life*	*Radiation energy (MeV)*
O	$^{16}O(n,p)^{16}N$	7.35 sec	β^-: 4.2, 10.3 γ: 6.14, 7.12
F	$^{19}F(n,p)^{19}O$	29.4 sec	β^-: 2.9, 4.5 γ: 0.200, 1.37
	$^{19}F(n,\alpha)^{16}N$	7.35 sec	β^-: 4.2, 10.3 γ: 6.14, 7.12
	$^{19}F(n,2n)^{18}F$	112 min	β^+: 0.649 (γ: 0.51)
Na	$^{23}Na(n,p)^{23}Ne$	40.2 sec	β^-: 4.4, 3.95 γ: 0.436
	$^{23}Na(n,\alpha)^{20}F$	10.7 sec	β^-: 5.41 γ: 1.63
Al	$^{27}Al(n,p)^{27}Mg$	9.45 min	β^-: 1.75, 1.59 γ: 0.84, 1.02
	$^{27}Al(n,\alpha)^{24}Na$	15.0 h	β^-: 1.39 γ: 1.37, 2.75

* Present address: Nippon Light Metal Research Laboratory Ltd., Shizuoka, Japan.

THEORETICAL

Table I shows the main component elements in baths and the radionuclei generated from each element through (n,p), (n,α) or (n,2n) nuclear reactions.

When samples that contain both oxygen and fluorine are irradiated by 14-MeV neutrons, the ratio of ^{16}N to ^{18}F ($^{16}N/^{18}F$) increases proportionally to the ratio of oxygen to fluorine(O/F). This relationship can be represented by a simple equation:

$$Y = \alpha RX + R \quad (1)$$

where Y is the $^{16}N/^{18}F$ activity ratio which can be replaced by the $^{16}N/^{18}F$ counting ratio under the same experimental conditions, X is the oxygen/fluorine content ratio in the sample, R is the $^{16}N/^{18}F$ activity or counting ratio given by a sample which contains fluorine but does not contain oxygen (*i.e.* O/F = 0.0), and α is the ratio of ^{16}N radioactivity induced from oxygen to that from the same amount of fluorine.

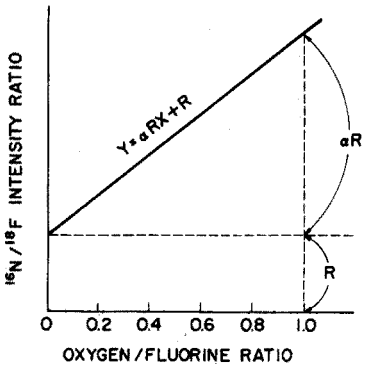

Fig. 1. Correlation of O/F and $^{16}N/^{18}F$ ratios.

The relationship is shown in Fig. 1. As values of R and α can be determined by experiment with some suitable standard substances, they can be used as constants in the following experiment under the same conditions. Then the oxygen/fluorine ratio (O/F) in the unknown sample can be determined by the equation;

$$X = (Y - R)/\alpha R \quad (2)$$

where Y is given by measuring the $^{16}N/^{18}F$ counting ratio in the neutron-irradiated sample. The oxygen content is obtained from the O/F ratio multiplied by the fluorine content; as much as about 50% fluorine can be efficiently determined by the ^{19}F-(n,2n)^{18}F reaction:

$$\text{oxygen (\%)} = (\text{O/F}) \cdot \text{fluorine (\%)}$$

EXPERIMENTAL

Apparatus

A Toshiba NAT-200 Cockcroft-Walton type neutron generator was used for activation of the samples. The samples were transferred between the target position

and the radiation detector by a pneumatic system. The effective neutron flux for generation of ^{16}N was automatically normalized by a CR-control system[7], and the relative neutron flux for generation of ^{18}F was normalized by using a neutron counter. γ-Spectra of the neutron irradiated samples were observed by a multichannel pulse-height analyser (TMC-401D). A single-channel pulse-height analyser was used for measuring the γ-rays from ^{16}N, and a γ,γ-coincidence counting system with two $2\times2''$ NaI scintillation detectors was used for measuring the annihilation γ-rays from ^{18}F. A $3\times3''$ well-type scintillation detector was used attached to the multi-channel and single-channel pulse-height analyser.

Standard substances

Pure alumina, succinic acid, sodium fluoride and cryolite were used for determining the values of α and R. The bath samples and standards were weighed (1.3–2.5 g) and were packed into polyethylene containers (15 mm diam. × 20 mm).

Procedure

The samples were transferred to the neighborhood of a tritium target, and then irradiated with neutrons for a suitable time interval that was automatically controlled

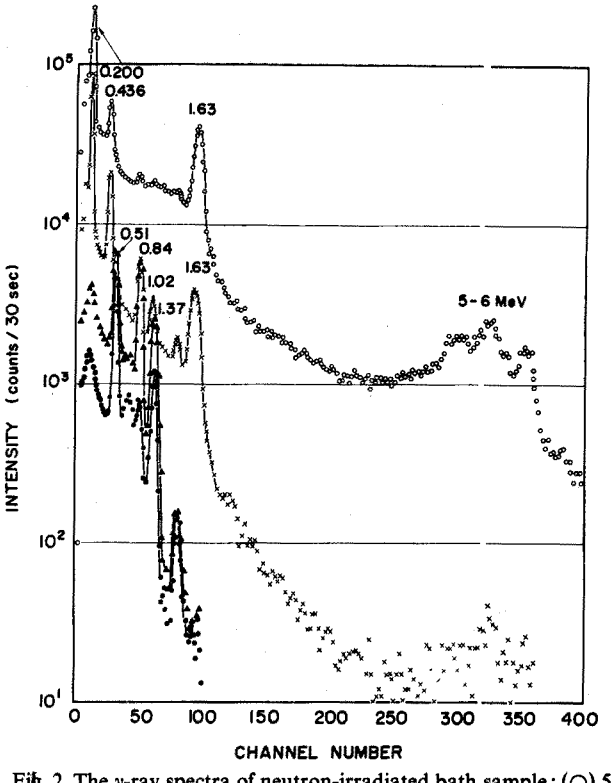

Fig. 2. The γ-ray spectra of neutron-irradiated bath sample: (○) 5 sec, (×) 50 sec, (▲) 5 min, (●) 50 min after cooling.

to 15–20 sec by the CR-control system. After irradiation, the samples were returned to the radiation detector by the pneumatic system and cooled for a few seconds. The γ-radiation of ^{16}N in the 5.0–7.5-MeV energy region was then counted for 30 sec, and the background was counted for 30 sec.

The annihilation γ-rays from ^{18}F in the 0.51 ± 0.05 MeV region were counted for 90 sec after cooling for more than 30 min. Then the counted value of each sample was corrected for the respective cooling time and was normalized to the same conditions in neutron flux by using a counted value from the neutron counter which accumulated the relative neutron output during the sample irradiation.

RESULTS AND DISCUSSION

γ-Spectra of the bath sample

Figure 2 shows the γ-spectra of neutron-irradiated bath sample after cooling for 5 sec, 50 sec, 5 min and 50 min. From these spectra, it appears that the γ-rays from ^{16}N in the energy region above 4 MeV are not overlapped by any other nuclei even just after the irradiation. Consequently, the counted value of the γ-radiation in the 5.0–7.5 MeV region should be reliable for the radiation from only ^{16}N. It was confirmed that the half-life of the radiation in this energy region as for bath samples was in good accordance with the half-life of ^{16}N.

The annihilation γ-rays from ^{18}F in the (0.51 ± 0.05)-MeV region were heavily overlapped by the Compton scattering γ-rays from many other nuclei; therefore, a considerable cooling time (more than 60 min) was necessary to allow the shorter-lived radionuclei to decay before the annihilation γ-rays from ^{18}F were measured with a single-channel pulse-height analyser. The γ,γ-coincidence counting system was very efficient for selective counting of the annihilation γ-rays, and the cooling time could then be shortened to 30 min.

TABLE II

DETERMINATION OF α-VALUE FROM THE SENSITIVITY RATIO OF $^{16}O(n,p)^{16}N$ TO $^{19}F(n,\alpha)^{16}N$ REACTION

Sensitivity for oxygen (counts/mg)			*Sensitivity for fluorine (counts/mg)*			*Oxygen/fluorine sensitivity ratio*
Succinic acid	*Alumina*	*Mean value*	*Cryolite*	*Sodium fluoride*	*Mean value*	
72.7	70.8	71.8	29.2	26.2	27.7	2.59
70.2	65.8	68.0	24.6	23.7	24.2	2.81
67.8	63.2	65.5	24.0	23.8	23.9	2.74
60.9	58.4	59.7	24.9	21.9	23.4	2.55
58.8	56.8	57.8	22.2	24.1	23.2	2.50
66.3	64.4	65.4	25.4	23.0	24.2	2.70
59.7	61.3	60.5	22.4	24.2	23.3	2.60
61.3	61.9	61.6	23.4	27.2	25.3	2.43
76.1	75.6	75.9	27.8	33.8	30.8	2.46
76.1	80.0	78.1	28.3	28.7	28.5	2.74
68.7	71.4	70.1	26.4	26.9	26.7	2.63
71.2	70.2	70.7	27.3	26.1	26.7	2.65
						2.62 ± 0.12

Determination of α-value

The value of α, which means the ratio of ^{16}N activity induced from oxygen to that from the same amount of fluorine, can be determined experimentally or mathematically as below.

1. The ratio of the ^{16}N sensitivity (*e.g.* counts per mg of oxygen or fluorine) of oxygen to that of fluorine is equal to the α-value, so that it can be determined from experiments with standard samples that contain oxygen or fluorine individually.

Table II shows the results of experiments in which alumina, succinic acid, sodium fluoride and cryolite were used as standards. From these results, the α-value was estimated as 2.62 ± 0.12.

2. The α-value can be also calculated from eqn. (1) by substituting the experimental value of $^{16}N/^{18}F$ to Y as for the standard samples which contain a known amount of oxygen and fluorine. Results of experiments in which cryolite–alumina mixed samples were used as standards are shown in Fig. 3. Estimation from eqn. (1) by the least-squares method gave a value of 2.65 ± 0.34 for α.

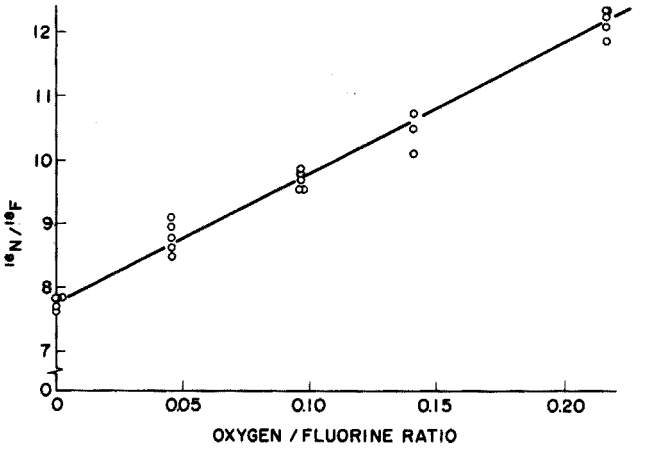

Fig. 3. Calibration curve of the O/F ratio.

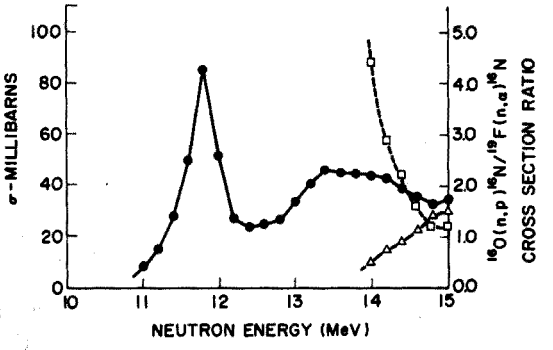

Fig. 4. Excitation curves of $^{16}O(n,p)^{16}N$ and $^{19}F(n,\alpha)^{16}N$ reactions: (●) $^{16}O(n,p)^{16}N$, (△) $^{19}F(n,\alpha)^{16}N$, (□) σ_o/σ_f ratio.

3. Theoretically, the α-value may be calculated from the following expression:

$$\alpha = \frac{N_o \cdot F \cdot \sigma_o}{N_f \cdot F \cdot \sigma_f} = \frac{19 \cdot \sigma_o}{16 \cdot \sigma_f} = 1.19 \cdot \frac{\sigma_o}{\sigma_f}$$

where N_o and N_f are the number of atoms in the same amount of oxygen and fluorine, respectively, F is the neutron flux used in the sample irradiation, and σ_o and σ_f are the cross-sections of the $^{16}O(n,p)^{16}N$ and $^{19}F(n,\alpha)^{16}N$ reactions.

However, the value of α was unsatisfactorily estimated as 2.9 ± 1.2 at a neutron energy of 14.1 MeV and as 1.9 ± 0.7 at a neutron energy of 14.5 MeV, because the exact values of the cross-section for the $^{19}F(n,\alpha)^{16}N$ reaction at neutron energies of about 14 MeV are not given in the literature[8]. The excitation curves of the $^{16}O(n,p)^{16}N$ and $^{19}F(n,\alpha)^{16}N$ reactions are shown in Fig. 4.

From the above-mentioned results, the value of α was estimated as 2.6 ± 0.1, and this value was used in the following experiments.

Determination of oxygen/fluorine ratio

In the determination of the O/F ratio by means of eqn. (2), the precision of the calculated O/F ratio mainly depends on the experimental precision of the $^{16}N/^{18}F$ counting ratio of the analytical sample and the R-value given by the standards.

TABLE III

EXPERIMENTAL PRECISION OF $^{16}N/^{18}F$ COUNTING RATIO

Sample (O/F ratio)	*^{16}N counts*	*^{18}F counts (corrected)*	*$^{16}N/^{18}F$ ratio*	*Mean value*	*Standard deviation*
S-0	52414	6811	7.70		
	51278	6695	7.66		
(0.000)	48060	6115	7.86		
	48115	6130	7.85		
	44673	5675	7.87	7.79	0.10
S-5	53340	6083	8.77		
	55232	6390	8.64		
(0.0456)	49840	5864	8.50		
	50590	5556	9.10		
	49422	5502	8.98	8.80	0.24
S-10	59644	6252	9.54		
	55092	5599	9.84		
(0.0964)	52435	5409	9.69		
	52460	5357	9.79		
	53320	5563	9.56	9.68	0.13
S-14	60768	5802	10.47		
	55325	5298	10.44		
(0.141)	54994	5430	10.13		
	53954	5167	10.44		
	54421	5066	10.74	10.44	0.22
S-20	62215	5083	12.24		
	60529	4908	12.33		
(0.217)	56368	4567	12.34		
	56158	4653	12.07		
	56913	4811	11.83	12.16	0.22

Since these are the constituents of a large subtraction, any deviation in either value causes a relatively large deviation in the calculated result. The experimental reproducibility of the $^{16}N/^{18}F$ counting ratio was found to be less than $\pm 2\%$ (relative standard deviation) as shown in Table III. It is, however, presumed that the relative standard deviation of the O/F ratio may be quite large, because the deviation of that ratio is mainly affected by the subtraction of R from Y in the following expression:

$$X(\mathrm{O/F}) = \frac{(Y \pm \sigma_y) - R \pm \sigma_r)}{(\alpha \pm \sigma_\alpha) \cdot (R \pm \sigma_r)} = \frac{(Y \pm \sigma_y) - (R \pm \sigma_r)}{(2.6 \pm 0.1) \cdot (R \pm \sigma_r)}$$

$$= \frac{Y-R}{2.6\,R}\left[1 \pm \left(\frac{\sigma_y^2+\sigma_r^2}{(Y-R)^2} + \frac{0.1^2}{2.6^2} + \frac{\sigma_r^2}{R^2}\right)^{\frac{1}{2}}\right] \quad (3)$$

where σ_y, σ_r, ynd σ_α are the standard deviations of the Y, R and α values, respectively.

The actual relative standard deviation was estimated as 10–15% at 0.1 for O/F, and as 15–20% at 0.05 for the O/F ratio.

Determination of fluorine in bath

Fluorine in amounts as high as about 50% in bath was determined efficiently by a simple radioactivation method based on the $^{19}F(n, 2n)^{18}F$ nuclear reaction. A γ, γ-coincidence counting system contributed to obtaining a high signal-to-noise ratio in measuring the annihilation γ-rays from ^{18}F. Table IV shows the analytical results for some bath samples, and it is apparent that quite a high precision (*i.e.* $\pm 1\%$ relative standard deviation) was obtained and that the values determined are in good accordance with those determined by a standard chemical analysis.

TABLE IV

PRECISION OF FLUORINE DETERMINATION

Method	*Electrolytic bath (A)* (%)	*Electrolytic bath (B)* (%)	*Cryolite* (%)	*Aluminum fluoride* (%)
Activation analysis	51.8 50.8	52.4 52.7	53.0 52.8	67.0
	51.5 50.6	53.5 52.0	52.8 53.6	66.5
	50.6 50.7	52.6 52.0	54.4 53.8	66.0
	50.8 51.9	52.4 52.3	53.0 52.7	67.0
	50.8 51.6	53.3 52.9		66.3
(Mean value)	51.1 ± 0.5	52.6 ± 0.5	53.3 ± 0.6	66.6 ± 0.5
Chemical analysis	50.6 ± 0.1[a]	52.2 ± 0.1[a]	53.0 ± 0.2[a]	65.0 ± 0.2[b]

[a] Distillation method with sulfuric acid.
[b] Fusion and titration method.

Determination of oxygen in baths

Table V shows the analytical results obtained for some practical bath samples. Each determined value was in good accordance with the value given by standard chemical analysis, and the relative standard deviation was 10–15%.

Consequently, it is considered that this method is applicable to routine determination of oxygen of alumina in baths; the method is rapid and would also lend itself to automation, whereas the chemical method requires a skilled analyst and

TABLE V

ANALYTICAL RESULTS FOR OXYGEN

Sample no.	*Oxygen (%)*					Al_2O_3 (%)	
	Determined values				*Mean value*	*Estimated*	*Chemical analysis*
1	3.5	4.1	3.7	4.4	3.7±0.5	7.8±0.9	8.4
	3.2	3.3	4.0	3.2			
2	7.5	7.2	7.1	6.8	7.0±0.4	14.8±0.8	14.7
	6.9	6.4	7.0				
3	5.4	4.7	5.1	4.4	4.8±0.4	10.3±0.8	10.0
	4.7						
4	4.0	3.9	3.8	3.2	3.8±0.4	8.1±0.8	7.8
	3.5	4.5					
5	4.7	4.3	4.7	4.7	4.7±0.2	9.8±0.4	10.2
	4.7	4.8					

time consumption of more than 3 h. The final precision of the analytical value mainly depends on the variation of the $^{16}N/^{18}F$ counting ratio which varies on account of the statistical variation of radioactive decays of ^{16}N and ^{18}F, and also by the mechanical gain shift of the radiation measuring equipment. The precision of this method may be improved in the future by using a higher neutron flux to obtain higher intensity for ^{16}N and ^{18}F, and also by using new counting equipment which can retain a very short resolving time and high stability in counting intensive γ-radiation.

SUMMARY

Oxygen in various materials can be determined by rapid, non-destructive fast-neutron activation analysis with a small neutron generator. The applicability of the method for determination of alumina in aluminum electrolytic baths, which is a very important factor in efficient aluminum metal production, has been studied. One of the major problems associated with this method is the interference of fluorine from cryolite. This difficulty has been eliminated by using a functional relation of the $^{16}N/-^{18}F$ activity ratio and the oxygen/fluorine ratio in the sample. The alumina content in baths can be determined with a precision of 10–15% to 15–20% for 10–5% alumina concentrations.

RÉSUMÉ

L'oxygène peut être dosé dans diverses substances par analyse rapide et non destructive, par activation neutronique, au moyen d'un petit générateur de neutrons. On examine l'application de cette méthode au dosage de l'alumine dans des bains électrolytiques d'aluminium; ce qui est un facteur très important pour la production d'aluminium métal. L'interférence du fluor, provenant de la cryolite, est considérable; cette difficulté est évitée en utilisant une relation fonctionnelle du rapport d'activité $^{16}N/^{18}F$ et du rapport oxygène/fluor dans l'échantillon. La teneur en alumine dans

les bains peut être déterminée avec une précision de 10–15% et 15–20% pour des concentrations d'alumine de 10 et 5% respectivement.

ZUSAMMENFASSUNG

Sauerstoff in verschiedenen Stoffen kann durch die schnelle, zerstörungsfreie Aktivierungsanalyse mit schnellen Neutronen aus einem kleinen Neutronengenerator bestimmt werden. Es wurde die Anwendbarkeit der Methode für die Bestimmung von Aluminiumoxid in Bädern der Aluminiumelektrolyse untersucht, was für eine wirkungsvolle Aluminiummetallgewinnung sehr wichtig ist. Eines der Hauptprobleme, die mit dieser Methode verbunden sind, ist die Störung durch das Fluor des Kryoliths. Diese Schwierigkeit wurde durch Anwendung einer funktionellen Beziehung von $^{16}N/^{18}F$-Aktivitätsverhältnis und Sauerstoff/Fluor-Verhältnis in der Probe beseitigt. Der Aluminiumoxidgehalt in den Bädern kann mit einer Reproduzierbarkeit von 10–15% bis 15–20% bei Aluminiumoxidkonzentrationen von 10–5% bestimmt werden.

REFERENCES

1 R. F. Coleman and J. L. Perkin, *Analyst*, 84 (1959) 233.
2 R. F. Coleman, *Analyst*, 87 (1962) 590.
3 D. J. Veal and C. F. Cook, *Anal. Chem.*, 34 (1962) 178.
4 E. L. Steele and W. W. Meinke, *Anal. Chem.*, 34 (1962) 185.
5 O. Anders and D. W. Briden, *Anal. Chem.*, 36 (1964) 287.
6 I. Fujii, K. Takada and H. Muto, *Japan Analyst*, 15 (1966) 1239.
7 I. Fujii, H. Muto, K. Ogawa and A. Tani, *J. At. Energy Soc. Japan*, 5 (1963) 455.
8 J. R. Stehn, M. D. Goldberg, R. W. Chasman, S. F. Mughabghab, B. A. Magurno and V. M. Mai, *Neutron Cross Sections, Vol. 1*, Z = 1 to 20, BNL-325, 2nd Edn., Suppl. No. 2, Brookhaven National Laboratory, 1964.

Analytica Chimica Acta
Elsevier Publishing Company, Amsterdam
Printed in The Netherlands

THE DETERMINATION OF VANADIUM IN BRINES BY ATOMIC ABSORPTION SPECTROSCOPY*

HANS J. CRUMP-WIESNER AND HERMAN R. FELTZ
U.S. Geological Survey, Washington, D. C. 20242 (U.S.A.)
AND
WILLIAM C. PURDY
Department of Chemistry, University of Maryland, College Park, Md. 20742 (U.S.A.)
(Received 8th January 1971)

Atomic absorption has become established as an important analytical tool and is practically indispensable in trace metal analysis. Ease of sample preparation, high sensitivity, and relative freedom from adverse inter-element effects are the chief reasons for this trend.

Certain elements, such as aluminum, silicon, titanium, and vanadium cannot be successfully determined with an air–acetylene flame because the flame is not hot enough to dissociate refractory oxides, providing only a very limited number of atoms for absorption. In 1962, Elwell and Gidley[1] listed vanadium as one of the elements which could not be determined by atomic absorption spectroscopy.

Flame conditions, however, play an important role in the determination of refractory elements. Gatehouse and Willis[2] noted that the optimum conditions for the atomic absorption detection of vanadium required a "very rich" air–acetylene flame, but they were unable to detect less than 1000 mg l^{-1}. Robinson[3] reported absorption by vanadium in an oxycyanogen flame with a detection limit of 300 mg l^{-1}.

In 1963, Fassel and Mossotti[4] reported that proper flame conditions inhibit the formation of oxides and hydroxides and produce an atomic vapor which absorbs at the resonance wavelengths. Vanadium was determined by using a fuel-rich oxyacetylene flame. Standards diluted with ethanol were aspirated into three Beckman integral-type burners giving a sensitivity of 10 mg l^{-1} for 1% absorption at the 318.398-nm resonance line. Slavin and Manning[5] confirmed this work and reported a slightly better sensitivity of 7 mg l^{-1} for 1% absorption under similar conditions. Poor signal-to-noise ratio due to the turbulent nature of the Zeiss total consumption burners, prevented the determination of more dilute vanadium solutions.

In 1965, Amos and Thomas[6] reported a sensitive method for measuring aluminum in aqueous solution using a long-path premix-type oxyacetylene burner. High burning speed and the explosive nature of the oxyacetylene mixture in a premix-type burner are serious limitations. Willis[7] overcame this difficulty by using a combination of nitrous oxide and acetylene which would not only dissociate refractory compounds, but also could be used safely in premix burners.

Spectrographic and spectrophotometric methods are the principal means

* Publication authorized by the Director, U.S. Geological Survey.

currently used to determine vanadium in natural waters. As previously reported by Crump-Wiesner and Purdy[8], the extraction of vanadium(V) and (IV) as the cupferrate into MIBK was superior to other chelating agents investigated and would be the best choice for an atomic absorption method. The increase in sensitivity gained in atomic absorption by use of organic solvents (especially water-immiscible) to concentrate a metal chelate in the organic phase, is well known. This paper describes a procedure for the extraction of vanadium from brines and subsequent measurement by atomic absorption spectroscopy with a premix-type burner assembly and a nitrous oxide–acetylene flame.

EXPERIMENTAL

Reagents

Reagent grade chemicals were used without further purification. A standard vanadium(V) stock solution (1 mg ml^{-1}) was prepared by dissolving 2.298 g of ammonium metavanadate in 1 l of distilled water. A working standard of vanadium(V) containing 1 μg ml^{-1} was prepared by dilution of this stock solution just before use. The stock solution was assayed by titration with standard ferrous ammonium sulfate to a potentiometric end-point[9] and by reduction with sodium sulfite followed by titration with potassium permanganate to a visual end-point[10].

A standard vanadium(IV) stock solution containing 1 mg ml^{-1} was prepared by dissolving 3.907 g of purified grade vanadyl sulfate (Fisher Scientific Co.)* in 1 l of distilled water. The working standard of vanadium(IV) containing 1 μg ml^{-1} was prepared by appropriate dilution of this stock solution. The vanadium(IV) stock solution was assayed as stated above to determine that all vanadium was present in the +4 oxidation state.

Cupferron in MIBK was prepared by dissolving 5.0 g of ACS certified reagent in 100 ml of 0.33 *M* hydrochloric acid and then extracting the hydrogen cupferrate with 100 ml of MIBK. The layers were separated and the organic phase was rinsed once more with 50 ml of demineralized water. This reagent must be freshly prepared just before use in the extraction procedure.

Apparatus

All measurements were made with a Perkin-Elmer Model 303 atomic absorption spectrophotometer fitted with a nitrous oxide–acetylene burner mounted on a premix-chamber-atomizer assembly. A shielded vanadium hollow-cathode lamp served as the light source. The absorption measurements were recorded on a Servo/Riter II potentiometric recorder (Texas Instruments, Inc.).

Recommended instrument settings

Grating:	ultraviolet
Wavelength:	318.4 nm
Scale expansion:	10×
Slit:	4 (1 mm, 0.7 nm)
Source:	shielded vanadium hollow-cathode lamp
Lamp current:	40 mA
Burner:	nitrous oxide–acetylene

Nitrous oxide pressure:	30 psi; 6.1 on flowmeter (arbitrary scale)
Acetylene pressure:	8 psi; 4.2 on flowmeter (arbitrary scale)
Noise suppression:	3
Recorder:	Servo/Riter II, set at zero % absorption with reagent blank.

Extraction procedure

Pipet equal volumes of sample (100 ml maximum) into four 250-ml beakers. Add to these beakers 0.0, 2.0, 4.0, and 6.0 ml of ammonium metavanadate solution (1.00 ml = 1.0 μg V), respectively. Adjust the pH to 1.0 with concentrated hydrochloric acid and transfer the samples to four 125-ml separatory funnels. Add 5 ml of 5% cupferron in MIBK and shake the funnels vigorously for 2.5 min. Allow the layers to separate and drain the organic phase into 10-ml test tubes. Centrifuge for 3 min to complete the phase separation. Aspirate the ketone layer as soon as possible. The complex deteriorates fairly rapidly, therefore, samples should not be left standing overnight for analysis on the following day. Repeat aspiration and average the duplicate results. MIBK or 5% cupferron in MIBK may be used to set the recorder to zero % absorption.

Interfering ion study

A 5.0-ml aliquot of vanadium(V) or (IV) standard (10 μg ml^{-1}), and 5.0 ml of solution of a series of metals (1000 μg ml^{-1}), were diluted to about 45 ml and the pH adjusted to 1.0 with hydrochloric acid. The solution was transferred to a 50-ml volumetric flask, diluted to the mark with water and mixed. A 15-ml portion was transferred into a 125-ml separatory funnel and extracted with 15 ml of 5% cupferron in MIBK. The absorption of this solution was compared with that from a standard prepared in a similar manner, but containing vanadium only.

Sample collection and treatment

Bottles (polyethylene) to be used for collection of samples for vanadium analysis should be given the following treatment. Fill the bottle with dilute nitric acid and allow it to stand overnight. Empty the bottle, rinse thoroughly with tap water, follow by thorough rinsing with distilled water, and allow to dry. Samples should be filtered at time of collection to eliminate the relatively high concentration of organisms that may be present. If these organisms are not removed, minor elements may be released into solution after the decomposition of biological material, or, under favorable conditions of growth, the organisms can deplete the minor elements. In either case, field filtration is necessary if the minor metals actually in solution at the time of collection are to be determined. A membrane-type filter, 0.45 μ average pore size, should be used in a pressure filter to minimize contamination of samples and speed the filtering process. Use the first 50 ml of filtrate to rinse the sample bottle. Discard this portion, and then collect the required volume of filtrate. In some cases, where samples cannot be filtered, they must be analyzed immediately upon receipt in the laboratory.

Filtered samples should not be acidified because of the slow formation of polyvanadates in acid medium[11]. These acids are rejected by cupferron in the extraction procedure. Only with heating in an alkaline medium can the polyvanadium acids be changed into the monomeric form. It is best to acidify the collected samples under controlled conditions in the laboratory just before extraction.

RESULTS AND DISCUSSION

Extraction of vanadium

The most stable form of vanadium in natural waters is the metavanadate anion (VO_3^-)[12]. Consideration of the chemistry of vanadium points to the ease with which this element will change its valence in response to changes in the redox potential of the environment. Vanadium(V) in the form of the metavanadate anion can be easily reduced to the quadrivalent vanadyl cationic complex VO^{2+}. The existence of VO^{2+} cannot be excluded under favorable conditions of pH and reducing environment. By careful adjustment of pH and concentration of the chelating agent, vanadium(V) and (IV) may be quantitatively extracted by cupferron into MIBK[8]. Further reduction leads to the trivalent V^{3+} ion, but only in a strongly acidic and reducing environment. The V^{2+} cation is very unstable.

Recorded absorption values are plotted with a connecting line extended back through zero % absorption. The intercept on the concentration axis is the concentration of the metal in the original sample. This line must be straight to obtain an accurate analysis. Owing to the variable solubility of MIBK in brines of differing salt content, the standard addition method was the preferred technique. Otherwise, the salt content of blanks used for the extraction of a series of standards must be matched to that of the brine sample. This is both difficult and cumbersome unless samples of the same salt concentration are analyzed routinely. The other alternative would be to dilute the recovered organic phase to a common volume, but this procedure would lower the sensitivity of the absorption measurement

$$\mu g \text{ per kg V} = (\text{density of brine sample})^{-1} \cdot \mu g \text{ V l}^{-1}$$

Effect of interfering ions

Table I shows the effect of other metals on the recovery of vanadium. With two exceptions, essentially no interference was observed for all metals present at a con-

TABLE I

EFFECT OF VARIOUS IONS ON THE RECOVERY OF VANADIUM
(Concentration of vanadium: 1 $\mu g\ ml^{-1}$; interfering ion: 100 $\mu g\ ml^{-1}$)

Interfering ion added	*Absorption*[a] (%)	*Vanadium recovered*[a] (%)	*Interfering ion added*	*Absorption*[a] (%)	*Vanadium recovered*[a] (%)
None	37.0	100.0	Ce^{4+}	38.0	102.7
Fe^{3+}	38.0	102.7	Bi^{3+}	37.0	100.0
Ni^{2+}	37.0	100.0	Ti^{4+}	37.0	100.0
Cu^{2+}	37.0	100.0	MoO_4^{2-}	36.0	97.3
Al^{3+}	36.6	99.0	Th^{4+}	38.0	102.7
Pb^{2+}	37.0	100.0	Zr^{4+}	38.0	102.7
Zn^{2+}	35.8	96.8	UO_2^{2+}	37.5	101.3

[a] These values represent the average of 3 independent determinations.

Interfering ion added	*Amount permissible* ($\mu g\ ml^{-1}$)
WO_4^{2-}	5
Sn^{4+}	10

centration 100 times that of vanadium before extraction. The levels at which tin (IV) and tungstate interfere are well below those normally encountered in brines.

Analysis of brines

An example of the standard addition technique for a Great Salt Lake Brine is shown in Fig. 1. Typical absorption signals obtained on the recorder are illustrated in Fig. 2. The maximum sensitivity is approximately 11 μg vanadium per liter per 1% absorption, and as little as 2.5 μg of vanadium per liter can be detected. Table II

TABLE II

VANADIUM IN CLOSED BASINS

Sample	*Date of collection*	*Density* ($g\ ml^{-1}$)	*Spectrographic*[a] ($\mu g\ kg^{-1}$)	*Atom. abs.* ($\mu g\ kg^{-1}$)
Deep Springs				
1	Aug. 1963	1.296	22	23
2	Aug. 1963	1.291	20	16
Great Salt Lake[b]				
1	July 1965	1.218	4–6	5
2	July 1965	1.174	4–6	7
Honey Lake				
1	Aug. 1963	1.040	—	1150
2	Aug. 1963	1.017	160	138
Alkali Valley	Aug. 1964	1.340	420	399
Abert Lake	Aug. 1963	1.284	42	30

[a] Spectrographic results were determined by the U.S. Geological Survey, Denver, Colo.
[b] All Great Salt Lake samples were diluted 1 + 1 at time of collection.

presents the results of vanadium analyses in brine samples from several lakes by atomic absorption and spectrographic methods. In the spectrographic procedure, 8-quinolinol, tannic acid, and thionalide were utilized to concentrate vanadium and a number of other metals[13]. Indium was added as a radiation buffer and palladium was used as an internal standard. The ashed oxides of these metals were subsequently subjected to direct current arcing conditions during spectrum analysis.

In most cases, atomic absorption values agree quite closely with those determined spectrographically. The trend of lower results by atomic absorption spectroscopy is due mainly to the long interval between collection and time of analysis, while spectrographic values were determined soon after sampling. All brines were unfiltered except for Abert Lake. Under favorable conditions of growth, the biological activity of algae can deplete the minor elements. Arnon and Wessell[14], working with algae, found that small quantities of vanadium gave increased growth. Sorption on walls of sample containers and sediments were noticed, particularly among the interstitial brine samples of Honey Lake. If any precipitation occurred, the density and ionic

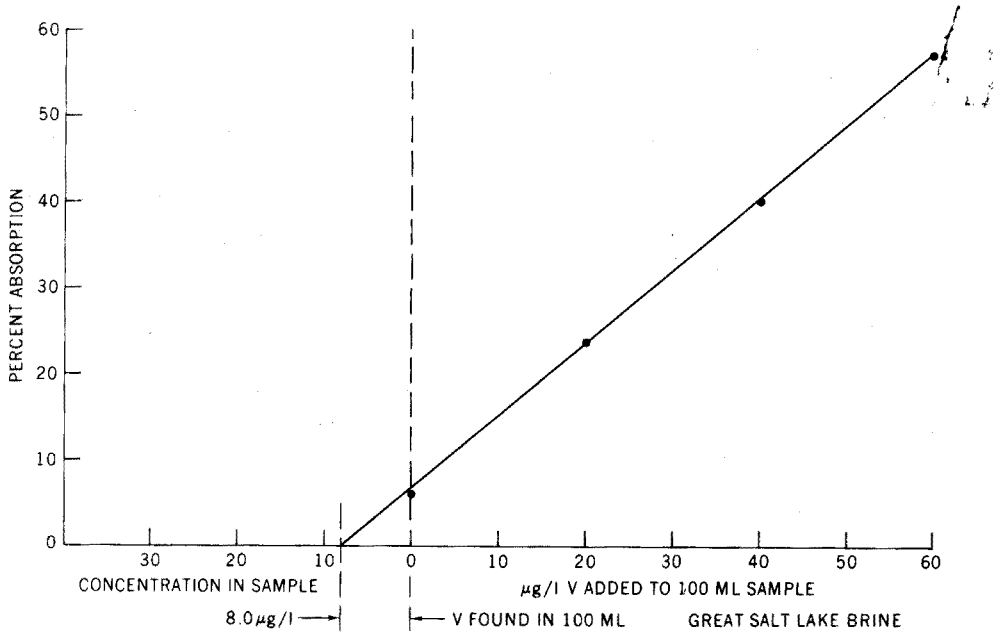

Fig. 1. Plot of atomic absorption values for a vanadium sample extracted directly with 5% cupferron in MIBK.

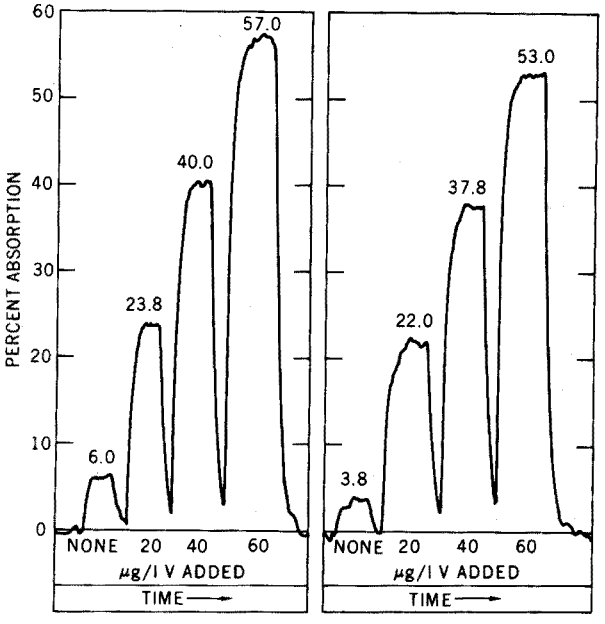

Fig. 2. Typical atomic absorption curves for vanadium added to two Great Salt Lake brines.

balance would be affected. No other reliable values for vanadium at these locations have been published which would have been helpful for comparison purposes.

CONCLUSIONS

Preliminary isolation and concentration of vanadium in brines is essential because of the severe limitations of the associated matrix, making a direct examination of the sample unfeasible by common techniques. The sensitivity and detection limit for the presence of vanadium is vastly improved with the aid of an extraction procedure and the enhancement effect of the organic solvent. The rapid, accurate, and sensitive atomic absorption method for the determination of trace quantities of vanadium in brines is a desirable approach to complement existing techniques.

SUMMARY

A standard addition method is described for the determination of vanadium in brines by atomic absorption spectroscopy with a nitrous oxide–acetylene flame. Sample pH is adjusted to 1.0 with concentrated hydrochloric acid and the vanadium is directly extracted with 5% cupferron in methyl isobutyl ketone (MIBK). The ketone layer is then aspirated into the flame and the recorded absorption values are plotted as a function of the concentration of the added metal. As little as 2.5 $\mu g\, l^{-1}$ of vanadium can be detected under the conditions of the procedure. Tungsten and tin interfere when present in excess of 5 and 10 $\mu g\, ml^{-1}$, respectively. The concentrations of the two interfering ions normally found in brines are well below interference levels.

RÉSUMÉ

On décrit une méthode de dosage spectroscopique par absorption atomique, avec étalon interne, pour le vanadium dans les saumures; on utilise une flamme oxyde nitreux–acétylène. Le pH est ajusté à 1.0 à l'aide d'acide chlorhydrique concentré; le vanadium est directement extrait à l'aide de cupferon à 5% dans la méthylisobutylcétone. La couche cétone est aspirée dans la flamme et les absorptions sont enregistrées. On peut détecter ainsi jusqu'à 2.5 $\mu g\, l^{-1}$ de vanadium. Tungstène et étain peuvent gêner à partir d'un excès de 5 et 10 $\mu g/ml$ respectivement. Les concentrations de ces deux éléments gênants sont normalement en dessous de ces quantités, dans les saumures.

ZUSAMMENFASSUNG

Es wird eine Standard-Additionsmethode beschrieben für die Bestimmung von Vanadin in Solwässern durch Atomabsorptionsspektroskopie unter Verwendung einer Lachgas–Acetylen-Flamme. Der pH-Wert der Probe wird mit konz. Salzsäure auf 1.0 eingestellt und das Vanadin unmittelbar mit 5% Cupferron in Methylisobutylketon (MIBK) extrahiert. Die Ketonphase wird dann in die Flamme gesprüht, und die aufgezeichneten Absorptionswerte werden als Funktion der Konzentration des zugefügten Metalls aufgetragen. Unter den Bedingungen des Verfahrens können 2.5 $\mu g\, l^{-1}$ Vanadin nachgewiesen werden. Überschüssiges Wolfram und Zinn von

5 bzw. 10 μg ml^{-1} stören. Die normalerweise in Solwässern gefundenen Konzentrationen der beiden störenden Ionen liegen unterhalb der Störungsbereiche.

REFERENCES

1 W. T. ELWELL AND J. A. F. GIDLEY, *Atomic Absorption Spectrophotometry*, Macmillan, New York, 1962, pp. 42–43.
2 B. M. GATEHOUSE AND J. B. WILLIS, *Spectrochim. Acta*, 17 (1961) 710.
3 J. W. ROBINSON, *Anal. Chem.*, 33 (1961) 1067.
4 V. A. FASSEL AND V. G. MOSSOTTI, *Anal. Chem.*, 35 (1963) 252.
5 W. SLAVIN AND D. C. MANNING, *Anal. Chem.*, 35 (1963) 253.
6 M. O. AMOS AND P. E. THOMAS, *Anal. Chim. Acta*, 32 (1965) 139.
7 J. B. WILLIS, *Nature*, 207 (1965) 715.
8 H. J. CRUMP-WIESNER AND W. C. PURDY, *Talanta*, 16 (1969) 124.
9 I. M. KOLTHOFF, R. BELCHER, V. A. STENGER AND G. MATSUYAMA, *Volumetric Analysis, Vol. 3*, Interscience, New York, 1957, p. 607.
10 N. H. FURMAN, *Standard Methods of Chemical Analysis, Vol. 1*, D. Van Nostrand, Princeton, N. J., 1962, pp. 1205–1227.
11 F. J. C. ROSSOTTI AND H. ROSSOTTI, *Acta Chem. Scand.*, 10 (1956) 957.
12 A. SZALAY AND M. SZILAGYI, *Geochim. Cosmochim. Acta*, 31 (1967) 1.
13 W. D. SILVEY AND R. BRENNAN, *Anal. Chem.*, 34 (1962) 784.
14 D. I. ARNON AND G. WESSELL, *Nature*, 172 (1953) 1039.

Analytica Chimica Acta
Elsevier Publishing Company, Amsterdam
Printed in The Netherlands

DOSAGE DE DIFFERENTES IMPURETES DANS LE PLUTONIUM PAR ABSORPTION ATOMIQUE

J. VIENNEY

Commissariat à l'Energie Atomique, Centre d'Etudes de Bruyères-le-Châtel, B.P. 61, Montrouge (92) (France)

(Reçu le 10 décembre 1970)

Les impuretés contenues dans un métal jouent un rôle important sur ses propriétés physiques et métallurgiques. L'analyse des impuretés doit être faite rapidement, avec précision et pour des métaux coûteux, sur une quantité minimale d'échantillon. Pour le plutonium, ces impuretés sont, en général, déterminées par spectrophotométrie ou polarographie, ce qui nécessite le plus souvent une séparation du plutonium, l'ajout de nombreux réactifs et entraîne un temps de mise en oeuvre très long.

Comme Graff et Mullin[1] pour l'uranium et Ganivet et Benhamou[2] pour le plutonium, on a cherché à utiliser l'analyse par absorption atomique sans séparation préalable.

Le plutonium est mis en solution par l'acide chlorhydrique. La solution est ajustée à une acidité 2 *M* et une concentration en plutonium de 20 g l^{-1}. La teneur en impuretés est déterminée en mesurant l'absorption de cette solution dans la flamme par rapport à une solution de plutonium connue. La source lumineuse est une lampe à cathode creuse de même nature que l'impureté à doser.

PARTIE EXPÉRIMENTALE

Appareillage

L'appareil utilisé est un spectrophotomètre d'absorption atomique Perkin-Elmer 303 dont le brûleur est placé en boîte à gants car les manipulations de solutions de plutonium nécessitent un certain nombre de précautions vis-à-vis de l'opérateur.

L'appareil est à l'extérieur de la boîte à gants, le faisceau lumineux de la cathode creuse traverse la flamme du brûleur par l'intermédiaire de deux fenêtres en "suprasil" qui assurent l'étanchéité de la boîte à gants.

L'évacuation des calories dégagées par le brûleur (150 kcal min^{-1} au maximum) est assurée par une ventilation permanente d'environ 1.25 m^3 min^{-1} et par un réfrigérant en cuivre de grande efficacité. La ventilation assure également la sécurité de l'installation par dilution des gaz en cas de fuite d'acétylène.

Le fait de travailler sans séparation préalable du plutonium nous oblige à débarrasser les gaz de combustion des particules d'oxyde de plutonium qu'ils peuvent entraîner. Ce piégeage est réalisé par un jeu de filtres montés en parallèle comprenant : (*a*) deux préfiltres en fibre de verre dont le pouvoir d'arrêt est voisin de 30 à 10 μm, (*b*) deux filtres en mousse de polyuréthane de très grande surface dont le pouvoir d'arrêt est voisin de 0.1 μm.

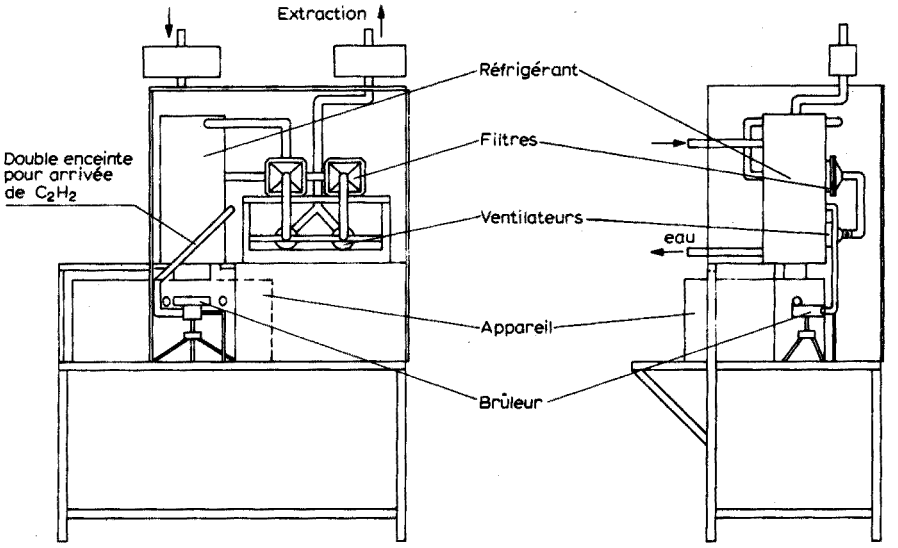

Fig. 1. Dispositif en boîte à gants d'absorption atomique.

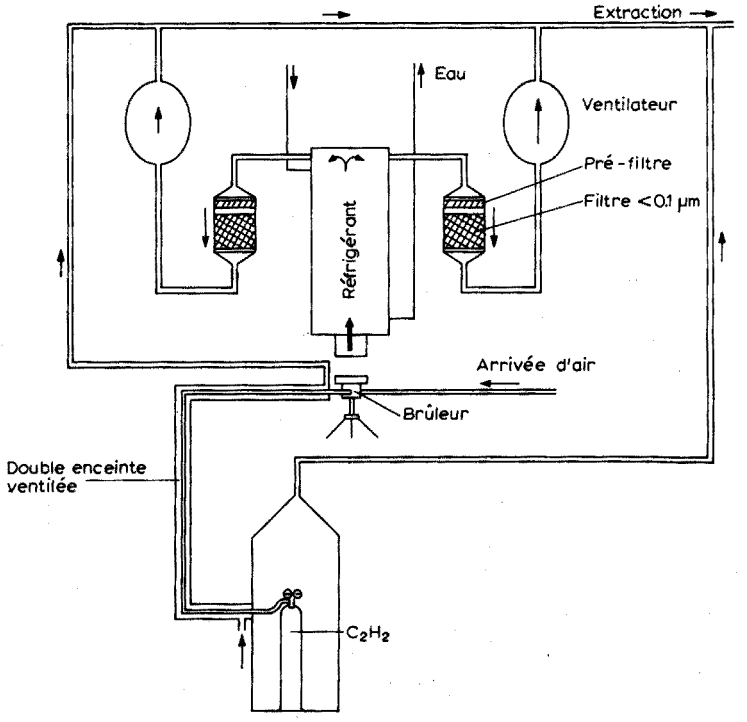

Fig. 2. Schéma de principe.

Cet ensemble de filtres constitue une perte de charge inférieure à 20 mm d'eau. L'expérience confirme l'efficacité d'un tel système de décontamination des gaz. La récupération des particules d'oxyde de plutonium peut s'effectuer par simple lavage des filtres.

Les Figs. 1 et 2 montrent l'ensemble de l'installation.

Mode opératoire

Environ 1 g du métal à analyser est mis en solution dans de l'acide chlorhydrique. La solution obtenue est ajustée à 20 g l^{-1} en plutonium et 2 *M* en acidité. La solution obtenue est vaporisée dans la flamme du brûleur air–acétylène. Les conditions de réglage du brûleur et du spectrophotomètre ainsi que les limites de dosage sont indiquées pour l'ensemble des éléments dosés dans le Tableau I.

Le tracé des courbes d'étalonnage est effectué à l'aide d'une solution chlor-

TABLEAU I

CONDITIONS OPÉRATOIRES ET LIMITES DE DOSAGE

Eléments	*Longueur d'onde (nm)*	*Absorption du plutonium*	*Limites en millionièmes*	*Flamme*	*Observations*
Ag	328	Nulle	2.5	Ox.	Dosage possible entre 2.5 et 20 millionièmes
Au	243	Importante	10	Ox.	
Bi	223.1	—	25	Red.	
Ca	422.7	Assez importante	2.5	Red.	Ajout de La pour obtenir une concentration de 1 mg La ml^{-1} dans la fiole finale
Cd	229	Faible 0.1[a]	1		
Co	240.7	—	2.5		
Cr	358	—	5	Red.	
Cu	325	Nulle	5		
Fe	248	Importante 0.5[a]	5		
Ga	287.4	Nulle	200		
K	766	—	1		Ajout d'un alcalin pour obtenir une concentration de 100 μg ml^{-1} de cet alcalin dans la fiole finale
Li	671	—	1		
Mg	285	Assez importante	1	Red.	idem Ca
Mn	280	Faible	2.5		
Mo	313.3	Importante	10	Red.	
Na	589	Faible	1		idem K
Ni	232	—	5		
Pb	217	—	5		Ajout d'EDTA (1 mg ml^{-1}) dans la solution vaporisée
Sb	217.6	Importante	50		
Sn	225	—	50	Red.	
Zn	213.8	Faible	2		

[a] Absorption du plutonium en μg ml^{-1} de l'élément à doser.

hydrique de plutonium purifiée, de concentration et d'acidité identiques à la solution à analyser, contenant des ajouts connus de solution étalon de l'élément à doser. Des ajouts peuvent aussi être effectués à une ou deux fractions de la solution à analyser de manière à vérifier l'absence d'éléments gênants.

L'absorption des solutions étalons ainsi préparées et l'absorption de la solution à analyser sont mesurées successivement par rapport à celle de la solution de plutonium purifiée sans retoucher au réglage des débits gazeux du brûleur.

DISCUSSION

On a examiné successivement l'influence des différents paramètres de la mesure d'absorption sur le résultat du dosage.

Influence des conditions de réglage du brûleur

Le réglage du débit d'air et acétylène ainsi que la hauteur du faisceau lumineux dans la flamme, sont deux paramètres de réglage importants. Le réglage optimum du débit d'air et d'acétylène pour un élément déterminé, est défini en mesurant l'absorption d'une solution contenant cet élément aux différents débits gazeux et en cherchant pour chaque valeur du débit gazeux la hauteur de flamme correspondant au maximum d'absorption. La Fig. 3 représente le faisceau de courbes obtenues dans ces conditions dans le cas d'une solution à 10 μg Cr ml^{-1} et 20 g Pu l^{-1}. Le réglage des débits gazeux

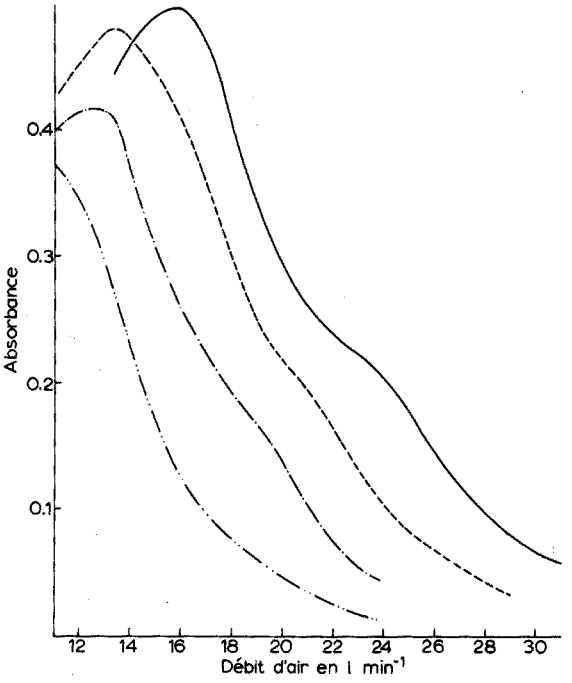

Fig. 3. Absorption du Cr 10 μg ml^{-1} dans une solution de plutonium à 20 g l^{-1} en fonction des débits gazeux. $\lambda = 3580$ Å, échelle 1, fente 3, atténuation 0, gain 5.5, alimentation lampe 20 mA. Débit d'acétylène fixé à: (——) 4.8 l min^{-1}; (– – –) 4.1 l min^{-1}; (–·–) 3.7 l min^{-1}; (–···–) 3.2 l min^{-1}.

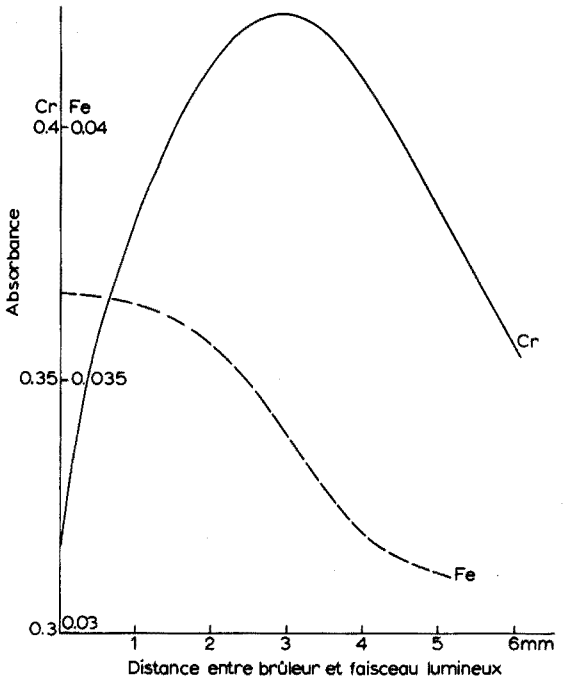

Fig. 4. Absorption en fonction de la zone de flamme. (——) Du chrome (10 μg ml^{-1}) dans une solution de plutonium à 20 g l^{-1}. $\lambda = 3580$ Å, échelle 1, fente 3, gain 5.5, atténuation 0, alimentation lampe 10 mA, débit d'air 14.6 l min^{-1}, débit d'acétylène 3.7 l min^{-1}. (– – –) Du fer (5 μg ml^{-1}) dans une solution de plutonium à 20 g l^{-1}. $\lambda = 2480$ Å, échelle 3, fente 3, gain 6, atténuation 2, alimentation lampe 20 mA, débit d'air 16 l min^{-1}, débit d'acétylène 3.7 l min^{-1}.

optimum étant ainsi défini, il faut connaître la hauteur optimum du faisceau lumineux dans la flamme. Cette mesure est effectuée de la façon suivante: le brûleur éteint, est remonté jusqu'à occulter une partie du faisceau lumineux issu de la lampe à cathode creuse; à ce moment, l'absorption est mesurée sur l'appareil, le brûleur est alors baissé lentement. La distance faisceau–brûleur sera considérée comme nulle dès que l'absorption sera nulle également. A ce moment le brûleur est allumé, le réglage des débits gazeux étant optimum, on mesure l'absorption d'une solution contenant l'élément considéré en baissant le brûleur lentement jusqu'à obtenir l'absorption maximum. La Fig. 4 représente la variation d'absorption d'une solution de chrome et de fer en fonction de la distance brûleur–faisceau lumineux.

L'expérience montre que la connaissance de ces paramètres est suffisamment précise pour ne pas avoir à les mesurer avant chaque dosage. Il faut toutefois les vérifier de temps en temps, surtout si les solutions utilisées sont corrosives et à chaque fois que l'on change le brûleur.

Influence des conditions de réglage du spectrophotomètre

Le paramètre dont l'influence est importante est essentiellement l'alimentation de la lampe à cathode creuse. Pour obtenir la meilleure sensibilité, on a intérêt à avoir le faisceau lumineux le plus intense possible donc le courant d'alimentation le plus

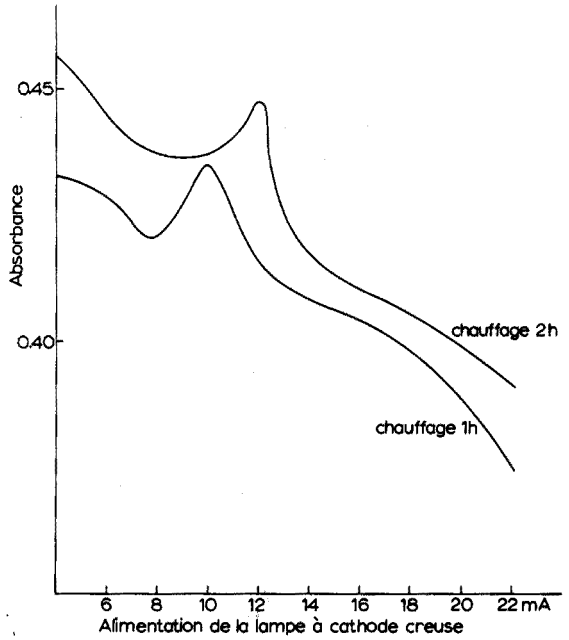

Fig. 5. Absorption du chrome (10 μg ml^{-1}) dans une solution de plutonium à 20 g l^{-1} en fonction de l'alimentation de la lampe à cathode creuse. $\lambda = 3850$ Å, échelle 1, fente 3, gain 5.5, atténuation 0, distance faisceau lumineux brûleur 3 mm, débit d'air 14.6 l min^{-1}, débit d'acétylène 3.7 l min^{-1}.

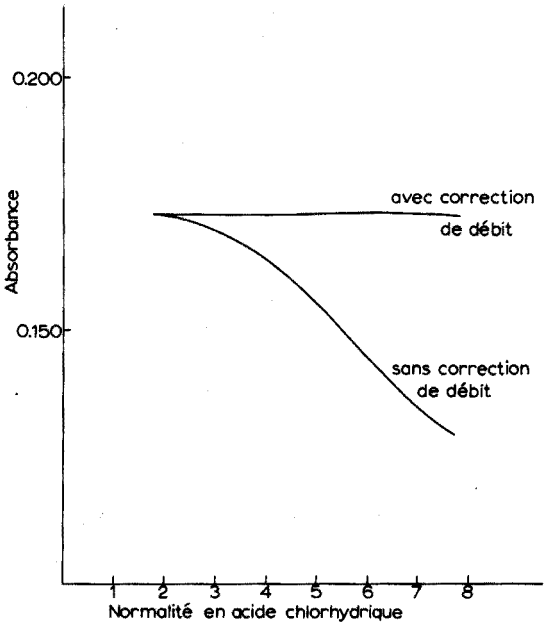

Fig. 6. Absorption du chrome (5 μg ml^{-1}) dans une solution de plutonium à 20 g l^{-1} en fonction de l'acidité (acide chlorhydrique). Alimentation lampe 10 mA, gain 6 et les autres paramètres de la Fig. 5.

élevé. Deux faits limitent ce courant: d'une part, le phénomène d'auto-absorption croît plus vite avec le courant que l'intensité lumineuse émise par la cathode creuse, d'autre part, le courant ne doit pas être trop élevé afin d'assurer aux cathodes creuses une durée de vie maximum. La Fig. 5 représente la variation d'absorption d'une solution de chrome en fonction de l'alimentation de la lampe. Cette Fig. met aussi en évidence l'importance du temps de chauffage de la lampe. Ce temps doit être le plus long possible, de manière à obtenir une meilleure stabilité du signal d'absorption.

D'autres facteurs de réglage du spectrophotomètre, tels que la largeur de fente, la finesse du réglage de la longueur d'onde, peuvent avoir une influence sur l'absorption de la solution à analyser. Dans la plupart des cas peu de moyens permettent d'intervenir sur ces paramètres.

Influence des paramètres physico-chimiques de la solution à analyser

Pour comparer l'absorption de la solution à analyser aux différentes solutions étalon, il faut que le débit des solutions injectées dans le brûleur soit le même pour toutes les solutions donc que la viscosité de ces solutions soit la même. Tous les facteurs intervenant sur la viscosité des solutions, doivent être surveillés (température, acidité, concentration en plutonium). Les Figs. 6 et 7 représentent les variations de l'absorption d'une solution de chrome en fonction de l'acidité de la solution et de la concentration en plutonium avec et sans correction du débit de la solution injectée dans le brûleur.

La valence du plutonium peut jouer un rôle important sur les mesures d'ab-

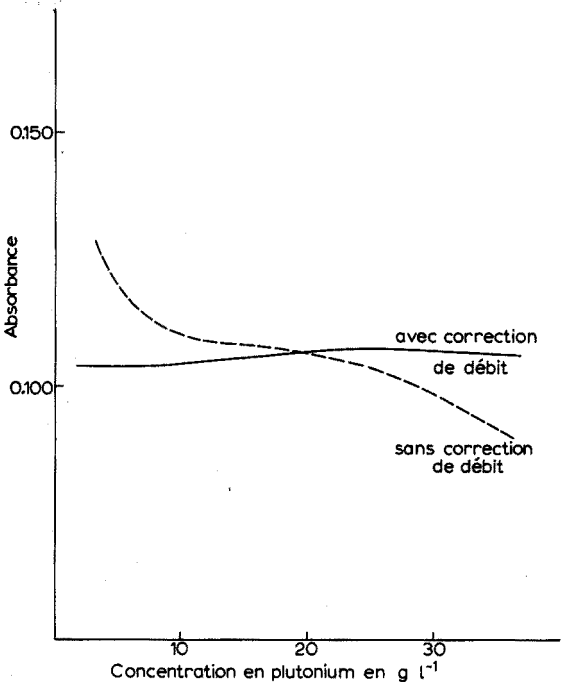

Fig. 7. Absorption du chrome (3 μg ml^{-1}) en fonction de la concentration en plutonium. Echelle 3, atténuation 2, autres paramètres comme en Fig. 6.

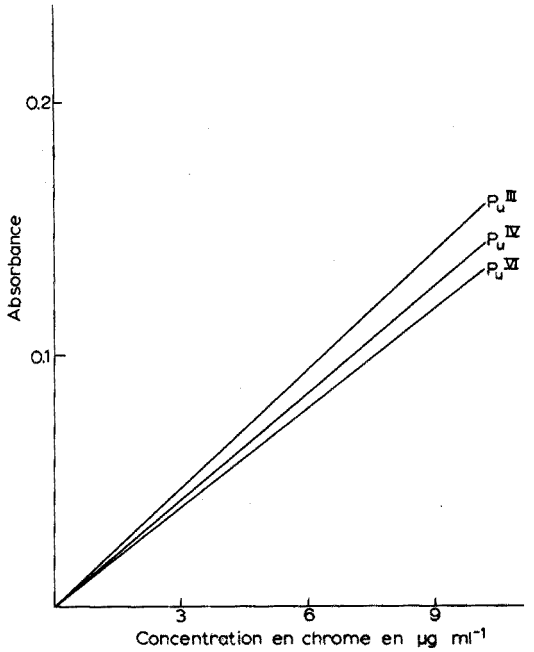

Fig. 8. Droites d'étalonnage du chrome suivant les valences du plutonium. Concentration: 20 g l^{-1}, en plutonium.

TABLEAU II

INTERFÉRENCES

(+ = Interférence positive; − = interférence négative; ○ = pas d'interférence)

Elément étranger / *Elément à doser*	*Ca*	*Cd*	*Cr*	*Cu*	*Fe*	*Ga*	*In*	*K*	*Li*	*Mg*	*Mn*	*Na*	*Ni*	*Pb*	*Sr*	*Zn*	F^-	SO_4^{2-}	ClO_4^-	NO_3^-
Ag	○	○	○	○	○	○	○	○	○	○	○	○	○	○	○	○	○	○	○	○
Au	○	○	○	○	○	○	○	○	○	○	○	○	○	○	○	○	○	○	○	○
Ca	×	○	○	○	○	○	○	○	○	○	○	○	○	○	+	○	−	○	○	○
Cd	○	×	○	○	○	○	○	○	○	○	○	○	○	○	○	○	○	○	○	+
Co	○	○	○	○	○	○	○	+	+	○	○	○	○	○	○	○	○	○	○	○
Cr	○	○	×	○	−	○	○	○	○	○	○	○	○	○	○	○	○	○	○	○
Cu	○	○	○	×	○	○	○	○	+	○	○	○	○	○	○	○	○	○	○	○
Fe	○	+	○	○	×	○	○	○	○	○	○	○	○	○	○	○	○	○	○	○
Ga	○	○	○	○	○	×	○	○	○	○	○	○	○	○	○	○	○	○	○	○
In	○	○	○	○	○	○	×	−	○	○	−	−	○	○	○	○	○	○	○	○
Mg	+	○	○	○	○	○	○	○	○	×	○	○	○	○	○	○	○	○	○	○
Mn	○	○	○	○	○	○	○	○	+	○	×	○	○	○	○	○	○	○	○	○
Ni	○	○	○	○	○	○	○	○	○	○	○	○	×	○	○	○	○	○	○	○
Sr	○	○	○	○	○	−	○	○	○	○	○	○	○	○	×	○	○	○	○	○
Zn	−	○	−	○	○	○	+	○	○	○	+	+	−	○	○	×	○	○	−	−
Mo	○	○	○	○	○	−	○	○	○	○	○	○	○	○	○	○	○	○	○	○

sorption des éléments dont le dosage nécessite une flamme réductrice. La Fig. 8 représente les différentes droites d'étalonnage du chrome obtenues en présence des trois valences stables du plutonium en solution. La valence du plutonium de la solution à analyser et celle des solutions étalons doivent être identiques pour l'analyse d'éléments en flamme très réductrice. Pour certains éléments on peut obtenir une absorption identique quelle que soit la valence du plutonium en modifiant les conditions de flamme (débit des gaz, hauteur du faisceau lumineux dans la flamme) suivant la valence du plutonium.

Etudes des interférences

D'une manière générale la présence du plutonium joue un rôle très favorable vis-à-vis des interférences.

Le Tableau II donne les résultats d'essais effectués sur des solutions dont la concentration de l'élément à doser correspond à une absorption de 0.300 en absorbance. Le rapport élément étranger/élément à doser est égal à 50 sauf pour le gallium où la concentration est de 2% par rapport au plutonium. La concentration des anions est de 10^{-4} *M*. Est considéré comme gênant tout élément qui modifie l'absorption de l'élément à doser de plus de 5%.

TABLEAU III

INTERFÉRENCES[a]

Elément étranger / *Elément à doser*	*Cd*	*Cr*	*Mn*	*Fe*	*Ni*	NO_3^-	F^-	PO_4^{3-}	SO_4^{2-}
Ca	1	1	1			×	×	×	×
Cr				5	5				
Fe	50	50							
Mg						×			
Mn						×			

[a] X, élément gênant pour une concentration 10^{-4} *M* ; valeurs chiffrées, rapport maximum élément étranger/élément à doser.

Pour une concentration en élément à doser 10 fois plus faible (absorption environ 0.030 en densité optique), d'autres éléments gênants apparaissent. Ces éléments sont signalés dans le Tableau III; la valeur du rapport: élément étranger/élément à doser est indiquée dans ce Tableau pour les cations. La concentration des anions est de 10^{-4} *M*. Dans ce Tableau est considéré comme gênant tout élément qui modifie l'absorption de l'élément à doser de plus de 10%.

On peut dans certains cas, éliminer l'effet gênant d'un élément en ajoutant cet élément aux solutions étalons à la même concentration que dans la solution à analyser.

L'analyse de traces dans le plutonium par absorption atomique est une méthode très rapide et précise[2], toutefois une étude détaillée des conditions du dosage doit être faite pour chaque élément à analyser.

RÉSUMÉ

On décrit une méthode d'analyse rapide de vingt et un éléments à l'état de

traces dans le plutonium sans séparation préalable. Une étude détaillée des différents facteurs jouant un rôle important en absorption atomique est réalisée.

SUMMARY

Atomic absorption spectrophotometry is applied for the rapid determination of 21 trace elements in plutonium without preliminary separation. A suitable arrangement to avoid atmospheric contamination is described. An extensive study of interferences has been made.

ZUSAMMENFASSUNG

Durch Atomabsorptionsspektrophotometrie ist die schnelle Bestimmung von 21 Spurenelementen in Plutonium ohne vorhergehende Abtrennung möglich. Es wird eine geeignete Anordnung zur Vermeidung atmosphärischer Kontamination beschrieben. Störungen wurden umfassend untersucht.

BIBLIOGRAPHIE

1 R. L. GRAFF ET H. R. MULLIN, *Xth Conference on Analytical Chemistry in Nuclear Technology*, Gatlinburg, Tenn., 1966.
2 M. GANIVET ET A. BENHAMOU, *Anal. Chim. Acta*, 47 (1969) 81.

Analytica Chimica Acta
Elsevier Publishing Company, Amsterdam
Printed in The Netherlands

SOME THEORETICAL OBSERVATIONS ON THE USE OF LESS-COMMON FLAMES IN ANALYTICAL ATOMIC SPECTROMETRY

J. E. CHESTER, R. M. DAGNALL AND M. R. G. TAYLOR
Department of Chemistry, Imperial College of Science and Technology, London, S.W.7 (England)
(Received 17th February 1970)

A digital computer technique based upon the minimisation of free energy has recently been used to study the flame gas compositions of the nitrous oxide–acetylene and air–acetylene flames[1]. The results followed closely the experimentally determined data and it was shown that the species most likely to be responsible for causing efficient atomisation of aluminium and silicon was atomic carbon, the CN radical or HCN. No conclusive evidence was available at that time, although it was believed that atomic carbon could be as important as the CN and HCN species. The work reported in this paper explores the characteristics of less-common flames, some of which cannot give rise to the CN and HCN species because of the preclusion of either nitrogen or carbon from the flame gas mixtures. In consequence further insight is gained concerning the atomisation properties of certain flames in analytical atomic spectrometry, and the advantages and disadvantages of some of the less-common flames are indicated.

The computer programme used in this study was the same as that previously described[1] for use with an IBM 7094 computer and a PUFFT compiler, and the results were calculated in a similar manner, *i.e.*, the concentrations were calculated in moles per mole of feed and those of the gaseous species in volume per cent. A variety of flame stoichiometries can be studied and the programme is capable of handling forty species at each of ten temperatures. The number of species can be increased, but there must be fewer condensed species than elements for solution of the equations. All flames in this study were evaluated with and without water and with the addition of certain "refractory type" elements at the 0.0001 g atom per mole of feed level. The amount of water used in the calculation was evaluated where possible from practical measurements taken with conventional analytical premixed flames. The limitations of the method employed have been discussed before[1].

THE OXYGEN–ACETYLENE FLAME

The stoichiometric flame reaction is:

$$\tfrac{3}{2}O_2 + C_2H_2 \rightarrow 2CO + H_2O$$

For the calculation the following equation was used:

$$\tfrac{3}{2}O_2 + x\,CH_2H_2 + 0.075\,H_2O + 0.0001\,Me \rightarrow \text{products}$$

where Me denotes an element. The value of x was varied from 1.0 to 2.0 in steps of 0.10,

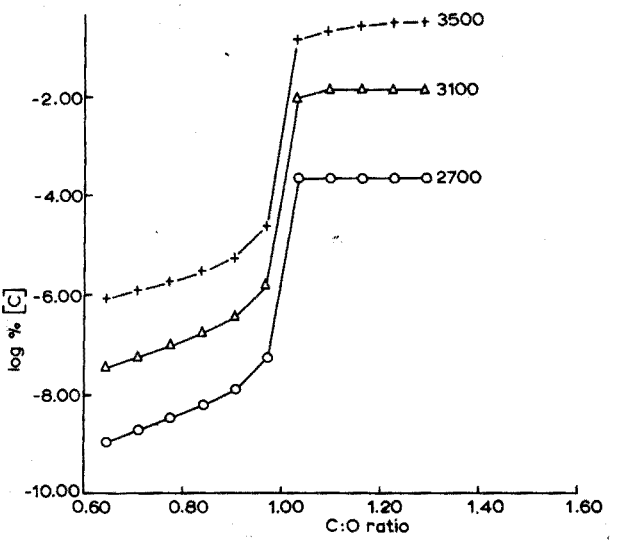

Fig. 1. Log (% concentration) C *vs.* C:O ratio for oxygen–acetylene flames; temperature in °K.

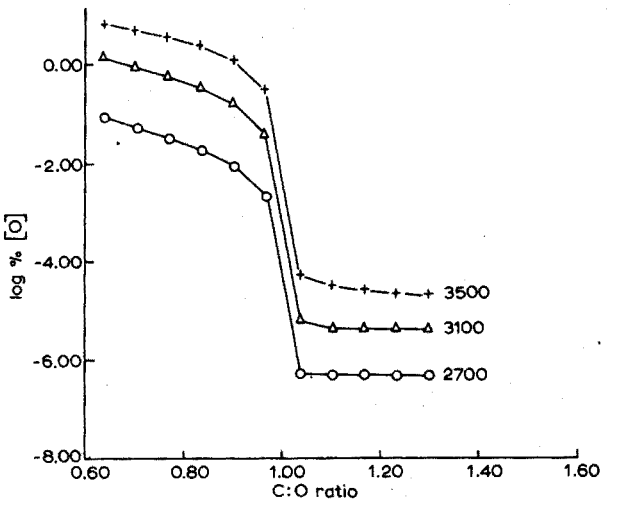

Fig. 2. Log (% concentration) O *vs.* C:O ratio for oxygen–acetylene flames; temperature in °K.

giving a range of flame stoichiometries. In the stoichiometric flame the ratio of C:O is 0.6504 and when the C:O ratio is unity the flame is 53.75% fuel rich.

The concentrations of the carbon-containing species present, particularly atomic carbon (Fig. 1), followed the same trends as their calculated concentrations in the nitrous oxide–acetylene and air–acetylene flames[1]. The CN and HCN species were absent in this instance because of the absence of nitrogen from the flame constituents (entrained air is not considered in the calculation). The concentration of atomic carbon increases rapidly at a C:O ratio of unity; above this ratio it is a maximum and approximately constant with excess of carbon being present as solid. The concentrations of the oxidising species such as atomic and molecular oxygen and the hydroxyl radical

TABLE I

CONCENTRATIONS OF THE MAJOR SPECIES IN OXYGEN–ACETYLENE FLAMES

Species	2700°K	3100°K	3500°K	2700°K	3100°K	3500°K
	Stoichiometric flame ($C:O = 0.6504$)			*Fuel-rich flame* ($C:O = 1.172$)		
CO	51.20	50.38	47.30	61.08	58.63	53.76
CO_2	12.81	9.72	4.25	$8.64 \cdot 10^{-5}$	$3.40 \cdot 10^{-5}$	$1.79 \cdot 10^{-5}$
C	$1.08 \cdot 10^{-9}$	$3.53 \cdot 10^{-8}$	$8.79 \cdot 10^{-7}$	$2.28 \cdot 10^{-4}$	$1.36 \cdot 10^{-2}$	$2.70 \cdot 10^{-1}$
H	2.00	7.04	17.78	3.32	11.11	24.48
H_2	12.45	11.09	9.15	34.64	27.55	17.36
H_2O	20.52	15.81	6.58	$3.23 \cdot 10^{-4}$	$1.18 \cdot 10^{-4}$	$4.62 \cdot 10^{-5}$
O	$8.68 \cdot 10^{-2}$	1.41	6.82	$4.90 \cdot 10^{-7}$	$4.23 \cdot 10^{-6}$	$2.53 \cdot 10^{-5}$
O_2	$5.86 \cdot 10^{-2}$	$8.06 \cdot 10^{-1}$	1.94	$1.87 \cdot 10^{-12}$	$7.30 \cdot 10^{-12}$	$2.67 \cdot 10^{-11}$
OH	$8.75 \cdot 10^{-1}$	3.75	6.16	$8.25 \cdot 10^{-6}$	$1.78 \cdot 10^{-5}$	$3.15 \cdot 10^{-5}$
Solid carbon[a]	0.0	0.0	0.0	11.9	6.66	0.0

[a] Moles per mole of feed; all other values in volume per cent.

are inversely related to the concentration of the carbon species and fall rapidly at a C:O ratio of unity to a minimum value (Fig. 2). The concentrations of the major species in the stoichiometric and fuel-rich flames are listed in Table I. The degrees of atomisation of aluminium and silicon exhibited a direct relationship with the concentrations of the reducing carbon-containing species and were inversely related to the concentrations of oxidising species (similarly to that reported in the nitrous oxide–acetylene flame[1]). The concentration of atomic hydrogen is appreciable, but it is considered unlikely to play a major role in these atomisation processes. The predominant aluminium species when the C:O ratio is less than unity at the lower temperature range studied (total range was 2600°K–3500°K) is solid aluminium oxide (Al_2O_3). This is in agreement with the results obtained in the air– and nitrous oxide–acetylene flames. In flames with a C:O ratio greater than unity the predominant aluminium species at all temperatures is atomic aluminium.

The main silicon species at all temperatures in flames with a C:O ratio less than unity and at the lower flame temperatures with a C:O ratio greater than unity is gaseous silicon monoxide (SiO). At higher temperatures in the latter flames, the principal silicon species is atomic silicon.

It was found that, at equivalent C:O ratios (greater than unity) and temperatures, the degree of atomisation of aluminium in the oxygen–acetylene flame is approximately equal to that in the nitrous oxide–acetylene flame, and that of silicon is somewhat greater in the oxygen–acetylene flame. Moreover, the concentrations of atomic carbon in the two flames (after correction of the carbon concentration in the nitrous oxide–acetylene flame to account for the extra 40% of nitrogen species) are approximately equal. These results would tend to indicate that a principal reducing species in acetylene flames is atomic carbon, because the CN and HCN species are absent from the oxygen–acetylene flame.

The oxygen–acetylene flame has been used[2–8] for the determination of many elements, including those subject to refractory oxide formation, by both thermal emission and atomic absorption spectrometry. Substantial enhancement in both atomic line emission and the absorption of many elements has been observed in the

expanded interconal zone formed in the fuel-rich premixed flame.

In view of the high burning velocity of the oxygen–acetylene flame, it is desirable to burn only very fuel-rich mixtures in order to avoid explosive flashbacks. Cowley *et al.*[7] have used a flame mixture of 0.80 moles oxygen and 1.00 moles acetylene; however, the use of such fuel-rich mixtures is associated with a considerable reduction in the flame temperature from the maximum theoretical value of 3383°K[9]. This flame has a carbon:oxygen ratio of 1.25, although the ethanolic solutions of the analyte elements which were nebulised in these studies increased this ratio somewhat. This flame is not strictly comparable with the "ideal" oxygen–acetylene flame because air entrainment, which occurs at the base of the premixing tube, introduces nitrogen into the gas mixture before combustion. Up to 25% of the total premixed gas is in consequence nitrogen and for this reason nitrogen-containing species, particularly the CN radical, are observed in such flames. More recently, Fiorino *et al.*[8] have used a long-path burner which is capable of supporting a premixed oxygen–acetylene flame without such a high degree of air entrainment. The use of this flame in atomic absorption spectrometry was compared by these workers with the nitrous oxide–acetylene flame supported on the same burner.

The experimental evidence of Cowley *et al.*[7] points to a very low free-oxygen content in the flame gases leaving the primary reaction zone of the fuel-rich flame. The computer calculations of low concentrations of oxidising species in the interconal region of the fuel-rich oxygen–acetylene flame are hence in good agreement with experimental observation. The calculations are in good agreement also with the experimental results obtained by Fiorino *et al.*[8]. They determined some fourteen elements, and, in most instances, the oxygen–acetylene flame gave limits of detection comparable to those obtained in the nitrous oxide–acetylene flame. For seven elements the oxygen–acetylene flame was found to give lower detection limits. Fiorino *et al.*[8] also found that the absorbance for strong monoxide-forming elements depended on the fuel to oxidant ratio. These workers noted, however, that the nitrous oxide–acetylene flame was easier to operate. Its substantially lower burning velocity allows greater flexibility with respect to mixture composition and total gas flow. They suggested that the oxygen–acetylene flame be used only when there is substantial background emission from the nitrous oxide–acetylene flame causing a noisy signal.

In practice, air is entrained into all types of flames, unless they are mechanically or gas sheathed, and hence some CN and HCN must be produced even in a premixed oxygen–acetylene flame. However, the interconal regions of premixed flames are not influenced greatly by such entrainment and it is concluded therefore that atomic carbon may play a major role in the atomisation processes of aluminium and silicon.

THE NITROUS OXIDE–HYDROGEN FLAME

A brief summary of calculations involving the analytical utility of this flame has been reported previously[10]. It was shown then that the concentration of atomic and molecular oxygen was considerably greater in the nitrous oxide–hydrogen flame than in the nitrous oxide–acetylene flame and that the atomisation of aluminium and silicon was considerably lower in the former flame under all conditions.

The stoichiometric flame reaction is:

$$N_2O + H_2 \rightarrow N_2 + H_2O\,.$$

TABLE II

CONCENTRATIONS OF MAJOR SPECIES IN NITROUS OXIDE–HYDROGEN FLAMES

Species[a]	2400°K	2800°K	3200°K	2400°K	2800°K	3200°K
	Stoichiometric flame ($H:O=2$)			*Fuel-rich flame* ($H:O=4$)		
H	$2.29\cdot10^{-1}$	2.04	9.35	$8.97\cdot10^{-1}$	4.49	14.54
H_2	2.10	6.26	11.16	32.13	30.41	27.01
H_2O	48.03	39.28	23.30	34.30	31.86	22.53
O	$7.10\cdot10^{-2}$	$7.42\cdot10^{-1}$	3.82	$3.31\cdot10^{-3}$	$1.24\cdot10^{-1}$	1.52
O_2	$6.80\cdot10^{-1}$	1.90	3.19	$1.48\cdot10^{-3}$	$5.31\cdot10^{-2}$	$5.10\cdot10^{-1}$
OH	1.00	3.74	7.81	$1.83\cdot10^{-1}$	1.37	4.85
N_2	47.61	45.15	39.64	32.47	31.56	28.43
NH	$6.81\cdot10^{-6}$	$1.23\cdot10^{-4}$	$9.13\cdot10^{-4}$	$2.20\cdot10^{-5}$	$2.27\cdot10^{-4}$	$1.20\cdot10^{-3}$
NO	$2.81\cdot10^{-1}$	$8.74\cdot10^{-1}$	1.72	$1.08\cdot10^{-2}$	$1.22\cdot10^{-1}$	$5.82\cdot10^{-1}$

All values in volume per cent.

For the calculation, the following equation was used:

$$N_2O + xH_2 + 0.0625\ H_2O + 0.0001\ Me \rightarrow \text{products}.$$

The value of x was varied from 1.0 to 2.0 in steps of 0.10 as before.

In the acetylene flames previously described it was found that there was a sharp increase in the degrees of atomisation of aluminium and silicon at a flame composition corresponding to a C:O ratio of unity. At this composition there was also an increase in the concentrations of the carbon-containing species such as atomic carbon, CN and HCN and a decrease in the concentrations of atomic oxygen and hydroxyl species. The concentration of atomic hydrogen, however, exhibited a linear dependence on the C:O ratio. In the nitrous oxide–hydrogen flame the highly reducing carbon species are all absent unless an organic solvent is nebulised into the flame and, even then, the C:O ratio is small and never approaches unity. This is apparent from consideration of flame reactions of the type:

$$N_2O + H_2 + 0.1\ C_6H_6 \rightarrow \text{products}.$$

The figure of 0.1 mole of solvent per mole of nitrous oxide was calculated from practical organic solvent uptake rates. Benzene was selected in this study because it contains no oxygen and therefore gives a high C:O ratio. In this instance a value of 0.6 is obtained which is insufficient to effect substantial atomisation of refractory type elements.

From consideration of the flame reaction it is apparent that the hydrogen analogue to the C:O ratio, namely the H_2:O ratio, is already unity in the stoichiometric flame, even when water is nebulised because the ratio of H_2:O in water is of course unity. Hence the only effect produced by the addition of water to the flame is to cause slight cooling because water does not make the flame more fuel-lean as with the acetylene-containing flames. It would therefore be expected that there should be no sharp increase in the degrees of atomisation of elements introduced, but that they should exhibit an approximately linear dependence on the H_2:O ratio. This was, in fact, found to be the situation.

Similarly, and as expected, the concentrations of atomic hydrogen (which must

be regarded as the principal reducing species) exhibit a direct, almost linear dependence on the H_2:O ratio. The concentrations of the oxidising species, atomic and molecular oxygen and hydroxyl, exhibit an inverse, approximately linear dependence on the H_2:O ratio. The concentrations of the major species in the stoichiometric and fuel-rich nitrous oxide–hydrogen flames are shown in Table II.

From these results it may be assumed that the high-temperature, low-background nitrous oxide–hydrogen flame is somewhat oxidising in nature owing to the high concentrations of the oxidising species in even the fuel-rich flame. It would seem, therefore, that any atomisation of refractory oxide-forming elements which may occur is caused principally by thermal dissociation of the oxide species rather than by chemical reduction associated with acetylene-containing flames. Some chemical reduction must take place because the degrees of atomisation of the elements studied were greater in the cooler, fuel-rich flames, although the differences were by no means as marked as in the acetylene-containing flames studied previously.

THE OXYGEN–CYANOGEN FLAME

The high-temperature oxygen–cyanogen flame has been used for the atomic absorption[11] and thermal emission[12] spectrometric determination of several elements. Emission was observed for many elements including aluminium[12], but Robinson[11] observed no atomic absorption of aluminium and noticed improvements in sensitivity, compared with the oxygen–hydrogen flame, for only vanadium and platinum.

The maximum theoretical temperature of the stoichiometric flame has been calculated by Gaydon and Wolfhard[13] to be 4853°K which is in agreement with experimentally determined temperatures.

The stoichiometric flame reaction in this instance is:

$$C_2N_2 + O_2 \rightarrow 2\,CO + N_2$$

and the equation used in the calculation was:

$$C_2N_2 + xO_2 + 0.05\,H_2O + 0.0001\,Me \rightarrow \text{products}\,.$$

The value of x was varied from 0.5 to 1.5 in steps of 0.10 to give a range of flame stoichiometries.

The flame composition is altered considerably by the introduction of water because there is substantial cooling and several important hydrogen-containing species, *e.g.* H, H_2, HCN, OH, H_2O are absent in the water-free flame. The effect of the addition of water on the composition of the stoichiometric flame is shown in Tables III and IV. The C:O ratio in the stoichiometric flame is 0.9756; when this ratio is unity the flame is about 2.5% fuel rich.

The concentrations of atomic carbon and the CN species follow identical trends to those associated with the other acetylene flames studied. In the case of the CN species, there is an increase in concentration of two orders of magnitude at a C:O ratio of unity. Identical trends are followed in the flames studied with and without the addition of water, although the concentrations of the carbon species are higher in the flames without water because these flames contain less oxygen. At C:O ratios greater than unity the concentration of CN decreases with rise in temperature; other carbon-containing species decrease similarly except for atomic carbon which

TABLE III

CONCENTRATIONS OF THE MAJOR SPECIES IN THE STOICHIOMETRIC OXYGEN–CYANOGEN FLAME

Species[a]	4100°K	4500°K	4900°K
CO	66.40	65.87	64.58
CO_2	$8.64 \cdot 10^{-3}$	$6.52 \cdot 10^{-3}$	$5.23 \cdot 10^{-3}$
C	$1.52 \cdot 10^{-2}$	$8.94 \cdot 10^{-2}$	$3.82 \cdot 10^{-1}$
C_2	$3.42 \cdot 10^{-5}$	$2.42 \cdot 10^{-4}$	$1.16 \cdot 10^{-3}$
CN	$1.47 \cdot 10^{-1}$	$3.59 \cdot 10^{-1}$	$7.30 \cdot 10^{-1}$
O	$1.39 \cdot 10^{-1}$	$4.15 \cdot 10^{-1}$	1.06
O_2	$6.09 \cdot 10^{-5}$	$1.41 \cdot 10^{-4}$	$2.99 \cdot 10^{-4}$
N	$1.45 \cdot 10^{-1}$	$5.12 \cdot 10^{-1}$	1.46
N_2	33.13	32.72	31.73
NO	$1.43 \cdot 10^{-2}$	$2.73 \cdot 10^{-2}$	$4.73 \cdot 10^{-2}$

[a] All values in volume per cent.

TABLE IV

CONCENTRATIONS OF THE MAJOR SPECIES IN THE STOICHIOMETRIC OXYGEN–CYANOGEN FLAME WITH THE ADDITION OF WATER

Species[a]	4100°K	4500°K	4900°K
CO	63.48	63.31	62.27
CO_2	$8.04 \cdot 10^{-2}$	$2.35 \cdot 10^{-2}$	$9.61 \cdot 10^{-3}$
C	$1.49 \cdot 10^{-3}$	$2.28 \cdot 10^{-2}$	$1.93 \cdot 10^{-1}$
C_2	$3.30 \cdot 10^{-7}$	$1.59 \cdot 10^{-5}$	$2.98 \cdot 10^{-4}$
CN	$1.41 \cdot 10^{-2}$	$8.97 \cdot 10^{-2}$	$3.62 \cdot 10^{-1}$
H	3.12	3.14	3.13
H_2	$2.72 \cdot 10^{-2}$	$8.33 \cdot 10^{-3}$	$3.01 \cdot 10^{-3}$
H_2O	$2.96 \cdot 10^{-4}$	$2.74 \cdot 10^{-5}$	$4.17 \cdot 10^{-6}$
HCN	$1.32 \cdot 10^{-4}$	$2.48 \cdot 10^{-4}$	$3.53 \cdot 10^{-4}$
O	1.35	1.56	2.02
O_2	$5.76 \cdot 10^{-3}$	$2.00 \cdot 10^{-3}$	$1.09 \cdot 10^{-3}$
OH	$2.16 \cdot 10^{-2}$	$7.68 \cdot 10^{-3}$	$3.65 \cdot 10^{-3}$
N	$1.42 \cdot 10^{-1}$	$5.01 \cdot 10^{-1}$	1.43
N_2	31.64	31.33	30.48
NO	$1.36 \cdot 10^{-1}$	$1.00 \cdot 10^{-1}$	$8.84 \cdot 10^{-2}$

[a] All values in volume per cent.

increases with rise in temperature. A possible explanation for this is that no solid carbon can be formed in this instance because the temperature is too high and the molecular carbon-containing species tend to dissociate. Thus, the concentration of atomic carbon (which cannot dissociate) will tend to rise with increasing temperature.

The concentrations of atomic oxygen and hydroxyl also exhibit a similar behaviour to that observed in the other acetylene flames studied. However, the concentration of hydroxyl is considerably smaller in this flame because hydrogen is only available from nebulised water. The concentrations of molecular oxygen and hydroxyl decrease with increase in temperature at C:O ratios less than unity, but they

increase with increase in temperature when the C:O ratio exceeds unity. The concentration of atomic oxygen is directly related to temperature throughout, which is presumably due to the variations in the concentrations of carbon species with temperature described above.

The degree of atomisation of silicon is again markedly dependent on the flame composition and silicon was observed to be completely atomised at all temperatures studied (4000°K–4900°K) when the C:O ratio exceeds unity. Until this ratio is attained the principal silicon species is gaseous silicon monoxide (SiO). This is further evidence for atomisation by chemical reduction rather than thermal dissociation in flames with carbon-containing fuels because even a temperature of 4900°K is insufficient to atomise silicon completely until the C:O ratio exceeds unity.

As would be expected from consideration of the results obtained in the other carbon-containing flames, the principal aluminium species at all temperatures is atomic aluminium. No data are available for condensed Al_2O_3 over the temperature range considered, but this species may be safely omitted because it does not appear at temperatures above its melting point (2700°K) in the acetylene flames studied. Aluminium is atomised to an extent of about 70% at the lowest temperature studied (4000°K) in the most fuel-lean flame (C:O = 0.4878). At a C:O ratio greater than unity, it is atomised to an extent of about 99.9% even at 4000°K. The other aluminium species present to any extent are AlO, AlOH and AlH in the fuel-lean flames and only AlH in the fuel-rich flames.

The oxygen–cyanogen flame has the highest temperature of the various flames that have found use in analytical flame spectroscopy. However, a temperature of 5200°K has been reported[14] for the ozone–cyanogen flame according to the reaction:

$$3\,C_2N_2 + 2\,O_3 \rightarrow 6\,CO + 3\,N_2$$

Very high temperatures may also be obtained by combustion of the nitrile of acetylene dicarboxylic acid (C_4N_2) with oxygen or ozone. The heat of formation of cyanogen is 73.6 kcal mole^{-1} (gaseous state at 298°K) and that of carbon subnitride (C_4N_2) under the same conditions is 149.8 kcal mole^{-1}, and this presumably accounts for the increase in temperature.

The stoichiometric oxygen flame reaction is:

$$C_4N_2 + 2\,O_2 \rightarrow 4\,CO + N_2$$

and the flame has a reported temperature of 5261°K[15].

The stoichiometric ozone flame reaction is:

$$C_4N_2 + \tfrac{4}{3}\,O_3 \rightarrow 4\,CO + N_2$$

and the reported flame temperature is 5516°K. The latter flame has not been used in flame emission studies because the gas mixture tends to decompose explosively to form nitrogen and carbon powder.

MISCELLANEOUS HYDROCARBON FLAMES

Other flames of interest were studied, but they do not merit extensive discussion because the same trends were observed as in those previously described. This is to be expected because the computer is clearly unable to distinguish between flame types,

TABLE V

CONCENTRATIONS OF THE MAJOR SPECIES IN NITROUS OXIDE–PROPANE FLAMES

Species	2400°K	2700°K	3000°K	2400°K	2700°K	3000°K
	Stoichiometric flame			*Fuel-rich flame*		
CO	29.09	28.75	27.92	27.87	27.48	26.59
CO_2	$2.09 \cdot 10^{-1}$	$1.86 \cdot 10^{-1}$	$1.66 \cdot 10^{-1}$	$4.20 \cdot 10^{-5}$	$2.41 \cdot 10^{-5}$	$2.10 \cdot 10^{-5}$
C	$9.43 \cdot 10^{-10}$	$2.34 \cdot 10^{-8}$	$3.05 \cdot 10^{-2}$	$4.29 \cdot 10^{-6}$	$1.65 \cdot 10^{-4}$	$2.19 \cdot 10^{-3}$
CN	$9.78 \cdot 10^{-6}$	$3.64 \cdot 10^{-5}$	$1.03 \cdot 10^{-4}$	$4.11 \cdot 10^{-2}$	$2.34 \cdot 10^{-1}$	$6.71 \cdot 10^{-1}$
H	$9.86 \cdot 10^{-1}$	3.44	9.06	1.04	3.60	9.50
H_2	38.79	37.07	33.19	43.26	40.62	36.52
H_2O	1.62	1.58	1.42	$3.78 \cdot 10^{-4}$	$2.34 \cdot 10^{-4}$	$2.08 \cdot 10^{-4}$
HCN	$5.49 \cdot 10^{-4}$	$5.11 \cdot 10^{-4}$	$4.61 \cdot 10^{-4}$	2.44	3.44	3.15
O	$1.29 \cdot 10^{-4}$	$2.24 \cdot 10^{-3}$	$2.18 \cdot 10^{-2}$	$2.71 \cdot 10^{-8}$	$3.04 \cdot 10^{-7}$	$2.90 \cdot 10^{-6}$
O_2	$2.25 \cdot 10^{-6}$	$3.92 \cdot 10^{-5}$	$3.77 \cdot 10^{-4}$	$9.94 \cdot 10^{-14}$	$7.19 \cdot 10^{-13}$	$6.65 \cdot 10^{-12}$
OH	$7.83 \cdot 10^{-3}$	$3.90 \cdot 10^{-2}$	$1.34 \cdot 10^{-1}$	$1.74 \cdot 10^{-6}$	$5.53 \cdot 10^{-6}$	$1.86 \cdot 10^{-5}$
N_2	29.30	28.93	28.08	24.99	24.03	23.12
NO	$4.02 \cdot 10^{-4}$	$2.76 \cdot 10^{-3}$	$1.26 \cdot 10^{-2}$	$7.80 \cdot 10^{-8}$	$3.40 \cdot 10^{-7}$	$1.51 \cdot 10^{-6}$
Solid C[a]	0.0	0.0	0.0	$4.48 \cdot 10^{-2}$	0.0	0.0
%Al	12.47	87.18	91.06	82.80	94.23	96.25
%Si	$2.02 \cdot 10^{-3}$	$1.05 \cdot 10^{-2}$	$3.99 \cdot 10^{-2}$	8.75	43.67	75.02

[a] Moles per mole of feed; all other values in volume per cent.

and merely distributes the available carbon, hydrogen, oxygen and nitrogen to the species considered to give the composition corresponding to minimum free energy. The only major variable therefore is flame temperature.

Nitric oxide–acetylene

This flame was used by Manning[16] for the determination of aluminium by atomic absorption spectrometry and yielded absorbances some 60% higher than the nitrous oxide–acetylene flame. This is presumably due to its higher temperature (*ca.* 3353°K) and low burning velocity (*ca.* 87 cm sec^{-1}).

The stoichiometric flame reaction used for calculation was:

$$2\,NO + C_2H_2(+0.1250\,H_2O) \rightarrow 2\,CO + N_2 + H_2\,.$$

The flame gas composition is very similar to that of the nitrous oxide–acetylene flame, the principal difference being the smaller proportion of nitrogen present.

Nitrous oxide–propane

The stoichiometric flame reaction considered was:

$$3\,N_2O + C_3H_8(+0.1875\,H_2O) \rightarrow 3\,CO + 3\,N_2 + 4\,H_2\,.$$

The red CN emission which is characteristic of the nitrous oxide–acetylene flame is not observed to any such extent in the corresponding propane flame. This may be explained by the fact that the concentration of CN increases with rise in temperature. The temperature of this flame is lower than that of the nitrous oxide–acetylene flame, hence the CN concentration is lower. The lower temperature also results in a decrease in emission. The composition of the nitrous oxide–propane flame and the

degrees of atomisation of aluminium and silicon are listed in Table V.

Air–propane

As in previous studies air was considered to be a mixture of nitrogen and oxygen in the ratio 4:1 by volume (carbon dioxide and other gases were neglected). The flame reaction considered was:

$$C_3H_8 + 5\ O_2 + 20\ N_2 (+ 1.25\ H_2O) \rightarrow 3\ CO_2 + 4\ H_2O + 20\ N_2$$

for which the maximum theoretical temperature is 2198°K. The practical stoichiometric flame has a C:O ratio less than 0.3 (it equals 0.3 in the absence of water) and is therefore rather oxidising in nature. A C:O ratio of unity is achieved only when the flame is some 275% fuel-rich. It is unlikely that such a flame could be supported on conventional burners and, if it were, then its temperature would be extremely low. Its low temperature and oxidising nature make it clearly unsuitable for the flame spectroscopic determination of any but the most easily atomised elements.

CONCLUSIONS

The calculations carried out in this and previous studies have shown that the main requirements for a flame which efficiently atomises elements which form refractory oxides are a high temperature and a carbon-containing fuel such that the ratio of carbon to oxygen is greater than unity. Both the nitrous oxide–acetylene and the oxygen–acetylene flames are capable of fulfilling to some degree these requirements. The nitrous oxide–acetylene flame achieves a carbon: oxygen ratio in excess of unity in a flame that is less than 10% fuel rich; under these conditions there is only a small drop in temperature from that in the stoichiometric flame. However, for the oxygen–acetylene flame it is necessary to achieve a flame more than 50% fuel rich to give a carbon: oxygen ratio greater than unity; a large decrease in flame temperature occurs in such flames. Thus, although the temperature of the stoichiometric nitrous oxide–acetylene flame is lower than that of the stoichiometric oxygen–acetylene flame, the nitrous oxide–acetylene flame with a carbon:oxygen ratio greater than unity is probably at a higher thermal temperature than an oxygen–acetylene flame of the same carbon: oxygen ratio. Moreover, the nitrous oxide–acetylene flame has a considerably lower burning velocity than the oxygen–acetylene flame (180 cm sec^{-1} against 2,480 cm sec^{-1}) and is therefore less likely to cause explosive flashbacks. For these reasons the nitrous oxide–acetylene flame is recommended for general use in analytical atomic spectrometry.

The nitrous oxide–hydrogen flame is shown to be an inefficient means of atomisation for refractory elements, and this appears to be due to the lack of the carbon-containing species which are present in the acetylene flames. Which of these species is principally responsible for chemical reduction cannot be determined unequivocally, but the high degrees of atomisation of aluminium and silicon in the fuel-rich oxygen–acetylene flames would tend to suggest that atomic carbon is the main species (CN and HCN are absent in such flames). This could perhaps be confirmed if it were possible to compare the capabilities of the nitrogen–oxygen–acetylene and argon–oxygen–acetylene flames.

Although the nitrous oxide–acetylene flame appears to be the most useful,

even this flame only gives very low degrees of atomisation for some elements, *e.g.* rare earth elements, boron, etc., such that the determination of these elements by atomic absorption spectrometry is either not possible, or at least, very poor. Unfortunately, combinations of nitrous oxide and air (or oxygen) with various fuel gases (or mixtures) will not give rise to a flame which is likely to be more generally useful than the nitrous oxide–acetylene flame. One possible method of increasing the thermal temperature, and hence the degree of atomisation, appears to be via electrical augmentation of the fuel-rich nitrous oxide–acetylene flame.

SUMMARY

The method of minimisation of free energy is used to calculate the flame gas composition and atomisation efficiency of a variety of flames, *viz.* oxygen–acetylene, oxygen–cyanogen, nitrous oxide–hydrogen, nitric oxide–acetylene, nitrous oxide–propane and air–propane. The results are compared with those obtained in the nitrous oxide–acetylene flame; atomic carbon appears to play a major role in the atomisation of aluminium and silicon in the oxygen–acetylene flame. For general analytical atomic spectroscopic purposes, however, the nitrous oxide–acetylene flame is most suitable.

RÉSUMÉ

La méthode de minimisation d'énergie libre est utilisée pour calculer la composition de la flamme et le rendement d'atomisation de diverses flammes: oxygène–acétylène, oxygène–cyanogène, oxyde nitreux–hydrogène, oxyde nitrique–acétylène, oxyde nitreux–propane et air–propane. Les résultats sont comparés avec ceux obtenus dans une flamme oxyde nitreux–acétylène.

ZUSAMMENFASSUNG

Die Methode der weitestgehenden Verringerung der freien Energie wird auf die Berechnung der Flammengaszusammensetzung und Atomisierungswirksamkeit einer Anzahl von Flammen nämlich Sauerstoff–Acetylen, Sauerstoff–Cyan, Lachgas–Wasserstoff, Stickstoffmonoxid–Acetylen, Lachgas–Propan und Luft–Propan angewendet. Die Ergebnisse werden mit jenen von Lachgas–Acetylen-Flammen verglichen; bei der Atomisierung von Aluminium und Silicium in der Sauerstoff–Acetylen-Flamme scheint atomarer Kohlenstoff eine grössere Rolle zu spielen. Für allgemeine Zwecke der analytischen Atomspektroskopie eignet sich jedoch die Lachgas–Acetylen-Flamme am besten.

REFERENCES

1 J. E. Chester, R. M. Dagnall and M. R. G. Taylor, *Anal. Chim. Acta*, 51 (1970) 95.
2 V. A. Fassel and D. W. Golightly, *Anal. Chem.*, 39 (1967) 466.
3 R. N. Kniseley, A. P. D'Silva and V. A. Fassel, *Anal. Chem.*, 35 (1963) 910.
4 A. P. D'Silva, R. N. Kniseley and V. A. Fassel, *Anal. Chem.*, 36 (1964) 1287.
5 W. Slavin and D. C. Manning, *Anal. Chem.*, 35 (1963) 253.
6 V. A. Fassel, R. B. Myers and R. N. Kniseley, *Spectrochim. Acta*, 19 (1963) 1187.

7 T. G. COWLEY, V. A. FASSEL AND R. N. KNISELEY, *Spectrochim. Acta*, 23B (1968) 771.
8 J. A. FIORINO, R. N. KNISELEY AND V. A. FASSEL, *Spectrochim. Acta*, 23B (1968) 413.
9 R. MAVRODINEANU AND H. BOITEUX, *L'Analyse Spectral Quantitative par la Flamme*, Masson, Paris, 1964.
10 J. E. CHESTER, R. M. DAGNALL AND M. R. G. TAYLOR, *Analyst*, 95 (1970) 702.
11 J. W. ROBINSON, *Anal. Chem.*, 33 (1961) 1067.
12 B. L. VALLEE AND A. E. BARTHOLOMAY, *Anal. Chem.*, 28 (1956) 1753.
13 A. G. GAYDON AND H. G. WOLFHARD, *Flames*, Chapman and Hall, London, 1960.
14 A. G. STRANG AND A. V. GROSSE, *J. Amer. Chem. Soc.*, 79 (1957) 5583.
15 A. D. KIRSCHENBAUM AND A. V. GROSSE, *J. Amer. Chem. Soc.*, 78 (1956) 2020.
16 D. C. MANNING, *At. Absorption Newslett.*, 4 (1965) 267.

Analytica Chimica Acta
Elsevier Publishing Company, Amsterdam
Printed in The Netherlands

THE DETERMINATION OF ANTIMONY IN GEOLOGICAL MATERIALS BY ATOMIC ABSORPTION SPECTROPHOTOMETRY, WITH PARTICULAR REFERENCE TO SOILS

D. J. NICOLAS*
The Corner House Laboratories (1968) (Pty) Limited, P.O. Box 1169, Johannesburg (South Africa)
(Received 4th January 1971)

Most methods currently in use for the determination of antimony in geological materials are too time-consuming and often involve the use of large quantities of reagents. Many are often inaccurate owing to the presence of interfering substances which occur in complex geological samples. Solvent extraction, which is laborious for routine analysis of large numbers of samples, is often used to remove interferences and increase sensitivity. Decomposition of different sample types varies tremendously, as a method must take into account the volatility of the chlorides and bromides and the hydrolytic tendencies of antimony. Owing to the increased interest in prospecting for antimony, there is a current demand for a rapid sensitive technique which permits good accuracy with high precision, the latter being extremely important for the statistical treatment of geochemical data.

For over 50 years antimony in ores has been determined by fusion with alkali carbonate or hydroxide, or digestion with concentrated sulphuric acid, usually followed by sulphide separation and iodimetric determination. Jankovsky[1] has determined antimony in ores by a sulphur–potassium carbonate fusion followed by solvent extraction and iodimetric determination. These methods are slow and large amounts of reagents are required, but a carbonate fusion is recommended for high-grade sulphide ores. Sodium carbonate fusions are not to be recommended for the analysis of antimony in soils, as losses can occur owing to the relatively high temperature at which fusion occurs. It is generally not known in what form the antimony exists and antimony readily volatilizes if present in organometallic form and also in inorganic forms such as antimony trichloride. Stanton and McDonald[2,3] determined antimony in soil and sediment samples by fusion with ammonium chloride and dissolution with hydrochloric acid; the antimony–brilliant green complex was extracted with toluene and the colour compared with standards. In this laboratory, ammonium chloride fusion has given low recoveries in analyzing soils, and the method could only handle 80 samples per 8-h man-day.

Very little work has been published on the determination of antimony by atomic absorption methods, which are generally rapid and reasonably free from interferences. Antimony in alloys has been determined by Mostyn and Cunningham[4]. Yanagisawa *et al.*[5] and Walker *et al.*[6] have used solvent extraction and atomic absorption for the analysis of metallurgical products. Atomic absorption analysis has

* Now at 3 Lisburn Avenue, Auckland 5, New Zealand.

been used in various South African laboratories for the determination of antimony in geochemical prospecting samples after treatment of the sample with acids, *e.g.* perchloric–nitric and mixtures, other base metals being determined on the same solution. Generally only instrumental parameters have been reported and information concerning the accuracy and precision of such methods is lacking. The author has found low recoveries for the determination of antimony in soils by such methods.

Solvent extraction–atomic absorption methods with ammonium pyrollidine-dithiocarbamate (APDC) as a general complexing agent have been described by Mulford[7]. St John[8] is currently investigating the use of APDC/MIBK systems followed by atomic absorption for the analysis of antimony in carbonate rocks and in waters.

The most efficient method for extracting antimony in the range 0–5% from many types of geological samples and suitable for rapid atomic absorption measurement was sought. An ammonium iodide fusion followed by dissolution of the quantitatively volatilised antimony iodide in 2 *M* hydrochloric acid proved to be fast, simple and reproducible.

EXPERIMENTAL

Instrumentation

The instrumental conditions used for the determination of antimony with a Varian-Techtron Model 1000 atomic absorption spectrophotometer are shown in Table I. The unit was fitted with an air–acetylene 10-cm burner and a standard nebulizer operating at 15 p.s.i. The liquid uptake rate was 4 ml min^{-1}. Two spectral lines 217.58 nm and 231.18 nm were used. The line at 208.83 nm was not used, because excessive flame absorption resulted in a higher noise level.

TABLE I

INSTRUMENTAL CONDITIONS FOR THE DETERMINATION OF ANTIMONY

Spectral line (nm)	*Sensitivity for 1% absorption ($\mu g\ ml^{-1}$)*	*Spectral slit width (nm)*
217.58	0.64	0.2
231.18	1.3	0.5

The light source was an A.S.L. neon-filled antimony hollow-cathode lamp operated at 10 mA. The burner was set 1.5–2.0 mm below the light beam. In all cases, a slightly fuel-rich air–acetylene flame was used, the mixture being adjusted for maximum signal. The Model 1000 is equipped with linear absorbance readout and continuous scale expansion and hence direct read-out in μg Sb ml^{-1} was possible.

The 231.18-nm resonance line was found to be more suitable because a more linear calibration was obtained at this line than at 217.58 nm. Moreover, since this line was more intense than the 217.58-nm line, and was sufficiently isolated with a spectral slit width of 0.5 nm, a much lower dynode voltage could be applied to the photomultiplier, so that the noise level was considerably reduced.

Reagents

A stock standard solution containing 500 μg Sb ml^{-1} was prepared by dissolving 0.5 g of antimony powder (min. 99%) in 30 ml of aqua regia; 300 ml of 70% (analytical grade) perchloric acid was added to prevent precipitation as antimony oxychloride and the solution was cooled and diluted to 1 l in a volumetric flask. Suitable working solutions were prepared by dilution of this solution with distilled water. These were stable for at least 3 months.

Antimony trioxide (min. 99%) was used for recovery experiments. Laboratory-reagent grade ammonium iodide was used.

Development of method

Ammonium iodide in 2 *M* hydrochloric acid had no effect on the absorbance of 25 μg Sb ml^{-1} provided that its concentration exceeded 3% (w/v). Figure 1 shows

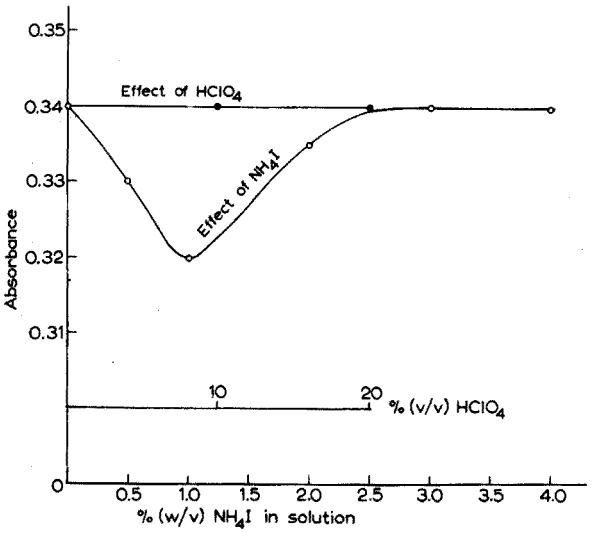

Fig. 1. The effect of ammonium iodide and perchloric acid on the absorbance of antimony (25 μg ml^{-1}) at 217.58 nm with 0.2 nm slit width.

that concentrations less than this produced a slight depression of the absorbance.

Concentrations up to 20% (v/v) perchloric acid had no effect on the antimony absorbance.

Ammonium iodide alone in 2 *M* hydrochloric acid up to 5% (w/v) showed an absorbance of less than 0.005 at 217.58 nm, which can be neglected unless high scale expansions are being used, when it should be subtracted as a reagent blank.

Procedure

Weigh a 0.250-g sieved soil sample (80-mesh soil fraction) or a finely ground rock or low-grade oxide ore into an 18 × 180-mm Pyrex test tube and mix thoroughly with 0.5 g of ammonium iodide crystals. Use 1.0 g if the sample contains more than 0.5% antimony. Rotate the tube in and out of an air-gas jet or Meker burner so that only the end is heated. Heat until all the ammonium iodide has sublimed. The fusion takes about 1 min. The sublimate should condense on the tube walls not higher than

100 mm up.

Allow the tube to cool and dissolve the sublimate by adding 10 ml of 2 *M* hydrochloric acid (analytical grade), warming to about 70° for 2–3 min. Add a further 20 ml if the antimony concentration is likely to be in the range 0.5–5.0%. Mix well, cool, allow the residue to settle, and aspirate the top layer for atomic absorption measurement.

Prepare suitable standards by dilution of the stock antimony solution with distilled water.

Read the absorbances of standards and samples in the standard way or read out directly in μg Sb ml^{-1}.

RESULTS AND DISCUSSION

Typical calibration curves of absorbance *vs.* concentration for antimony in weakly acidic solution are shown in Fig. 2.

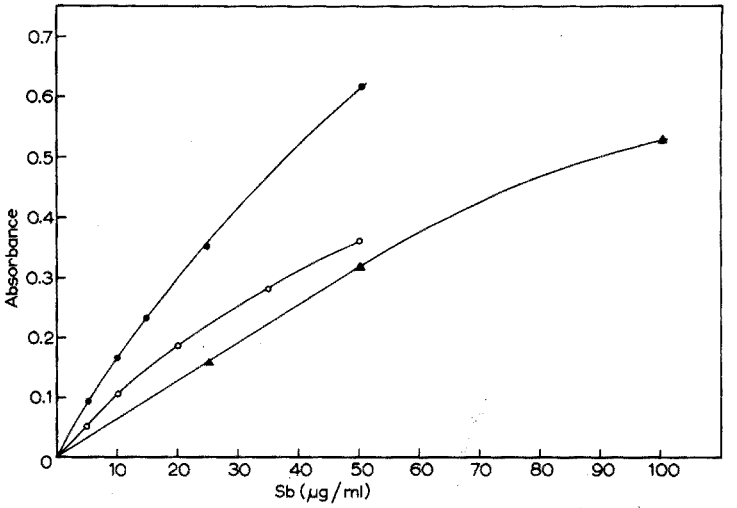

Fig. 2. Calibration curves for antimony at 217.58 nm and 231.18 nm in dilute perchloric acid solution. (●) 217.58 nm, 0.2 nm slit; (○) 217.58 nm, 0.5 nm slit; (▲) 231.18 nm, 0.2 nm slit.

Typical applications

The results for two soil samples containing anomalous antimony values by five different methods are shown in Table II. Values given are the average of two

TABLE II

COMPARISON OF DIFFERENT METHODS FOR THE DETERMINATION OF ANTIMONY IN SOILS

(Results given as % antimony; final determination by atomic absorption unless otherwise stated)

Sample	*NH_4I fusion*	*K_2CO_3/S fusion*[a]	*NH_4Cl fusion*	*$HClO_4/HNO_3$ (1 : 2)*	*Aqua regia hot extraction*
Brown earth 1	0.20	0.19	0.11	0.006	0.01
Brown earth 2	0.15	0.12	0.08	0.005	0.01

[a] Iodimetric titration.

determinations. To eliminate sampling variations, the 80-mesh soil fraction was analyzed after grinding to pass a 100-mesh nylon sieve.

The standard chemical method involving a potassium carbonate/sulphur fusion, extraction and reextraction from chloroform, and titration with iodine yielded slightly lower values than those obtained for the ammonium iodide fusion–atomic absorption method. Probably some antimony volatilizes during the initial stages of the fusion if it is present in a volatile form. The perchloric–nitric acid attack gave extremely low results, owing to the loss of volatile antimony perchlorates. Shaking the sample with hot aqua regia gave a very low recovery of antimony, showing that antimony is still associated with the silica. Fusion with ammonium iodide produced results that were 82% and 88% higher (samples 1 and 2, respectively), than similar fusion with ammonium chloride. This is due to the volatility of antimony chlorides. The boiling points of the halides are compared in Table III.

TABLE III

BOILING POINTS OF ANTIMONY HALIDES

Compound	*B.p.* (°)
$SbCl_3$	223
$SbCl_5$	140
SbI_3	401
SbI_5	400.6
$SbBr_3$	280

TABLE IV

DETERMINATION OF ANTIMONY IN TIN CONCENTRATES

Sample type	*Sb* (%)	
	NH_4I fusion/ atomic absorption	*Chemical method*
Cassiterite 1	0.75	0.73
Cassiterite 2	0.45	0.46

Results are given in Table IV for the determination of antimony in tin concentrates. The results from the chemical method were obtained in another laboratory, and the two sets show excellent agreement.

Recovery trials for the atomic absorption method

It is not known how accurate the results obtained in Table II for the ammonium iodide fusion–atomic absorption method are, as more reliable results could not be obtained by standard chemical methods. To check the recovery of antimony from antimony trioxide by this method, the oxide was added to weighed soil samples containing low antimony values. The results of these experiments are shown in Table V.

TABLE V

RECOVERY EXPERIMENTS FOR THE NH_4I FUSION–ATOMIC ABSORPTION METHOD

Sb in sample (p.p.m.)	*Sb in 0.2 g sample (μg)*	*Sb added as Sb_2O_3 (μg)*	*Sb total (μg)*	*Sb recovered (μg)*	*Recovery (%)*
195	42	3340	3382	3200	95
105	22	3340	3362	3300	98
0	0	2185	2185	2180	100

The level of recovery shown is quite acceptable for geochemical soil analysis. However, as it is not known generally in which form the antimony is present, these recoveries may change with sample type.

A soil from the same area containing 0.65% antimony was diluted down by mixing with similar soils (80-mesh fractions) containing less than 5 p.p.m. antimony to determine whether the recovery was constant. A series of samples down to 0.001% antimony was made and analysed according to the procedure given; the results are shown in Table VI.

TABLE VI

EFFECT OF MATRIX ON RECOVERY FOR THE NH_4I FUSION/ATOMIC ABSORPTION METHOD

Sample no.	*Dilution ratio*	*1. p.p.m. Sb*	*2. p.p.m Sb*	*Average of 2 values*	*Calculated value*	*Recovery (%)*
1.	0	0.66	0.64	0.65	—	—
2.	2 : 3	0.49	0.52	0.50	0.43	116
3.	1 : 2	0.35	0.36	0.355	0.33	108
4.	1 : 3	0.20	0.20	0.20	0.22	91
5.	1 : 4	0.15	0.15	0.15	0.16	94
6.	1 : 8	0.068	0.073	0.07	0.08	87.5
7.	1 : 16	0.039	0.036	0.037	0.04	92.5
8.	1 : 32	0.020	0.019	0.019	0.02	95
9.	1 : 64	0.010	0.009	0.010	0.01	100

The variation in the recoveries occurs because calculated values are based on known dilutions of sample 1 and some mixing variations must occur. The matrix does not significantly affect the recovery of antimony.

One sample (195 p.p.m. Sb) was analyzed ten times from which the coefficient of variation was calculated as 4%. This precision would enable one to be able to distinguish between background and anomalous samples with a high degree of confidence.

Interferences

No interferences were found for 10 p.p.m. of antimony owing to cations or anions which could be present in solution after ammonium iodide fusion and dissolution with 2 *M* hydrochloric acid.

Lead, tin, iron, calcium and magnesium present in 100-fold amounts were found not to interfere with the antimony absorption at 217.58 nm with a 0.2-nm slit.

These metals also had no effect on antimony in the presence of 0.02 *M* iodine. Slavin and Sattur[9] demonstrated that lead caused spectral interference at the 217.0-nm antimony line. This is not serious at spectral slit widths less than 0.3 nm and at lead concentrations less than 5000 $\mu g\ ml^{-1}$. Owing to the limited solubility of lead iodide this interference is therefore not a problem.

CONCLUSION

One of the advantages of the ammonium iodide fusion is the ease with which sample weights up to 1 g can be treated so that the final volume is small. Therefore sensitivity is very good. Wood[10] has discussed the extension of an ammonium chloride fusion for antimony, to the decomposition of other geological sample types. It appears, therefore, that an ammonium iodide fusion could also be used to determine antimony in rocks and other materials.

The method proved to be very rapid and allowed 150 soil samples per 8-h man-day to be determined in this laboratory. With approximately 5 × scale expansion and damping at the 217.58-nm line, the detection limit, taken as twice the peak-to-peak noise level, was 10 p.p.m. on a 250-mg sample and a 10-ml volume.

SUMMARY

A method is described for the determination of antimony in various geological materials. After an ammonium iodide fusion and dissolution with dilute hydrochloric acid, antimony is measured by atomic absorption measurement in an air–acetylene flame. The method is interference-free; the limit of detection is 10 p.p.m. antimony on the basis of a 250-mg sample. The method has good precision and is suitable for application to geochemical prospecting samples.

RÉSUMÉ

On décrit une méthode de dosage de l'antimoine dans divers matériaux géologiques. Après fusion au iodure d'ammonium et dissolution dans l'acide chlorhydrique dilué, l'antimoine est dosé par absorption atomique, dans une flamme air–acétylène. Cette méthode ne présente pas d'interférence; la limite de détection est de 10 p.p.m. d'antimoine, pour un échantillon de 250 mg. La précision est bonne et convient pour des échantillons géochimiques de prospection.

ZUSAMMENFASSUNG

Es wird eine Methode für die Bestimmung von Antimon in verschiedenen geologischen Proben beschrieben. Nach einem Ammoniumjodidaufschluss und Auflösung mit verdünnter Salzsäure wird Antimon durch Atomabsorptionsmessung in einer Luft–Acetylen-Flamme bestimmt. Die Methode ist störungsfrei; die Nachweisgrenze liegt bei einer Probe von 250 mg bei 10 p.p.m. Antimon. Die Methode hat eine gute Reproduzierbarkeit und eignet sich für die Anwendung auf geochemische Sondierungsproben.

REFERENCES

1 J. JANKOVSKY, *Z. Anal. Chem.*, 201 (1964) 325.
2 R. E. STANTON AND A. J. MCDONALD, *Trans. Inst. Mining Met.*, 71 (1962) 501.
3 R. E. STANTON AND A. J. MCDONALD, *Analyst*, 87 (1962) 299.
4 R. A. MOSTYN AND A. F. CUNNINGHAM, *Anal. Chem.*, 39 (1967) 433.
5 M. YANAGISAWA, M. SUZUKI AND T. TAKEUCHI, *Anal. Chim. Acta*, 47 (1969) 121.
6 C. R. WALKER, O. A. VITA AND R. W. SPARKS, *Anal. Chim. Acta*, 47 (1969) 1.
7 C. E. MULFORD, *Atomic Absorption Newsletter*, 5 (1966) 88.
8 B. E. ST. JOHN, *J. Sediment. Petrol.*, 40 (1966) 537.
9 S. SLAVIN AND T. W. SATTUR, *Atomic Absorption Newsletter*, 7 (1968) 99.
10 G. A. WOOD, *Ph.D. Thesis*, London University, 1957.

Analytica Chimica Acta
Elsevier Publishing Company, Amsterdam
Printed in The Netherlands

SEMI-QUANTITATIVE ANALYSIS BY MEANS OF THE LASER MICROPROBE

M. S. W. WEBB AND R. J. WEBB
Analytical Sciences Division, A.E.R.E., Harwell, Berks. (England)
(Received 5th March 1971)

The description and characteristics of the laser-spark microprobe have been well documented[1-3] and there are numerous reports of specific applications of the technique. While the qualitative applications demonstrate its potential power and versatility as an analytical tool, there are serious inherent problems when attempts are made to make quantitative measurements, notably the difficulty in standardisation and in many cases the impracticability of incorporating an internal standard into the sample. Thus most quantitative applications are restricted to one type of material where it can be assumed that a reproducible amount of sample is volatilised and excited in each exposure so that the intensity of the element line is proportional to the concentration, or to cases where there is a natural internal standard. In both instances, standardised samples can be used for calibration provided that they are homogeneous in relation to the spatial resolution of the instrument. More general methods such as the impregnated gel technique of Rosan[4] and the powder method used by Whitehead and Heady[5] involve an appreciable amount of sample preparation and the laser-spark becomes, in effect, another method of excitation for the quantitative spectrographic analysis of powders and solutions, whereas it was originally developed for the *in situ* spectrochemical analysis of microsamples (0.1–1 μg), such as inclusions and surface deposits.

In general, the conventional methods of quantitative analysis cannot be used without curtailing this important characteristic or otherwise limiting the versatility of the method. In this report an alternative method of assessing semi-quantitatively the photographic recordings of spectrograms is considered which does not demand any uniformity as to type or form of samples and standards.

If the laser pulse length is short (*ca.* 30 nsec), the sample area can be converted directly from the solid to the vapour phase without an intermediate liquid state and under these conditions the vapour should have the same relative concentration of atoms as the solid sample.

When a spark is used to excite an atomic cloud of vapour, conditions are ideal for the production of optical spectra which should be free from the interference effects normally associated with the matrix material and in these circumstances the intensity of a particular spectral line should be a simple function of its concentration. Breck[6] has predicted that this type of excitation process should be relatively free from the influence of the matrix, and this view is supported to some extent by the data published by Rasberry *et al.*[3] and Whitehead and Heady[5].

Assuming these two hypotheses to be true, an equation has been derived

empirically, which enables the intensity of the spectrum line of a particular element to be expressed in terms of relative concentration by the use of a weighting factor; the latter is derived experimentally for each element line by the analysis of suitable standards. It is a constant for any particular line and, once it has been determined, it enables quantitative analysis to be undertaken without further reference to standards.

The following expression was finally adopted for evaluating the relative intensity of the analytical line in terms of the concentration of the originating element.

$$C_A = F_A \cdot (R_A)^2 / \Sigma R \qquad (1)$$

where C_A = relative concentration of element A, F_A = weighting factor of A, R_A = relative intensity of a specific spectral line of A, ΣR = total of the relative intensities of all the elements measured. Although there is no obvious theoretical explanation for the unusually low emission factor of 0.5 implied by this expression, it fits the data in this paper and a similar figure has been reported by other authors[3].

When the relative concentration of each element has been found, it is straightforward to normalise these to 100%, *i.e.*

$$\%\,A = C_A/\Sigma C \cdot 100 \qquad \%\,B = C_B/\Sigma C \cdot 100\,, \quad \text{etc.} \qquad (2)$$

where ΣC is the sum of the relative concentration of all the elements. This automatically corrects for any variation in the weight of sample volatilised, but it must be remembered that the final answer gives only the percentage of the elements actually measured relative to themselves which is usually, but not necessarily, the same as the concentration in the sample, *i.e.* it is only applicable to the complete analysis of a sample.

EXPERIMENTAL

Exposure conditions

Standardised conditions, summarised in Table I, were used for exciting and recording the spectra. A two-step filter was placed at the slit to extend the usable range of the element lines. For powder samples it was found that satisfactory shots could be obtained by forming a thin compress of the powder between two pieces of thin polythene adhesive tape.

TABLE I

EXCITATION AND RECORDING CONDITIONS

Spectrograph	Hilger medium quartz
External optics	Source focused on to the collimator with a sphero-cylindrical lens
Photographic plate	Kodak Scientific 0-0 Developer: Ilford D19B for 4 min at 20°
Microprobe	Jarrell-Ash Q-switched ruby laser Pulse length 30 nsec Attenuated power output 0.2 J
Cross-excitation supply	Operated at 92% power with capacitance 20 μF inductance 100 μH residual resistance

Plate characteristics

It was clear from the first plates that the repeatability of microphotometer readings was not good enough to warrant an elaborate plate calibration procedure for each plate, and that in general it would be better to establish the plate characteristics on the first plate by replicate readings and then maintain controlled development procedures and assume the same parameters for the other plates in the batch. The necessary Kaiser functions[7] were established to give straight-line characteristic curves for the range of wavelengths required and the slope of each determined. For the subsequent calculations the equation of this straight line was taken in its simplest form, namely:

$$\text{Kaiser function} = (1-k)D + kS = m \log R \tag{3}$$

where k = Kaiser constant, D and S = normal and Seidel densities, respectively, m = slope.

Calibration

A finely ground synthetic mixture of metal oxides containing equal concentrations of some 30 elements was prepared and replicate exposures were taken of this mixture. The elements and wavelengths selected for measurement are tabulated in Table II. These were chosen to give maximum sensitivity consistent with freedom from inter-element line interferences.

The line and background were measured in each case and hence by substituting in eqns. (3) and (1), the weighting factor for each element was calculated. For the calibration of less sensitive lines of the elements which are more commonly encountered as major constituents, suitable analysed samples were selected, their spectra recorded, and the weighting factors calculated. The minor constituents provided an overlap of elements for which the weighting factors had already been determined, so that the two sets of weighting factors could be rationalised. Similarly, if it is desired to add weighting factors for any other elements, there must be an overlap of elements in the new standards so that the factors for the additional elements can be calculated relative to those already evaluated.

Evaluation of sample spectra

The analytical lines of the elements present in the spectra were measured on the microphotometer together with their associated backgrounds. Where both the alternative lines for a particular element were measurable, the less sensitive one was used. Computation of the composition of the sample then followed the sequence of calculations:

1. the relative intensity of each element line from the microphotometer readings for line and background,

2. corrections as required for inter-element line interference. This was done by subtracting a predetermined proportion of the relative intensity of the analytical line of the interfering element from the apparent relative intensity of the element line. Thus if a line of element B is coincident with the analytical line of A then

$$\text{corrected } R_A = \text{calculated } R_A - x\% \text{ of } R_B$$

3. the relative concentration of each element,

4. the normalisation of the relative concentrations to equal 100%.

When many elements are present these calculations can be long and tedious and it was expedient to use the computer for this stage. The programme required is straightforward and an outline of the one used is shown in Fig. 1. The data regarding

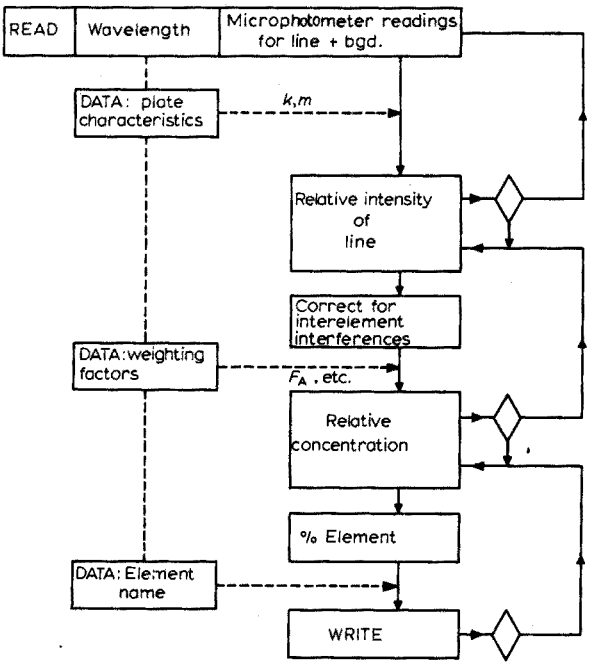

Fig. 1. Outline of computer programme.

the plate characteristics and weighting factors were incorporated in the programme and the wavelength of the element line as given in Table II was used as the label for the input data and other constants, thus allowing the readings for any number of analytical lines to be read in any order.

RESULTS

Duplicate, or in some cases triplicate, exposures were taken of a variety of materials of known composition and the mean concentrations as calculated from the spectra are summarised in Tables III–VI. In some cases the sample was analysed on two different occasions, and these are recorded separately.

Accuracy and reproducibility

Tables III–VI give a general indication of the accuracy attained by this technique. This is shown more clearly in Fig. 2 where observed concentrations of all elements are shown plotted against their nominal values. There appears to be no significant bias for any of the samples analysed, and, for the most part, results below 10% are within a factor of two of the nominal figure (*i.e.* equivalent to a coefficient of

TABLE II

ANALYTICAL LINES USED

Element	*Wavelength (nm)*	*Factor*	*Interfering elements*
Manganese	257.6	1	
Cobalt	258.0	6.5	
Iron	259.9	4	
	259.1[a]	88	
Hafnium	264.7	150	
Molybdenum	281.6	35	Aluminium
Platinum	283.0	80	
Tin	284.0	60	Chromium
Chromium	284.3	4.4	
Magnesium	285.2	10.8	
Silicon	288.2	12.3	
Bismuth	306.7	30	
Niobium	309.4	8	
Vanadium	311.1	7	Titanium
Calcium	315.9	15	
	364.4[a]	800	
Copper	324.7	3.7	Iron
	282.4[a]	400	
Silver	328.0	3	
Sodium	330.2	300	Zinc
Zinc	334.5	50	
	255.8[a]	500	
Titanium	334.9	0.8	
Zirconium	339.2	1.5	
Strontium	346.4	15	
Nickel	349.3	50	Iron
Scandium	361.4	0.3	
Palladium	363.5	33	
Lead	368.3	70	
Yttrium	371.0	0.8	
Aluminium	396.1	10.3	
	257.5[a]	600	
Lanthanum	398.8	20	
Tungsten	400.9	300	
Gallium	417.2	15	

[a] Alternative line used for higher concentration of these elements.

variation of 50%) and considerably better at higher concentrations. It is an inherent characteristic of the method of calculating the results that the error tends to zero at 100%. While this represents the precision attainable when the technique is used as a general-purpose method of analysis, it gives an unfavourably biassed impression of the reproducibility of the method of analysis itself, because the very small amount of sample consumed, about 0.1 μg, must inevitably introduce large sampling errors for most materials and this is included in the above results.

Although this sampling error cannot be eliminated completely, it was considered that a sample of bronze should be reasonably homogeneous and provide a more realistic estimate of reproducibility. The results from 10 spectra taken of a

TABLE III

OBSERVED COMPOSITION OF MINERAL AND CERAMIC SAMPLES
(Nominal concentrations in brackets)

	BCS No. 174/1 *Basic slag* (%)		*BCS No.* 268 *Firebrick* (%)		*NBS No.* 1014 *Portland cement* (%)		*Standard glass No.* 1 (%)	
Fe_2O_3	10	(13.7)	5	(3.5)	2	(2.5)	0.1	(0.15)
MgO	9	(8.1)	0.3	(0.93)	6	(2.8)	0.6	(3.56)
SiO_2	16	(16.7)	65	(56.7)	21	(19.5)	76	(71.74)
CaO	56	(50.9)	0.3	(0.33)	65	(63.1)	5	(8.49)
TiO_2	0.7	(0.81)	1.0	(1.48)	0.2	(0.25)	0.02	(0.05)
Al_2O_3	3	(1.95)	29	(33.9)	6	(6.38)	0.5	(1.55)
MnO	5	(5.8)	0.02	(—)	0.06	(0.07)		
Cr_2O_3	0.2	(0.30)						
V_2O_5	0.5	(1.36)						
Na_2O					—	(0.24)	18	(13.25)
SrO					0.2	(0.28)		

TABLE IV

OBSERVED COMPOSITION OF LOW-ALLOY STEEL SAMPLES
(Nominal concentrations in brackets)

Sample no.	*SS* 1 (%)		*SS* 4 (%)		*SS* 7 (%)		*SS* 8 (%)		
							(*1*)	(*2*)	
Fe	95	(94)	93	(94)	94	(94)	95	92	(94)
Mo	0.2	(0.185)	3	(1.29)	0.2	(0.32)	0.2	0.3	(0.42)
Cr	<0.2	(0.044)	0.3	(0.54)	1.6	(1.72)	3	4	(3.07)
Si	0.2	(0.013)	0.5	(0.30)	0.5	(0.38)	0.6	0.7	(0.81)
Mn	0.1	(0.165)	0.6	(0.53)	1.5	(1.42)	0.7	0.5	(0.79)
V	0.2	(0.03)	1.2	(0.52)	0.3	(0.11)	0.7	1.1	(0.65)
Cu	0.5	(0.09)	0.4	(0.11)	1.8	(0.30)	0.5	0.4	(0.19)
Ni	5	(5.15)	1.3	(2.08)	0.2	(0.84)	—	—	(0.05)

standard sample are summarised in Table VII. These figures are very similar to the reproducibilities quoted by other authors who used conventional methods of computation, *e.g.* 11% for intensity ratios in various refractory matrices by Whitehead and Heady[5] and 15% to 40% in the analysis of high temperature alloys by Rasberry *et al.*[3].

Another limiting factor is the fast, grainy type of photographic plate which has to be used for this analysis although, as was mentioned earlier, it is far from ideal for quantitative analysis. Repeat microphotometry on a few of the spectra indicates an effective photometric error of about 15% or 10% on a single measurement.

TABLE V

OBSERVED COMPOSITION OF FERROUS ALLOY SAMPLES
(Nominal concentrations in brackets)

Sample no.	3528 *Stainless steel* (%)			6099 *Stainless steel* (%)		*B* 7018 *Nimonic* (%)		*Austenitic steel* (%)	
	(*1*)	(*2*)							
Fe	64	59	(68.0)	60	(70.6)	1.5	(1.5)	38	(44)
Mo						5	(4.63)	0.3	(1.0)
Cr	16	13	(17.4)	15	(18.1)	7	(14.95)	18	(18.5)
Si	0.9	1.0	(0.65)	5	(0.78)	1.3	(1.02)	2	(0.66)
Mn	0.9	1.8	(1.28)	1.5	(0.75)			0.6	(1.24)
Cu	0.3	0.5	(—)	2	(—)	0.5	(0.20)	0.2	(—)
Ni	17	23	(11.9)	14	(9.12)	55	(52.2)	36	(32.3)
Ti				0.7	(0.51)	1.1	(0.97)	1.1	(0.69)
Co						20	(20.0)		
Al				1.2	(—)	10	(4.58)	2	(0.65)
Nb	1.0	0.5	(0.74)					1.2	(0.9)

TABLE VI

OBSERVED COMPOSITION OF NON-FERROUS ALLOY SAMPLES
(Nominal concentrations in brackets)

Sample no.	*Aluminium alloys*						*Copper-based alloys*			
	S 17 (%)		*D* 14 (%)		*Y* 9 (%)		*YCW* 22 (%)		*YCW* 31 (%)	
Al	85	(87)	89	(93)	87	(88)	1.6	(1.3)	0.3	(0.10)
Mn	0.3	(0.21)	0.6	(0.55)			0.2	(0.4)	0.03	(0.03)
Fe	0.4	(0.30)	0.8	(0.45)	1.7	(1.02)	0.3	(0.14)	0.08	(0.03)
Mg	1.1	(0.16)	1.0	(0.59)	1.8	(2.14)	0.04	(0.005)	0.2	(0.20)
Si	12	(11.7)	0.7	(0.52)	1.1	(0.90)	0.11	(0.14)	0.2	(0.05)
Cu	0.7	(0.22)	3	(4.04)	3	(5.08)	75	(70)	58	(57)
Zn	0.1	(0.20)	0.2	(0.16)			23	(26.6)	34	(39)
Ti	0.3	(0.16)	0.3	(0.25)	0.5	(0.19)	0.03	(—)	0.03	(—)
Ni	0.2	(0.18)	0.2	(0.20)	4	(2.33)	<0.08	(0.005)	0.3	(0.25)
Pb	0.3	(0.17)	1.2	(0.19)			0.4	(0.2)	3	(2.3)
Co							<0.02	(0.01)	0.01	(0.1)
Sn							0.3	(0.2)	0.4	(0.6)
Bi							0.05	(0.04)		
Nb							0.2	(0.01)	0.1	(—)
Ag							0.08	(0.14)	0.2	(0.20)

CONCLUSION

The above results appear to justify the empirical expression quoted earlier and as far as mineral and metal samples are concerned support the view that the laser/spark source is for all practical purposes free from any matrix effect. This method of assessing the recorded spectra gives results which are comparable in accuracy and reproducibil-

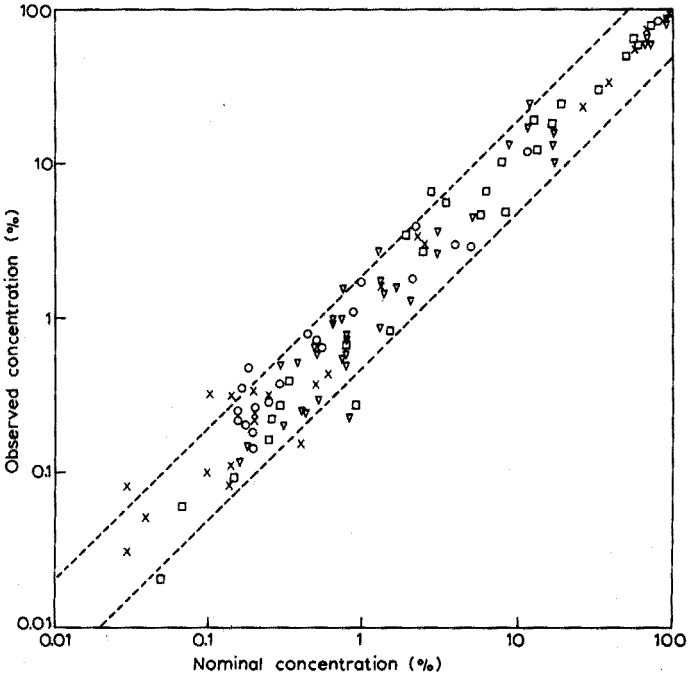

Fig. 2. Recovery from different matrices. (▽) Iron alloys, (⊙) aluminium alloys, (□) minerals, (×) copper alloys.

ity to other attempts at quantitative analysis by laser with the added advantage that it is applicable to any type of metal or mineral sample. With organic-based materials the analysis gives only the relative concentrations of the metals (or metal oxides) in the sample which is, in effect, equivalent to the analysis of the ash of the sample and an independently determined ash content is required to convert these to concentrations in the sample. Since the method depends on the inter-relationship of all the elements in the discharge plasma, isolated elements or groups of elements cannot be determined; only the complete analysis provides meaningful results. Thus, in the field of general spectrochemical analysis, while the precision may not be so good as other methods, it could provide a rapid general survey method of a semi-quantitative nature.

The fact that this method gives only the concentrations of the elements measured, relative to themselves, opens up several possible applications, for example,

TABLE VII

REPRODUCIBILITIES—SAMPLE OF BRONZE

Element	*Concentration* (%)		*Coeff. of variation* (%)
	Nominal	*Found*	
Cu	97	96.5	1
Zn	2.5	2.97	19
Sn	0.5	0.37	40

the analysis of very thin platings where the laser shot penetrates to the base material. If it can be assumed that elements present in the base are not present in, or are very minor constituents of, the coating, then by ignoring the analytical lines of these elements when measuring the plate, an analysis of the coating material is obtained. Likewise, a similar technique could be used for very small inclusions.

SUMMARY

Conventional methods of quantitative spectrochemical analysis cannot, in general, be applied to spectra produced by the laser microprobe. An alternative procedure is given for quantifying the recorded spectra from the laser/spark excitation of any type of material, thus providing a complete survey analysis of the metallic constituents of the sample or part of the sample under examination. No systematic bias has been observed in the accuracy of the results obtained, and, in the main, results below 10% were within a factor of two of the nominal figure and were considerably better at higher concentrations.

RÉSUMÉ

Les méthodes conventionnelles d'analyse spectrochimique quantitative ne peuvent pas en général être appliquées aux spectres produits par laser. Un procédé est donné pour quantifier les spectres enregistrés lasor/étincelle de n'importe quel type de substance; ce qui permet une analyse complète des constituants métalliques de l'échantillon, ou d'une partie de l'échantillon à examiner.

ZUSAMMENFASSUNG

Konventionelle Methoden der quantitativen spektrochemischen Analyse können im allgemeinen nicht auf Spektren angewendet werden, die mit der Laser-Mikrosonde erhalten werden. Ein Alternativverfahren zur quantitativen Behandlung der Spektrogramme, die durch Laser-Funkenanregung einer beliebigen Materialart entstehen, erlaubt eine vollständige Übersichtsanalyse der metallischen Bestandteile der Probe oder eines zu prüfenden Teils davon. Systematische Abweichungen in der Genauigkeit der erhaltenen Ergebnisse wurden nicht beobachtet; die Ergebnisse unter 10% lagen innerhalb des Faktors zwei vom gegebenen Wert und waren bei höheren Konzentrationen erheblich besser.

REFERENCES

1 Y. KATSUNO, T. TAKEUCHI, K. SUNAHARA AND K. MORITA, *J. Japan Soc. Anal. Chem.*, 3 (1968) 376.
2 S. D. RASBERRY, B. F. SCRIBNER AND M. MARGOSHES, *Appl. Opt.*, 6 (1967) 81.
3 S. D. RASBERRY, B. F. SCRIBNER AND M. MARGOSHES, *Appl. Opt.*, 6 (1967) 87.
4 R. C. ROSAN, *Appl. Spectrosc.*, 19 (1965) 97.
5 A. B. WHITEHEAD AND H. H. HEADY, *Appl. Spectrosc.*, 22 (1968) 7.
6 F. BRECK, *Current Status and the Potentials of Laser Excited Spectrochemical Analysis*, Reprint No. 2, Jarrell-Ash Co.
7 H. KAISER, *Spectrochim. Acta*, 3 (1948) 159.

Analytica Chimica Acta
Elsevier Publishing Company, Amsterdam
Printed in The Netherlands

THE ULTRAVIOLET SPECTROPHOTOMETRIC DETERMINATION OF NITRITE BY THE ANTIPYRINE METHOD

K. G. WEISS AND D. F. BOLTZ
Department of Chemistry, Wayne State University, Detroit, Mich. 48202 (U.S.A.)
(Received 21st December 1970)

The most extensively used spectrophotometric method for the determination of nitrite is based on the Griess[1] reaction which involves the diazotization of sulfanilic acid and subsequent coupling with 1-naphthylamine. Numerous modifications have been suggested, primarily on the basis of changing either the reagent being diazotized or coupled[2-10]. A critical study of the diazotization and coupling reactions by Rider and Mellon[11] delineated the optimum conditions for maximum development of the azo dye using the sulfanilic acid and 1-naphthylamine reagents. Sawicki *et al.*[12] reviewed 52 spectrophotometric methods for nitrite emphasizing the relative sensitivities and color stabilities of the various systems. New methods based on the formation of free radical chromogens have been proposed[13].

There are relatively few ultraviolet spectrophotometric methods proposed for the determination of nitrite. Although nitrite has a molar absorptivity of 23 l mole^{-1} cm^{-1} at 355 nm[14,15], conversion to a species of much larger absorptivity is necessary for trace analysis. Pappenhagen and Mellon[16] developed a sensitive ultraviolet spectrophotometric method ($\varepsilon = 1.55 \cdot 10^4$) based on diazotization of 4-aminobenzenesulfonic acid. In an ultraviolet spectrophotometric study of 9 diazonium compounds Kuemmel and Mellon[17] observed high molar absorptivities ($\varepsilon = 1.2 \cdot 10^4$ to $4.0 \cdot 10^4$) and that many readily underwent photochemical changes. Additional ultraviolet spectrophotometric methods have been proposed by Ziegler and Glemser[18] based on the nitrite–thioglycollic acid reaction and by Wiersma[19] based on the formation of 2,3-naphthotriazole by the reaction of nitrite and 2,3-diaminonaphthalene. An indirect spectrophotometric method for the determination of calcium proposed by Akiyama and Matsumura[20] in which a calcium hexanitritonickelate(II) precipitate was dissolved in acetic acid and treated with antipyrine to give a green color suggested the desirability of further study of antipyrine as a reagent for the direct spectrophotometric determination of nitrite. Schaak[21] reported the use of the formation of 4-nitrosoantipyrine for the colorimetric determination of antipyrine shortly after the first synthesis of antipyrine by Knorr[22]. Schuyten[23] used antipyrine for the colorimetric determination of nitrite but no systematic spectrophotometric study of this method was found in the literature although the nitrosation of antipyrine had been studied[24] and the certain spectral characteristics of 4-nitrosoantipyrine had been documented[25]. During the preparation of this paper a recent Abstract revealed that Perez[26] had used antipyrine in the photometric determination of nitrite. There are many synonyms for antipyrine found in the literature. The most generally accepted name is 2,3-dimethyl-1-phenyl-3-pyrazolin-5-one.

EXPERIMENTAL

Reagents

Standard nitrite solution. Dissolve approximately 6.9 g of analytical reagent grade sodium nitrite in distilled water and dilute to 1 l. Standardize this stock solution by a titrimetric method using standardized 0.1 *N* permanganate as titrant and a micro-buret. Use a micro-buret to measure the appropriate volume of stock nitrite solution required to prepare a solution containing 25 mg of nitrite per liter of standard solution.

Antipyrine reagent solution. Transfer exactly 5.5 ml of concentrated sulfuric acid (s.g. 1.84); 98.0% H_2SO_4 to approximately 700 ml of distilled water in a 1-1 volumetric flask. Dissolve 18.823 g of dry, recrystallized antipyrine (Aldrich) in the

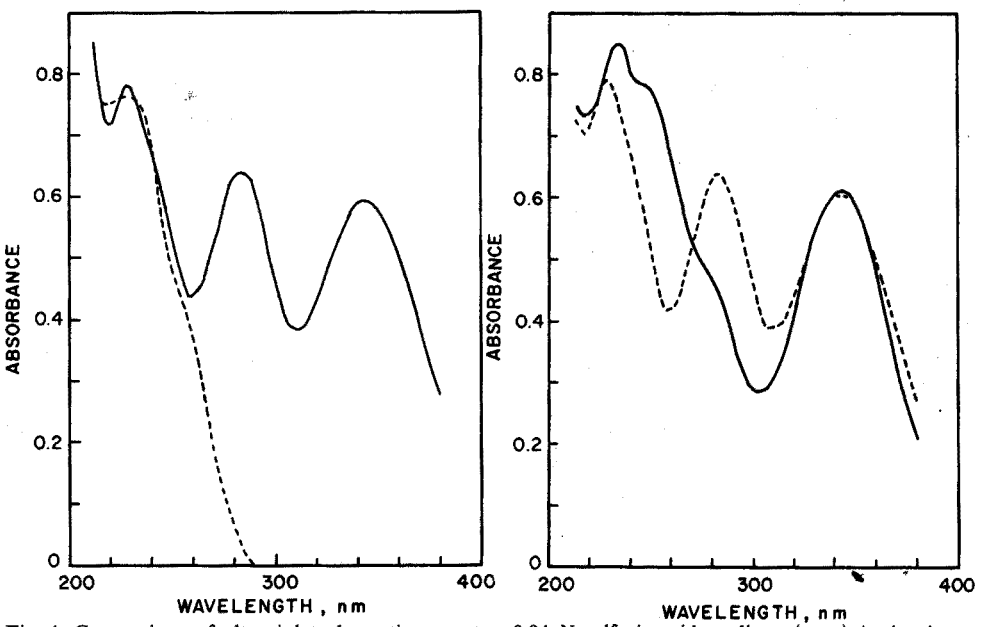

Fig. 1. Comparison of ultraviolet absorption spectra. 0.04 *N* sulfuric acid medium. (------) Antipyrine; (——) 4-nitrosoantipyrine.

Fig. 2. Effect of solvent on ultraviolet absorption spectra of 4-nitrosoantipyrine. (------) Water; (——) absolute methanol.

acidic solution and dilute to volume. This reagent solution is 0.1 *N* in sulfuric acid and 0.1 *M* in antipyrine.

Diverse ion solutions. Prepare these solutions from reagent-grade chemicals so that 1 ml of solution contains 5.0 mg of diverse ion.

Apparatus

Spectrophotometric measurements were made in 1.000-cm silica cells with a Cary 14 spectrophotometer.

General procedure

Transfer 10 ml of sample solution containing 0.25–30 μg of nitrite per ml to a 25-ml volumetric flask. Add 10.0 ml of the sulfuric acid–antipyrine reagent solution and dilute to volume with distilled water. Measure the absorbance at 343 nm in 1.000-cm silica cells using a reagent blank solution in the reference cell. Refer the absorbance readings to a calibration graph prepared using standard solutions.

RESULTS

Nature of ultraviolet absorption

In order to make a thorough investigation of the characteristic ultraviolet absorption spectra 4-nitrosoantipyrine was synthesized. It was found that the recrystallization of 4-nitrosoantipyrine from an acetone–methanol mixture gave a product of highest purity as indicated by a molar absorptivity of $7.55 \cdot 10^3$ at 343 nm. The ultraviolet absorption spectra of antipyrine and 4-nitrosoantipyrine are shown in Fig. 1. In the case of antipyrine a hypsochromic shift and a hyperchromic effect were observed in changing from an aqueous to a 0.04 *N* sulfuric acid medium although this is inconsequential when absorbance is measured at 343 nm. There is no appreciable difference in the ultraviolet absorption spectra for 4-nitrosoantipyrine in water and 0.04 *N* sulfuric acid media. However, 4-nitrosoantipyrine in absolute methanol gave a distinctly different absorption spectrum but the absorbance maximum at 343 nm was not altered which is very significant (see Fig. 2). Thus, 4-nitrosoantipyrine in aqueous solutions exhibits three absorbance maxima at 227, 282, and 343 nm. Examination of Fig. 1 shows that even a solution with a very low concentration of antipyrine has an appreciable absorptivity below 285 nm and would cause difficulties if absorbance measurements were attempted at the 227 or 282 nm wavelengths.

Nitrite concentration

The ultraviolet absorption spectra for solutions of various nitrite concentra-

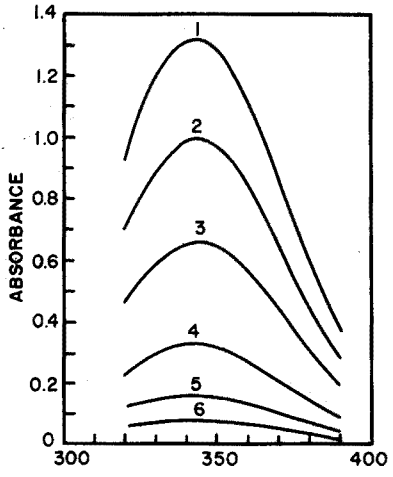

Fig. 3. Effect of nitrite concentration. p.p.m. of NO_2^- : (1) 8, (2) 6, (3) 4, (4) 2, (5) 1, (6) 0.5.

tions prepared according to the recommended general procedure are shown in Fig. 3. Conformity to Beer's law was observed over 0.1 to 12 p.p.m. of nitrite concentrations when absorbance measurements were made at 343 nm. The optimal concentration range based on a Ringbom plot is 1.5–4 p.p.m. of nitrite. The molar absorptivity at 343 nm is $7.61 \cdot 10^3$ l mole^{-1} cm^{-1}.

Antipyrine concentration

The effect of antipyrine was determined for 3 p.p.m. of nitrite, maintaining a constant 0.004 *N* sulfuric acid concentration and using 1.0 to 10 ml of a 0.1 *M* antipyrine solution. The absorbance increased rapidly until 3.0 ml of the reagent had been added and then increased very gradually. When 8.0, 9.0 and 10.0 ml of the reagent had been added, the corresponding absorbance values of 0.490, 0.494 and 0.493 were obtained at 343 nm. This study indicated that the antipyrine concentration should be at least 0.012 *M* at this low acidity of 0.004 *N* and at the 3 p.p.m. of nitrite level.

Effect of acidity

The volume of 0.1 *N* sulfuric acid used in preparing a solution corresponding to 3 p.p.m. of nitrite and 0.004 *M* in antipyrine was varied and the resulting absorbance at 343 nm measured. The absorbance changed inappreciably after 3.0 ml of the 0.1 *N* sulfuric acid had been used. It was concluded that a final acidity corresponding to 0.024–0.04 *N* sulfuric acid was sufficient even for the low (0.004 *M*) concentration of antipyrine.

Effect of mixed reagent

On the basis of the three preliminary studies on the effect of acidity and antipyrine concentration it was decided to prepare a mixed reagent 0.1 *M* in antipyrine and 0.1 *N* in sulfuric acid. The use of 10 ml of this reagent for 25 ml of final solution would give a final concentration of 0.04 *M* in antipyrine and 0.04 *N* in sulfuric acid. However, because of the low acidity used for studying the effect of antipyrine concentration and the low antipyrine concentration used in studying the effect of acidity, a study was made to determine the efficiency of this mixed reagent in which the sulfuric acid and antipyrine concentrations were being increased simultaneously. For 5 p.p.m. of nitrite it was found that at least 3 ml of the mixed reagent had to be added, thus indicating a minimal antipyrine concentration of about 0.01 *M*, and a minimal acidity of approximately 0.01 *N* in sulfuric acid.

Stability of absorptive system

The absorbance of a 5-p.p.m. sample of nitrite solution was monitored for a period of 5 min after preparation of solution to 5.75 h. The change in absorbance was less than 0.5% per hour indicating that the 4-nitrosoantipyrine is a stable species.

Effect of diverse ions

The effect of 500 p.p.m. of 26 diverse ions in the determination of 3 p.p.m. of nitrite by the recommended procedure was determined. Non-interference was based on a deviation 3 times the relative standard deviation or 1.1%.

The following did not interfere: copper(II), manganese(II), mercury(II), magnesium, nickel, calcium, bromide, chloride, fluoride, nitrate, oxalate, phosphate,

TABLE I

EFFECT OF DIVERSE IONS

Ion	*Added as*	*Amount added (p.p.m.)*	*% Relative error*	*Permissible amount*[a]
Cr^{3+}	$CrCl_3$	500	+3.6	100
Fe^{2+}	$FeSO_4$	500	+1.3	300
Fe^{3+}	$Fe(NH_4)(SO_4)_2$	10	100	0
Pb^{2+}	$Pb(C_2H_3O_2)_2$	500	−0.2	500[b]
I^-	NaI	100	−1.2	75
$Cr_2O_7^{2-}$	$K_2Cr_2O_7$	25	>100	0
WO_4^{2-}	Na_2WO_4	500	+1.8	300[b]
MoO_4^{2-}	Na_2MoO_4	13	+1.0	15[b]
MnO_4^-	$KMnO_4$	25	>100	0
VO_3^-	NH_4VO_3	10	1.1	10
SO_3^{2-}	Na_2SO_3	100	−70	1
$S_2O_3^{2-}$	$Na_2S_2O_3$	100	−97	0
SCN^-	NH_4SCN	500	−1.4	300

[a] Non-interference based on error less than 3 times relative standard deviation, *i.e.* 1.1%.
[b] Precipitate removed by centrifugation prior to absorbance measurement.

and perchlorate. The interfering ions or ions requiring additional treatment are listed in Table I.

Precision

An estimate of the precision obtainable with this proposed ultraviolet method was determined by performing a series of 8 determinations of 3 p.p.m. of nitrite. An average absorbance of 0.496, a standard deviation of $1.7 \cdot 10^{-3}$ absorbance unit, and a percentage relative standard deviation of 0.35% were obtained. In an analogous precision study 8 reagent blank solutions were prepared and their absorbances measured. An average absorbance of 0.005, a standard deviation of $1.5 \cdot 10^{-3}$ absorbance unit, and a percentage relative deviation of 0.3% were obtained. According to Kaiser's[27] criteria for detection limit, 0.057 μg of nitrite per ml can be detected.

SUMMARY

An ultraviolet spectrophotometric study of 4-nitrosoantipyrine has resulted in the development of a method for the determination of 0.1–12 p.p.m. of nitrite. The recommended procedure is rapid and simple, and yields very reproducible results. The molar absorptivity for the proposed method is $7.61 \cdot 10^3$ l mole^{-1} cm^{-1} at 343 nm. The detection limit is 0.057 μg of nitrite per ml.

RÉSUMÉ

Une étude par spectrophotométrie dans l'ultraviolet a été effectuée sur la nitroso-4-antipyrine; ce qui a permis de développer une méthode de dosage de 0.1 à 12 p.p.m. de nitrite. Ce procédé est rapide, simple et fournit des résultats très reproductibles. Le coefficient d'absorption molaire est de 7.61×10^3 l mol^{-1} cm^{-1}, à 343 nm. La limite de détection est de 0.057 μg de nitrite par ml.

ZUSAMMENFASSUNG

Ultraviolett-spektrophotometrische Untersuchungen an 4-Nitrosoantipyrin führten zur Entwicklung einer Methode für die Bestimmung von 0.1–12 p.p.m. Nitrit. Das empfohlene Verfahren ist schnell, einfach und hat sehr gut reproduzierbare Ergebnisse. Der molare Extinktionskoeffizient ist $7.61 \cdot 10^3$ l mol^{-1} cm^{-1} bei 343 nm, die Nachweisgrenze 0.057 μg Nitrit pro ml.

REFERENCES

1 P. GRIESS, *Ber.*, 12 (1879) 426.
2 R. WARINGTON, *J. Chem. Soc.*, 39 (1881) 229.
3 M. L. ILOSVAY, *Bull. Soc. Chim.*, 2 (1889) 388.
4 M. B. SHINN, *Ind. Eng. Chem., Anal. Ed.*, 13 (1941) 33.
5 N. F. KERSHAW AND N. S. CHAMBERLAIN, *Ind. Eng. Chem., Anal. Ed.*, 14 (1942) 312.
6 H. BARNES AND A. R. FOLKARD, *Analyst*, 76 (1951) 599.
7 F. G. GERMUTH, *Ind. Eng. Chem., Anal. Ed.*, 1 (1929) 28.
8 J. C. GIBLIN AND G. CHAPMAN, *Analyst*, 61 (1936) 686.
9 E. E. GARCIA, *Anal. Chem.*, 39 (1969) 1605.
10 A. KIERUCZENKO, *Chem. Anal. (Warsaw)*, 12 (1967) 1031.
11 B. F. RIDER AND M. G. MELLON, *Ind. Eng. Chem., Anal. Ed.*, 18 (1946) 96.
12 E. SAWICKI, T. W. STANLEY, J. PFAFF AND A. D'AMINCO, *Talanta*, 10 (1963) 641.
13 E. SAWICKI, T. W. STANLEY, J. PFAFF AND H. JOHNSON, *Anal. Chem.*, 35 (1963) 2183.
14 A. D. ALTSHULLER AND A. F. WARTBURG, *Anal. Chem.*, 32 (1960) 174.
15 J. H. WETTERS AND K. L. UGLUM, *Anal. Chem.*, 42 (1970) 336.
16 J. M. PAPPENHAGEN AND M. G. MELLON, *Anal. Chem.*, 25 (1953) 341.
17 D. F. KUEMMEL AND M. G. MELLON, *Anal. Chem.*, 28 (1956) 1674.
18 M. ZIEGLER AND O. GLEMSER, *Z. Anal. Chem.*, 144 (1955) 190.
19 J. H. WIERSMA, *Anal. Lett.*, 3 (1970) 123.
20 T. AKIYAMA AND S. MATSUMURA, *Kazoto Yakka Daigaku Gakubo*, 14 (1966) 37.
21 M. F. SCHAAK, *Amer. J. Pharm.*, 66 (1894) 321.
22 L. KNORR, *Ber. Deut. Chem. Ges.*, 17 (1884) 546.
23 M. C. SCHUYTEN, *Chemiker Ztg.*, 20 (1896) 723.
24 M. A. EL F. IBRAHIM, H. A. EL-MANGOURI AND Y. M. ABOU-ZIED, *Boll. Chim. Farm.*, 101 (1962) 603.
25 L. LANG (Editor), *Absorption Spectra in the Ultraviolet and Visible Region, Vol. VI*, Academic Press, New York, 1965, pp. 193, 194.
26 Z. PEREZ, M., *Acta Cient. Compostelana*, 5 (1968) 159; *Chem. Abstr.*, 73 (1970) 2697p.
27 H. KAISER, *Anal. Chem.*, 42 (4) (1970) 26A.

Analytica Chimica Acta
Elsevier Publishing Company, Amsterdam
Printed in The Netherlands

AUTOMATIC QUANTITATIVE INFRARED ANALYSIS OF MEPROBAMATE. BIPHASIC METHOD

JAMES A. RYAN, EUGENE McGONIGLE AND JOSEPH M. KONIECZNY

Department of Pharmaceutical Research and Development, Merck Sharp & Dohme Research Laboratories, Division of Merck and Company, Inc., West Point, Pa. 19486 (U.S.A.)

(Received 10th December 1970)

A need has become increasingly apparent in recent years for analytical methods capable of producing rather large volumes of data coupled with high selectivity of measurement. This is particularly true in the drug industry where automatic analysis systems have been employed to measure functional groups or changes in a structural moiety by application of colorimetric reactions[1,2]. There are instances when few or no colorimetric, fluorescence or ultraviolet detection techniques are available or when development time is limited. In other cases, the selectivity of existing methods is not adequate. A research infrared spectrophotometer which can operate with sufficient stability in the absorbance *vs.* time mode at fixed wavelength may be directly applicable to filling this need when used as a detector for autoanalysis. This concept dates to 1964[3]. Remote stripchart recorders may be applied to certain spectrophotometers lacking this mode. Ordinate scale expansion may be desirable.

Several authors have reported the use of infrared measurement of on-stream organic solutions. An example is the work of Carr-Brion and Gadsden[4]. These methods were generally oriented toward process control and had limited frequency capability in the infrared range.

An important advantage of the proposed method over that of Carr-Brion and Gadsden is that a two-phase system is employed, offering automatic extraction and analysis. The biphasic feature makes possible modifications which could result in separations from interfering components in mixtures, and allows an increase in the effective sensitivity by concentrating the compound to be determined. The method also involves the use of equipment already available in many laboratories and requires little modification. Another feature is that structurally specific infrared bands may be chosen. These structural frequency assignments are, of course, usually well supported by literature references.

Several authors[5,6] have emphasized the fact that infrared quantitative methods may be successfully applied to analyses in which the material to be determined is present at low concentration levels. The use of cell pathlengths in excess of the usual 1 mm can be noted in these papers. In an application of infrared analysis to steroid esters, it has been shown[7] that provided the proper solvent is selected, adequate energy transmission for quantitative work can be obtained over much of the fundamental infrared when 3-mm pathlength cells are used. Provided that these energy considerations as well as solubility and concentration effects are considered, there is little reason to doubt that many quantitative infrared methods already published could be successfully automated by this general technique.

Determination of meprobamate

Meprobamate (2-methyl-2-propyl-1,3-propanediol dicarbamate) was measured by infrared spectrophotometry by employing a band near 6.32 μm[8]. Ryan[9] proposed a measurement of the carbamate carbonyl near 1728 cm^{-1} in chloroform solution as a method offered for inclusion in USP XVII in 1961. This band affords greater sensitivity and is free from water interference; a relative standard deviation of about $\pm 1\%$ was obtained. Hamilton[10] recently reported a similar procedure.

Development of method

The initial application of the method was intended for the determination of meprobamate resulting from dissolution studies of pharmaceutical dosage forms in aqueous media. Direct determination in aqueous solution was obviously not considered owing to high infrared absorption. The problems caused by moisture which had to be overcome in order to complete the analysis successfully were two-fold: absorption cell deterioration had to be prevented and the presence of appreciable amounts of water which might act as a variable interference, had to be avoided. These problems were overcome by extraction of an aqueous solution of the meprobamate with chloroform. Dilution of the initial chloroform extract served to prevent cell etching. To prevent excessive mixing in the cell while maintaining the desirable 3-mm path, a minimum volume 3-mm cell was constructed as shown in Fig. 1.

Early work involved the use of methylene chloride as an organic phase;

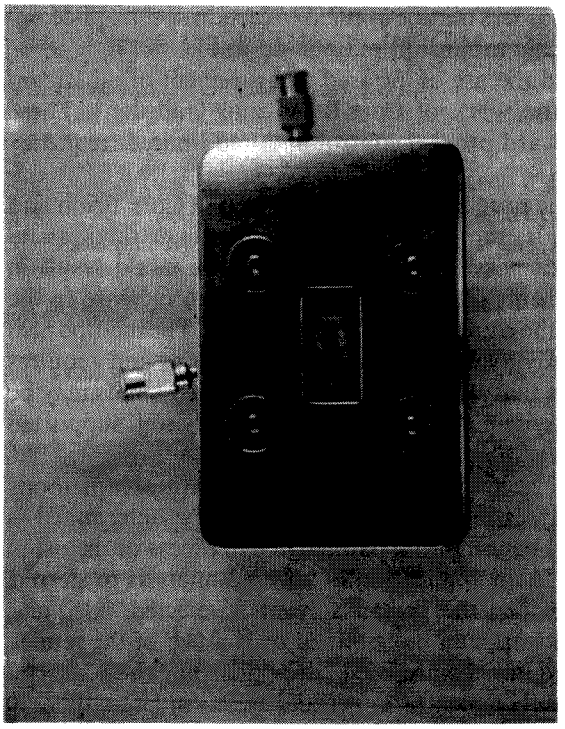

Fig. 1. Minimum volume 3-mm pathlength cell.

however, it was found to cause air bubbles in the transmission tubes which resulted in an erratic baseline.

EXPERIMENTAL

Construction of 3-mm cell

An ordinary demountable cell mount was used with 25.2 mm diameter × 5 mm thick NaCl windows. A lead spacer of the same diameter was used. The lead was cast around two luer lock syringe needles to provide solvent flow. A beam aperture of about 2.5 mm × 9 mm placed an estimated 0.68 ml of solution in the beam at one time. The cell was sealed by amalgamation.

Instruments

Technicon Controls AutoAnalyzer components (Technicon Instruments Corp., New York) were used including a Sampler II and proportioning pump. A Perkin-Elmer Model 521 Infrared Spectrophotometer was employed, equipped with the specially-fabricated flow cell.

Acidflex tubing was used throughout except where noted.

Reagents and standards

The purge solvent consisted of 5% methanol in ethanol.

For standards, an accurately weighed 50-mg portion of meprobamate was transferred to a 50-ml volumetric flask, dissolved in 0.1 *M* hydrochloric acid, with mild heating and stirring, cooled and diluted to volume with the same solvent. Individual serial dilutions of 6, 8, 10 and 12 ml of this solution were diluted to 50-ml volumes with the 0.1 *M* hydrochloric acid.

Samples

Samples such as those from dissolution studies were prepared at a concentration level of about 0.2 mg ml^{-1} in 0.1 *M* hydrochloric acid.

Procedure

The AutoAnalyzer equipment was assembled as shown in Fig. 2. The system was flushed with distilled water, followed by 5% methanol in ethanol. Chloroform (Merck reagent-grade) was then introduced into those tubes that would be pumping chloroform; after several minutes 0.1 *M* hydrochloric acid was introduced into the "aqueous" tubing and the system was allowed to come to equilibrium. The preceding steps were conducted before connection of the flow cell to prevent severe damage to the salt cell window resulting from its exposure to significant amounts of water or methanol–ethanol. When only the chloroform phase was exiting through the glass tubing leading to the flow cell, it was connected with acidflex tubing. The sampler was then activated at a sampling rate of 20 per h. The standards and samples in a predetermined order were then started through the system. Sampling cups (8.5 ml) were alternated with 0.1 *M* hydrochloric acid to serve as a wash. A 0.2 mg ml^{-1} standard solution was inserted after every fourth sample to allow compensation for drift or other variations. A reproduction of the spectral record of standard data used in the measurement of precision may be seen in Fig. 3. A relative standard deviation of ±1.08% was obtained.

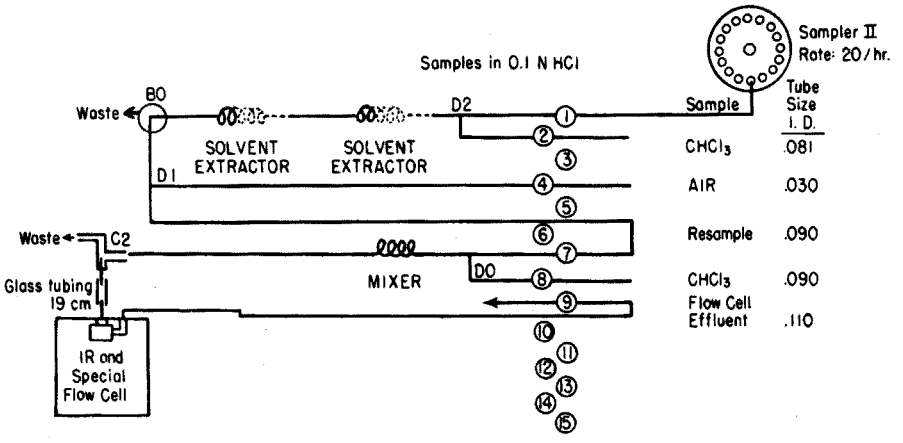

Fig. 2. Autoanalyzer flow diagram for meprobamate.

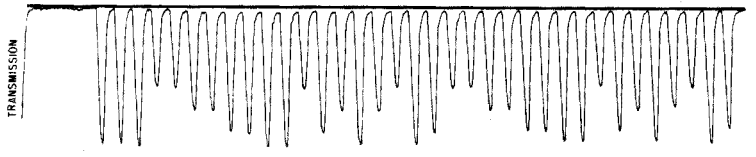

Fig. 3. Spectral record of meprobamate standards at various concentrations.

Route of sample. A portion of the sample solution was drawn through the proportioning pump and extracted with chloroform. After separation, the organic phase was diluted and passed into the spectrophotometer cell for measurement of absorbance.

Spectrophotometer parameters. The following parameters were found adequate for the equipment used.

Amplifier—balanced
Slits—fixed at 206 μm
Attenuator speed 780
Gain 6.2

Scan clutch—out
Frequency—fixed at 1728 cm^{-1}

Attenuation—adjust AT-02 (Attenuator R.I.I.C.) as required (see Fig. 3) for proper baseline position

Source 0.78 A
Suppression 4.5
Chart—absorbance ordinate
Scan time—internal gears adjusted for slow abscissa travel

Scale expansion—2 × to 4 × as required for adequate chart presentation of absorption peaks in ordinate direction

SUMMARY

The construction of a long-path, minimal-volume infrared cell has made

possible the use of a research infrared spectrophotometer as a detector system for automatic analyzer system. Application to the automated assay of meprobamate is described. The method involves aqueous solutions of the drug, such as those resulting from dissolution studies of pharmaceutical dosage forms, and extraction into chloroform before measurement. A relative standard deviation of $\pm 1.08\%$ was obtained. Sample measurement rate was about 20 per h.

RÉSUMÉ

On propose un système permettant l'utilisation d'un spectrophotomètre infrarouge comme détecteur pour l'analyse automatique. Un dosage de méprobamate est décrit, avec extraction préalable de cette drogue dans le chloroforme. Vingt déterminations peuvent être effectuées par heure, avec une déviation standard relative de $\pm 1.08\%$.

ZUSAMMENFASSUNG

Der Bau einer Infrarotküvette für langen Lichtweg bei kleinstem Volumen ermöglichte die Anwendung eines Forschungs-Infrarotspektrophotometers als Detektorsystem für einen automatischen Analysator. Die Anwendung auf die automatisierte Probe auf Meprobamat wird beschrieben. Bei der Methode wird das Arzneimittel aus wässrigen Lösungen, wie sie sich bei Auflösungsuntersuchungen an pharmazeutischen Dosierungsformen ergeben, mit Chloroform extrahiert und dann gemessen. Es wurde eine relative Standardabweichung von $\pm 1.08\%$ erhalten. Pro Stunde konnten etwa 20 Proben gemessen werden.

REFERENCES

1 D. MERCALDO AND F. GALLO, *Abstracts, N.Y.A.S. Second Conference on Automation, March, 1967.*
2 J. R. LANE AND P. J. WEISS, *Automation in Analytical Chemistry, Vol. 1*, Mediad Inc., 1966, p. 224.
3 J. A. RYAN, Wyeth Laboratories, Radnor, Pa., unpublished work, 1964.
4 K. G. CARR-BRION AND J. A. GADSDEN, *J. Sci. Instr.*, 2 (1969) 155.
5 L. HAHN AND L. PAULING, *Anal. Chem.*, 40 (1948) 1283.
6 R. K. RITCHIE AND D. KULOWIC, *Anal. Chem.*, 40 (1948) 1283.
7 J. A. RYAN, L. J. CALI AND E. MCGONIGLE, *Anal. Chim. Acta*, 54 (1971) 105.
8 W. R. MAYNARD, JR., *J. Assoc. Offic. Agr. Chemists*, 43 (1960) 791.
9 J. A. RYAN, Wyeth Laboratories, Radnor, Pa., unpublished work, 1961.
10 J. L. HAMILTON, JR., *J. Assoc. Offic. Agr. Chemists*, 53 (1970) 594.

Analytica Chimica Acta
Elsevier Publishing Company, Amsterdam
Printed in The Netherlands

SPECTROPHOTOMETRIC DETERMINATION OF VANADIUM AND IRON WITH β-ISOPROPYLTROPOLONE

O. MENIS AND C. S. P. IYER*
Analytical Chemistry Division, National Bureau of Standards, Washington, D.C. 20234 (U.S.A.)
(Received 30th November 1970)

A new spectrophotometric procedure has been developed for the determination of vanadium and for the simultaneous determination of vanadium and iron with β-isopropyltropolone (IPT). Also known as thujplacin, the reagent was first described by Japanese workers[1,2]. The formation of stable complexes with various metals by this reagent has been reported by several authors[3-10]. Dyrssen has studied extensively the extraction equilibria of twenty-seven metal ions in the IPT–chloroform system[4,5,8]. However, vanadium was not included in these studies. In the work described here, it was observed initially that vanadium gave a color reaction with IPT and that the reaction rate of the colored complex was slow. To overcome this problem, the procedure was modified to include the addition of an alcoholic solution of IPT to the aqueous medium. Under these conditions, equilibrium was attained rapidly within 30 min. This modification was applied to the determination of low concentrations of vanadium in steels.

Vanadium, an important addition to certain types of steels, high-temperature alloys, and reactor materials, is generally determined at high concentrations by titrimetric methods and by spectrophotometry in low concentrations or trace quantities. The literature on this subject has been summarized[11]. Separation and spectrophotometric determinations are discussed by Sandell[12].

In the present studies, it was established that IPT forms a colored complex with vanadium which can be extracted from strong acid solutions, thus eliminating a large number of interferences. However, in ferrous analyses, a mercury cathode separation is recommended for the removal of high concentrations of iron and chromium. Complete separation from iron is not essential since a two-wavelength measurement provides a precise correction. NBS Standard Reference Materials of ferrous metals containing traces of vanadium were tested to establish accuracy of the method.

EXPERIMENTAL

Apparatus

Spectrophotometric measurements were made on a quartz prism spectrophotometer with matched 1-cm cells. Spectra scanning was conducted on a dual-grating spectrophotometer. The absorption cells were thermostated at constant

* Present address: 54 Kenilworth, Peddar Road, Bombay 26, India.

temperature. The wavelength scale of the spectrophotometer was verified with a neodymium glass standard. pH measurements were made with an expanded scale pH meter. Studies of the effect of temperature were carried out in a water-jacketed separatory funnel controlled by a constant temperature bath.

Reagents

Standard vanadium solution (100 $\mu g\ ml^{-1}$) was prepared by dissolving 0.2295 g of reagent-grade ammonium metavanadate in water and diluting to 100 ml. Aliquots of this solution were diluted to provide a solution containing 10 μg V ml^{-1}.

β-Isopropyltropolone (IPT) was recrystallized twice from petroleum ether. The purity was tested by determining the m.p. (51°–52°) and by taking a thin-layer chromatogram on a silica impregnated plate with butanol, water and ethanol as the developer in the ratio of 5:11:4. A stock solution of 10^{-1} *M* IPT was prepared by dissolving 16.42 g of IPT in alcohol and diluting to 1 l. When necessary, appropriate dilutions were made with alcohol.

Spectra of the reagent and the complexes of V(V), V(IV), Fe(III) and Fe(II) (not shown) with IPT were taken after the aqueous phase of the particular element in the desired valence state had been extracted with 5 ml of $2 \cdot 10^{-2}$ *M* IPT in chloroform, the aqueous phase being maintained at an acidity of 1 *M* perchloric acid. Spectra of the organic extract were scanned from 400–650 nm and are shown in Fig. 1.

Analysis of ferrous alloys

Dissolve 1 g of sample in 10 ml of nitric acid (3:5). After the reaction subsides, add 5 ml of perchloric acid and fume the solution twice to remove nitric acid. Remove any silica by filtration and wash with dilute perchloric acid (1:100). Dilute the solution to 200 ml and reduce electrolytically overnight with a mercury cathode at 10 A. Transfer the solution to a beaker and boil. Add 5 ml of the nitric acid to the boiling solution to oxidize vanadium to the pentavalent state. Then evaporate the solution to dryness and dilute to 100 ml with 1 *M* perchloric acid. Transfer an aliquot representing 20–25 μg of vanadium to a separatory funnel, adjust the acidity to 1 *M* in perchloric acid and add 2 ml of $5 \cdot 10^{-2}$ *M* IPT in alcohol. Extract this solution with 5 ml of chloroform which has been preequilibrated with a solution containing the same volumes of alcohol and acid as the sample. Measure the absorbances at 470 nm and 540 nm. Make any necessary corrections for iron and calculate the percent vanadium in the sample.

Effect of variables

Effect of acidity. Extractions were conducted on solutions adjusted to pH 0–7, as well as 0.1–2 *M* perchloric acid. No change of absorbance was noted when measured at 470 nm over this acidity range. The ionic strength of the aqueous phase from 0.1 to 7 by the addition of sodium perchlorate did not affect the absorbance of the complex.

Effect of alcohol addition. Initial studies with IPT in chloroform solutions showed that the color development for the vanadium and iron complexes required more than 24 h for full development. The rate of the formation of the colored vanadium species was considerably faster than that of the iron complex. Three hours after extraction of the organic phase, only 90% of the vanadium and 50% of the iron complexes were formed. However, on addition of the alcoholic solution of IPT, the color

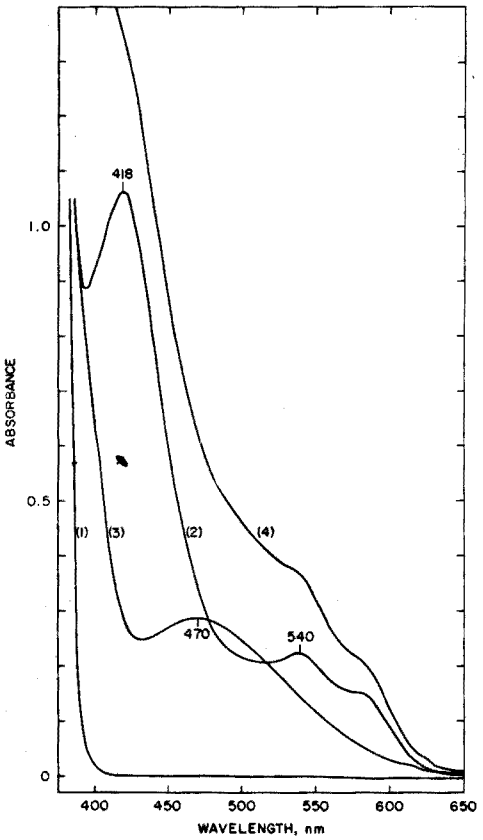

Fig. 1. Spectra of β-isopropyltropolone complexes in chloroform. (1) Reagent ($2 \cdot 10^{-2}$ *M*); (2) iron(III)–IPT complex; (3) vanadyl–IPT complex; (4) iron(III) + vanadyl–IPT complex.

development for both complexes reached a maximum within 2–30 min and remained constant over 24 h.

Effect of temperature. Temperatures of 15°, 25°, 35° and 45° were tested for the extraction and measurement of the absorbance of the vanadium complex. There was a relative increase of absorbance with an increase in temperature. However, it was more difficult to separate the phases at high temperatures. All extractions were therefore carried out at 25° ± 1°.

Effect of reagent concentration. A 2:1 ratio of metal ion to ligand was observed on the addition of $1 \cdot 10^{-3}$ *M* IPT in alcohol to $1 \cdot 10^{-3}$ *M* vanadyl solution. In all extraction work, a 5–10-fold excess of organic ligand was used. At higher ligand concentration, 0.1 *M*, side reactions were observed, involving the reduction of vanadium(V) to vanadium(IV).

Effect of diverse ions. Spectra of reactant solutions containing 1 mg of diverse ions and 20 μg of vanadium were scanned to determine their relative interferences. Nickel(II), chromium(III), molybdenum(VI) and zirconium(IV) did not interfere, while chromium(VI), iron(III) and titanium(IV) did interfere. The interference of chromium(VI) can be overcome by reduction to chromium(III). Titanium–IPT does

not absorb at 540 nm. Vanadium, however, can be measured without interference at this wavelength. Up to 50 μg of titanium can be tolerated even when measurements are made at the vanadium peak at 470 nm. Fluoride, sulfate, phosphate and tartrate do not interfere.

Preparation of calibration curves

Vanadium. Use 20–50 μg of vanadium in 1 *M* perchloric acid and add 2 ml of $1 \cdot 10^{-2}$ *M* IPT in alcohol. Preequilibrate chloroform with the same volumes of alcohol, water and acid as are used for the samples. Extract with 5 ml of this pre-equilibrated chloroform by shaking for 2 min and allowing to settle for 30 min. Measure absorbances at 470 nm, and 540 nm (Table I).

Iron. Proceed in the same way as above, using 20–50 μg of iron(III) (Table I).

Additive properties of iron and vanadium complexes. Absorbances of the vanadium and iron complexes with IPT were additive (Table II).

DISCUSSION

In the search for a method for the determination of microgram quantities of vanadium, preliminary tests indicated that its β-isopropyltropolone chelate could be extracted from strongly acid media. From the extensive studies by Dyrssen of the IPT metal complexes, it was expected that only iron, uranium, copper and thorium would interfere[5]. Dyrssen also reported that the extraction of the iron was slow, taking more than 4 days to reach completion. In the current studies it was found that vanadium, while not as slow to reach equilibrium, required 24 h to develop the colored

TABLE I

CALIBRATION CURVE FOR VANADIUM AND IRON β-ISOPROPYLTROPOLONE

V (μg)	*Absorbance at 470 nm*	*Fe* (μg)	*Absorbance at 470 nm*
Blank	0.004	Blank	0.003
10	0.172	10	0.174
20	0.342	20	0.357
30	0.511	30	0.517
50	0.861	50	0.861
Least square slope:	0.0174 ± 0.0001		0.0171 ± 0.0001

TABLE II

ADDITIVE PROPERTIES OF VANADIUM– AND IRON–IPT COMPLEXES

Concn. (*V* + *Fe*) (μg)	*Absorbance* (470 *nm*)			*Absorbance* (540 *nm*)		
	Found	*Calc.*	*Diff.*	*Found*	*Calc.*	*Diff.*
10+10	0.354	0.354	0.00	0.200	0.198	0.002
20+20	0.712	0.703	0.09	0.412	0.397	0.005
25+25	0.885	0.886	0.001	0.503	0.494	0.009

complex fully when measured at 470 nm. In the case of $Fe(IPT)_3$, Dyrssen postulated from spectrophotometric data that the slow step was $Fe(IPT)_2^+ + IPT = Fe(IPT)_3$.

The addition of alcohol to the two-phase system enabled the measurement of the complex within 30 min. Iron, however, under these conditions also reached equilibrium rapidly. Therefore, because of its interference, it must be eliminated by mercury cathode electrolysis, or if present in correspondingly trace quantities, corrected from two wavelength measurements. In Fig. 1, the spectra of the iron(III) and vanadyl complexes are additive and the two can be simultaneously determined by measuring at two wavelengths: 470 and 540 nm when the ratio of $VO_2^+ : Fe^{3+}$ is one or at 418 and 470 when the ratio of $VO_2^+ : Fe^{3+} \geqq 10$.

When several reaction media were evaluated, the mixed solvent system, by the addition of 0.01 *N* HIPT in alcohol to a 1 *M* perchloric acid solution of the sample followed by extraction with preequilibrated chloroform proved to yield the most satisfactory results. It has the advantage of speed and best precision and accuracy. Of the other choices, the direct measurement in the aqueous media suffered from lower sensitivity and instability, the complex decomposing with time. The other possibility, the extraction of HIPT into chloroform solution is a slow process, especially when iron is present. A more rapid extraction rate of the vanadyl complex can be attained by increasing the concentration of HIPT from 0.01 to 0.1 *M*. However, even in this case the extraction time has to be at least 1 h. Under those conditions a fairly stable solution is obtained, the absorbance increasing at a rate of *ca.* 2.5 % per h, and reaching equilibrium only after 29 h. In another study[13] with radioactive tracer ^{49}V, it was shown that extraction is complete in 5 min. The slow step, therefore, is assumed to be the formation of the final absorbing adduct VO_2^+ IPT–HIPT. The extraction with chloroform alone therefore suffers from the disadvantage of slow reaction and also incomplete extraction of iron. At high reagent concentration, 0.1 *M* or higher, the extraction proceeds rapidly, but because of side reaction with the reagent a green VO^+ complex forms, and leads to imprecision. This effect becomes especially evident with a reagent which is over one week old. This evidence leads one to postulate that decomposition products of the reagent contribute to the reduction of the vanadyl ion and cause erratic results. With the recommended procedure only 2 min for color development is required, and the colored complex is relatively stable. For best precision, however, the absorbance should be measured within 30–60 min, since there is still a slow increase of absorbance at the rate of 1 % per h. Data presented in Table I indicate a relative standard deviation of better than 1 % for the slope of the Beer's law

TABLE III

ANALYSIS DATA ON NBS STANDARD REFERENCE MATERIALS

SRM[a]	*Vanadium (p.p.m.)*	
	Found	*Certified*
8i, Bessemer steel	1165 ± 13[b]	120_0
30e, Low alloy steel	1507 ± 13	149_0
30f, Low alloy steel	1790 ± 17	180_0

[a] Three determinations for each sample.
[b] Standard deviation of a single determination.

plot of the vanadium and iron complexes, and Table II shows the agreement of the additive absorbances on the two metals. The procedure was evaluated for precision and accuracy by an analysis of NBS Standard Reference Materials (Table III). The method is relatively simple. A relative standard deviation of better than 1% on a number of ferrous materials was obtained for trace quantities of vanadium.

The assistance of E. R. Deardorff in carrying out some of the experimental work is acknowledged.

SUMMARY

A spectrophotometric procedure is described for the determination of vanadium and for the simultaneous determination of iron and vanadium by means of two wavelength measurements, at 470 and 540 nm or 418 and 470 nm. It is based on the formation of chelate complexes with β-isopropyltropolone. The complex is extracted with chloroform and in the presence of alcohol the color develops rapidly and is stable for at least 24 h. The precision of the calibration curve is 1% relative standard deviation. The application to the analysis of NBS Standard Reference Material steel samples is presented.

RÉSUMÉ

Une méthode spectrophotométrique est décrite pour le dosage du vanadium et pour le dosage simultané fer–vanadium; on effectue les mesures à deux longueurs d'onde: 470 et 540 nm ou 418 et 470 nm. Ce procédé est basé sur la formation de chélates avec la β-isopropylropolone. Le complexe est extrait dans le chloroforme; en présence d'alcool, la coloration se développe rapidement; elle est stable pendant 24 h au moins. La précision de la courbe d'étalonnage est de 1% de déviation relative standard. On donne les résultats obtenus avec des substances de référence NBS.

ZUSAMMENFASSUNG

Es wird ein spektrophotometrisches Verfahren beschrieben für die Bestimmung von Vanadin und für die Simultanbestimmung von Eisen und Vanadin mit Hilfe von Messungen bei zwei Wellenlängen, nämlich bei 470 und 540 nm oder 418 und 470 nm. Die Methode beruht auf der Bildung von Chelatkomplexen mit β-Isopropyltropolon. Der Komplex wird mit Chloroform extrahiert; in Gegenwart von Alkohol entwickelt sich die Färbung schnell und ist für wenigstens 24 h beständig. Die Reproduzierbarkeit der Eichkurve beträgt 1% relative Standardabweichung. Über die Anwendung auf die Analyse von NBS-Standard-Stahlproben wird berichtet.

REFERENCES

1 T. Nozoe, *Bull. Chem. Soc. Japan*, 11 (1936) 295.
2 T. Nozoe, *J. Pharm. Soc. Japan*, 3 (1949) 174.
3 K. Pan and T. M. Hsew, *J. Chinese Chem. Soc., Ser. II*, 2, No. 1 (1955) 23.
4 D. Dyrssen, *Acta Chem. Scand.*, 15 (1961) 1614.

5 D. DYRSSEN, *Trans. Roy. Inst. Technol. (Stockholm)*, 1962, No. 188.
6 T. M. HSEW, *J. Chinese Chem. Soc., Ser. II*, 7, No. 2 (1960) 124.
7 D. DYRSSEN, *Acta Chem. Scand.*, 16 (1962) 785.
8 D. DYRSSEN, *Extraction of Metal Ions with Chelating Acids*, 16th Annual Anal. Summer Symposium, Tucson, Arizona, 1962.
9 Y. DUTT AND R. P. SINGER, *Indian J. Chem.*, 4 (1966) 424.
10 B. P. GUPTA, Y. DUTT AND R. P. SINGER, *Indian J. Chem.*, 5 (1967) 214.
11 I. M. KOLTHOFF AND P. J. ELVING, *Treatise on Analytical Chemistry*, Part II, Vol. 8, Interscience, New York, p. 180.
12 E. B. SANDELL, *Colorimetric Determination of Traces of Metals*, 1959, Interscience, New York, p. 923.
13 B. E. MCCLELLAN AND O. MENIS, *Anal. Chem.*, 43 (1971) 436.

Analytica Chimica Acta
Elsevier Publishing Company, Amsterdam
Printed in The Netherlands

THE DETERMINATION OF SMALL AMOUNTS OF SULPHUR IN COPPER

H. PUGH AND W. R. WATERMAN
Imperial Metal Industries Ltd., Witton, Birmingham B6 7BA (England)
(Received 1st March 1971)

The determination of sulphur at about the 2–50 p.p.m. level in any metallurgical material presents a problem, and whilst existing procedures[1,2] provide useful information, occasions arise when it is necessary to know the sulphur content of copper within closer limits than can be established by the usual laboratory methods.

Sulphur is frequently determined in copper by a procedure in which the sample is heated at about 1150° in oxygen; oxides of sulphur in the evolved gas can be determined in several ways, *e.g.* by titration with a standard borate solution. Such methods are satisfactory, provided that standard samples of known sulphur content are available, and the sulphur content of the sample is greater than about 50 p.p.m.

In this combustion procedure, the provision of standard samples is necessary for calibration purposes, because conversion of the sulphur to oxides of sulphur is not quantitative. The efficiency of the reaction, which is usually between 80 and 90%, is variable, though reasonably constant for any prescribed set of conditions, and this enables an empirical factor to be used.

For samples in which the sulphur contents are below about 50 p.p.m., the combustion–borate titration method has known limitations, *e.g.* the volume of titrant, even with a very dilute (0.005 *N*) sodium borate solution, is small, and the colour change of the indicator at the end-point is difficult to establish with reasonable accuracy.

If the weight of sample exceeds about 2 g, the resulting copper oxide, which becomes molten at the combustion temperature, has an increased tendency to penetrate the combustion boat and damage the combustion tube; this imposes a practical limitation on the weight of sample that can be used.

Sulphur has been determined in copper at levels below 50 p.p.m., by means of a combustion–titrimetric method in which the titrant is very dilute, *e.g.* 0.0007 *N* potassium iodate solution[3]. Our experience with this alternative iodimetric method, especially in view of the equally uncertain end-point of the titration, has not been entirely satisfactory.

An alternative and more sensitive approach involves a direct procedure in which sulphur in the sample is evolved as hydrogen sulphide[1]. The sample is dissolved in a mixture of nitric and hydrochloric acids, which oxidises the sulphur to sulphate, and the excess of nitric acid is decomposed by formic acid. The sulphate is reduced by boiling the solution with a mixture of hydriodic and hypophosphorous acids, and the evolved hydrogen sulphide is scrubbed, then absorbed in a zinc acetate solution, and finally determined colorimetrically by the methylene blue method. It is claimed that the method is capable of determining down to about 5 p.p.m. of sulphur in copper,

but it is time-consuming, and the reagents have to be purified by distillation to obtain satisfactory blank values.

In preliminary trials with this method, difficulty was experienced in obtaining reproducible sulphur values, and in preparing the calibration graph the final absorbances showed wide variations. It is known that the conditions for obtaining quantitative evolution and absorption of the hydrogen sulphide are critical, particularly the amount of water present in the distillation flask, and it was established that the major difficulty in applying this procedure is associated with this distillation stage. Experimental work with this method was, therefore, discontinued.

Barabas and Kaminski[3] have described another method for the determination of sulphur in copper, in which the sample is heated at a high temperature in an atmosphere of oxygen. The evolved sulphur dioxide is absorbed in a sodium tetrachloromercurate solution, and the product is reacted with *p*-rosaniline hydrochloride and formaldehyde, to form a purple sulphonic acid derivative of *p*-rosaniline[4]. This procedure was chosen for further investigation.

Feigl[5] states that when sulphite is added to a mercury(II) solution, the very stable disulphitomercurate(II) ion, $Hg(SO_3)_2^{2-}$, is formed. West and Gaeke[6] made a detailed investigation of this reaction, and found that the disulphitomercurate(II) ion is most stable in a solution of mercury(II) chloride and sodium chloride of molar ratio 1:2, *i.e.* sodium tetrachloromercurate.

The reaction involved in the absorption of sulphur dioxide in a solution of sodium tetrachloromercurate, is thought to be as follows:

$$HgCl_4^{2-} + 2\,SO_2 + 2\,H_2O \rightarrow Hg(SO_3)_2^{2-} + 4\,Cl^- + 4\,H^+$$

West and Gaeke further showed that potassium permanganate oxidises this complex only at a very slow rate, and that when air is bubbled for several hours (at about 2 l min^{-1}) through 0.1 *M* sodium tetrachloromercurate solution containing about 250 μg of sulphur dioxide, there is no detectable oxidation of the disulphitomercurate(II) complex.

EXPERIMENTAL

Apparatus

This is shown schematically in Fig. 1.

1. Compressed-air supply to give a steady flow of 2 l min^{-1}, via a reduction valve.
2. Fine-control needle valve.
3. Purification tower, containing soda asbestos (6–12 mesh), and then silica gel (self-indicating, 6–12 mesh).
4. Flowmeter (0.4–4 l min^{-1}).
5. Air-stabilising reservoir (20-l aspirator); this also stabilises the flowmeter float. The reservoir is essential to prevent suckback during the oxidation process.
6. Translucent silica combustion tube, about 90 cm long, internal diameter about 22 mm, and reduced at the exit end to about 4 mm.
7. Tube furnace, capable of maintaining a working temperature of 1150°.
8. Plastic connecting tube of minimum length to give a butt joint between the exit of the combustion tube and the entry tube of the absorption vessel.

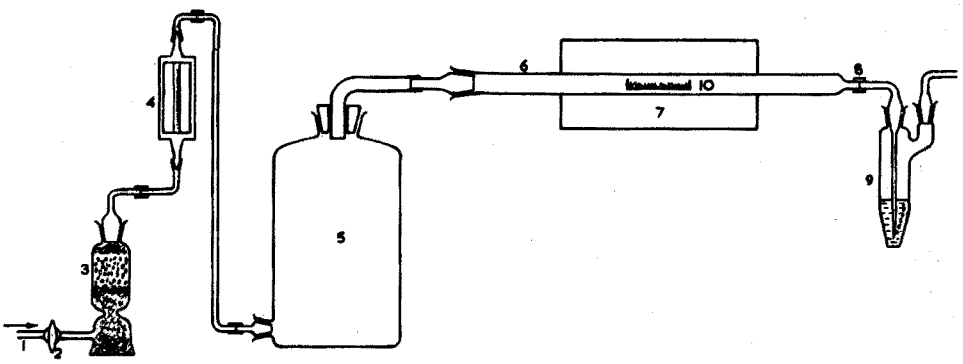

Fig. 1. Schematic outline of combustion apparatus.

9. Glass absorption vessel.

10. Refractory combustion boat, about $75 \times 15 \times 10$ mm, heated in air at 1150°, preferably overnight, then cooled in a desiccator.

Special reagents

High-purity copper. Heat vacuum-cast copper drillings in a stream of hydrogen at about 800° for several hours, then cool in an atmosphere of hydrogen. The sulphur content of this material should not exceed about 2 p.p.m. when analysed by the proposed method.

Standard sample of copper. This should be in the form of drillings or millings and the sulphur content must be known accurately and, preferably, be between 100 and 200 p.p.m.

Sodium tetrachloromercurate solution (0.2 *M*). Dissolve 23.4 g of sodium chloride in about 200 ml of water, and transfer the solution to a beaker containing 54.4 g of mercury(II) chloride. Stir to dissolve the mercury(II) chloride, dilute the solution to 1 l and mix.

p-*Rosaniline hydrochloride solution* (0.04%). Transfer 1 g of *p*-rosaniline hydrochloride to a beaker (150 ml), add 2 ml of water and stir for 1–2 min; then gradually add during stirring, 85 ml of water, and allow to stand for 24 h. Stir the solution, filter it through a Whatman No. 541 filter paper into a 100-ml calibrated flask, dilute to the mark and mix. Transfer 10.0 ml of this solution to a 250-ml calibrated flask, add 15 ml of concentrated hydrochloric acid, mix well, dilute to the mark and mix.

Formaldehyde solution (0.2%). Transfer 5.0 ml of formaldehyde solution (40% w/v) to a 1-l calibrated flask, dilute to the mark and mix.

Preparation of calibration graph

Pickle all samples of copper in nitric acid (1 + 4) for 2–3 min, to clean the surface, wash thoroughly with water, and then with acetone; dry finally in warm air, preferably from a hair dryer.

To five combustion boats, add a series of known weights of a standard copper sample, equivalent to 10.0, 20.0, 30.0, 40.0, and 50.0 μg of sulphur, and high-purity

copper so that the total weight of copper in each boat is 2 g. Proceed with each boat as follows.

Adjust the furnace temperature to 1150°, and pass purified air through the combustion tube at 2 l min^{-1} for about 30 min to condition the apparatus. Remove the furnace-tube closure, add 12 ml of the sodium tetrachloromercurate solution to the absorption vessel, and transfer the boat to the hot zone of the combustion tube. Replace the furnace-tube closure; maintain the air-flow at 2 l min^{-1} for 8 min and then, with the air still flowing, lower the absorption vessel and wash the outlet jet with water.

Transfer the contents of the absorption vessel to a 100-ml calibrated flask, rinse the vessel with a few millilitres of water, and add the washings to the calibrated flask.

Remove the furnace-tube closure and withdraw the combustion boat from the furnace.

To the calibrated flask, add 5.0 ml of the *p*-rosaniline hydrochloride solution and 5.0 ml of the formaldehyde solution; dilute to 100 ml, mix, and allow the solution to stand at room temperature for 1 h. Measure the absorbance of the solution at 560 nm, with water in the reference cell; use 20-mm cells.

Subtract the absorbance obtained on the high-purity copper, corrected for the weight taken (because it is less than 2 g) from that of the standard samples, and plot a graph of absorbance against μg of sulphur. The graph should be almost linear (there is slight curvature towards the concentration axis).

Procedure

Clean the sample as described above for the standards, and transfer 2 g of the sample to a combustion boat; use a second (empty) boat for the boat blank. Proceed exactly as described under *Preparation of calibration graph.*

Since there is a tendency for the slope of the calibration graph to change slightly, check three points on the graph (as in *Preparation of calibration graph*). These three simulated standards should contain 10, 20, and 40 μg of sulphur (corresponding to 5, 10, and 20 p.p.m. of sulphur, based on a 2-g sample). A further boat containing 2 g of the high-purity copper must also be taken through the procedure.

Evaluate the corrected absorbance of the standard samples as described under *Preparation of calibration graph*, subtract the absorbance of the boat blank from the sample, and calculate the sulphur content of the sample.

RESULTS AND DISCUSSION

Preparation of calibration graph

A calibration graph was prepared as described by Barabas and Kaminski. The standard sulphur solution (10 μg S ml^{-1}) was made by dissolving anhydrous sodium sulphite (assayed to be 99% by iodimetric titration) in water. To a series of 100-ml calibrated flasks were added 12 ml of 0.2 *M* sodium tetrachloromercurate solution, and varying amounts of the standard sulphite solution to cover the range 0–50 μg of sulphur. Colour development was carried out as described above. A slight increase (5–10%) in absorbance was found after the solution had stood for 30 min, but the absorbance then remained unchanged after 60 min. In all subsequent measurements,

therefore, absorbances were measured 1 h after the reagents had been added. The graph, which had a slight curve towards the concentration axis, was almost linear.

However, when this calibration was repeated several days later, with the original sodium sulphite stock solution (100 μg S ml^{-1}), freshly diluted to give the working solution (10 μg S ml^{-1}), the absorbances were only about half of those obtained originally. Further tests with freshly prepared sodium sulphite stock and working solutions showed that the absorbances were not reproducible on a day-to-day basis.

When the standard sulphite solution was prepared by dissolving the sodium sulphite in the sodium tetrachloromercurate solution, instead of in water, and each aliquot of the standard sulphite solution was diluted to 12 ml with the sodium tetrachloromercurate solution (it was proposed to use 12 ml of this absorption solution in all tests), the absorbances were considerably improved. The resulting calibration graph remained almost linear, but its slope was significantly higher than that obtained with the aqueous sodium sulphite solution. The difference in slope was almost certainly due to oxidation of the dilute aqueous sodium sulphite solution. The absorbance of a solution containing 50 μg of sulphur was consistently about 0.82, compared with values ranging from 0.3 to 0.5 when an aqueous sulphite solution was used—depending on the interval between preparing the sodium sulphite solution and adding the other reagents.

In the well-established combustion–titrimetric method[1], it is known that conversion of the sulphur (probably present in copper as copper(I) sulphide) to oxides of sulphur (mainly sulphur dioxide) is not stoicheiometric, and an empirical factor is usually calculated from the recovery obtained when a standard sample of copper of known sulphur content is analysed under identical conditions; in the authors' laboratory, the recovery is about 80%. It seemed, therefore, that the recovery of sulphur in the proposed procedure would be of the same order, although this is in conflict with the observations of Barabas and Kaminski[3], who claimed a 100% recovery. It is possible that a compensation of errors occurred in the earlier work, because an aqueous sulphite solution was used for calibration purposes.

To establish the extent of the conversion of sulphur to oxides of sulphur under the proposed conditions, it was necessary to analyse samples of copper with known (low) sulphur contents.

Preparation of a standard sample

Several BCS and NBS standard samples of known sulphur content are available commercially, but these copper-based standards are all either bronzes or copper–nickel alloys, and the spread of individual sulphur values reported by the cooperating laboratories in the standardisation precluded the use of these samples for present calibration purposes.

A small copper ingot to which sulphur was added to simulate copper containing about 150 p.p.m. of sulphur, was specially cast. This material (A) was analysed for sulphur by a gravimetric method (ASTM method E-56, which involves converting the sulphur to barium sulphate), and duplicate sulphur contents of 160 and 165 p.p.m. were established.

Two samples of copper, (B) and (C), were also available; these had been analysed independently by a gravimetric procedure, and the sulphur contents were shown to be 0.15 and 0.30%, respectively.

As a further check on the sulphur content of A, a 2-g sample of the material was analysed by the conventional combustion–borate method. For calibration purposes, samples B and C were used to simulate two independent samples of copper, each containing a calculated sulphur content of 150 p.p.m. (2-g basis). The weight deficiency in each was made up to 2 g by adding "sulphur-free" copper.

When this method was used, duplicate values of 155 and 160 p.p.m. of sulphur were obtained for sample A, and the overall average of the four sulphur values on this material was 160 p.p.m.

Combustion of copper samples

Samples of vacuum-cast copper were first analysed as described under Experimental, except that a stream of oxygen at 1 l min^{-1} was used instead of air.

With a 1-g sample of copper the oxidised and fused residue only penetrated the combustion boat slightly; the use of a 2-g sample could be tolerated, but sample weights in excess of 2 g gave trouble because the oxidised residue penetrated the boat, and occasionally stuck to the inside of the combustion tube. Samples were, therefore, restricted to a maximum weight of 2 g.

It was intended to prepare a calibration graph by taking appropriate weights of sample A and making each sample weight up to 2 g with vacuum-cast copper, to cover the range "0"–50 μg of sulphur *i.e.* the equivalent of "0"–25 p.p.m. of sulphur, on a 2-g sample basis. By reducing the composite sample weight (by adding less vacuum-cast copper), this range could be extended.

When an empty combustion boat was used in the procedure, an absorbance of about 0.06 was obtained, and a 2-g sample of vacuum-cast copper gave a net absorbance of about 0.24. To lower the sulphur content of the vacuum-cast copper, the bulk material was reduced in an atmosphere of hydrogen for several hours at 800°, and a repeat test on the copper gave a net absorbance of about 0.07. This hydrogen-reduced vacuum-cast copper is subsequently referred to as "high-purity copper". It was not known whether this absorbance was due to sulphur present in the copper, or to sulphur released from the boat during the exothermic oxidation of the copper.

To resolve this problem, 2 g of the high-purity copper was heated at 1150° in a combustion boat in the usual way; the combustion boat was then removed from the furnace and allowed to cool in a desiccator. A further 2-g sample of this copper was added to the same boat, and it was again heated, etc., as before. From the second addition of copper, a net absorbance of about 0.07 was again obtained, indicating that the (additional) sulphur originated from the copper and not from the boat. This corresponds to a sulphur content of the high-purity copper of about 2 p.p.m.

Calibration with the standard copper sample

Increasing weights of sample A were taken; the weights ranged from 0.06 to 0.3 g, corresponding to 10–50 μg of sulphur (5–25 p.p.m. on a 2-g sample basis); high-purity copper was added to each sample to give a total weight of 2 g. These composite samples were heated at 1150° in oxygen, etc., as before, and the colorimetric procedure as described earlier was applied.

The resulting calibration graph was almost linear. However, a comparison of this calibration graph with that obtained by using a standard sodium sulphite

solution in the sodium tetrachloromercurate solution showed that the recovery of sulphur was only about 75%, although the conditions were essentially the same as those used by Barabas and Kaminski, who claimed complete recovery of the sulphur.

It is known that higher temperatures increase the sulphur dioxide/sulphur trioxide ratio in the evolved gas, and at 1427° in an atmosphere of oxygen, the theoretical yield of sulphur dioxide is about 98%[7]. However, with samples of copper it is not advisable to raise the temperature much above 1150°, because the oxidised residue tends to penetrate the combustion boat and damage the combustion tube.

Horn and Kendler[8] state that the law of mass action as applied to the sulphur dioxide/sulphur trioxide system, indicates that the use of air, in place of oxygen, is more satisfactory, and a reduction in the relative amount of oxygen should reduce or eliminate the formation of sulphur trioxide. Most workers, including Barabas and Kaminski, use high-purity oxygen, but air has recently been used for this combustion.

In the determination of sulphur in steel by a combustion–titrimetric procedure, it has been reported[9] that the use of air at about 1450° gives quantitative conversion of the sulphur to sulphuric acid, after absorption of the products of combustion in a dilute hydrogen peroxide solution.

In an attempt to improve the conversion obtained with samples of copper, oxygen and nitrogen were individually metered into, and mixed, in the stabilising (20-l) reservoir, immediately before passing the mixed gas into the heated combustion tube. The proportion of oxygen was varied between 10 and 50% (v/v), and it was shown that maximum absorbance of the final solution was obtained when the volume of oxygen was about 20–30%.

This observation led to the use of the normal laboratory compressed-air supply, after its purification through soda asbestos and silica gel. The flow-rate of the air through the furnace tube was varied; in all previous experiments, an oxygen rate of 1 l min^{-1} had been used. Increase in the oxygen flow-rate from 1 to 2 l min^{-1} caused an increase in the absorbance from 0.48 to 0.59. Similarly, when air was used instead of oxygen, the absorbance increased from 0.55 to 0.66, at flow-rates of 1 and 2 l min^{-1}, respectively.

A flow-rate of 2 l min^{-1} was thought to be the best practical upper limit, because of the fast rate of the effluent gas through the absorption solution, with the possibility of incomplete absorption. With the original absorber, some spraying occurred, hence a special design of absorption vessel[10] was used in all subsequent experiments. It was confirmed, by placing a second absorber in series that, with an air flow-rate of 2 l min^{-1}, all the sulphur dioxide produced during the combustion was absorbed in the first vessel.

In previous experiments a combustion time of 5 min had been used, as recommended by Barabas and Kaminski, but, when the increased air flow was adopted, tests were made to establish the optimum combustion time. Several composite samples containing 0.25 g of sample A and 1.75 g of high-purity copper were taken through the procedure, with combustion times of 4, 6, 8, and 10 min. It was established that maximum absorbance was obtained after an 8-min combustion period.

With these optimised conditions, *viz.*, furnace temperature 1150°, air flow 2 l min^{-1}, and a combustion time of 8 min, the calibration was repeated with 2-g composite samples of sample A and high-purity copper, as described under Experimental. For comparison, the calibration was also repeated under the same ex-

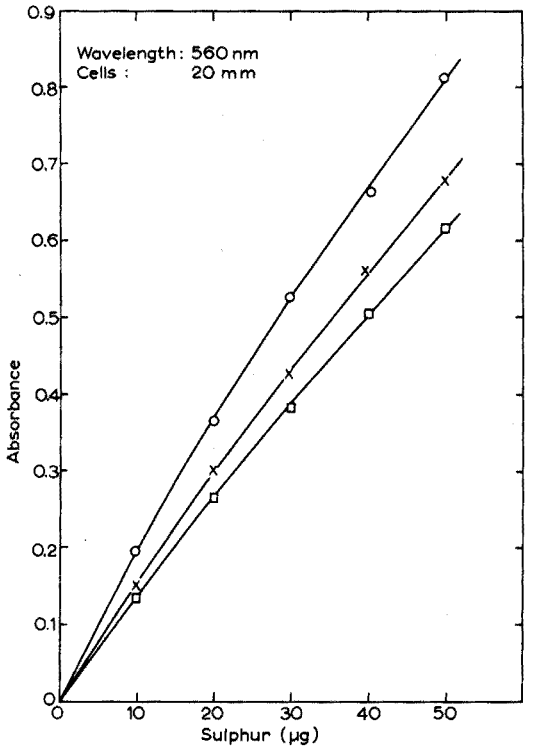

Fig. 2. Calibration graphs. Calibration with: (○) sodium sulphite, (×) standard copper sample burned in air, (□) standard copper sample burned in oxygen.

perimental conditions, except that oxygen (instead of air) was used at a flow-rate of 2 l min^{-1}. These two graphs, and a third graph, prepared from a standard sodium sulphite solution in sodium tetrachloromercurate (0.2 *M*), all with the same batch of *p*-rosaniline hydrochloride and the same formaldehyde, are shown in Fig. 2. These calibration graphs show that with air the conversion to sulphur dioxide is about 85%, compared with about 75% when oxygen is used.

With these optimum conditions, the reproducibility of the proposed method was evaluated by examining six independent samples of sample A (0.25 g made up to 2 g with high-purity copper), simulating a sample containing 20 p.p.m. of sulphur. The six results obtained corresponded to sulphur contents of 19.7, 19.8, 20.1, 19.7, 20.3, and 19.6 p.p.m.; a precision of about ±1 p.p.m. at the 20-p.p.m. level therefore seems probable, although the accuracy of the method, depending upon the accuracy of the determined sulphur values of the standard samples, is probably less favourable than this.

The sulphur content of sample A was evaluated with the copper samples B and C as standards. The "sensitivity" of the method was reduced by using a 1-g sample, and a final volume of 250 ml instead of 100 ml; the volumes of the reagents were increased in proportion. Small sample weights (0.05–0.1 g) of B and C were made up to 1 g with the high-purity copper, so that the amount of sulphur present in each composite sample was similar to that present in 1 g of sample A. The sulphur values

obtained on Sample A were 165, 165 and 169 p.p.m.; an average of 166 p.p.m. of sulphur, compared with the previous average of 160 p.p.m.

This standard sample of copper was accepted as containing 163 p.p.m. of sulphur, and this value was used in all subsequent calculations.

Application of proposed method to typical samples

Two samples of copper wire (about 2.5 mm dia.) were available; the reported sulphur contents were 2 and 4 p.p.m. When these samples were analysed by the proposed combustion–colorimetric procedure, sulphur contents of 6 and 8 p.p.m., respectively, were obtained.

The NBS Cast Bronze Sample No. 52C was also analysed, and duplicate sulphur values of 20 and 21 p.p.m. were obtained; the certified sulphur value is given as "0.002%".

CONCLUSIONS

The proposed combustion–colorimetric procedure is suitable for determining sulphur in copper at about the 2–25 p.p.m. level. The precision of the method is probably about 1–2 p.p.m. over this range. Higher sulphur contents can be determined in copper by suitable adjustment of the sample weight.

Primarily to compensate for the non-stoicheiometric conversion of sulphur in the sample to sulphur dioxide, the provision of samples of copper with known sulphur contents is essential. Since it is difficult to acquire standard samples of copper in which the sulphur contents (*e.g.* 2–50 p.p.m.) are known with indisputable accuracy, composite samples may be provided by "diluting" a standard copper sample of known (relatively high) sulphur content with high-purity copper. Sulphur in this standard copper sample can be determined with a high degree of accuracy by more conventional combustion–titrimetric methods, or by a standard gravimetric procedure.

Until such time as more reliable copper samples become available, the proposed method of providing simulated standard samples of copper is recommended. About twenty samples can be analysed in a normal working day.

The authors thank Dr. W. T. Elwell, Chief Scientist (Chemistry and Analysis) for helpful advice, and for his assistance in the preparation of this paper.

SUMMARY

A combustion method for the determination of sulphur in copper is proposed. The sample is heated at 1150° in a stream of air; the evolved gas is passed into a solution of sodium tetrachloromercurate, and the product is reacted with *p*-rosaniline hydrochloride and formaldehyde to form a purple sulphonic acid derivative of *p*-rosaniline, which is measured spectrophotometrically. The problem of providing a suitable range of (low sulphur) copper standards for calibration purposes is circumvented by using a standard sample of copper with a relatively high (certified or determined) sulphur content, and a calibration graph is prepared with samples obtained by "diluting" the standard sample with high-purity copper. Evidence is provided for

the validity of the method for the determination of sulphur in copper, at the 2–50 p.p.m. level, with a precision probably of the order of 1–5 p.p.m. over this range. Higher sulphur contents can be determined by suitable adjustment of the sample weight. About twenty samples can be analysed in a normal working day.

RÉSUMÉ

On propose une méthode de combustion pour le dosage du soufre dans le cuivre. L'échantillon est chauffé à 1150° dans un courant d'air. Le gaz formé est envoyé dans une solution de tétrachloromercurate de sodium; le produit réagit ensuite avec chlorhydrate de *p*-rosaniline et formaldéhyde pour donner un dérivé sulfoné de la *p*-rosaniline, violet, On procède finalement à un dosage spectrophotométrique. Cette méthode convient très bien pour le dosage de 2 à 50 p.p.m. de soufre dans le cuivre, avec une précision de l'ordre de 1 à 5 p.p.m. Il est possible d'analyser ainsi environ vingt échantillons par jour.

ZUSAMMENFASSUNG

Für die Bestimmung von Schwefel in Kupfer wird eine Verbrennungsmethode vorgeschlagen. Die Probe wird im Luftstrom auf 1150° erhitzt und das entwickelte Gas in eine Lösung von Natriumtetrachloromercurat eingeleitet. Das Produkt wird mit *p*-Rosanilinhydrochlorid und Formaldehyd umgesetzt; das hierbei gebildete purpurfarbene Sulfonsäurederivat von *p*-Rosanilin wird spektrophotometrisch gemessen. Die Schwierigkeit, für die Erstellung der Eichkurve eine geeignete Reihe von Kupfereichproben mit niedrigem Schwefelgehalt einzusetzen, wurde umgangen, indem eine Kupfereichprobe mit bekanntem, relativ hohem Schwefelgehalt für die einzelnen Eichproben mit hochreinem Kupfer "verdünnt" wurde. Die Leistungsfähigkeit der Methode für die Bestimmung von Schwefel in Kupfer wird belegt; im Bereich 2–50 p.p.m. ist die Reproduzierbarkeit wahrscheinlich von der Grössenordnung 1–5 p.p.m. Höhere Schwefelgehalte können durch entsprechende Angleichung des Probengewichts bestimmt werden. An einem normalen Arbeitstag können etwa 20 Proben analysiert werden.

REFERENCES

1 W. T. ELWELL AND I. R. SCHOLES, *Analysis of Copper and its Alloys*, Pergamon Press, Oxford, 1967.
2 *Book of ASTM Standards, 1964, Chemical Analysis of Metals, Part 32*, American Society for Testing Materials, Philadelphia.
3 S. BARABAS AND J. KAMINSKI, *Anal. Chem.*, 35 (1963) 1702.
4 R. V. NAUMAN, P. W. WEST, F. TRON AND G. C. GAEKE, *Anal. Chem.*, 32 (1960) 1307.
5 F. FEIGL, *Chemistry of Specific, Selective and Sensitive Reactions*, Academic Press, New York, 1949, p. 75.
6 P. W. WEST AND G. C. GAEKE, *Anal. Chem.*, 28 (1956) 1816.
7 W. G. RICE-JONES, *Anal. Chem.*, 25 (1953) 1383.
8 H. HORN AND E. KENDLER, *Neue Huette*, 8 (1963) 31.
9 H. GREEN, *BCIRA J.*, 16 (1968) 244.
10 N. W. HANSON, D. A. REILLY AND H. E. STAGG (Editors), *The Determination of Toxic Substances in Air—A Manual of ICI Practice*, Heffer, Cambridge, 1965, p. 14.

Analytica Chimica Acta
Elsevier Publishing Company, Amsterdam
Printed in The Netherlands

DETERMINATION OF HUMAN SERUM ALKALINE PHOSPHATASE BY SEMI-SOLID STATE FLUORIMETRIC ANALYSIS

G. G. GUILBAULT AND A. VAUGHAN

Department of Chemistry, Louisiana State University in New Orleans, New Orleans, La. 70122 (U.S.A.)

(Received 21st December 1970)

Guilbault and Zimmerman[1] have described the measurement of the rate of reaction of cholinesterase with N-methyl indoxyl acetate deposited on a solid surface using a fluorescence detection method. The rate of reaction was measured directly from the pads by means of a fluorimeter which had been converted to accommodate the pad in a specially designed cell holder.

In recent publications, Guilbault and Vaughan[2,3] and Johnson[4] have described the use of naphthol AS-BI phosphate and naphthol AS-MX phosphate, respectively, for the determination of human serum alkaline phosphatase. Naphthol AS-BI phosphate was found[3] to be more sensitive towards alkaline phosphatase than other naphthol AS phosphates investigated.

This system lends itself to application in the determination of serum alkaline phosphatase by a "solid surface" fluorimetric method of analysis.

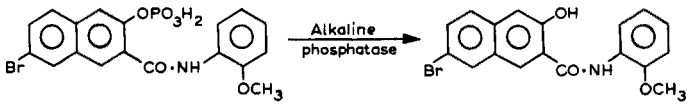

Naphthol AS-BI phosphate (Non-fluorescent) — Naphthol AS-BI (Fluorescent)

In the method developed, naphthol AS-BI phosphate was deposited on the surface of a silicone rubber pad and given volumes of buffer solution and serum were placed on the pad. The drop was mixed and spread into a uniform shape. The pad which was held on a blackened metal plate was placed in a cell holder in a fluorimeter. The cell and metal plate were constructed in such a way that the pad was horizontal with the excitation light entering the cell parallel to the surface of the pad and the detector at right angles to the surface of the pad. The enzymatic rate recorded from the drop is proportional to the serum alkaline phosphatase value. The method can be applied to all serum samples except those which are highly jaundiced.

The effects of pad color, shape and size, drop volume and shape and pad position with reference to the excitation light were investigated.

EXPERIMENTAL

Instrumentation

All measurements were recorded on an Aminco Bowman filter fluorimeter

fitted with a Wratten 7-54 primary filter and Wratten combination 8/65A secondary filters. The instrument was turned on its end and supported by two wooden blocks which were placed parallel to the primary filter holder. This was done so that the pad could be held horizontally thus preventing instability of the drop on the pad. The base of the instrument was supported with a piece of wood to prevent electronic noise in the recorder.

Syringes. Hamilton syringes capable of measuring to 0.1 ml were used in all experiments.

Fluorimeter cell holder. An Aminco-Bowman cell adapter, catalogue number A6-63019, was constructed of black Delrin to hold a metal plate with the dimensions shown in Fig. 1, view A. The metal strip was painted black.

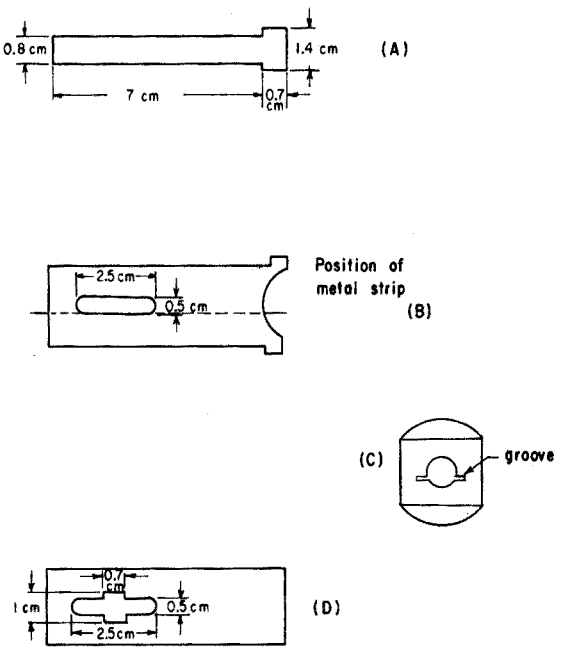

Fig. 1. Construction of the cell holder and metal plate. (A) Dimensions of metal plate; (B) side view of cell holder showing position of metal plate; (C) end view of cell holder showing position of groove; (D) top view of cell holder showing the filed aperture.

Two grooves were cut in the cell adapter in such a way that the plate could be slid into the cell adapter with the plate lying flush to the base of the two opposing port-holes. The position of the plate is shown in Fig. 1, view B. The groove was cut parallel to the lower side of the port-holes with reference to the port-hole on the top of the cell holder.

View C shows the top end of the cell holder. The groove does not pass centrally through the cell holder.

The top of the cell is shown in view D. The port-hole was filed so that the light emitted from the sample on the silicone rubber pad would not be blocked out by the sides of the cell holder.

Solutions

Enzyme substrate. The dihydrogen phosphate ester of naphthol AS-BI (Isolab, Inc., Akron, Ohio) was dissolved as a 10^{-2} *M* solution in 95% ethanol.

Buffer. 2-Amino-2-methyl-propanol buffer, 1 *M*, pH 9.8, was prepared by dissolving the pure compound in water and adjusting the pH with hydrochloric acid.

Standard naphthol AS-BI. Naphthol AS-BI (0.0124 g) was dissolved in 1.0 *M*, pH 9.8, 2-amino-2-methyl-propanol–HCl buffer (100 ml). This solution which contains 10^{-2} μM naphthol AS-BI in 0.03 ml was used as a working standard.

Silicone rubber. The following silicone rubbers from Dow Corning Corporation, Midland, Mich. were used:

Adhesive sealants, Catalogue numbers 3145 RTV (grey), 3140 RTV (clear), 732 RTV (black).

A white silicone rubber preparation from General Electric Company was also used.

Preparation of pads

Silicone rubber pads were prepared by pressing a strip of silicone rubber between two strips of greased glasseine paper. The strip which had a V-shape in the center was cut into small pads which had dimensions of 9 mm × 7 mm with the V in the center of the longer length. The thickness of the pad was 1 mm at the center and 2 mm at the edges.

Determination of serum alkaline phosphatase

Onto a series of grey silicone rubber pads (adhesive sealant 3145 RTV) was placed 10^{-2} *M* naphthol AS-BI phosphate (0.01 ml). The ethanol was allowed to evaporate off so that the naphthol AS-BI phosphate was deposited on the surface of the pad. These pads can be used immediately or stored below 0° for at least three weeks without any deterioration.

The pad was placed on the blackened metal strip, which was then slid into the cell holder, in such a way that the pad was centrally positioned below the filed aperture of the cell holder. Onto the pad was placed from syringes pH 9.8, 1 *M*, 2-amino-2-methyl-propanol–HCl buffer (0.02 ml) and then serum (0.01 ml). The drop formed was mixed with the needle of a syringe so that the drop covered half the area of the pad.

The cell holder was placed in the fluorimeter and the rate of reaction recorded. It may be necessary to wait 15 sec before the reaction starts; this is particularly noticeable with serum samples having low alkaline phosphatase values. The serum alkaline phosphatase value can be obtained from the initial rate determined in two ways.

1. A plot of serum alkaline phosphatase values obtained from an alternative procedure *vs.* initial rate of reaction gives a straight line. In the study carried out, the rate of reaction was plotted against units alkaline phosphatase obtained from a procedure[5] in which phenolphthalein phosphate was used as substrate. The rate can be converted directly into phenolphthalein units by multiplying the rate by 31.5. The units are then expressed as μmole phenolphthalein min^{-1} l^{-1} serum.

2. The method was calibrated with a standard solution of naphthol AS-BI. The fluorimeter was adjusted to give a reading of 1.2 fluorescent units with pH 9.8, 1 *M* 2-amino-2-methyl-propanol buffer (0.03 ml). A fluorescent reading of 12.0 on the 0.1 scale was obtained with the naphthol AS-BI working standard (0.03 ml). The

difference between these two readings corresponds to the fluorescence of 10^{-2} μmoles naphthol AS-BI in 0.03 ml. Under these conditions the serum alkaline phosphatase value, expressed as μmole naphthol AS-BI liberated min^{-1} l^{-1} serum, is obtained directly by multiplying the rate by 93.

RESULTS AND DISCUSSION

In the method described, many parameters affect the reproducibility, sensitivity and accuracy of the method. Two problems encountered were of particular importance: (*a*) *background fluorescence*—the residual or background fluorescence of the method is very high and as a result the sensitivity and accuracy of the method can be very poor; (*b*) *jaundiced serum*—it was found that jaundiced serum samples, which usually have high alkaline phosphatase values, gave low values. These two problems were partly overcome by investigating the effects of changes in pad color and filter systems.

Besides the major problems described above, many other parameters affecting the reproducibility and sensitivity of the method were investigated.

Cell construction

In the original paper of Guilbault and Zimmerman[1] the cell holder was constructed in such a way that pad was held in a vertical position at a 45° angle to the excitation radiation. This system had two disadvantages: (*a*) the pad was in a vertical position so there was a tendency for the drop to fall off, and (*b*) the pad and pad holder were at a 45° angle to the excitation light. Under these conditions much light is reflected directly into the photomultiplier; as a result high backgrounds were obtained.

In order to reduce the background a cell was constructed as described. The fluorescence back ground was negligible when the metal plate was placed parallel to the light source, and when a silicone rubber pad was placed in position, the background was at a minimum. The fluorimeter was turned on its end so that the pad and cell holder were horizontal. In this position the drop no longer tended to fall off the pad. No detrimental effects on the fluorimeter were observed.

pH and buffer system

In solution serum alkaline phosphatase was shown to act optimally at pH 9.8 with naphthol AS-BI phosphate. This was also found to be the case with the "solid surface" fluorimetric method. Because serum has a high buffer capacity, it was found necessary to use a buffer at high concentration in order to maintain a constant pH.

Drop shape and volume

The shape of the drop is critical. Because of the geometry of the system, the drop can act as a lens and the excitation light passing into the drop can be internally reflected many times. This implies that the background and rate will vary from sample to sample. In order to prevent this variation the drop was spread over half the surface of the pad. This also helps to mix the sample. Without this precaution irreproducible results are obtained.

The volume of the drop is also critical. As the drop volume increases, the background increases which is not desirable. It is, however, not possible to use volumes which are too small because difficulties are encountered in measuring volumes smaller than 0.01 ml. It is also desirable that the ratio of buffer to serum should be high enough to prevent variations in the pH of the system. It was found that a total drop volume of 0.03 ml constituted from buffer (0.02 ml) and serum (0.01 ml) was satisfactory.

Pad shape

The shape of the pad should be kept constant. Differences between pads change the background and reaction rates. Both these factors increase as the pad size increases. Only pads which gave identical backgrounds (no substrate or solution present) were used in the determinations.

Background, filter systems and serum samples

Initial studies showed that jaundiced samples gave very low rates and in some cases no rates at all. All these samples were found to have high alkaline phosphatase values when determined by other methods. These low values are obtained because the components of the serum absorb the radiant energy, therefore decreasing the degree of activation of the liberated naphthol AS-BI. Consequently, decreases in the intensity of fluorescence and in the reaction rate occur. Figure 2 shows an absorption spectrum

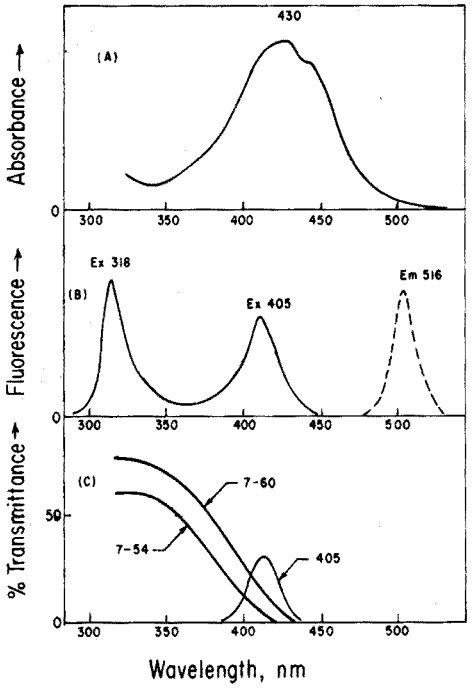

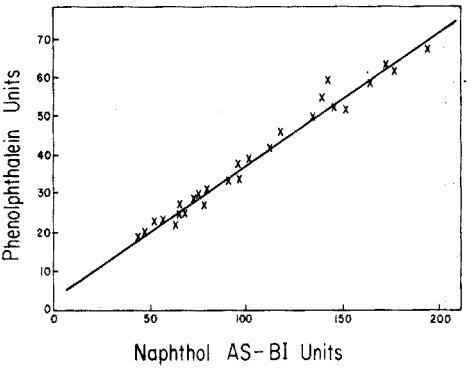

Fig. 2. (A) Absorption spectra of serum at pH 9.8. (B) Excitation and emission spectra of naphthol AS-BI. (C) Transmittance characteristics of Wratten filters 405, 7-60 and 7-54.

Fig. 3. Correlation between results obtained with naphthol AS-BI method and phenolphthalein method.

of jaundiced serum at pH 9.8 (A), the fluorescence spectra of naphthol AS-BI (B), and the transmission spectra of three Wratten filters 405, 7-60 and 7-54 (C).

From the Fig. it can be seen that the jaundiced serum sample absorbs very strongly between 400 and 450 nm and that the light passing through the 405 filter will be partially absorbed by the serum. The 405-nm excitation peak of naphthol AS-BI will therefore be incompletely activated.

The Wratten 7-60 and 7-54 filters, however, pass more light into the system and give the possibility of activation of both the 318-nm and 405-nm excitation peaks. With either of these filters better rates were obtained with both normal and jaundiced serum. A comparison of the three filters showed that the background increased in the order 405 < 7-60 < 7-54 and that the rate of reaction with serum also increased in the same order. Although the 7-54 filter gave the highest rates with all samples, the background increased so much (white pads) that the method was very inaccurate.

The color of the silicone rubber however, affects both the background and reaction rates. With any of the filter systems, the background and reaction rates increase in the order black < grey < clear < white. Each possible combination of pad color and filter was examined and it was found that the most accurate results could be obtained if a combination of 7-54 filter and grey silicone rubber pads were used.

Table I shows the results obtained from a series of serum samples. Over 80 serum samples were analyzed with a relative error of $\pm 5\%$.

Figure 3 shows the correlation between the serum alkaline phosphatase values obtained from the "solid surface" method and alkaline phosphatase values obtained from a solution method employing phenolphthalein phosphate[5]. The graph

TABLE I

DETERMINATION OF SERUM ALKALINE PHOSPHATASE

Units alkaline phosphatase taken[a]	*Units alkaline phosphatase found*[a-c]
20	21.5
22	19
24	24.5
26	23
28	25
30	31
31	31
33	37
37	34
39	40
41	39
43	42
48	49
53	54[d]
61	60[d]
64	64[d]

[a] Units expressed as μmole phenolphthalein liberated min^{-1} l^{-1} serum.
[b] Obtained by multiplying the rate by 31.5.
[c] Average from 3 or more different samples—each analysis in duplicate.
[d] One sample—average of 2 determinations.

shows good agreement between the two methods over a wide range of serum values. If the serum values are expressed as μmole phenolphthalein liberated min^{-1} l^{-1} serum, then normal serum has 9–35 units alkaline phosphatase. If the serum values are expressed as μmoles naphthol AS-BI liberated min^{-1} l^{-1} serum, then normal serum has 27–105 units.

TABLE II

ANALYTICAL RESULTS OBTAINED FROM JAUNDICED SERUM SAMPLES

Units alkaline phosphatase taken[a]	*Units alkaline phosphatase found*[a,b]
27	18
34	21
59	30
86	21
135	44
185	115
200	138

[a] Units expressed as μmole phenolphthalein liberated min^{-1} l^{-1} serum.
[b] Average of 3 results.

Table II shows the alkaline phosphatase values obtained from highly jaundiced serum compared to the phenolphthalein phosphate method. All the results from these samples were low and implied a limitation on the method. It is however, possible to predict which samples will give low results. Generally, it is those samples which are very dark yellow or orange-yellow in color. The light-yellow serum gave good results as did haemolyzed serum. The low values obtained from jaundiced serum is the main limitation of the method but it is possible to recognize these solutions and carry out the analysis by an alternative method.

SUMMARY

A solid surface fluorimetric method for the analysis of human serum alkaline phosphatase is described. In this method, a layer of the enzyme substrate, naphthol AS-BI phosphate is deposited on the surface of a silicon rubber pad. Serum and buffer solution are placed on the pad and the rate of formation of the fluorescent naphthol AS-BI is measured. This initial rate is proportional to the serum alkaline phosphatase content. The parameters, *i.e.*, pH, incubation time, drop volume and size, shape, and the shape and color of the pads, which affect the rate of reaction and reproducibility of the method, are discussed.

RÉSUMÉ

Une méthode fluorométrique sur surface solide est décrite pour l'analyse de phosphatase alcaline de sérum humain. On dépose sur caoutchouc silicone une couche de substrat d'enzyme, et de phosphate de naphtol AS-BI. Sérum et tampon sont placés sur ce support; on mesure la vitesse de formation du naphtol AS-BI fluorescent. On examine divers paramètres tels que pH, durée d'incubation, volume

des gouttes, forme et couleur du support, pouvant influencer la vitesse de réaction et la reproductibilité.

ZUSAMMENFASSUNG

Es wird eine fluorimetrische Methode unter Verwendung einer festen Oberfläche für die Bestimmung alkalischer Phosphatase des menschlichen Serums beschrieben. Bei dieser Methode wird eine Schicht des Enzymsubstrates Naphthol-AS-BI-Phosphat auf der Oberfläche eines Silikonkautschukträgers aufgetragen. Nach Zugabe von Serum und Pufferlösung wird die Bildungsgeschwindigkeit des fluoreszierenden Naphthol AS-BI gemessen. Die Anfangsgeschwindigkeit ist proportional dem Gehalt des Serums an alkalischer Phosphatase. Die Parameter wie pH, Inkubationszeit, Tropfenvolumen und -form sowie Anordnung und Farbe der Träger, die die Reaktionsgeschwindigkeit und die Reproduzierbarkeit der Methode beeinflussen, werden diskutiert.

REFERENCES

1 G. G. GUILBAULT AND R. ZIMMERMAN, *Anal. Lett.*, 3 (1970) 145.
2 G. G. GUILBAULT AND A. VAUGHAN, *Anal. Lett.*, 3 (1970) 1.
3 G. G. GUILBAULT, A. VAUGHAN AND D. HACKNEY, *Anal. Chem.*, to be published.
4 R. B. JOHNSON, *Clin. Chem.*, 15 (1969) 108.
5 A. L. BABSON, *Clin. Chem.*, 11 (1965) 789.

Analytica Chimica Acta
Elsevier Publishing Company, Amsterdam
Printed in The Netherlands

PHOTOMETRIC DETERMINATION OF SILVER AND MERCURY WITH GLYOXAL DITHIOSEMICARBAZONE

B. W. BUDESINSKY AND J. SVEC
Department of Chemistry, University of Waterloo, Waterloo, Ontario (Canada)

(Received 11th December 1970)

Glyoxal dithiosemicarbazone (GDTS) has been tested for its biological activity[1], but its complexation properties and analytical utility are unknown. Since

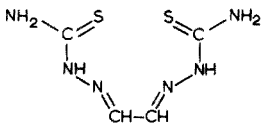

it is a tetradentate ligand with convenient steric arrangement of its donor groups and contains a conjugated system of π-electrons connected with the donor system, an investigation of its complexing properties and its possible analytical use as a reagent for spectrophotometry seemed worthwhile.

EXPERIMENTAL

Apparatus

All photometric measurements were made with a double-beam Unicam 800B recording spectrophotometer. Quartz cells (1 cm) were used throughout. An Orion Model 801 pH-meter with a glass and calomel electrode pair, was used for pH measurements.

Preparation of GDTS

The substance was prepared as described by Gingras *et al.*[1]. The yield was 80%. The product forms fine yellow crystals, m.p. $>300°$. The R_F value is 0.72 (yellow spot) on Whatman paper No. 1 at 25° in aqueous 1 *M* ammonia. The product obtained was chromatographically pure. It was analyzed with the following results: 23.6% C, 4.1% H, 41.0% N, 31.5% S; required for $C_4H_8N_6S_2$: 23.5% C, 3.9%H, 41.1% N, 31.4% S.

Reagents

GDTS solution. Prepare a $1.00 \cdot 10^{-4}$ *M* solution daily by dissolving 20.23 mg of the substance in 10 ml of 0.1 *M* sodium hydroxide and diluting to 1 l with water.

Metal ion solutions. $1.00 \cdot 10^{-4}$ *M* and $1.00 \cdot 10^{-2}$ *M* stock solutions of the metal salts (usually perchlorates or chlorides) were used.

The pH was adjusted by means of perchloric acid and hexamine (pH 1.10–6.90), perchloric acid and borax (pH 7.58–9.01), borax and sodium hydroxide (pH 9.26–10.82), and sodium hydroxide (pH 10.93–12.95). The ionic strength was kept constant (0.10 *N*) by means of sodium perchlorate. The sequence of buffer, metal ion and reagent was adhered to during the preparation of all measured solutions; the temperature was kept at $25 \pm 1°$. The absorbance of solutions was measured against a buffer blank.

Determination of silver and mercury

Add 0.5 ml of 0.1 *M* EDTA-disodium salt solution to a sample solution containing 0.05–0.40 μmole of silver(I) or mercury(II). Adjust to pH 4–7 by means of 0.5 *M* perchloric acid and 0.5 *M* sodium hydroxide. Add 5.0 ml of perchloric acid and mix. Then, add 5.00 ml of $1.00 \cdot 10^{-4}$ *M* GDTS solution, dilute to 25 ml in a volumetric flask and mix. During 10 min, measure the absorbance at 335 nm of the GDTS blank against sample solution. Construct the calibration curve for the given range of silver(I) or mercury(II) concentrations under the same conditions. Straight lines similar to those shown in Fig. 3 should be obtained.

RESULTS AND DISCUSSION

Spectral characteristics

Typical spectral curves corresponding to the appearance of individual hydrogen complexes (see below) of the ligand are presented in Fig. 1. Similar curves for the silver(I), mercury(II), copper(II) and palladium(II) complexes are shown in Fig. 2.

Influence of acidity and adherence to Beer's law

The decrease in absorbance of GDTS caused by the complexation with silver(I)

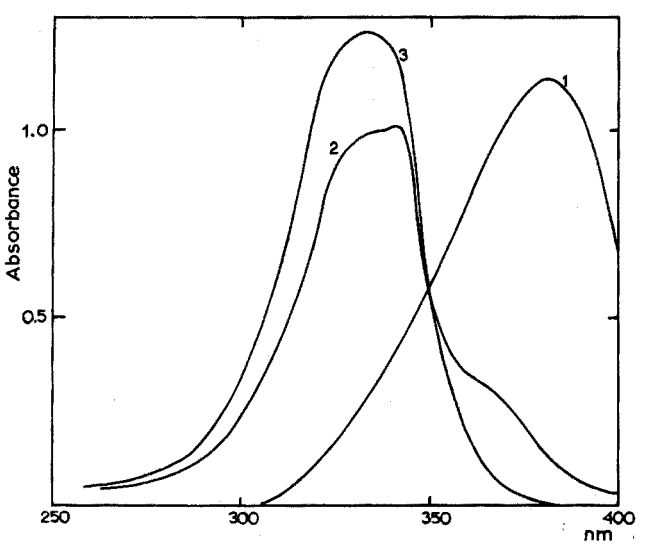

Fig. 1. Absorbance spectra of GDTS at different pH: (1) 11.79, (2) 9.71, (3) 6.94. $c_L = 2.50 \cdot 10^{-5}$ *M*.

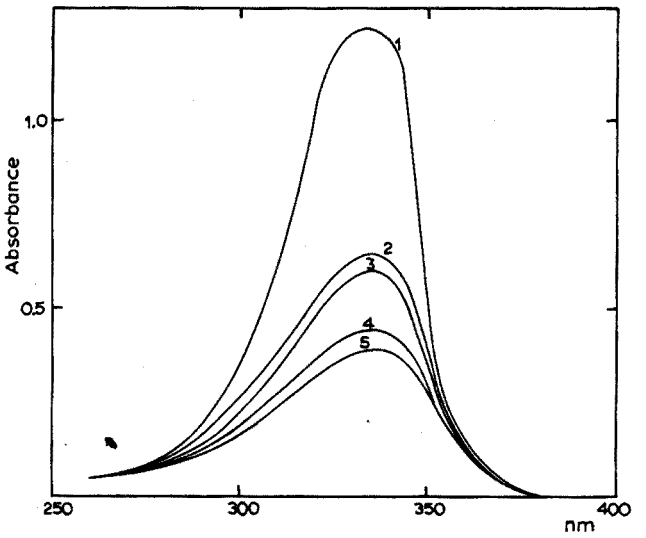

Fig. 2. Absorbance spectra of GDTS (1) and its palladium(II) (2), copper(II) (3), silver(I) (4) and mercury(II) (5) complex at pH 1.10. $c_L = 2.50 \cdot 10^{-5}$ *M*, $c_M = 2.00 \cdot 10^{-5}$ *M*.

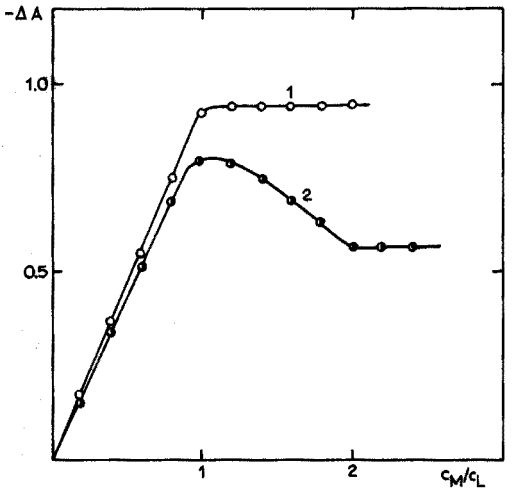

Fig. 3. Dependence of absorbance difference on the concentration of mercury(II) (1) and silver(I) (2) at pH 1.10 and 335 nm. $c_L = 2.00 \cdot 10^{-5}$ *M*.

and mercury(II) is constant in the pH interval 1.0–7.0. A pH of 1.1 ± 0.1 was selected for determinations because of elimination of many interfering reactions of other ions. The adherence to Beer's law is shown in Fig. 3.

Effect of time

The stability of aqueous solution of GDTS was investigated at 25° and 50° for 24 h. It may be seen from Table I that the stability is quite satisfactory in the usual

TABLE I

STABILITY OF AQUEOUS REAGENT SOLUTION
($2.00 \cdot 10^{-5}$ *M*, pH 7.58)

Time (min)	*5*	*10*	*20*	*40*	*60*	*120*	*180*	*300*	*600*	*1440*
Absorbance (335 nm)	[a] 1.000	1.000	1.000	0.998	0.997	0.995	0.993	0.990	0.900	0.810
	[b] 1.000	0.995	0.908	0.880	0.801	0.750	0.680	0.603	0.511	0.435

[a] 25°.
[b] 50°.

TABLE II

DETERMINATION OF SILVER IN THE PRESENCE OF FOREIGN IONS

Foreign ion	$-\Delta A$			*Foreign ion*	$-\Delta A$		
	a	*b*	*c*		*a*	*b*	*c*
—	0.344	0.344	0.344	Y	0.342	0.340	0.345
Cu(II)	0.342	0.347	0.420	Hg(II)	0.696	0.880	0.880
Mg	0.345	0.344	0.346	Ca	0.343	0.343	0.346
Zn	0.344	0.345	0.348	Pb(II)	0.344	0.345	0.347
Mn(II)	0.345	0.345	0.350	Co(II)	0.345	0.348	0.410
Cd	0.346	0.346	0.351	Ni	0.344	0.345	0.348
Fe(II)	0.344	0.347	0.345	Sn(II)	0.345	0.346	0.348
Fe(III)	0.345	0.346	0.522	Sc	0.344	0.344	0.346
Sr	0.345	0.345	0.344	Ba	0.344	0.345	0.345
Hf	0.344	0.345	0.345	Zr	0.344	0.344	0.346
Al	0.345	0.346	0.347	La	0.346	0.346	0.348
Li	0.345	0.346	0.346	Be	0.347	0.345	0.390
U(VI)	0.346	0.345	0.345	Ti(IV)	0.345	0.346	0.346
Th	0.346	0.345	0.346	V(V)	0.347	0.348	0.410
Pd(II)	0.347	0.348	0.620	Mo(VI)	0.345	0.349	0.390
Cr(III)	0.346	0.345	0.348	SO_4^{2-}	0.346	0.345	0.340
Cl^-	0.340	0.250	0.192	NO_3^-	0.346	0.380	0.680
Br^-	0.335	0.241	0.172	AcO^-	0.345	0.346	0.346
I^-	0.320	0.202	0.010	Oxalate	0.345	0.347	0.380
F^-	0.345	0.346	0.345	Tartrate	0.345	0.348	0.390
SCN^-	0.336	0.202	0.025	Citrate	0.348	0.348	0.401
CN^-	0.345	0.303	0.207	PO_4^{3-}	0.345	0.340	0.310
$S_2O_3^{2-}$	0.310	0.187	0.025	EDTA	0.345	0.348	0.347

[a] 0.5 μmole of foreign ion present.
[b] 5.0 μmole of foreign ion present.
[c] 50.0 μmole of foreign ion present.

temperature conditions and in the range 0–5 h. The silver(I) and mercury(II) complexes prepared in this time interval were also of reasonable stability.

Effect of foreign ions on the determination of silver(I) and mercury(II)

The effects of 30 cations and 15 anions on the silver(I) and mercury(II) determinations were investigated. The limiting value of the concentration of a foreign ion

TABLE III

DETERMINATION OF MERCURY IN THE PRESENCE OF FOREIGN IONS

Foreign ion	$-\Delta A$			*Foreign ion*	$-\Delta A$		
	a	*b*	*c*		*a*	*b*	*c*
—	0.352	0.352	0.352	Y	0.353	0.352	0.355
Cu(II)	0.357	0.360	0.425	Ag(I)	0.695	0.860	0.860
Mg	0.353	0.355	0.353	Ca	0.352	0.352	0.354
Zn	0.355	0.354	0.360	Pb(II)	0.351	0.355	0.356
Mn(II)	0.352	0.355	0.360	Co(II)	0.352	0.358	0.425
Cd	0.353	0.358	0.359	Ni	0.353	0.353	0.360
Fe(II)	0.354	0.356	0.352	Sn(II)	0.352	0.356	0.358
Fe(III)	0.353	0.360	0.510	Sc	0.353	0.352	0.357
Sr	0.352	0.353	0.352	Ba	0.352	0.353	0.354
Hf	0.355	0.354	0.354	Zr	0.353	0.355	0.355
Al	0.353	0.354	0.353	La	0.349	0.350	0.354
Li	0.352	0.353	0.355	Be	0.354	0.358	0.388
U(VI)	0.354	0.353	0.360	Ti(IV)	0.352	0.352	0.355
Th	0.353	0.352	0.352	V(V)	0.353	0.356	0.415
Pd(II)	0.355	0.362	0.622	Mo(VI)	0.354	0.355	0.395
Cr(III)	0.352	0.353	0.355	SO_4^{2-}	0.353	0.355	0.350
Cl^-	0.350	0.351	0.345	NO_3^-	0.352	0.381	0.685
Br^-	0.349	0.320	0.250	AcO^-	0.354	0.355	0.354
I^-	0.350	0.205	0.020	Oxalate	0.354	0.355	0.381
F^-	0.354	0.352	0.354	Tartrate	0.355	0.356	0.380
SCN^-	0.350	0.240	0.035	Citrate	0.352	0.354	0.392
CN^-	0.348	0.349	0.340	PO_4^{3-}	0.353	0.359	0.305
$S_2O_3^{2-}$	0.250	0.126	0.018	EDTA	0.352	0.350	0.348

[a,b,c] See Table II.

was taken as that which caused an error of less than $\pm 5\%$ in the determination of 0.2 μmole of silver(I) or mercury(II). The results obtained are summarized in Tables II and III. For silver(I), the interfering ions (in μmole) are: mercury(II) (0.001), bismuth (30), copper(II) (30), iron(III) (30), palladium(II) (30), cobalt(II) (30), beryllium (40), vanadium(V) (30), molybdenum(VI) (30), chloride (2), bromide (1), iodide (0.5), thiocyanate (1), cyanide (3), thiosulfate (0.5), nitrate (5), oxalate (40), tartrate (40), citrate (40) and phosphate (20). The determination of mercury(II) is affected by: silver(I) (0.001), bismuth (30), copper(II) (30), iron(III) (30), palladium(II) (30), cobalt(II) (30), beryllium (40), vanadium(V) (30), molybdenum(VI) (30), chloride (6), bromide (2), iodide (1), thiocyanate (2), thiosulfate (0.5), nitrate (5), oxalate (40), tartrate (40), citrate (40) and phosphate (20). Other ions in amounts up to 50 μmole do not interfere. In the presence of 5 μmole of chloride, mercury may be determined in presence of up to 2 μmole of silver.

Precision data

These were obtained by multiple analyses of series of solutions containing 0.3 μmole of silver(I) or mercury(II). The precision of the absorbance measurement for silver(I) is $\pm 1.6\%$ (relative standard deviation), corresponding to 0.0048 μmole of silver; for mercury it is $\pm 1.5\%$ corresponding to 0.0045 μmole.

Sensitivity of determination

The sensitivity is expressed as effective molar absorptivity for silver(I) and mercury(II) corresponding to the linear part of the dependence between relative absorbance (blank minus sample solution) and the total concentration of metal. The results compared with sensitivities for copper(II) and palladium(II) are presented in Table VI.

Composition and stability of complexes

The stability constants of hydrogen complexes of GDTS were determined by usual spectrophotometric methods[2]. The absorbance–pH plot was constructed for wavelengths 335 and 372 nm. Since the molecule of GDTS is symmetrical and the distance between the dissociatable protons is relatively long, the values of both constants K_1 and K_2 would be expected to lie close together. Therefore the equation

$$A_0 = A + (A - \varepsilon_1 c_L)[H]K_1 + (A - A_2)[H]^2 K_1 K_2 \quad (1)$$

was used for calculation of the values of K_1, K_2 and ε_1. A is the measured absorbance; A_0 and A_2 are the constant absorbances corresponding to pH > 12.0 and < 8.0, and the species of L^{2+} and H_2L, respectively. Hence the molar absorptivities ε_0 and ε_2 are:

$$\varepsilon_0 = A_0/c_L; \quad \varepsilon_2 = A_2/c_L \quad (2a,b)$$

The values found are given in Table IV.

TABLE IV

STABILITY CONSTANTS, MOLAR ABSORPTIVITIES AND ISOSBESTIC POINTS OF HYDROGEN COMPLEXES

Complex	L^{2-}	HL^-	H_2L
log K_n[a]	—	10.2±0.2	9.3±0.3
λ_{max} (nm)	372	341	335
$\varepsilon_{\lambda(max)} \cdot 10^{-4}$	4.50	4.08	5.00
λ_{isos} (nm)	350	348	

[a] $K_n = [H_nL][H_{n-1}L]^{-1}[H]^{-1}$.

According to the bathochromic shift connected with the deprotonization of H_2L, the following reaction can be assumed:

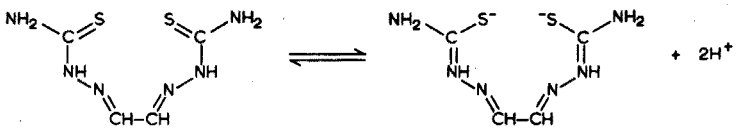

The ratio of metal to ligand in the complexes formed was determined by the method of continuous variations in equimolar solutions. The corrected curves are given in Fig. 4. A ratio of 1 : 1 was found throughout. According to the structure of GDTS and coordinating properties of the metal ions studied, only a mononuclear composition of complexes seems probable.

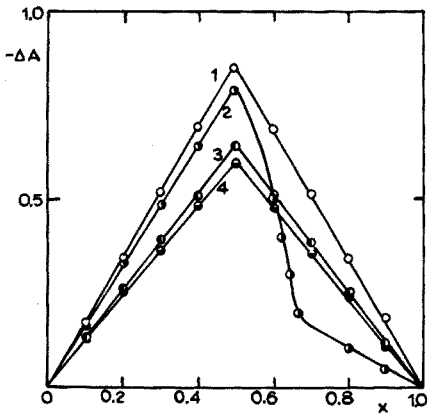

Fig. 4. Continuous variation in equimolar solutions. (1) mercury(II), (2) silver(I), (3) copper(II) and (4) palladium(II) at 335 nm and pH 1.10. $x = c_M/(c_M + c_L)$, $c_M + c_L = 4.00 \cdot 10^{-5}$ *M*.

The effective stability constants of the complexes, K_{11}, were determined by the method of proportional absorbances[3]. Since the values originally found were too high and therefore their determination was very inaccurate, they were decreased by the masking effect of EDTA. In this case, it is necessary to use for calculation of the overall stability constant β of the complex MH_jL, the equation

$$\log \beta = j\,\mathrm{pH} + \log K_{11} + \log \alpha_{M(Y)} + \log \alpha_{L(H)} \tag{3}$$

where $\alpha_{M(Y)}$ and $\alpha_{L(H)}$ are the coefficients of side-reactions of the metal ion with EDTA (ligand Y) and ligand L with hydrogen ions respectively. Thus[4]:

$$\alpha_{M(Y)} = [M]^{-1} \sum_0^x [MH_xY] = \sum_0^x (c_Y/\alpha_{Y(H)})[H]^x \beta_x \tag{4}$$

where c_Y is the total concentration of EDTA, $\alpha_{Y(H)}$ is the coefficient of side-reactions of EDTA with hydrogen ions, and β_x are the overall stability constants of complexes MH_xY. Equation (4) is valid if $c_Y \gg c_M$. For $\alpha_{L(H)}$,

$$\alpha_{L(H)} = [L]^{-1} \sum_0^2 [H_nL] = \sum_0^2 [H]^n \beta_n \tag{5}$$

where $\beta_n = \prod_0^2 K_n$. A similar equation may be written for $\alpha_{Y(H)}$. The hydrolysis of metal ions may be ignored within the given pH interval. The results obtained (Table V) indicate that $j = 0$ for each complex. The data for EDTA complexes were taken from Schwarzenbach and Flaschka's monograph[5].

In given acidity conditions, the absorbance difference ΔA, obtained by measurement of the sample solution against a reagent blank solution, is given by

$$\Delta A = (\varepsilon - \varepsilon_2)[ML] \tag{6}$$

where ε is the molar absorptivity of the complex; the value of ε_2 is expressed by eqn. (2b). For the effective stability constant K_{11}:

$$K_{11} = [ML](c_M - [ML])^{-1}(c_L - [ML])^{-1} \tag{7}$$

TABLE V

COMPOSITION AND EFFECTIVE AND OVERALL STABILITY CONSTANTS OF SOME GDTS COMPLEXES

Complex composition	*pH*	$\Delta A_1/\Delta A_2$[a]	*log* K_{11}	*log* $\alpha_{M(Y)}$	*log* $\alpha_{L(H)}$	*log* β
HgL	2.32	2.315	5.6	7.7	14.9	28.2
	3.15	2.327	5.6	9.1	13.2	27.9
	4.45	2.214	5.9	11.6	10.6	28.1
AgL	1.10	2.154	6.2	0.0	17.3	23.5
	1.25	2.086	6.7	0.0	17.0	23.7
	1.54	2.043	7.1	0.0	16.4	23.5
CuL	0.80	3.030	4.7	0.1	17.9	22.5
	1.10	2.800	4.8	0.5	17.3	22.6
	1.25	2.222	5.9	1.1	17.0	22.5
PdL	0.80	2.490	5.2	0.1	17.9	23.2
	1.10	2.430	5.3	0.5	17.3	23.0
	1.25	2.377	5.4	1.1	17.0	23.5

[a] Proportions of absorbance differences for $\lambda = 335$ nm, $c_M = 2.00 \cdot 10^{-5}$ *M* and $c_Y = 2.00 \cdot 10^{-3}$ *M* EDTA.

where c_M and c_L are the total concentrations of the metal and ligand, respectively. If c_L is constant, differentiation of eqn. (7) gives:

$$\frac{d[ML]}{dc_M} = \frac{c_L - [ML]}{K_{11}^{-1} + c_L - c_M} \tag{8}$$

and for the point $[ML] \to 0$, $c_M \to 0$,

$$(d[ML]/dc_M)_0 = ([ML]/c_M)_0 = 1/(K_{11}^{-1} c_L^{-1} + 1) \tag{9}$$

If eqns. (6) and (9) are combined, then:

$$(\Delta A/c_M)_0 = (\varepsilon - \varepsilon_2)/(K_{11}^{-1} c_L^{-1} + 1) = \Delta\varepsilon \tag{10}$$

where $\Delta\varepsilon$ is the effective molar absorptivity. If the error of photometric measurement is assumed to be $\pm 1\%$, eqn. (10) shows that $\Delta\varepsilon$ is independent of concentration of c_L only if

$$K_{11} c_L \geqq 10^2 \tag{11}$$

The values of log $K_{11} c_L$, ε and $\Delta\varepsilon$ together with average values of the logarithmic overall stability constants are presented in Table VI.

TABLE VI

AVERAGE LOGARITHMIC OVERALL STABILITY CONSTANTS AND MOLAR ABSORPTIVITIES OF COMPLEXES AND EFFECTIVE MOLAR ABSORPTIVITIES

Complex	*log* β	λ (*nm*)	$\varepsilon \cdot 10^{-4}$	$-\log K_{11} c_L$	*pH*	$-\Delta\varepsilon \cdot 10^{-4}$
HgL	28.1	235	0.6	6.1	1.10	4.4
AgL	23.6	235	0.6	1.5	1.10	4.3
CuL	22.5	235	0.7	0.5	1.10	3.3
PdL	23.2	235	1.6	1.2	1.10	3.1

According to the composition and stability, the following structure of complexes seems probable

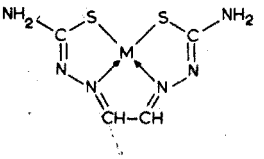

In the case of the silver(I) complex, the coordination of only sulfur donors is likely. Figures 3 and 4 indicate the formation of the complex Ag_2L, if silver is present in excess. The hypsochromic shift connected with complexation may be explained by the decrease of π-electron delocalization caused by complexation. A similar hypsochromic shift appears on complexation of derivatives of *o,o'*-dihydroxyazobenzene at pH about 10.

The authors are grateful for the grant afforded them by the National Research Council, Ottawa, Ontario.

SUMMARY

Glyoxal dithiosemicarbazone forms hypsochromic complexes of ML with silver(I), mercury(II), copper(II) and palladium(II); the logarithmic overall stability constants are 28.1, 23.6, 22.5 and 23.2, respectively. The complexes are formed in the pH interval 1.0–7.0. Complexes of silver(I) and mercury(II) may be used for the photometric determination of these elements at pH 1.1 ± 0.1 in the presence of EDTA. Effective molar absorptivities are 43,000 and 44,000 cm^2 $mmole^{-1}$ at 335 nm. Of 30 cations and 15 anions studied, only bromide, iodide, thiocyanate and thiosulfate interfere at molar ratios of 2.5–5 for 0.2 μmole of silver(I) or mercury(II). Other ions usually interfere only above the molar ratio 150. With regard to mutual interference of silver(I) and mercury(II), silver(I) may be masked by chloride so that the determination of mercury(II) is possible up to the molar ratio 10.

RÉSUMÉ

La glyoxaldithiosémicarbazone forme des complexes hypsochromiques avec argent(I), mercure(II), cuivre(II) et palladium(II); les constantes logarithmiques de stabilité sont 28.1, 23.6, 22.5 et 23.2 respectivement. Ces complexes se forment dans l'intervalle de pH de 1.0 à 7.0. Les complexes d'argent(I) et de mercure(II) peuvent être utilisés pour le dosage photométrique de ces éléments au pH 1.1 ± 0.1, en présence d'EDTA. Les coefficients d'extinction molaires, à 335 nm, sont 43,000 et 44,000 cm^2 $mmol^{-1}$. Parmi les 30 cations et les 15 anions examinés, seuls bromure, iodure, thiocyanate et thiosulfate interfèrent, pour un rapport molaire de 2.5–5 et 0.2 μmole d'argent(I) ou de mercure(II). Les autres ions gênent généralement pour un rapport molaire supérieur à 150. En ce qui concerne le dosage de mercure(II), en présence d'argent, il est possible de masquer ce dernier comme chlorure.

ZUSAMMENFASSUNG

Glyoxaldithiosemicarbazon bildet hypsochrome ML-Komplexe mit Silber(I), Quecksilber(II), Kupfer(II) und Palladium(II); die zugehörigen logarithmischen Gesamtstabilitätskonstanten sind 28.1, 23.6, 22.5 und 23.2. Die Komplexe bilden sich im pH-Bereich 1.0–7.0. Die Komplexe von Silber(I) und Quecksilber(II) können für die photometrische Bestimmung dieser Elemente bei pH 1.1 ± 0.1 in Gegenwart von EDTA verwendet werden. Die wirksamen molaren Extinktionskoeffizienten sind 43000 und 44000 $cm^2\ mmol^{-1}$ bei 335 nm. Von den untersuchten 30 Kationen und 15 Anionen stören nur Bromid, Jodid, Thiocyanat und Thiosulfat bei molaren Verhältnissen von 2.5–5 bei 0.2 μmol Silber(I) oder Quecksilber(II). Andere Ionen stören gewöhnlich nur oberhalb des molaren Verhältnisses 150. Mit Rücksicht auf die gegenseitige Störung von Silber(I) und Quecksilber(II) kann Silber(I) durch Chlorid maskiert werden, so dass die Bestimmung von Quecksilber(II) bis zum molaren Verhältnis 10 möglich wird.

REFERENCES

1 B. A. GINGRAS, T. SUPRUNCHUK AND C. H. BAYLEY, *Can. J. Chem.*, 40 (1962) 1053.
2 B. BUDESINSKY, *Talanta*, 16 (1969) 1277.
3 B. BUDESINSKY, *J. Inorg. & Nucl. Chem.*, 31 (1969) 1345.
4 B. BUDESINSKY, *Anal. Chem.*, 42 (1970) 928.
5 G. SCHWARZENBACH AND H. FLASCHKA, *Complexometric Titrations*, Methuen, London, 1969.

Analytica Chimica Acta
Elsevier Publishing Company, Amsterdam
Printed in The Netherlands

AN EXTRACTIVE–PHOTOMETRIC STUDY OF SOME BIVALENT HEAVY METAL CHELATES OF PYRIDINE-2-ALDEHYDE-2-QUINOLYL-HYDRAZONE

R. W. FREI, G. H. JAMRO AND O. NAVRATIL*
Department of Chemistry, Dalhousie University, Halifax, N.S. (Canada)
(Received 17th November 1970)

Substituted heterocyclic hydrazones have been applied successfully in analytical chemistry as tridentate chelating agents. Their reactions with many metal ions are as a rule fairly selective because of the steric restrictions in the molecule of the complex. One of them, pyridine-2-aldehyde-2-quinolylhydrazone, PAQH, has been recommended as a very sensitive colorimetric and fluorimetric reagent[1] and has been used for the spectrophotometric determination of palladium[2,3], cobalt and nickel[4,5] and for the fluorimetric determination of zinc[6]. The chromatographic properties of some transition metal complexes of PAQH after its use as a semiquantitative scavenging agent have also been investigated[7]. The extractability of the chelates into water-immiscible organic solvents has been generally observed to be very good and renders the reagent suitable for many practical applications[2–7]. The lack of quantitative information on the extractability of these chelates into some common organic solvents prompted this study, which involved an investigation of the distribution of the reagent and its complexes between two liquid phases. Two of the solvents were chosen because of their suitability in atomic absorption spectroscopy.

EXPERIMENTAL

Apparatus, reagents and solutions

The transmission spectra were measured in the visible region with Bausch and Lomb Spectronic 505 and Unicam SP 8000 recording spectrophotometers in 1-cm glass cuvettes. Atomic absorption spectrophotometers (Perkin-Elmer Model 290 and Beckman 1301 DB-G) equipped with Cd, Zn–Cu, Co, Ni, Fe and Cu hollow-cathode lamps were used for the measurement of the metal concentrations in aqueous and organic phases. A Radiometer pH meter, Model 28 (Denmark) was used for pH measurements in the aqueous phase.

The aqueous stock solutions of the cations were prepared from weighed amounts of the salts; if necessary, a small amount of sulphuric acid was added to prevent hydrolysis. In the preparation of the iron solution, ascorbic acid was used to prevent oxidation of iron(II). The reagent has been described elsewhere[1]. Reagent solutions in organic solvents were always freshly prepared; stock solutions in hydrochloric acid medium were prepared from weighed amounts. Acetate and borate buffers and solutions of perchloric acid, sodium perchlorate and sodium hydroxide were used. Reagent-grade chemicals were used throughout.

* On leave from the University of Brno, Czechoslovakia.

Procedure

Aqueous solutions (5–25 ml) containing $5 \cdot 10^{-6}$—$5 \cdot 10^{-4}$ *M* metal ion, $5 \cdot 10^{-2}$–$5 \cdot 10^{-4}$ *M* reagent (as a solution in dilute hydrochloric acid), and appropriate amounts of perchlorates and/or buffer solutions were added to an equal volume of organic solvent containing $5 \cdot 10^{-2}$–$5 \cdot 10^{-4}$ *M* reagent. These systems were shaken for 3–4 h in test tubes with ground-glass stoppers in a homemade rotator (1.5 turns/sec), or in separatory funnels in a mechanical mixer, in order to establish equilibrium. After the layers had been separated, an aliquot part was taken from the organic phase for spectrophotometric measurements or from both phases for atomic absorption measurements. With the benzene phase, direct spraying into the flame was not feasible because smoky flames were obtained. After evaporation of the benzene, the residue was dissolved in dilute hydrochloric acid and then measured. The concentrations of the metals were determined with the use of suitable calibration curves.

The distribution of PAQH (HA) alone between benzene, isoamyl alcohol and methyl isobutyl ketone (MIBK) and aqueous buffer solutions was studied spectrophotometrically as described above. When the concentration of PAQH in the aqueous phase was determined, a definite volume of 0.1 *M* hydrochloric acid solution was added to an aliquot of the aqueous phase so that PAQH was completely transformed to the cationic form (H_2A^+). The concentration of HA in the organic phase or H_2A^+ in the aqueous phase was measured against a blank, by means of suitable calibration curves.

All experiments were carried out at $20 \pm 2°$.

RESULTS AND DISCUSSION

The distribution and acid–base properties of PAQH

The acid dissociation constant K_2 and the distribution constant Q of HA in

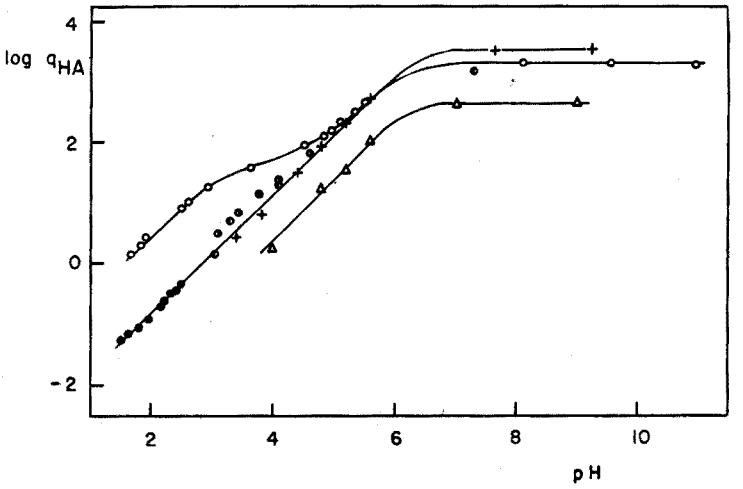

Fig. 1. Effect of pH of the aqueous phase on the distribution of PAQH between an aqueous solution of inorganic ions with ionic strength 0.1 and benzene, MIBK or isoamyl alcohol. Systems: (△) benzene–acetates; (+) MIBK-acetates; (○) isoamyl alcohol–perchlorates; (◑) isoamyl alcohol–acetates; (◐) isoamyl alcohol–chlorides; (●) isoamyl alcohol–sulfates.

benzene, isoamyl alcohol and MIBK were determined from extraction curves (Fig. 1). The results are shown in Table I; some earlier results are also given for comparison. The acid dissociation constants of the ligand and cationic acid and the distribution constant are defined by the equations

$$K_1 = \frac{[H^+][A^-]}{[HA]} \tag{1}$$

$$K_2 = \frac{[HA][H^+]}{[H_2A^+]} \tag{2}$$

$$Q = \frac{[HA]_o}{[HA]} \tag{3}$$

where $[H_2A^+]$, $[HA]$, $[A^-]$ and $[H^+]$ represent the concentrations of the protonated reagent, unprotonated ligand, reagent anion and hydrogen ion respectively in the aqueous phase; $[HA]_o$ represents the concentration of the unprotonated reagent in the organic phase.

The distribution of PAQH between aqueous solutions and organic solvents is given by eqns. (4) and (5):

$$q_{HA} = \frac{[HA]_o}{[H_2A^+]+[HA]+[A^-]} \tag{4}$$

or

$$q_{HA} = \frac{Q}{1+K_1/[H^+]+[H^+]/K_2} \tag{5}$$

which permits the determination of all constants from one experimental curve. The constant K_1 could not be determined from the curves obtained in Fig. 1, because of the very small decrease of equilibrium ratio of HA in the region of high pH values (pH 10–12.3); in the systems used in this work the value for K_1 must therefore be lower than $1 \cdot 10^{-11}$ mole l^{-1}. There is also the possibility of a further dissociation constant K_3 for the double-protonated form H_3A^{2+}:

$$K_3 = \frac{[H^+][H_2A^+]}{[H_3A^{2+}]} \tag{6}$$

TABLE I

ACID DISSOCIATION AND EQUILIBRIUM CONSTANTS OF THE REAGENT

	pK_1	pK_2	pK_3	$\log Q$	*Remarks*
Benzene–water		6.25 ± 0.15		2.65 ± 0.05	
MIBK–water	>11	6.40 ± 0.15	<2	3.52 ± 0.05	This work
Isoamyl alcohol–water		6.15 ± 0.15		3.31 ± 0.05	
Dioxane–water	12.91	5.26	—		Ref. 1

The constant K_3 must be greater than $1 \cdot 10^{-2}$ mole l^{-1}, because the slope of the straight line +1 in the pH region investigated (see Fig. 1) has not shown any tendency to

change to a larger value in the left-hand portion of the distribution curve.

The deformation of the extraction curve in the isoamyl alcohol system HA–H_2A^+–ClO_4^- in Fig. 1 indicates that the extraction of ionic pairs of the type (H_2A^+, ClO_4^-) is not negligible; therefore, the total concentration of the reagent in the organic phase is higher in the presence of perchlorates than in the presence of acetates, chlorides or sulfates. The formation of extractable ionic pairs is more difficult with the latter anions[8].

The difference in pK_2 values between reference 1 and this work could be due to the presence of different liquid systems; *e.g.* water saturated by organic solvent and a 1 : 1 dioxane–water system.

The extraction of metal complexes of PAQH

The organic solvents isoamyl alcohol, MIBK and benzene were chosen for the extraction of metal complexes of PAQH; isoamyl alcohol and MIBK were found to be most suitable for atomic absorption spectrophotometric determination of the bivalent metal complexes because they permit direct aspiration of the samples into the flame (with the exception of benzene as mentioned above).

The reagent PAQH, being a weak acid, can lose the acidic hydrogen in the hydrazone group and incorporate the electron pair independently of the type of chelated metal into a new stable resonating system:

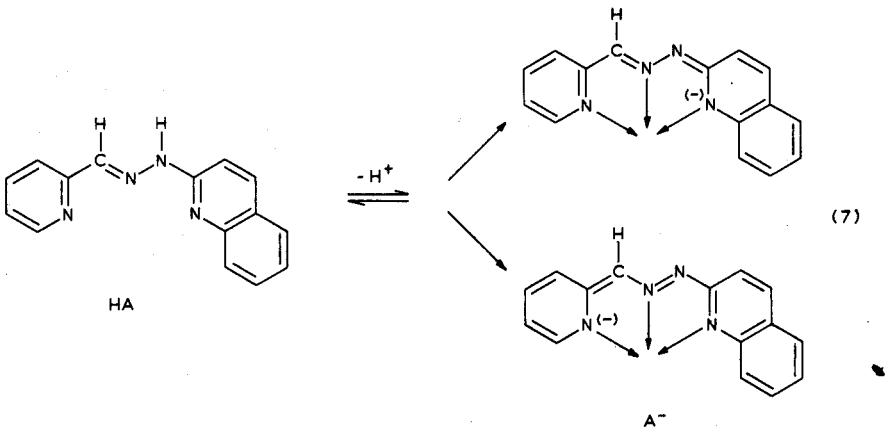

(7)

This being the case, very similar spectral characteristics must result in the visible region of the spectrum for the metal chelates formed, and the extractability between two liquid phases should adhere to the well-known equations for the distribution of metal chelate species, *e.g.* of the type MA_n[9]:

$$M^{2+} + A^- \overset{k_1}{\rightleftarrows} MA^+ \tag{8}$$

$$MA^+ + A^- \overset{k_2}{\rightleftarrows} MA_2 \tag{9}$$

$$MA_2 \rightleftarrows (MA_2)_o \; ; \qquad Q_{MA_2} = \frac{[MA_2]_o}{[MA_2]} \tag{10}$$

where the subscript o denotes the organic phase.

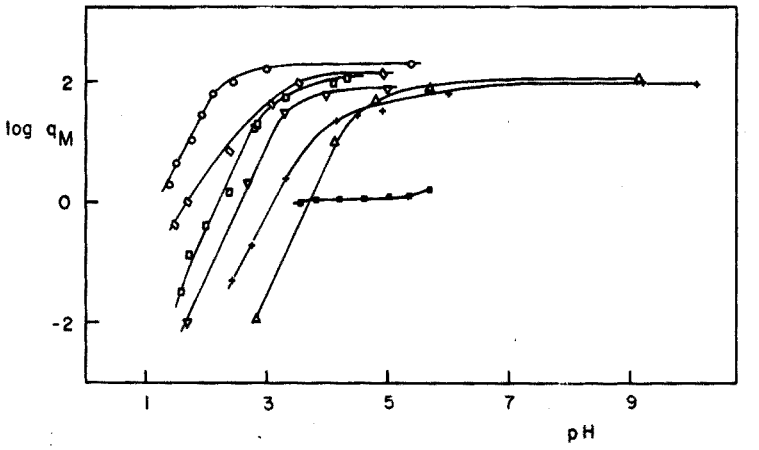

Fig. 2. Effect of pH of the aqueous phase on the distribution of some bivalent metals between 0.1 *M* perchlorate solution and $5 \cdot 10^{-3}$ *M* PAQH in MIBK. (○) Ni, (◇) Cu, (□) Co, (△) Cd, (+) Zn, (▽) Fe, (■) Co. Acetates only.

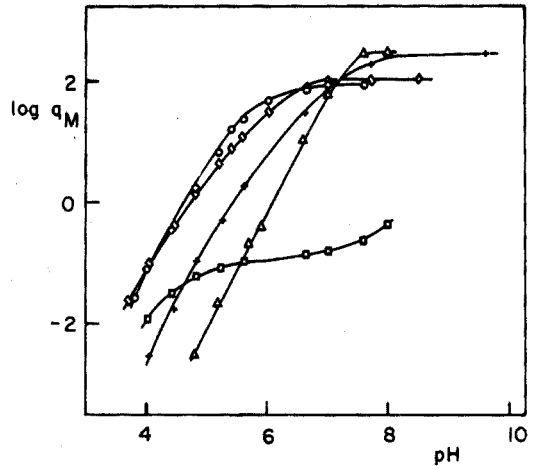

Fig. 3. Effect of pH of the aqueous phase on the distribution of some bivalent metals between 0.1 *M* acetate solution and $5 \cdot 10^{-3}$ *M* PAQH in benzene. (○) Ni, (◇) Cu, (□) Co, (△) Cd, (+) Zn.

The distribution of bivalent metal M is then described by the equilibrium ratio q_M:

$$q_M = \frac{[MA_2]_o}{[M^{2+}]+[MA^+]+[MA_2]} = \frac{Q_{MA_2} k_1 k_2 [A]^2}{1+k_1[A]+k_1 k_2 [A]^2} \quad (11)$$

Effect of acidity

A pH–extraction study in the presence of MIBK, benzene or isoamyl alcohol as organic phase (Figs. 2–4) showed that quantitative extraction of nickel, copper, iron(II), cadmium and zinc was possible in the pH range 3–7. A perchlorate medium

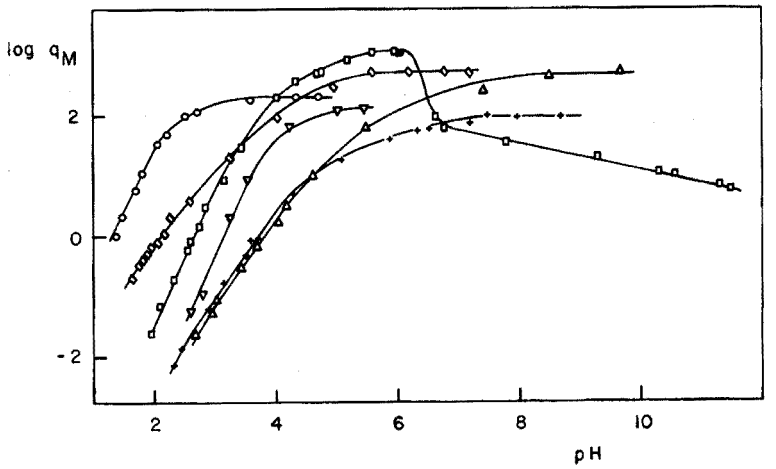

Fig. 4. Effect of pH of the aqueous phase on the distribution of some bivalent metals between 0.1 *M* perchlorate solution and $5 \cdot 10^{-3}$ *M* PAQH in isoamyl alcohol. (○) Ni, (◇) Cu, (□) Co, (△) Cd, (+) Zn, (▽) Fe, (■) Co. Acetates only.

was used with the systems isoamyl alcohol and MIBK and an acetate medium with benzene. Perchlorate was not suitable for the benzene system because a third phase was formed. Of the metals investigated, only cobalt demonstrated an anomalous extractability, being very poorly extracted in the benzene or MIBK system, with only acetates present in the aqueous phase (see Fig. 3).

All extraction curves in Figs. 2–4 (except for cobalt) adhere to eqn. (11). The different shapes of the left-hand portion of the curves depend on the stability of the 1 : 1 complexes (the less steep the curve, the more stable is the 1 : 1 complex). This fact is demonstrated clearly by the very stable copper complex (Figs. 2–4) and is in accordance with earlier results[1]. The fact that all the metals investigated are extractable from acidic media is surprising (especially in the case of nickel) and could be attributed to the high stability of the complexes MA_n. There are several suitable methods for the calculation of stability constants[9], but the present results do not permit such a computation for the following reasons: (*a*) the exact value of k_1 is unknown, (*b*) the distribution of HA in the presence of perchlorates is complicated and cannot be defined by Q_{HA}. A suitable evaluation of the extractability of these chelates can however be given on the basis of the $pH_{\frac{1}{2},0.005}$ values[9] (*e.g.*, 50% extractability in the presence of 0.005 *M* PAQH in the system). The values of $pH_{\frac{1}{2}}$ and log Q_{MA_2} are shown in Table II.

Cobalt complex

The cobalt chelate has been shown in earlier work to be a 2 : 1 reagent–cobalt-(III) complex with a positive charge[10]. It has also been shown that charged complexes can be extracted after suitable ion-pair formation [11,12]. Therefore, the main difference in the behavior of cobalt is probably its low extractability in the presence of anions such as acetates, which cannot properly form extractable ionic pairs. On the other hand, in the presence of perchlorates and especially picrates (Fig. 5), the extractability improves dramatically with an increase in their concentration. The plot log q_{Co} *vs.* log $c_{\text{picric acid}}$ shows a slope of +1 for the straight line; hence picric acid alone is not able to extract cobalt ions in the absence of PAQH.

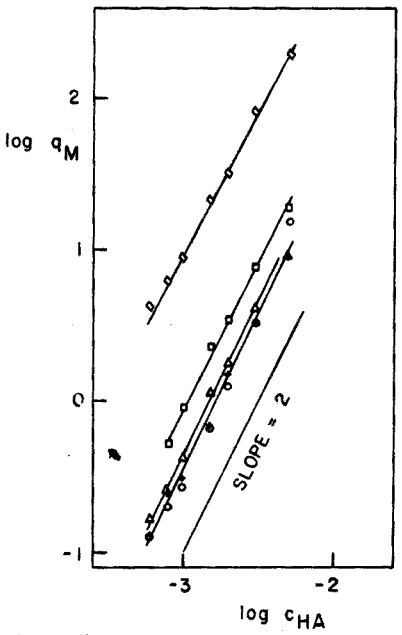

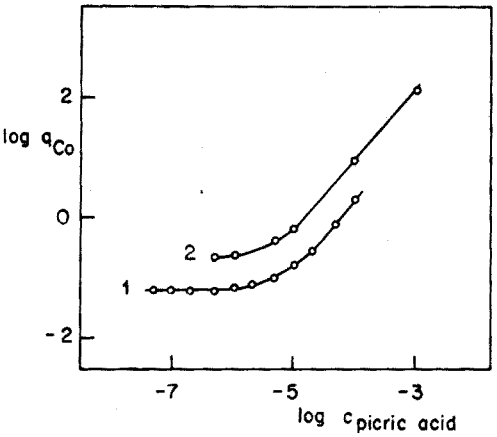

Fig. 5. Effect of the analytical concentration of PAQH on the distribution of some bivalent metals between 0.1 *M* perchlorate solution and PAQH solutions in isoamyl alcohol. pH of the aqueous phase: Cu (◇), Zn (+), Cd (△), 4.57±0.03; Co (□), 3.29±0.03; Ni (○), 1.90±0.03.

Fig. 6. Effect of the analytical concentration of picric acid on the distribution of cobalt between 0.1 *M* acetate solution and PAQH solution in benzene. (1) pH 4.8; (2) 7.5.

TABLE II

$pH_{\frac{1}{2},0.005}$ VALUES AND DISTRIBUTION COEFFICIENTS OF THE COMPLEXES MA_n
(Ionic strength of the water phase = 0.1)

Metal	*System*					
	Benzene–acetates		*Alcohol*[a]*–perchlorates*		*MIBK–perchlorates*	
	$pH_{\frac{1}{2}}$	$\log Q_{MA_2}$	$pH_{\frac{1}{2}}$	$\log Q_{MA_2}$	$pH_{\frac{1}{2}}$	$\log Q_{MA_2}$
Ni^{2+}	4.26	2.0	1.38	2.29	1.28	2.29
Cu^{2+}	4.68	2.05	2.10	2.70	1.72	2.15
Co^{3+}	—	—	2.65	3.05[b]	2.20	2.08[b]
Fe^{2+}	—	—	3.08	2.12	2.55	1.93
Zn^{2+}	5.42	2.5	3.71	1.98	3.10	2.00
Cd^{2+}	6.05	2.5	3.81	2.72	3.70	2.00

[a] Isoamyl alcohol.
[b] Probable composition CoA_2X (see text).

Composition of the extracted species

The results shown in Figs. 2–5 indicate that the complexes extracted in the organic phase are of the MA_2 type. This assumption is supported by the fact that all

the organic extracts absorb in the same wavelength region[13]. Since the oxidation of cobalt(II) to cobalt(III) was reported recently to occur in similar systems[14], a Co(III) A_2X complex is probably extracted, where X is a suitable inorganic or organic anion which can form an extractable ionic pair. The decrease of the equilibrium ratio of cobalt in the alkaline medium is probably due to the hydrolysis of the metal complex.

CONCLUSIONS

The systems studied in this work show good potential for utilization in analytical chemistry, depending on the ionic character of the aqueous phase and especially on pH. The extractability in acidic media is of particular advantage. Bivalent heavy metals investigated in this work can be extracted into isoamyl alcohol or MIBK and determined directly by atomic absorption spectroscopy.

This work was supported by grants from the National Research Council and the Department of Energy, Mines and Resources of Canada.

SUMMARY

Extraction properties of chelates of Ni^{2+}, Cu^{2+}, Co^{3+}, Fe^{2+}, Zn^{2+} and Cd^{2+} with pyridine-2-aldehyde-2-quinolylaldehyde (PAQH) have been studied by means of transmission and atomic absorption spectroscopy. Of the three organic solvents investigated (benzene, isoamyl alcohol and methyl isobutyl ketone) the latter two were suitable for direct aspiration into the flame after addition of equal amounts of ethanol. The charged cobalt complex is believed to be extractable under suitable conditions as an ion pair. The composition of the other quantitatively extractable chelates is of the general nature MA_2. The systems studied show good potential for utilization in analytical chemistry.

RÉSUMÉ

Une étude est effectuée sur les propriétés d'extraction des chélates de Ni^{2+}, Cu^{2+}, Co^{3+}, Fe^{2+}, Zn^{2+} et Cd^{2+} avec le pyridine-2-aldéhyde-2-quinolylaldéhyde (PAQH) par spectroscopie par absorption atomique et transmission. Parmis les trois solvants organiques examinés: benzène, alcool isoamylique et méthylisobutylcétone, les deux derniers conviennent pour une aspiration directe dans la flamme, après addition d'un égal volume d'éthanol. Les systèmes étudiés semblent intéressants pour une utilisation en chimie analytique.

ZUSAMMENFASSUNG

Die Extraktionseigenschaften der Chelate von Ni^{2+}, Cu^{2+}, Co^{3+}, Fe^{2+}, Zn^{2+} und Cd^{2+} mit Pyridin-2-aldehyd-2-chinolylaldehyd (PAQH) wurden mittels Transmissions- und Atomabsorptionsspektroskopie untersucht. Von den drei untersuchten organischen Lösungsmitteln (Benzol, Isoamylalkohol und Methylisobutylketon) eigneten sich die beiden letzten nach Zugabe gleicher Mengen Äthanol für die direkte Versprühung in die Flamme. Es wird angenommen, dass der geladene Kobaltkomplex

unter geeigneten Bedingungen als Ionenpaar extrahierbar ist. Die anderen quantitativ extrahierbaren Chelate haben die allgemeine Zusammensetzung MA_2. Die untersuchten Systeme zeigen gute Eigenschaften für die Verwendung in der analytischen Chemie.

REFERENCES

1 M. L. HEIT AND D. E. RYAN, *Anal. Chim. Acta*, 32 (1965) 448.
2 M. L. HEIT AND D. E. RYAN, *Anal. Chim. Acta*, 34 (1966) 407.
3 R. E. JENSEN AND R. T. PFLAUM, *Anal. Chim. Acta*, 37 (1967) 397.
4 S. P. SINGHAL AND D. E. RYAN, *Anal. Chim. Acta*, 37 (1967) 91.
5 B. K. AFGHAN AND D. E. RYAN, *Anal. Chim. Acta*, 41 (1968) 167.
6 R. E. JENSEN AND R. T. PFLAUM, *Anal. Chem.*, 38 (1966) 1268.
7 R. W. FREI, D. E. RYAN AND C. A. STOCKTON, *Anal. Chim. Acta*, 42 (1968) 59.
8 Y. MARCUS AND A. S. KERTES, *Ion Exchange and Solvent Extraction of Metal Complexes*, Wiley–Interscience, 1969, p. 29.
9 J. STARY, *The Solvent Extraction of Metal Chelates*, Pergamon Press, London, 1964.
10 R. W. FREI AND H. ZEITLIN, *Can. J. Chem.*, 47 (1969) 3902.
11 O. NAVRATIL AND R. W. FREI, *Can. J. Chem.*, 49 (1971) 173.
12 O. NAVRATIL AND R. W. FREI, *Anal. Chim. Acta*, 52 (1970) 221.
13 R. W. FREI, G. H. JAMRO AND O. NAVRATIL, *J. Environ. Anal. Chem.*, in press.
14 J. E. GOING AND R. T. PFLAUM, *Anal. Chem.*, 42 (1970) 1098.

Analytica Chimica Acta
Elsevier Publishing Company, Amsterdam
Printed in The Netherlands

THE EXTRACTION OF CHROMIUM(III) FROM AQUEOUS EDTA BY SOLUTIONS OF TETRA-*n*-HEXYLAMMONIUM CHLORIDE IN DICHLOROETHANE

H. M. N. H. IRVING AND R. H. AL-JARRAH
Department of Inorganic and Structural Chemistry, University of Leeds, Leeds (England)
(Received 29th December 1970)

Little is known about the liquid–liquid extraction of metal complexes of ethylenediaminetetraacetic acid (EDTA; H_4Y). Vickery[1] failed to extract metal–EDTA complexes into chloroform but Moore[2] has recently employed various primary-, secondary- and tertiary-amine and quaternary-ammonium salts of high molecular weight to extract anionic complexes of tervalent actinides and lanthanides from aqueous solutions of organic acids such as EDTA into hexone and xylene. Pre-treatment of the amine salt with EDTA was found to improve the extraction efficiency. Zolotov *et al.*[3] have described the extraction of iron and thorium from solutions containing EDTA by tetraphenylarsonium or diphenylguadinium chloride. The percentage of extraction was greater in mixtures of coordination-active solvents such as alcohols with highly polar ones such as nitromethane or nitrobenzene.

A few complexones other than EDTA have been examined. Thus the extraction of anionic complexes of americium and europium with hydroxyethylenediamine-triacetic acid (HEDTA) and diethylenetriaminepentaacetic acid (DTPA) by solutions of Aliquat-336 (tricaprylmethylammonium chloride) in xylene has been reported by Moore[4].

The present paper describes the extraction of chromium(III) from solutions in EDTA by solutions of quaternary *n*-hexylammonium chloride ($NR_4^+Cl^-$; R = *n*-hexyl) in 1,2-dichloroethane. Furlani *et al.*[5] have shown that aqueous solutions of chromium(III) and EDTA can contain four different species depending on the pH, *viz.* the uncharged violet species $CrHY(H_2O)$ ($pK_1 = 2.27$), the violet singly charged $CrY(H_2O)^-$ ($pK_2 = 7.41$), the blue doubly charged species $CrY(OH)^{2-}$ ($pK_3 = 12.2$), and in very strongly alkaline solution the triply charged green species $CrY(OH)_2^{3-}$.

A sample containing the violet complexes was prepared by boiling aqueous solutions of 0.1005 *M* chromium(III) chloride and 0.1500 *M* Na_2H_2Y and adjusting the pH within the range 3–6 where the absorbance at ~550 nm is known to be insensitive to small changes in the proportion of the species present[5–7]. On equilibration with a solution of tetrahexylammonium chloride in dichloroethane a violet coloured extract was obtained whose absorption spectrum (λ_{max} 550 nm; Fig. 1, curve 2) showed

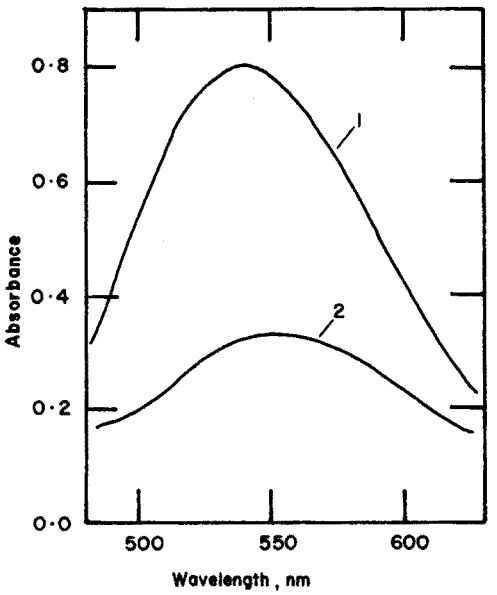

Fig. 1. The absorption spectrum of $CrY(H_2O)^-$ in the aqueous phase (curve 1) and in 1,2-dichloroethane (curve 2).

a small bathochromic shift compared with that of the original aqueous phase (Fig. 1, curve 1).

The question now arises whether the formally uncharged species $CrHY(H_2O)$ is extracted as well as the uninegative anion $CrY(H_2O)^-$ since both are violet coloured. Since the organic phase remained completely colourless when a violet solution prepared from $1.66 \cdot 10^{-3}$ *M* EDTA and $3.95 \cdot 10^{-3}$ *M* chromium(III) chloride adjusted to pH 0.33 (where at least 99% must have been in the form $CrHY(H_2O)$) was equilibrated with an equal volume of 0.1324 *M* tetrahexylammonium chloride in dichloroethane, it follows that the uncharged species is not extracted. Similar experiments with a green solution at pH *ca.* 13 containing predominantly the species $CrY(OH)_2^{3-}$, showed that this too was not extracted by a solution of tetrahexylammonium chloride that had been preequilibrated with 1 *M* sodium hydroxide.

The distribution ratio, *q*, between the organic and aqueous phases defined by

$$q = \frac{\text{total concentration of Cr(III) in the organic phase}}{\text{total concentration of Cr(III) in the aqueous phase}}$$

was determined experimentally while various parameters, such as the pH, the total concentration of liquid anion exchanger $[NR_4^+Cl^-]_{tot}$, and the total concentration of chloride ion $[Cl^-]_{tot}$, were varied. The concentration of complex in each phase was determined absorptiometrically. The value $\varepsilon_{max} = 202$ at 542 nm is well established for the species $CrY(H_2O)^-$ in the aqueous phase[5]. The value $\varepsilon_{max} = 201.6 \pm 0.3$ for the violet complex in the organic phase was determined by stripping a solution of known absorbance with an aqueous solution of 0.1 *M* sodium perchlorate containing EDTA, as described in the experimental section.

Since only the two anions $CrY(H_2O)^-$ and $CrY(OH)^{2-}$ are potentially extractable, we can write

$$q = \frac{[NR_4^+CrY(H_2O)^-]_{org} + [(NR_4^+)_2CrY(OH)^{2-}]_{org}}{[CrHY(H_2O)] + [CrY(H_2O)^-] + [CrY(OH)^{2-}] + [CrY(OH)_2^{3-}]} \quad (1)$$

By introducing extraction constants for the reactions

$$(NR_4^+Cl^-)_{org} + CrY(H_2O)^- \overset{\bar{K}_1}{\rightleftharpoons} (NR_4^+CrY(H_2O)^-)_{org} + Cl^-$$

and

$$2(NR_4^+Cl^-)_{org} + CrY(OH)^{2-} \overset{\bar{K}_2}{\rightleftharpoons} ((NR_4^+)_2CrY(OH)^{2-})_{org} + 2Cl^-$$

namely,

$$\bar{K}_1 = [NR_4^+CrY(H_2O)^-]_{org}[Cl^-]/[NR_4^+Cl^-]_{org}[CrY(H_2O)^-] \quad (2)$$

and

$$\bar{K}_2 = [(NR_4^+)_2CrY(OH)^{2-}]_{org}[Cl^-]^2/[NR_4^+Cl^-]_{org}^2[CrY(OH)^{2-}] \quad (3)$$

and the stoicheiometric acid dissociation constants

$$K_1 = [CrY(H_2O)^-][H^+]/[CrHY(H_2O)] \quad (4)$$

$$K_2 = [CrY(OH)^{2-}][H^+]/[CrY(H_2O)^-] \quad (5)$$

$$K_3 = [CrY(OH)_2^{3-}][H^+]/[CrY(OH)^{2-}] \quad (6)$$

eqn. (1) can be rewritten in the form

$$q = \frac{(\bar{K}_1[NR_4^+Cl^-]_{org}/[Cl^-]) + (\bar{K}_2 \cdot K[NR_4^+Cl^-]_{org}^2/[H^+][Cl^-]^2)}{([H^+]/K_1) + 1 + (K_2/[H^+]) + (K_2K_3/[H^+]^2)} \quad (7)$$

Measurements of q were carried out with different concentrations of the liquid anion exchanger while the concentrations of chromium, chloride and hydrogen ions were kept constant (Table I). The plot of log q against log $[NR_4^+Cl^-]_{org}$ was linear and of unit slope (Fig. 2) showing that, under these conditions, only the uni-

TABLE I

THE EXTRACTION OF CHROMIUM(III) FROM EDTA SOLUTIONS BY VARYING CONCENTRATIONS OF LIQUID ANION-EXCHANGER

$[Cr(III)]_{tot} = 0.00488\ M$; $[Cl^-]_{added} = 0.1002\ M$; $[EDTA] = 0.0129\ M$)

$[NR_4^+Cl^-]_{tot}$	q	*pH after extraction*	$[Cl^-]_{tot}$	$[NR_4^+Cl^-]$	f_H	$\bar{K}_1$
0.1428	0.0749	3.94	0.1152[a]	0.1425	1.0215[b]	0.062
0.1785	0.0919	3.96	0.1153	0.1781	1.0207	0.061
0.2142	0.1135	3.94	0.1153	0.2138	1.0216	0.062
0.2650	0.1516	3.89	0.1153	0.2646	1.0240	0.067
0.3835	0.1995	3.83	0.1153	0.3831	1.0250	0.062
				Average	0.063 ± 0.003	

[a] $[Cl^-]_{tot} = 0.1002 + 3 \cdot 0.00488 + [NR_4^+CrY(H_2O)^-]$.

[b] $f_H = \{([H^+]/K_1) + 1 + (K_2/[H^+])\}$ with $pK_1 = 2.27$ and $pK_2 = 7.41$.

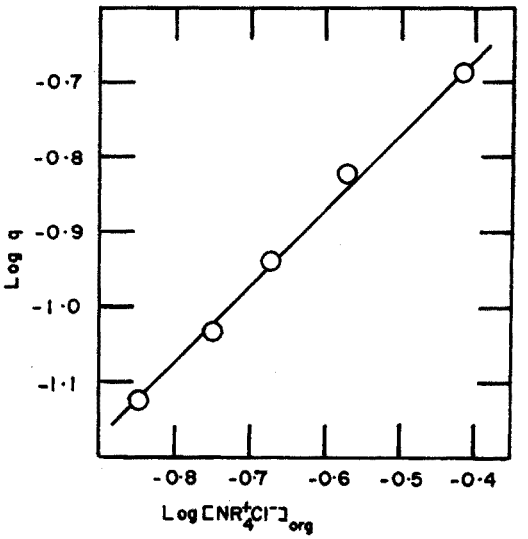

Fig. 2. A plot of log q against log $[NR_4^+Cl^-]_{org}$ for the extraction of 0.00488 M chromium(III) in 0.0129 M EDTA at constant pH and chloride ion concentration by different concentrations of tetrahexylammonium chloride in dichloroethane.

TABLE II

THE EXTRACTION OF CHROMIUM(III) FROM EDTA SOLUTIONS OF VARYING CHLORIDE ION CONCENTRATION
($[Cr]_{tot}=[CrY(H_2O)^-]_{tot}=0.0048\ M$; $[NR_4^+Cl^-]_{tot}=0.4357\ M$)

pH	q	$[Cl^-]_{added}$	$[Cl^-]_{tot}$	$[NR_4^+Cl^-]$	f_H	$\bar{K}_1$
3.94	0.5954	0.0360	0.0522[a]	0.4339	1.0211[b]	0.073
3.97	0.4564	0.0480	0.0639	0.4342	1.0199	0.069
3.98	0.3064	0.0720	0.0875	0.4346	1.0193	0.063
4.01	0.2219	0.0960	0.1112	0.4349	1.0179	0.058
4.03	0.1854	0.1200	0.1351	0.4350	1.0185	0.059
4.05	0.1440	0.1440	0.1590	0.4351	1.0166	0.054
4.07	0.1203	0.1800	0.1949	0.4352	1.0158	0.055
					Average	0.062 ± 0.007

[a] $[Cl^-]_{tot}=[Cl^-]_{added}+3\cdot0.0048+[NR_4^+CrY(H_2O)^-]$.
[b] $f_H=\{([H^+]/K_1)+1+(K_2/[H^+])\}$ with $pK_1=2.27$ and $pK_2=7.41$.

negatively charged species $CrY(H_2O)^-$ is extracted. Equation (7) can thus be simplified by omitting the final term in the numerator and denominator.

On taking decadic logarithms:

$$\log q=\log \bar{K}_1+\log [NR_4^+Cl^-]-\log [Cl^-]+$$
$$-\log \{([H^+]/K)+1+(K_2/[H^+])\} \qquad (8)$$

By substituting the experimental values for $[NR_4^+Cl^-]$ and $[Cl^-]$ (in each case taking into account the changes in concentration due to the partition equilibrium), the value $\bar{K}_1=0.063\pm0.003$ is obtained for the extraction constant.

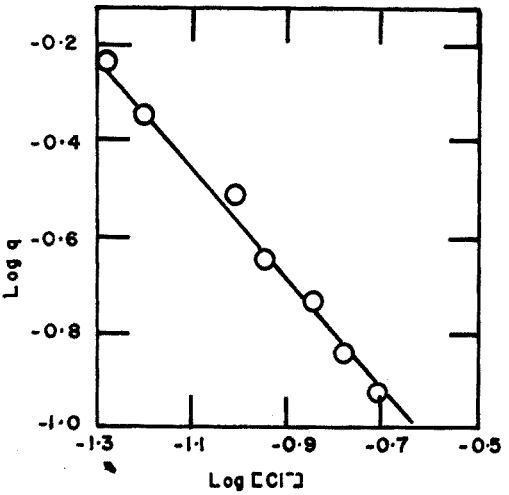

Fig. 3. A plot of log q against log $[Cl^-]$ for the extraction of chromium(III) from aqueous solutions of constant pH and EDTA concentration but variable chloride ion content by a constant concentration of tetrahexylammonium chloride in dichloroethane.

TABLE III

THE EXTRACTION OF CHROMIUM(III) FROM SOLUTIONS OF EDTA AT VARIOUS pH VALUES BY A CONSTANT CONCENTRATION OF TETRA-*n*-HEXYLAMMONIUM CHLORIDE IN DICHLOROETHANE

($[Cr]_{tot} = 5 \cdot 10^{-3}\,M$; $[EDTA]_{tot} = 10^{-2}\,M$; $[NR_4^+Cl^-]_{tot} = 0.3121\,M$)

pH	$[Cl^-]^a$	$[NR_4^+Cl^-]$	*Distribution ratio, q*		
			Exptl.	*Calcd. (i)*[b]	*Calcd. (ii)*[c]
2.08	0.1730	0.3117	0.087	0.044	0.061
2.60	0.1396	0.3115	0.133	0.094	0.111
2.79	0.1296	0.3115	0.140	0.114	0.128
3.66	0.1161	0.3115	0.158	0.155	0.158
5.03	0.1161	0.3114	0.162	0.161	0.161
5.56	0.1161	0.3114	0.159	0.160	0.159
6.02	0.1161	0.3115	0.152	0.156	0.155
6.79	0.1160	0.3115	0.112	0.134	0.116
7.39	0.1157	0.3118	0.060	0.085	0.061
7.56	0.1156	0.3119	0.048	0.069	0.047
7.80	0.1156	0.3120	0.033	0.048	0.036

[a] This value includes the chloride ion added as NaCl, the contribution from the displaced quaternary ammonium salt and that added as HCl to bring the pH below 5.0.
[b] Calculated with $K_1 = 0.62$, $pK_1 = 2.27$ and $pK_2 = 7.41$.
[c] Calculated with $K_1 = 0.62$, $pK_1 = 2.00$ and $pK_2 = 7.15$.

A series of measurements was then conducted with samples of the violet complex $CrY(H_2O)^-$ containing different concentrations of chloride ions in the range $0.036 \leqq [Cl^-] \leqq 0.18\,M$ and buffered to pH *ca.* 4. Each sample was equilibrated with an equal volume of 0.4357 M quaternary ammonium chloride (Table II). In agreement with eqn. (8) a plot of log q against log $[Cl^-]$ was a straight line of unit

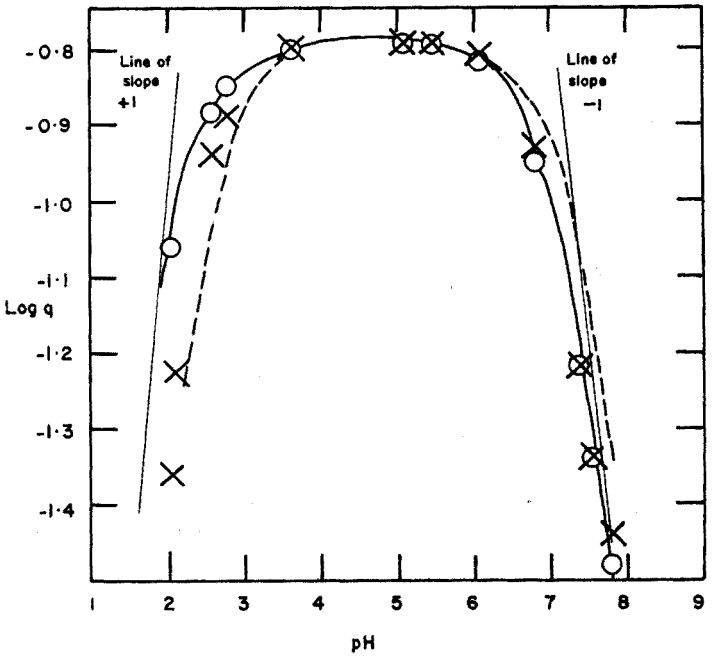

Fig. 4. The effect of pH on the extraction of chromium(III) from solutions in EDTA by a 0.3121 M solution of tetrahexylammonium chloride in dichloroethane. Experimental results shown as open circles and continuous line. The curve calculated from eqn. (8) with $\bar{K}_1 = 0.62$, $pK_1 = 2.41$ and $pK_2 = 7.41$ is shown with broken lines. Values calculated for $\bar{K}_1 = 0.62$, $pK_1 = 2.00$ and $pK_2 = 7.15$ shown as crosses. The measurements at pH 3.66 and above correspond to constant $[Cl^-]$ but the concentration of chloride ion varied in the more acid solutions.

negative slope (Fig. 3) confirming the extraction of chromium in the form $CrY(H_2O)^-$. The calculated value of the extraction constant is $\bar{K}_1 = 0.062 \pm 0.007$.

The variation in the value of q with pH when both $[NR_4^+Cl^-]_{tot}$ and $[Cl^-]_{tot}$ are kept constant is shown in Table III and Fig. 4 (open circles). At sufficiently low pH values the term $1+(K_2/[H^+])$ can be neglected in comparison with $([H^+]/K_1)$ so that eqn. (8) reduces to

$$\log q = \log \bar{K}_1 + \log [NR_4^+Cl^-]_{org} - \log [Cl^-] + pH - pK_1 \qquad (9)$$

and the graph of $\log q$ against pH at constant $[NR_4^+Cl^-]_{org}$ and $[Cl^-]$ should have a limiting slope of $+1$ if only the anion $CrY(H_2O)^-$ is extracted. At sufficiently high pH values the term $([H^+]/K_1)+1$ can be neglected in comparison with $K_2/[H^+]$ and eqn. (8) reduces to

$$\log q = \log \bar{K}_1 + \log [NR_4^+Cl^-]_{org} - \log [Cl^-] + pK_2 - pH$$

so that the limiting slope will be -1.

The observed decrease in q at high pH values (Fig. 4; open circles, continuous

line) is consistent with the replacement of $CrY(H_2O)^-$ by $CrY(OH)^{2-}$ and $CrY(OH)_2^{3-}$ in the aqueous phase. The decrease at low pH is consistent with the protonation of $CrY(H_2O)^-$ to $CrHY(H_2O)$ which is not extracted or extracted to a much smaller extent. The theoretical plot of eqn. (8) calculated with $\bar{K}_1 = 0.062$ and Furlani's values $pK_1 = 2.27$ and $pK_2 = 7.41$ is shown in Fig. 4 as a broken line. Although this fits the experimental results (open circles) over a limited range there are deviations both at high acidities where it underestimates the amount of chromium extracted and at high alkalinities where this is overestimated. These discrepancies at high pH values cannot be due to ignoring the possible extraction of the dominant species $CrY(OH)^{2-}$ since the limiting slope is certainly -1 and the slopes of Figs. 2 and 3 are 1 and not 2. If, however, in place of Furlani's acid dissociation constant the modified value $pK_2 = 7.15$ is used, the calculated curve (Fig. 4, crosses) exactly reproduces the experimental curve over the pH range 4–8. The difference between 7.15 and Furlani's value of 7.41 could be due in large measure to differences in experimental conditions. The discrepancies at low pH values cannot, however, be eliminated by any reasonable modification in the value adopted for pK_1. The crosses in Fig. 4 are calculated with $pK_1 = 2.00$ and a value as low as 1.8 would be needed to give an acceptable fit. Trial calculations showed that the assumption that the uncharged species $CrY(H_2O)$ was being extracted with a small partition coefficient of the order of 0.05–0.1 would enable the experimental curve to be matched easily—but direct evidence for this (*v.s.*) could not be found.

It follows from eqn. (8) that maximum extraction occurs when $\partial(\log q)/\partial \mathrm{pH} = 0$ and $([H^+]/K_1) + 1 + (K_2/[H^+])$ is at its minimum value given by $\mathrm{pH} = (pK_1 + pK_2)/2 = (2.27 + 7.41)/2 = 4.84$. This is confirmed by the experimental results (Fig. 4). The mean value $\bar{K}_1 = 0.062 \pm 0.004$ was obtained from 22 measurements reported above.

In a subsequent paper we shall report on the extraction of a group of transition metals in various oxidation states.

EXPERIMENTAL

Chemicals

The preparation and standardisation of stock solutions of the liquid anion-exchanger tetra-*n*-hexylammonium chloride in 1,2-dichloroethane has been described elsewhere[8].

Solutions of chromium(III) complexes were prepared by boiling 5 ml of an 0.1005 *M* solution of AnalaR chromium(III) chloride with 5 ml of 0.1500 *M* EDTA ($Na_2H_2Y \cdot 2H_2O$) for 10 min. The violet solution was then cooled and diluted to 25 ml. A 0.00166 *M* solution of the complex $CrHY(H_2O)$ was prepared by adjusting a diluted aliquot portion with hydrochloric acid to pH 0.34. Solutions of the violet complex $CrY(H_2O)^-$ were prepared by diluting an aliquot portion and adjusting the pH within the range 3–6 by adding sodium hydroxide. The green complex $CrY(OH)_2^{3-}$ was prepared similarly by adjusting the pH to *ca.* 13.

Methods

Equilibrations were carried out by shaking in stoppered centrifuge tubes 5 ml of solutions of chromium–EDTA complexes containing known added amounts of

chloride ion with an equal volume of tetrahexylammonium chloride for 5 min. After centrifugation the layers were separated and the concentration of each phase was determined at 542 nm with a Unicam SP500 Spectrophotometer and matched cells of the appropriate length from 0.5 to 4.0 cm. The pH values of aqueous phases were measured after equilibration, with a Radiometer pH-meter (type PHM4C) fitted with a glass electrode and a saturated calomel reference electrode.

Before the absorbance of any aqueous phase of volume x ml was measured, the pH was adjusted by adding a known volume, y ml, of hydrochloric acid or sodium hydroxide to be within the range 3 to 6, where the absorbance is known to be insensitive to small changes in the concentrations of the species present[5-7]. The corrected absorbance is then given by (absorbance at 542 nm) $(x+y)/x$.

The molecular extinction coefficient of the violet complex $CrY(H_2O)^-$ in the organic phase was obtained by equilibrating a 5-ml aliquot with an equal volume of 0.0996 M sodium perchlorate. The absorbance of the separated organic phase was zero showing that the reaction

$$(NR_4^+CrY(H_2O)^-)_{org} + ClO_4^- \rightleftharpoons (NR_4^+ClO_4^-)_{org} + CrY(H_2O)^-$$

had proceeded quantitatively to the right. The concentration of the complex $CrY(H_2O)^-$ transferred to the aqueous phase (pH 4.27) was determined absorptiometrically at 542 nm by means of Furlani's value $\varepsilon_{max} = 202$. The following results were obtained.

Absorbance of organic phase at 550 nm (1-cm cell)	0.503	0.506	0.503	0.310	0.310	0.311
$10^3[CrY(H_2O)^-]_{org}$	2.490	2.504	2.495	0.770	0.770	0.775
ε_{max}	202.0	202.1	201.6	201.4	201.4	201.3
	Average 201.6 ± 0.3					

The validity of this procedure rests on the assumption that the absorption spectrum of the complex $CrY(H_2O)^-$ is unaffected by high concentrations of sodium perchlorate. To test this 10 ml of 0.0196 M aqueous $CrY(H_2O)^-$ was diluted to 25 ml (*a*) with pure water and (*b*) with a 0.1017 M solution of sodium perchlorate. The spectra (1-cm cell) were indistinguishable over the range 470–600 nm.

One of us (R. H. Al-J.) is indebted to the Iraqi Ministry of Oil for financial support.

SUMMARY

When a solution of chromium(III) in aqueous ethylenediaminetetraacetic acid (H_4Y) is equilibrated with a solution of the liquid anion-exchanger tetra-*n*-hexylammonium chloride in 1,2-dichloroethane, only the violet complex $CrY(H_2O)^-$ is extracted as the ion pair $NR_4^+CrY(H_2O)^-$ (where R = *n*-hexyl) over the pH range 3.6–6.0. Maximal extraction occurs at pH 4.7 and the extraction constant $\bar{K}_1 = (NR_4^+CrY(H_2O)^-]_{org}[Cl^-]/[NR_4^+Cl^-]_{org}[CrY(H_2O)^-] = 0.062 \pm 0.004$. The formally neutral species $CrHY(H_2O)$ and the anionic species $CrY(OH)^{2-}$ and $CrY(OH)_2^{3-}$ are not extractable.

RÉSUMÉ

Lorsqu'une solution aqueuse chrome(III)–acide éthylènediaminotétracétique (H_4Y) est mise en présence d'une solution d'échangeur anionique liquide, chlorure de tétra-*n*-hexylammonium dans dichloro-1,2-éthane, on constate que seul le complexe violet $CrY(H_2O)^-$ est extrait comme $NR_4^+CrY(H_2O)^-$ ($R = n$-hexyl) à un pH compris entre 3.6 et 6.0. L'extraction maximum se fait au pH 4.7, avec la constante d'extraction : $\bar{K}_1 = [NR_4^+CrY(H_2O^-)]_{org}\,[Cl^-]/[NR_4^+Cl^-]_{org}\,[CrY(H_2O)^-] = 0.062 \pm 0.004$. $CrHY(H_2O)$ et les particules anioniques $CrY(OH)^{2-}$ et $CrY(OH)_2^{3-}$ ne sont pas extractibles.

ZUSAMMENFASSUNG

Aus einer Lösung von Chrom(III) in wässriger Äthylendiamintetraessigsäure (H_4Y) wird mit einer Lösung des flüssigen Anionenaustauschers Tetra-*n*-hexylammoniumchlorid in 1,2-Dichloräthan im pH-Bereich 3.6–6.0 nur der violette Komplex $CrY(H_2O)^-$ als Ionenpaar $NR_4^+CrY(H_2O)^-$ ($R = n$-Hexyl) extrahiert. Die maximale Extraktion erfolgt bei pH 4.7; die Extraktionskonstante ist $\bar{K}_1 = [NR_4^+CrY(H_2O)^-]_{org}\,[Cl^-]/[NR_4^+Cl^-]_{org}\,[CrY(H_2O)^-] = 0.062 \pm 0.004$. Der formal neutrale Komplex $CrHY(H_2O)$ und die anionischen Spezies $CrY(OH)^{2-}$ und $CrY(OH)_2^{3-}$ sind nicht extrahierbar.

REFERENCES

1 R. C. VICKERY, *J. Chem. Soc.*, (1951) 1817.
2 F. L. MOORE, *Anal. Chem.*, 37 (1965) 1235.
3 N. A. ZOLOTOV, O. M. PETRUKHIN AND I. P. ALIMARIN, *Zh. Analit. Khim.*, 20 (1965) 347.
4 F. L. MOORE, *Anal. Chem.*, 38 (1966) 905.
5 C. FURLANI, G. MORPURGO AND G. SATORI, *Z. Anorg. Chem.*, 303 (1960) 1.
6 H. M. N. H. IRVING AND W. R. TOMLINSON, *Chem. Analyst*, 55 (1966) 14.
7 G. DEN BOEF AND B. C. POEELER, *Z. Anal. Chem.*, 199 (1964) 398.
8 H. M. N. H. IRVING AND A. H. NABILSI, *Anal. Chim. Acta*, 41 (1968) 505.

Analytica Chimica Acta
Elsevier Publishing Company, Amsterdam
Printed in The Netherlands

ON ACIDIC ORGANODIPHOSPHORUS EXTRACTANTS

PART IV. EXTRACTION OF EUROPIUM(III) BY A DIPHOSPHONIC ACID IN DIFFERENT ORGANIC SOLVENTS

M. JAMIL, P. ZUR NEDDEN AND G. DUYCKAERTS
Department of Analytical and Nuclear Chemistry, University of Liège, Sart Tilman (Belgium)

(Received 12th March 1971)

Organophosphorus extractants such as dialkylphosphoric acids and phosphine oxides have been widely studied for the extraction of different metal ions. Current research work is more concerned with the organodiphosphorus extractants of the diphosphine oxide and diphosphonic acid types.

Gorican, Grdenic *et al.* have described the extraction of different metal ions by dialkylmethane-diphosphonic acids: Zr and Ge[1], Ti[2], Ge and As[3], Nb and Ta[4].

zur Nedden[5] has observed that di-*n*-alkylethane-(1,2)-diphosphonic acids (RO-(OH)-PO-$(CH_2)_2$-PO-(OH)-OR, where R is a *n*-butyl or *n*-octyl group) are monomeric in benzene containing 4% pentanol-1 and he suggested that the stoichiometry of metal complexes in the same organic phase is $Eu(AH)_3$[6].

In this paper the results are reported of a distribution study of di-*n*-butyl-ethane-(1,2)-diphosphonic acid and the stoichiometry of the europium complexes in different organic solvents.

EXPERIMENTAL

Reagents

The extractant, di-*n*-butyl-ethane-(1,2)-diphosphonic acid (C_4H_9-O-(OH)-PO-$(CH_2)_2$-PO-(OH)-O-H_9C_4, H_2B_2EDP) was synthesized in this laboratory. A ^{32}P-labelled H_2B_2EDP extractant was prepared by irradiating it in a nuclear reactor and the labelled compound was separated from the other irradiation products[7]. All other chemicals were reagent-grade products (E. Merck, West Germany) and were used without further purification. The γ-active nuclide $^{152,154}Eu$ was prepared by neutron irradiation of Eu_2O_3. The stock solution of $^{152,154}Eu$ was prepared by first evaporating the nitrate solution and then dissolving the residue in 1 *M* (H,Na) ClO_4. The concentration of europium(III) was less than 10^{-6} *M*. In all these experiments the ionic strength in the aqueous phase was adjusted to a value of 1.0 by the addition of sodium perchlorate and the concentration of perchloric acid was 0.1 *M*.

Procedure

In studies of the distribution of the extractant, the organic phase was a solution of a mixture of labelled and unlabelled H_2B_2EDP. In studies of the distribution of the metal ion, the organic phase was a solution of inactive H_2B_2EDP and the aqueous phase contained $^{152,154}Eu$; 3 ml of both phases shaken for 30 min in a thermostated

shaker at 25°. The two phases were then separated by centrifugation.

The ^{32}P β-activity was measured with a GM dipping detector and the $^{152,154}Eu$ γ-activity was measured with a scintillation counter (well-type NaI(Tl) crystal).

The spectrophotometric determination of H_2B_2EDP in the organic phase was carried out as follows: H_2B_2EDP from the organic phase was precipitated by equilibration with an aqueous phase containing an excess amount of iron(III). The remaining iron(III), complexed by sulfosalicylic acid, gave an intense pinkish red colour with maximal absorbance at 510 nm. In some cases, the concentration of H_2B_2EDP in the organic phase was determined by a two-phase titration with a standard solution of sodium hydroxide.

RESULTS AND DISCUSSION

Distribution of the extractant

The distribution coefficient of the extractant AH_2 is expressed as:

$$E_{(A)} = [AH_2]\text{org. total}/[AH_2]\text{aq. total} \tag{1}$$

If we assume that only one species of the extractant is present in the organic phase at a time and that there is no association of the extractant in the aqueous phase, the distribution coefficient of the extractant can be written as:

$$E_{(A)} = n[A_nH_{2n}]_o/([AH_2] + [AH^-] + [A^{2-}]) \tag{2}$$

where $[A_nH_{2n}]_o$ and $[AH_2]$, $[AH^-]$, $[A^{2-}]$ are the equilibrium concentrations of the extractant in the organic and aqueous phase, respectively.

Introducing into eqn. (2) the different constants, we obtain

$$E_{(A)} = \frac{n \cdot \beta_{(A)n} \cdot [AH_2]_o^n}{[AH_2]\{1 + K_{(H)1}/[H^+] + K_{(H)1} \cdot K_{(H)2}/[H^+]^2\}} \tag{3}$$

where $\beta_{(A)n} = [A_nH_{2n}]_o/[AH_2]_o^n$ is the association constant, and

$K_{(H)1} = [AH^-]\,[H^+]/[AH_2]$ and $K_{(H)2} = [A^{2-}]\,[H^+]/[AH^-]$ are the acidity constants.

At constant pH and for a given value of n, eqn. (3) can be written as:

$$E_{(A)} = K \cdot [AH_2]^{n-1} \tag{4}$$

or in logarithmic form as

$$\log E_{(A)} = \log K + (n-1) \log [AH_2] \tag{5}$$

If $\log E_{(A)}$ is plotted *versus* the logarithm of the concentration of the undissociated form of the extractant at equilibrium, $[AH_2]$, a straight line of slope $n-1$ is obtained (n is the degree of association of the extractant in the organic phase).

In the case of benzene, the experimental results are shown in Fig. 1. The points shown are the results obtained by the radiometric, colorimetric and acid–base titration methods, as indicated. When these results are analysed, it is found that the slope of the straight line is zero ($n=1$) up to a concentration of the undissociated form of the extractant equal to $4 \cdot 10^{-3}$ M in the aqueous phase. This means that the extractant remains monomeric in the above concentration range. The curve starts bending up-

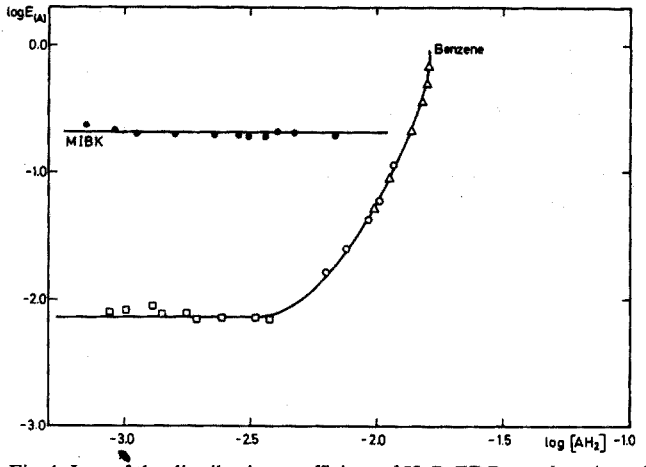

Fig. 1. Log of the distribution coefficient of H_2B_2EDP as a function of the log of the concentration of the undissociated form of the extractant in the aqueous phase. (●) MIBK; (□, △, ○) benzene; (□) radiometry; (△) acid–base titration; (○) colorimetry.

wards for AH_2 superior to $5 \cdot 10^{-3}$ *M*. Its slope indicates an average degree of association of approximately 9 near saturation.

Since it is not very probable that polar groups like P=O and P–OH can exist in the free state in non-hydrogen bonding solvents such as benzene up to a concentration of $4 \cdot 10^{-3}$ *M*, two explanations can be suggested for the deactivation of these polar groups of the extractant molecule: (*a*) through hydrogen bond formation with water molecules; or (*b*) by formation of intramolecular bonds.

At higher concentrations the extractant obviously starts associating by the formation of intermolecular bonds.

In the case of methyl isobutyl ketone (Fig. 1), a line of slope zero is obtained throughout the whole concentration range up to saturation. Although the extractant concentration in the aqueous phase is the same for the two solvents, the distribution coefficient of the extractant and its concentration is 30 times greater in MIBK than in benzene. Nevertheless, the extractant remains monomeric in MIBK. This state of the extractant in the ketone could be explained by the formation of hydrogen bonds between the C=O group of the ketone and the P–OH group of the extractant. The partition constants of the monomer extractant ($K_{p(A)} = [AH_2]_o/[AH_2]$) with its standard deviations determined for the two solvents were found to be:

$$K_{p(A)} \text{ in benzene} = (1.43 \pm 0.20) \cdot 10^{-2}$$

$$K_{p(A)} \text{ in MIBK} = (4.24 \pm 0.16) \cdot 10^{-1}.$$

From the above distribution study, it is possible to conclude that this diphosphonic acid remains a monomer in the organic phase over a wide range of concentration.

The extraction of europium(III)

The extraction of europium(III) was carried out with an aprotic solvent (benzene), two protogenic solvents ($CHCl_3$ and $CHBr_3$), a protophilic solvent (MIBK), and

a highly protogenic mixture of two solvents (benzene containing 12% pentanol-1). It is assumed that only neutral metal complexes are extracted into the organic phase and that there is no formation of polynuclear complexes. It was found that the extractant remains monomeric in benzene, in MIBK and in benzene containing 4% of pentanol-1 in the concentration range studied during the extraction of europium(III). The equilibrium concentration of the extractant in the aqueous phase at constant pH is therefore proportional to its total concentration. Under these conditions, the distribution coefficient of the metal ion ($E_{(Me)}$) can be expressed as follows:

$$E_{(Me)} = K \cdot C_t^m \tag{6}$$

where $C_t = [AH_2]/k$

$$K = k \cdot \beta_{(Me)} \cdot K_{p(Me)}$$

$$\beta_{(Me)} = [Me(A_mH_{2m-3})]/[Me^{3+}]\,[AH_2]^m$$

$$K_{p(Me)} = [Me(A_mH_{2m-3})]_o/[Me(A_mH_{2m-3})]$$

C_t is the total concentration of the extractant in the aqueous and organic phase (the two phases have the same volume), m is the number of extractant molecules present in the metal complexes, $\beta_{(Me)}$ is the formation constant of the complex in the organic phase, and $K_{p(Me)}$ is the partition constant of the complex.

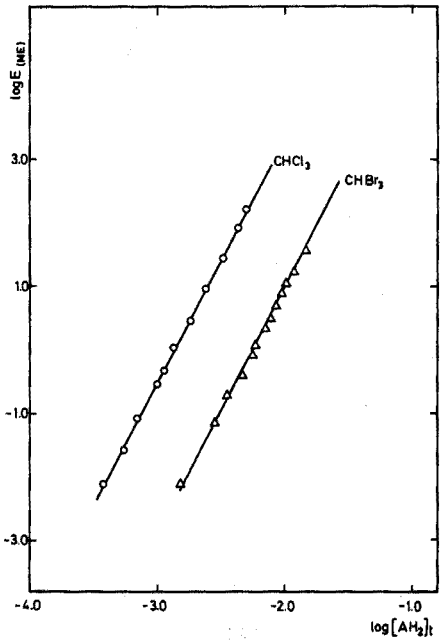

Fig. 2. Log of the distribution coefficient of Eu(III) as a function of the log of the total concentration of H_2B_2EDP. (○) $CHCl_3$; (△) $CHBr_3$.

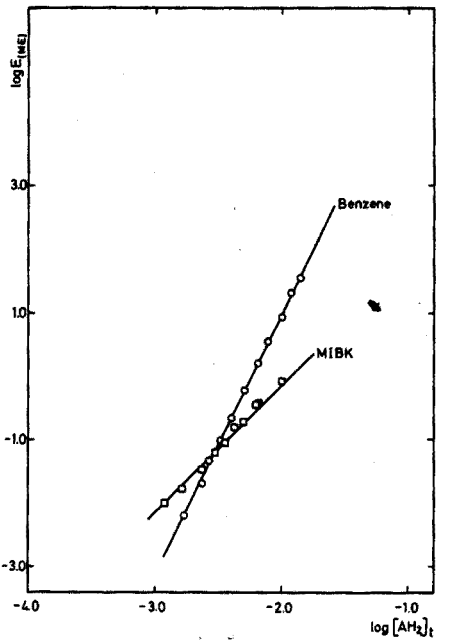

Fig. 3. Log of the distribution coefficient of Eu(III) as a function of the log of the total concentration of H_2B_2EDP. (○) Benzene; (□) MIBK.

Equation (6) becomes in logarithmic form

$$\log E_{(Me)} = \log K + m \log C_t$$

The plot of $\log E_{(Me)}$ *versus* the logarithm of the total concentration of the extractant gives a straight line with the slope equal to m.

In the plot of $\log E_{(Me)}$ *versus* $\log C_t$, straight lines with a slope of 4 were obtained for the protogenic solvents $CHCl_3$ and $CHBr_3$ (Fig. 2); in the case of benzene a slope of 4 was also obtained (Fig. 3). A straight line with a slope of 2 was obtained for the protophilic solvent MIBK (Fig. 3), while, in the case of benzene containing 12% pentanol-1, a straight line with a slope of 3 was obtained (Fig. 4).

The extraction of europium(III) into benzene, chloroform and bromoform is given by the following reaction.

$$Eu^{3+} + 4\,AH_2 \rightleftharpoons Eu(AH)_3\,AH_{2_o} + 3\,H^+$$

It is seen that the metal complex extracted into benzene contains one molecule of the extractant in excess. This may be due to the fact that benzene has a low solvating power and the additional molecule of the extractant could be associated to some of the free polar groups present in the metal complex as shown in the scheme below:

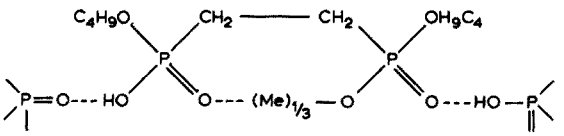

On the other hand, the fourth molecule could also occupy vacant positions on the coordination shell of the europium(III) ion.

The metal complex extracted into proton donor solvents contains 4 molecules of the extractant. There seems to be only a poor association between the protogenic solvents $CHCl_3$ and $CHBr_3$ and free polar groups present in the metal complex. This could explain the presence of an additional molecule of the extractant in the complex extracted into these solvents.

From Fig. 4 it is seen that the slope of the straight line is 3. This means that the metal complex extracted into benzene containing 12% pentanol-1 has three molecules of the extractant. In this case, it is considered that some of the free polar groups present in the metal complex are saturated by pentanol-1 molecules. The formula of the metal complex may be proposed as $Eu(AH)_3 \cdot xROH$.

The metal complex extracted into the ketone contains two molecules of the extractant. The ketone being a Brönsted base, would certainly solvate the metal complex, which can be represented by $EuA(AH) \cdot xRR'C{=}O$.

CONCLUSIONS

The extractant, a diphosphonic acid, is found to be monomeric in a wide range of concentration in benzene and MIBK. At higher concentrations it starts associating

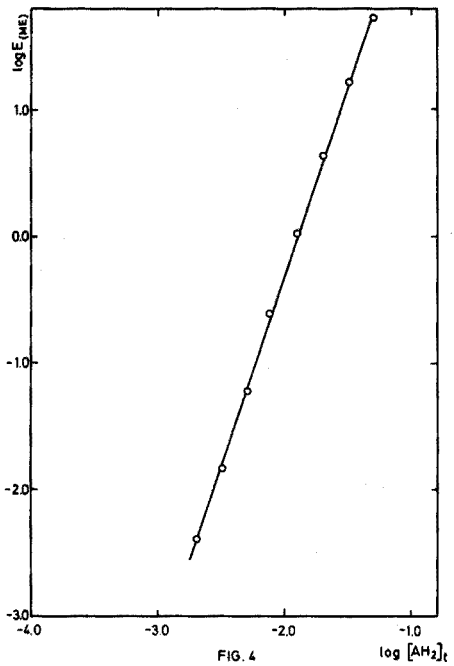

Fig. 4. Log of the distribution coefficient of Eu(III) as a function of the log of the total concentration of H_2B_2EDP. Benzene containing 12% pentanol-1.

in benzene. zur Nedden[5] found that the extractant is converted into a monomeric state in nearly the whole concentration range up to saturation, by the addition of 4% pentanol-1 to benzene. On this basis, it is assumed that H_2B_2EDP remains monomeric in benzene containing 12% pentanol-1 in the concentration range used during the extraction of europium(III).

It appears that the proton donor and acceptor properties of the organic solvents play an important role in determining the stoichiometry of the metal complex extracted into the organic phase. It was found that the complex extracted into benzene containing 12% pentanol-1 has the stoichiometry $Eu(AH)_3$, while that extracted into benzene, chloroform and bromoform contains 4 molecules of the diphosphonic acid. The complex extracted into methyl isobutyl ketone contains 2 molecules of the extractant.

The work has been supported by the "Office de la Coopération au Développement" and the "Institut Interuniversitaire des Sciences Nucléaires", Brussels (Belgium).

SUMMARY

The distribution of di-*n*-butyl-ethane-(1,2)-diphosphonic acid (H_2B_2EDP) between 1 *M* (H, Na)ClO_4 and benzene or methyl isobutyl ketone has been studied radiometrically. The partition constants of H_2B_2EDP are calculated. The results indicate that H_2B_2EDP remains monomeric in benzene up to a total concentration of $1.3 \cdot 10^{-2}$ *M*, while it is monomeric throughout the whole concentration range up to saturation in methyl isobutyl ketone. Europium is extracted from an aqueous phase

1 *M* (H, Na)ClO_4 by H_2B_2EDP into benzene, $CHCl_3$, $CHBr_3$, methyl isobutyl ketone and into benzene containing 12% pentanol-1. The extraction data indicate that europium is extracted into benzene as $Eu(AH)_3AH_2$, while the stoichiometry of the complexes extracted into methyl isobutyl ketone and into benzene containing 12% pentanol-1 seems to be $EuA(AH)\cdot xRR'C{=}O$ and $Eu(AH)_3\cdot xROH$, respectively. On the assumption that during the extraction of europium(III) the extractant also remains a monomer in $CHCl_3$ and $CHBr_3$ in the concentration range studied, it is concluded that the formula of the europium complex extracted is $Eu(AH)_3AH_2$.

RÉSUMÉ

L'étude de la distribution de l'acide di-*n*-butyl-éthane-(1,2)-diphosphonique (H_2B_2EDP) entre une solution 1 *M* en (H, Na)ClO_4 et le benzène ou la méthylisobutylcétone est réalisée par une méthode radiométrique. Les résultats indiquent que H_2B_2EDP reste monomère dans le benzène jusqu'à une concentration totale de $1.3\cdot10^{-2}$ *M* et qu'il est monomère dans tout le domaine de concentration jusqu'à saturation dans la méthylisobutylcétone. L'extraction de l'europium est ensuite réalisée à partir d'une phase aqueuse 1 *M* en (H, Na)ClO_4 par H_2B_2EDP dans le benzène, le chloroforme, le bromoforme, la méthylisobutylcétone et dans le benzène contenant 12% de pentanol-1. Il semble que l'europium est extrait dans le benzène sous la forme $Eu(AH)_3AH_2$ et que la stoechiométrie des complexes extraits dans la cétone et dans le benzène contenant 12% de pentanol-1 est probablement $EuA(AH)\cdot xRR'C{=}O$ et $Eu(AH)_3\cdot xROH$ respectivement. Si on admet que l'extractant reste monomère dans $CHCl_3$ et $CHBr_3$, dans le domaine de concentration étudié, la formule du complexe extrait dans ces solvants est $Eu(AH)_3AH_2$.

ZUSAMMENFASSUNG

Die Verteilung der Dibutyläthan-(1,2)-diphosphonsäure, H_2B_2EDP, zwischen einer 1 *M* (H,Na)ClO_4-Lösung und Benzol oder Methylisobutylketon wurde radiometrisch untersucht. Die Ergebnisse zeigen, dass H_2B_2EDP monomer bleibt: in Benzol unterhalb einer Gesamtkonzentration von $1.3\cdot10^{-2}$ *M* und in Methylisobutylketon im ganzen Konzentrationsbereich bis zur Sättigung. Europium(III) wurde aus wässriger 1 *M* (H,Na)ClO_4-Lösung durch H_2B_2EDP in Benzol, Chloroform, Bromoform, Methylisobutylketon und Benzol, das 12% Pentanol-1 enthält, extrahiert. In Benzol liegt es als $Eu(AH)_3AH_2$ Komplex vor. Die Stöchiometrie der Verbindungen, die in das Keton und in das Benzol–Pentanol-Gemisch extrahiert werden, ist wahrscheinlich $EuA(AH)\cdot xRR'C{=}O$ bzw. $Eu(AH)_3\cdot xROH$. Nimmt man an, dass die Diphosphonsäure im untersuchten Konzentrationsbereich in Chloroform und Bromoform gleichfalls monomer bleibt, so ist die Formel der in diesen Lösungsmitteln vorliegenden Komplexe $Eu(AH)_3AH_2$.

REFERENCES

1 H. GORICAN AND D. GRDENIC, *Proc. Chem. Soc.*, (1960) 288.
2 H. GORICAN AND D. GRDENIC, *J. Chem. Soc.*, (1964) 513.
3 D. GRDENIC AND V. JAGODIC, *J. Inorg. Nucl. Chem.*, 26 (1964) 167.
4 C. DJORDJEVIC AND H. GORICAN, *J. Inorg. Nucl. Chem.*, 28 (1966) 1451.
5 P. ZUR NEDDEN, paper to be published.
6 P. ZUR NEDDEN, *Z. Anal. Chem.*, 247 (1969) 236.
7 M. JAMIL, *Thèse de Doctorat*, Liège, 1970.

Analytica Chimica Acta
Elsevier Publishing Company, Amsterdam
Printed in The Netherlands

THE SOLVENT EXTRACTION OF ALIPHATIC SULFIDES WITH COPPER(II) AND MERCURY(II) SOLUTIONS

TAKAO YOTSUYANAGI, TAMIO KAMIDATE AND KAZUO AOMURA
Laboratory of Analytical Chemistry, Faculty of Engineering, Hokkaido University, Sapporo (Japan)
(Received 28th October 1970)

Since mercury(II) ion was first introduced by Birch and McAllan[1] as a suitable extractant for *n*-butyl sulfide, metal ions such as mercury(II) and zinc(II) have been used as reagents for the solvent extraction and subsequent purification of a number of organic sulfides[2-5].

Recently, Orr[4,5] suggested that organic sulfides can be separated and determined by liquid–liquid chromatography with mercury(II) or zinc(II) solution as the stationary phase. For the mercury(II) acetate–organic sulfide system, Orr[4] postulated the adduct formation reaction:

$$R_2S_{(o)} \rightleftarrows R_2S_{(a)} \overset{xHg(OAc)_2}{\longleftrightarrows} R_2S : xHg(OAc)_{2(a)} \qquad (1)$$

where the subscripts o and a indicate the organic and aqueous phases, respectively. However, he did not give any other information concerning the mechanism of the reaction.

In view of the scanty information available in the literature on metal ion–organic sulfide complexes in solution, further investigation seemed desirable. The present work was undertaken to determine the stoichiometry and the formation constants of the various metal–organic sulfide complexes in solution. Studies were also made on the effect of anionic ligands on the extraction equilibrium and on the extraction rate.

EXPERIMENTAL

Reagents

All chemicals used were of analytical-reagent grade.

Extraction and analytical procedure

Equal volumes (9 ml) of organic solvent containing 60 μl of sulfide and internal reference (Table I) and of the aqueous solution of metal salt were shaken for 1–2 h in 40-ml stoppered test tubes. After separation of the phases, the concentration of sulfide in the organic phase was determined with a Yanagimoto-G 8 model gas chromatograph, and then the distribution ratio, D (the ratio of the equilibrium concentration of sulfide in the aqueous phase to that in the organic phase) was calculated.

TABLE I

COMPOSITION OF ORGANIC PHASE

Sulfide	*Solvent*	*Internal standard material*
Dimethyl sulfide (DMS)	*n*-Heptane	Benzene
Diethyl sulfide (DES)	*n*-Pentane	Toluene
n-Propyl sulfide (*n*PS)	*n*-Pentane	*p*-Xylene

Ultraviolet spectral measurements

For the evaluation of the composition and the stability constants of the metal–sulfide complexes in aqueous solution, the ultraviolet spectra were determined by a Hitachi model 124 double-beam spectrophotometer equipped with 1-cm quartz cells. The pH values of the aqueous solutions were determined with a Tōadenpa HM-5A model pH meter and a glass electrode.

RESULTS AND DISCUSSION

Stoichiometry of the extracted metal–aliphatic sulfide complexes

It has been reported[6] that the stoichiometry of the addition compounds of aliphatic sulfides with mercury(II) chloride is $R^1R^2S(HgCl_2)_n$ with $n=1$, 1.5 and 2 in the solid state, and these complexes are classified as substitution compounds. Recently, Orr[4] postulated that the stoichiometry of the extraction reaction of sulfides with mercury(II) acetate may be expressed by eqn. (1). However, the value of x in eqn. (1), *i.e.* the formula of the metal–aliphatic sulfide complexes in aqueous solution, is not known.

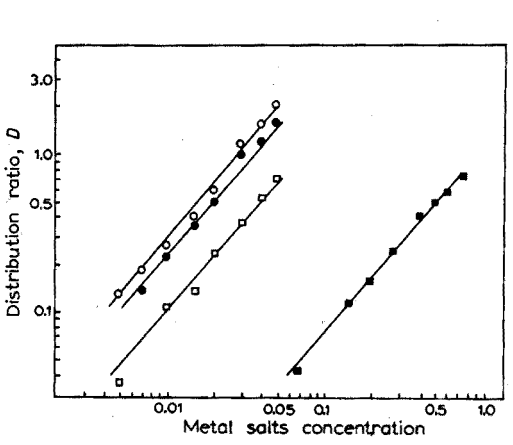

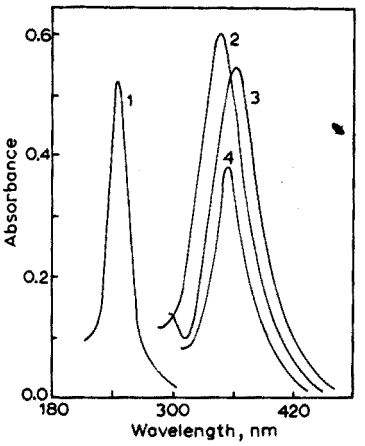

Fig. 1. Relationship between distribution ratio and metal ion concentration. $[Hg(II)]+[Na^+]=0.05$ *M* const., $[Cu(II)]+[Ca(II)]=4.57$ *M* const. (○) Hg(II)–DMS, (●) Hg(II)–DES, (□) Hg(II)–*n*PS, (■) Cu(II)–DMS.

Fig. 2. Absorption spectra for the DMS-metal ion complex. (1) $Hg(CH_3COO)_2=0.003$ *M*, (2) $CuBr_2=0.15$ *M*, (3) $CuCl_2=0.11$ *M*, (4) $Cu(ClO_4)_2=0.12$ *M*.

The extraction of aliphatic sulfides from organic solutions at an initial sulfide concentration of 60 μl dissolved in 9 ml of organic solvent, with aqueous solutions of copper(II) chloride or mercury(II) acetate was examined at various metal ion concentrations. Figure 1 shows the log–log plots of the distribution ratio for the sulfides *vs.* the metal ion concentration. All the plotted curves obtained for copper(II) or mercury(II) with several kinds of aliphatic sulfides gave straight lines with slopes of 1.0–1.1, which suggests a first-power dependence of the distribution ratio on the metal ion concentration. Hence, the following equilibrium expression is given for the extraction of sulfides from organic solvents by aqueous solutions of metal ions:

$$Me^{x+}{}_{(a)} + n'L^-{}_{(a)} \rightleftarrows MeL_{n'}^{(x-n')+}{}_{(a)} \quad (2)$$

$$R_2S_{(o)} \rightleftarrows R_2S_{(a)} \quad (3)$$

$$MeL_{n'}^{(x-n')+}{}_{(a)} + mR_2S_{(a)} \rightleftarrows MeL_{n'}(R_2S)_{m(a)} \quad (4)$$

$$MeL_{n'}(R_2S)_{m(a)} \rightleftarrows MeL_{n'}(R_2S)_{m(o)} \quad (5)$$

where Me and L^- represent the metal ion and the anionic ligand, respectively. The distribution ratio of the sulfides, D, is given:

$$D = \frac{[R_2S]_{(a)} + \Sigma m[MeL_{n'}(R_2S)_m^{(x-n')+}]_{(a)}}{[R_2S]_{(o)} + \Sigma m[MeL_{n'}(R_2S)_m^{(x-n')+}]_{(o)}} \quad (6)$$

In this extraction system, both the concentration of the free sulfides in the aqueous phase and the concentration of the sulfide complexes in the organic phase were extremely low compared with that of the other species in eqn. (6). Thus, eqn. (6) can be reduced to:

$$D = \Sigma m[MeL_{n'}(R_2S)_m^{(x-n')+}]_{(a)}/[R_2S]_{(o)} = \Sigma mK \cdot K_n \cdot \beta_{n'} \cdot [Me]_{(a)} \cdot [R_2S]^{m-1}{}_{(a)} \cdot [L^-]^{n'}{}_{(a)} \quad (7)$$

where K, K_n and $\beta_{n'}$ represent the distribution coefficient of the sulfides in eqn. (3), the formation constant of sulfide complexes in eqn. (4), and the cumulative formation constant of the complexes in eqn. (2), respectively. Under the experimental conditions shown in Fig. 1, the total concentration of the anionic ligands was kept effectively constant. Thus, the distribution ratio is given by the following expression:

$$\log D = \log [Me]_{(a)} + (m-1) \log [R_2S] + \text{constant} \quad (8)$$

The slopes of all the plots in Fig. 1, $\log D/\log [Me]_{(a)}$, were very close to unity. Thus the value of m in eqns. (4)–(7) is one. Consequently, it is thought that the aliphatic sulfides are extracted into the aqueous solution of metal ion by the following overall reaction:

$$MeL_{n'}^{(x-n')+}{}_{(a)} + R_2S_{(o)} \rightleftarrows MeL_{n'}(R_2S)^{(x-n')+}_{(a)} \quad (9)$$

Ultraviolet spectrophotometric study

The ultraviolet absorption spectra of the copper(II) and mercury(II) complexes of dimethyl sulfide (DMS) were measured (Fig. 2). The absorbance maximum of the mercury(II)–DMS–OAc^- complex occurs at 245 nm whereas that of the copper(II)–DMS–L^- complex ($L^- = ClO_4^-$, Cl^-, Br^-) occurs at 350–360 nm. In the case of

copper(II) complexes, Fig. 2 shows that the wavelength of maximum absorbance and the apparent absorbance of the complexes were affected by the nature of the anionic ligand existing in the solution; this suggests the presence of the complex containing the anionic ligand. The rate of complex formation in aqueous solution and the stability of the absorbance were examined by measuring the absorbance at the peak wavelength. The rate of formation was found to be very high and the absorbance was stable for at least 40 min. Based on these preliminary examinations, the composition of the metal–DMS complexes in solution was estimated by Job's method of continuous variations, where the total concentration of metal ion and sulfide were kept at 0.2 *M* for the copper(II) system and at 0.01 *M* for the mercury(II) system. The pH values of these solutions were 2.6 for the copper(II) system and 1.7 for the mercury(II) system. At these pH values, the hydrolysis reaction of copper(II) and mercury(II) can be neglected[7]. The Job plots (Fig. 3) show that the copper(II)– and mercury(II)–DMS complexes contained [Me] : [DMS] = 1 : 1.

These results were in accordance with the results obtained from the linear correlation between the metal ion concentration and the distribution ratio, *D*, for sulfide. Thus, the stoichiometry of eqn. (9) is also confirmed by spectrophotometry.

For copper(II)–DMS complexes, Fig. 3 shows that anionic ligands had no effect on the composition, but did affect the stability constants and the absorbances.

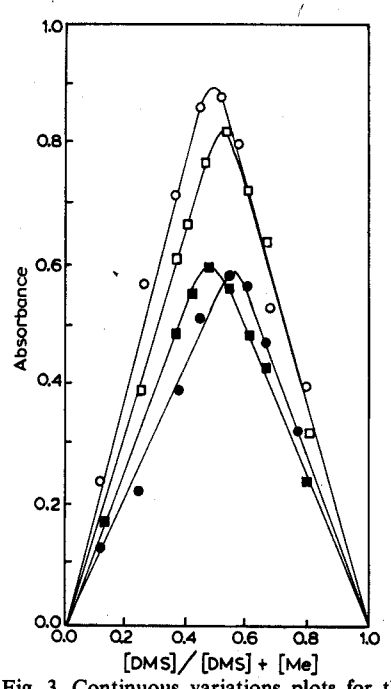

Fig. 3. Continuous variations plots for the DMS–metal complex. [Cu(II)] + [DMS] = 0.20 *M* const., [Hg(II)] + [DMS] = 0.01 *M* const. (○) $Hg(CH_3COO)_2$, (□) $CuBr_2$, (■) $CuCl_2$, (●) $Cu(ClO_4)_2$.

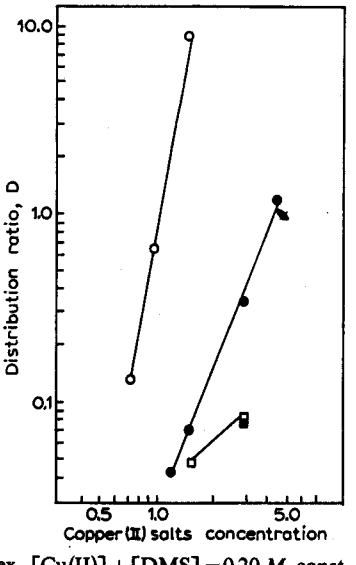

Fig. 4. Relationship between distribution ratio (DMS) and the initial concentration of copper(II) salts. (○) $CuBr_2$, (●) $CuCl_2$, (■) $Cu(NO_3)_2$, (□) $Cu(ClO_4)_2$.

From the curves in Fig. 3, the apparent stability constants, K^{app}, for each system were calculated by means of eqn. (10):

$$K^{app} = \frac{\left(\frac{As}{As_{ext}}\right)}{\left(1 - \frac{As}{As_{ext}}\right)^2 [Me]_{total}} \quad (10)$$

where As and As_{ext} represent the absorbance of the solutions and that of the extrapolated value, respectively. The stability constants found (Table II) show that the

TABLE II

STABILITY CONSTANT OF METAL–DMS COMPLEX

	Complex	*Anionic ligands* (L^-)			
		Br^-	Cl^-	ClO_4^-	CH_3COO^-
log K	Cu–L–$(CH_3)_2S$	4.23	3.52	2.91	—
	Hg–L–$(CH_3)_2S$	—	—	—	5.19

stability of the sulfide complex decreases in the order $Br^- > Cl^- > ClO_4^-$; this suggests that the halogenocopper(II) complex ion, $CuL_{n'}^{(2-n')+}$, is a better complexing agent for sulfides than the aquocopper(II) ion. The stability constant of the chlorocopper(II) compound is larger than that of the bromocopper(II) compound (K_1 for $CuCl^+$ 1.3 and for $CuBr^+$ 0.23)[8], and this order is not in accordance with that of K^{app} shown in Table II. This apparent discrepancy could be explained by the nature of the ligands, Cl^-, Br^- and R_2S. It is thought that the electron-donating power of R_2S is very strong, so that the auxiliary ligands, which can reduce the charge accumulation on the central metal ion by charge transfer with a π-acceptor orbital on the ligand (bromide having a better acceptor orbital than chloride), favor the formation of the metal–R_2S bond.

Effect of anionic ligands on the extraction efficiency of metal ion for dimethyl sulfide

From the K^{app} value of the copper(II)–DMS complexes, the extraction efficiency of copper(II) ion for sulfide could be expected to be enhanced by the presence of the anionic ligands. Figure 4 shows representative results for different copper(II) salts used in the extraction of DMS. The extraction efficiency of copper(II) solution was obviously strongly influenced by the anionic ligands, and decreased in the order $Br^- > Cl^- > ClO_4^- \sim NO_3^-$. This order is in accordance with the order of the apparent stability of the sulfide complexes (Table II).

In order to obtain more detail on the mechanism of this effect, the extraction efficiency was measured with 2.0 *M* zinc(II) nitrate solution, 1.5 *M* copper(II) nitrate solution and 0.02 *M* mercury(II) acetate solution which were 2.0 *M*, 1.5 *M* and 0.02 *M* in the calcium salts of the anionic ligands, respectively. The results (Table III) showed that, among these metal ions, only copper(II) notably increased its extraction efficiency in the presence of suitable anionic ligands; the value of the distribution ratio increased

TABLE III

EFFECT OF ANIONS ON THE DISTRIBUTION RATIO OF DIMETHYL SULFIDE

Metal salt	*Concentration (M)*	*Distribution ratio, D*				
		Salting out agent[a]				
		Not added	$CaBr_2$	$CaCl_2$	$Ca(CH_3COO)_2$	$Ca(NO_3)_2$
$Cu(NO_3)_2$	1.50	0.001	17.8	0.17	—	0.035
$Zn(NO_3)_2$	2.00	0.000	0.04	0.02	—	0.02
$Hg(CH_3COO)_2$	0.02	0.53	0.50	0.47	0.60	0.81

[a] [salting out agent]/[metal salt] = 1.0.

TABLE IV

STABILITY CONSTANT OF METAL–ANION COMPLEX[8]

	Br^-	Cl^-	CH_3COO^-	NO_3^-	ClO_4^-
$\log K^{Cu-L}$	−0.64	0.11	1.62	No evcpx[b]	—[a]
$\log K^{Zn-L}$	2.3	2.2	1.59	No evcpx[b]	No evcpx[b]
$\log K^{Hg-L}$	17.3	13.2	8.43	−0.21	Evcpx[c]

[a] $\log K^{s} = \log[Cu^{2+}][OH^-]^{1.71}[ClO_4^-]^{0.29} = -17$.
[b] No evidence for the existence of the complex.
[c] Evidence for the existence of the complex.

more than 10^3 times in the presence of bromide ion. The extraction efficiency of mercury(II) for DMS decreased slightly when chloride or bromide was present, presumably because these anions form very stable complexes with mercury(II) (Table IV) and inhibit the formation of mercury(II)–DMS complexes. Anions forming stable complexes are not necessarily suitable agents for increasing the extraction efficiency of the metal ion. In the presence of anions forming unstable complexes such as nitrate and perchlorate ion, the observed increase in the extraction efficiency of all the metal ions shown in Table III was mainly attributed to the salting out effect of calcium ion[9]. Thus, in the case of zinc(II), Tables III and IV show that co-ordinated chloride and bromide ion have almost no effect on the extraction efficiency of zinc(II) for DMS. These differences in the effect of the anion on the extraction efficiency of the metal ions can probably be explained in terms of the difference in the stereochemistry of the metal complexes.

From these studies, copper(II) was the most useful agent for the extraction and the liquid–liquid chromatographic separation of sulfides, because its extraction efficiency could be readily controlled by changing the concentrations of copper(II) and bromide ion as shown in Table III and Fig. 5. Orr[4,5] reported that for the zinc(II) and mercury(II) systems, the logarithm of the distribution ratios of sulfides decreased linearly as a function of the carbon number of the aliphatic sulfides. This was also observed for the copper(II) system. Di-*n*-butyl sulfide (C_8) could be quantitatively extracted into an aqueous phase containing 4.92 *M* copper(II) bromide (saturated solution). Thus, it may be expected that the copper(II)–bromide system can be

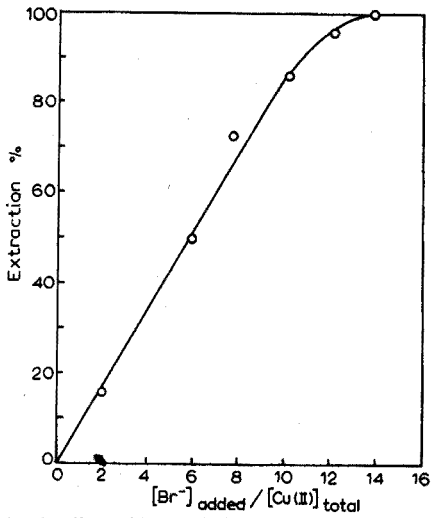

Fig. 5. Effect of bromide ion on the percentage extraction for DMS. Cu(II) = 0.50 *M* const.

successfully applied for the extraction of C_2–C_{10} sulfides.

Extraction rate study

In preliminary experiments, it was shown that a shaking time of 1–2 h was sufficient for the extraction system to attain equilibrium. However, because of possible application to liquid–liquid chromatography, further investigations of the extraction rate were considered desirable. The extraction of solutions containing 60 μl of DMS in 9 ml of *n*-heptane with various concentrations of copper(II) ion solution containing 8.0 *M* anionic ligand gave the results shown in Fig. 6 (for bromide) and Fig. 7 (for

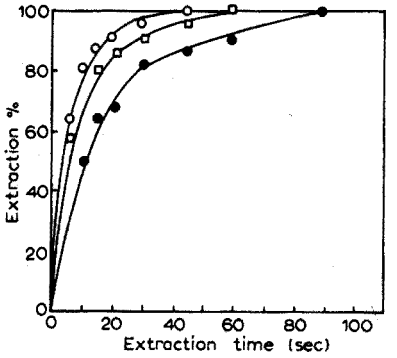

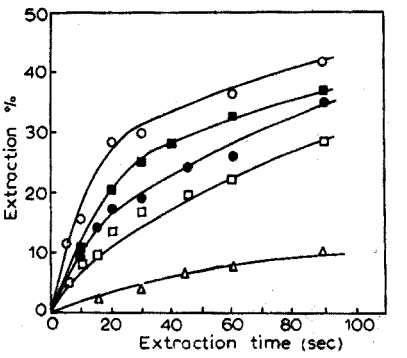

Fig. 6. Variation of extraction efficiency with extraction time for the extraction of DMS by various concentrations of copper(II) bromide solutions. (○) $CuBr_2 = 1.5$ *M*, (□) $CuBr_2 = 1.0$ *M*, (●) $CuBr_2 = 0.5$ *M*, $[CuBr_2] + [CaBr_2] = 4.0$ *M*.

Fig. 7. Variation of extraction efficiency with extraction time for the extraction of DMS by various concentrations of copper(II) chloride and copper(II) perchlorate solutions. $[CuCl_2] + [CaCl_2] = 4.0$ *M* const., $[Cu(ClO_4)_2] + [NaClO_4] = 4.0$ *M* const. (○) $CuCl_2 = 4.0$ *M*, (■) $CuCl_2 = 3.0$ *M*, (●) $CuCl_2 = 2.0$ *M*, (□) $CuCl_2 = 1.0$ *M*, (△) $Cu(ClO_4)_2 = 4.0$ *M*.

chloride and perchlorate). This shows that the extraction rate increases with the concentration of copper(II) and also depends on the anionic ligand added. In the presence of bromide ion, DMS can be quantitatively extracted into the aqueous phase within 1–2 min. Plots of $\log [DMS]_{total}/[DMS]_{(o)}$ against extraction time, calculated from the data in Fig. 7, gave straight lines (Fig. 8), which suggested a first-order dependence of the extraction rate on the concentration of DMS in the organic phase. From the slope of the curves shown in Fig. 8, the apparent first-order rate constant k_{app} was evaluated. The plots of k_{app} against the total concentration of copper(II) ion also gave straight lines (Fig. 9). Thus, the empirical rate expression can be given as:

$$-\frac{d[DMS]_{(o)}}{dt} = k_{app}[DMS]_{(o)} = k'[Cu]_{total} \cdot [DMS]_{(o)}$$

where k' is the rate constant. The relative values of k' were evaluated from the plots of Fig. 9 as $k'_{Br^-} : k'_{Cl^-} : k'_{ClO_4^-} = 360 : 13 : 1$. This order is in accordance with that of the stability of the sulfide complex and the extraction efficiency for sulfide. Under these experimental conditions, the concentration of copper(II) ion is about 10 times larger than that of DMS. Thus, the predominant copper(II) species in the aqueous solutions are Cu^{2+} and CuX^+, and the rate is expressed by the sum of the two terms as:

$$-\frac{d[DMS]_{(o)}}{dt} = \{k'_1[Cu^{2+}] + k'_2[CuX^+]\}[DMS]_{(o)}$$

where k'_1 and k'_2 are the rate constants. This expression could also be easily deduced from the stoichiometry of the extraction reaction established in the earlier part of this paper.

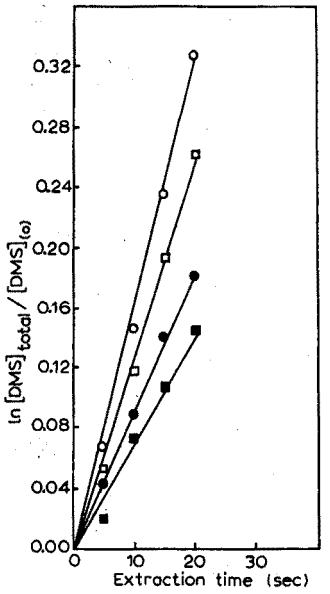

Fig. 8. First-order plot $\ln [DMS]_{total}/[DMS]_{(o)}$ against extraction time. (○) $CuCl_2 = 4.0$ *M*, (□) $CuCl_2 = 3.0$ *M*, (●) $CuCl_2 = 2.0$ *M*, (■) $CuCl_2 = 1.0$ *M*.

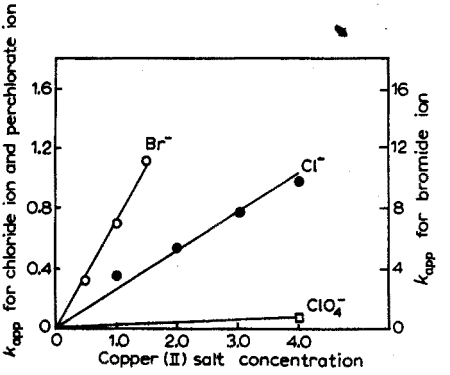

Fig. 9. Relationship between the apparent first-order rate constant k_{app} and the initial (total) copper(II) salts concentration. (○) $CuBr_2$, (●) $CuCl_2$, (□) $Cu(ClO_4)_2$.

The anionic ligands, bromide and chloride, not only enhanced the extraction efficiency of copper(II) ion for sulfide, but also accelerated the extraction reaction. According to the mechanism proposed on p. 157, a ligand with a better acceptor π-orbital than bromide should strongly enhance the efficiency and rate of the extraction of sulfides with copper(II) ion. This was confirmed by extracting the sulfides with a solution containing 1.0 *M* copper(II) perchlorate and 1.0 *M* potassium cyanide. However, the difficulty of controlling the copper(II)–cyanide system at its optimal condition limited the application of this system for analytical purposes. Copper(II) solutions containing bromide ion or some other ligand with a better acceptor orbital than bromide ion should be very useful as extracting agents or stationary phases for liquid–liquid chromatography for sulfide.

SUMMARY

A basic study of the extraction of aliphatic sulfides with copper(II), zinc(II) or mercury(II) is described. The stoichiometry of the extraction was established from the extraction equilibrium and by Job's method, to be:

$$MeL_{n'}^{(x-n')+}{}_{(a)} + R_2S_{(o)} \rightleftarrows MeL_{n'}(R_2S)^{(x-n')+}{}_{(a)}$$

An investigation of the effect of the anionic ligand, L^-, on the extraction showed that the efficiency (D) and rate (k') of the extraction and the stability of the sulfide complexes of copper(II) depended remarkably on the anion used. The effectiveness decreased in the order $Br^- > Cl^- > NO_3^- \sim ClO_4^-$, ($D_{Br^-}/D_{ClO_4^-} = 1000$, $k'_{Br^-}/k'_{ClO_4^-} = 360$). Similar effects were not observed for mercury(II) or zinc(II). The copper(II)–bromide system is useful for extraction of aliphatic sulfides.

RÉSUMÉ

Une étude est effectuée sur l'extraction de sulfures aliphatiques, au moyen de cuivre(II), de zinc(II) ou de mercure(II). La stoechiométrie de l'extraction est établie à partir de la constante d'équilibre de l'extraction et par la méthode de Job; elle est:

$$MeL_{n'}^{(x-n')+}{}_{(a)} + R_2S_{(o)} \rightleftarrows MeL_{n'}(R_2S)^{(x-n')+}{}_{(a)}$$

Le rendement et la vitesse d'extraction, ainsi que la stabilité des sulfures complexes de cuivre(II) dépendent grandement de la nature de l'anion ligand L^-. L'efficacité diminue dans l'ordre $Br^- > Cl^- > NO_3^- \sim ClO_4^-$ ($D_{Br^-}/D_{ClO_4^-}$) = 1000, $k'_{Br^-}/k'_{ClO_4^-} = 360$). Une influence similaire n'a pas été observée pour le mercure(II) ou pour le zinc(II). Le système cuivre(II)–bromure est interessant pour l'extraction des sulfures aliphatiques.

ZUSAMMENFASSUNG

Die Extraktion aliphatischer Sulfide mit Kupfer(II), Zink(II) und Quecksilber(II) wurde untersucht. Aus dem Extraktionsgleichgewicht und nach der Jobschen Methode ergab sich folgende Stöchiometrie der Extraktion:

$$MeL_{n'}^{(x-n')+}{}_{(a)} + R_2S_{(o)} \rightleftarrows MeL_{n'}(R_2S)^{(x-n')+}{}_{(a)}$$

Eine Untersuchung des Einflusses des anionischen Liganden, L^-, auf die Extraktion zeigte, dass Extraktionseffekt (D) und Extraktionsgeschwindigkeit (k') und die Beständigkeit der Sulfidkomplexe von Kupfer(II) erheblich von dem verwendeten Anion abhing. Die Effektivität nahm in der Reihenfolge $Br^- > Cl^- > NO_3^- \sim ClO_4^-$ ab ($D_{Br^-}/D_{ClO_4^-} = 1000$; $k'_{Br^-}/k'_{ClO_4^-} = 360$). Ähnliche Einflüsse wurden bei Quecksilber(II) und Zink(II) nicht beobachtet. Das Kupfer(II)–Bromid-System ist für die Extraktion aliphatischer Sulfide von Nutzen.

REFERENCES

1 S. A. BIRCH AND D. T. MCALLAN, *J. Inst. Petroleum Technol.*, 37 (1951) 443.
2 R. EMMOTT, *J. Inst. Petroleum*, 39 (1953) 695.
3 R. L. HOPKINS, H. J. COLEMAN, C. J. THOMPSON AND H. T. RALL, *U.S. Bur. Mines, Rept. Invest.*, 1964, p. 6458.
4 W. L. ORR, *Anal. Chem.*, 38 (1966) 1558.
5 W. L. ORR, *Anal. Chem.*, 39 (1967) 1163.
6 P. BISCARINI AND G. D. NIVELLINI, *J. Chem. Soc.*, A (1969) 2206.
7 G. CHARLOT, *l'Analyse Qualitative et les Réactions en Solution*, Masson, Paris, 1957.
8 L. G. SILLÉ AND A. E. MARTELL, *Stability Constants*, Spec. Publ. No. 17, The Chemical Society, London, 1963.
9 T. YOTSUYANAGI, T. KAMIDATE AND K. AOMURA, *Japan Analyst*, 18 (1969) 1487.

Analytica Chimica Acta
Elsevier Publishing Company, Amsterdam
Printed in The Netherlands

EFFECT OF SUBSTITUENTS ON THE DISTRIBUTION COEFFICIENTS OF ALKYL-SUBSTITUTED β-DIKETONES AND THEIR COPPER AND IRON CHELATES

HIDEO KOSHIMURA
The Tokyo Metropolitan Industrial Research Institute, Tokyo (Japan)
AND TEIJI OKUBO
Government Chemical Industrial Research Institute Tokyo, Tokyo (Japan)
(Received 13th January 1971)

Extractions of metal chelates are very useful for the separation of metals and studies of new improved ligands for such separations are numerous. Recently, the effects of substituents on the distribution of metal chelates have been reported for 8-quinolinol[1], dithizone[2], alkylmalonic acid[3], dialkylphosphoric acid[4], β-diketones[5] and alkylamines[6].

Fresco and Freiser[7] have studied comprehensively the distributions of 8-methylquinolinols and of their copper chelates. Dyrssen *et al.*[8] have studied the change in the distribution coefficient in a variety of chelate series and reported that the distribution coefficients increased fourfold per additional carbon atom.

In the previous paper of this series[9], the separation of various metals with the alkyl-substituted β-diketones, dipropionylmethane, diisobutyrylmethane, pivaloylacetylmethane and dipivaloylmethane was reported. In this paper, eight alkyl-substituted β-diketones including four newly synthesized reagents, were investigated in order to establish the effect of substituents on the extraction constants and the acid dissociation constants. Further, the relationship between the distribution coefficients of these chelating agents and of their copper chelates was examined. An investigation of the iron chelates was also carried out.

EXPERIMENTAL

The structural formula, common and systematic names of each of the newly prepared β-diketones are given in Table I with the abbreviation used in this paper. Di-*n*-butyrylmethane, di-*n*-valerylmethane, di-*n*-caproylmethane and diisovalerylmethane were synthesized by the method of Hauser and Adams[10]. The compositions were confirmed by elemental analysis. Acetylacetone (Dojindo & Co) was purified by washing with dilute ammonia solution, followed by distillation.

All of the reagents used were of reagent grade.

The experimental procedures for the acid dissociation constants and the distribution coefficients of β-diketones and metal ions were exactly the same as previously described[9].

TABLE I

NEWLY SYNTHESIZED ALKYL-SUBSTITUTED β-DIKETONES USED IN THIS STUDY[a]

Common name and structural formula	*Systematic name*	*Abbreviation*
Di-*n*-butyrylmethane $CH_3-(CH_2)_2-C(=O)-CH_2-C(=O)-(CH_2)_2-CH_3$	Nonane-4,6-dione	DNBM
Di-*n*-valerylmethane $CH_3-(CH_2)_3-C(=O)-CH_2-C(=O)-(CH_2)_3-CH_3$	Undecane-5,7-dione	DNVM
Di-*n*-caproylmethane $CH_3-(CH_2)_4-C(=O)-CH_2-C(=O)-(CH_2)_4-CH_3$	Tridecane-6,8-dione	DNCM
Di-isovalerylmethane $CH_3-CH(CH_3)-CH_2-C(=O)-CH_2-C(=O)-CH_2-CH(CH_3)-CH_3$	2,8-Dimethylnonane-4,6-dione	DIVM

[a] For DPrM, DIBM, DPM, see ref. 9.

RESULTS AND DISCUSSION

The distributions of copper and iron between 0.1 *M* sodium perchlorate and benzene containing 0.1 *M* β-diketones are shown at varying pH values in Figs. 1–4. The plots of log *D* *vs.* pH in these systems almost fall on a straight line with a slope 2 or

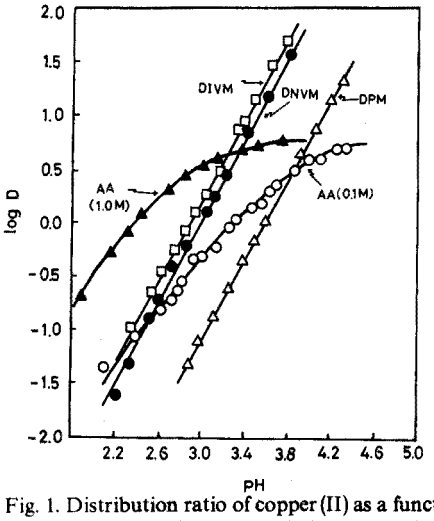

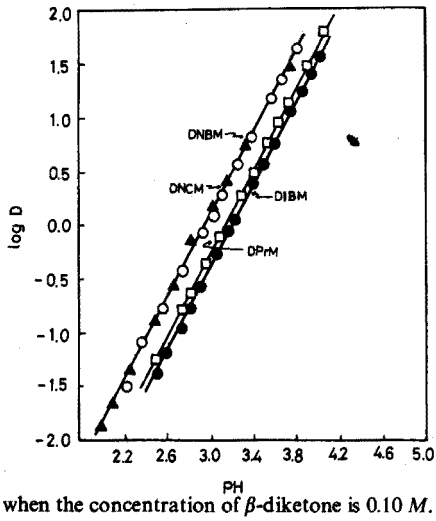

Fig. 1. Distribution ratio of copper(II) as a function of pH when the concentration of β-diketone is 0.10 *M*. (○) AA; (▲) AA; (△) DPM; (●) DNVM; (□) DIVM.

Fig. 2. Distribution ratio of copper(II) as a function of pH when the concentration of β-diketone is 0.10 *M*. (●) DIBM; (□) DPrM; (○) DNBM; (▲) DNCM.

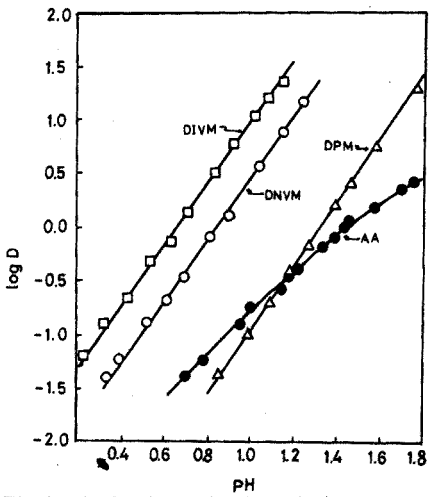

Fig. 3. Distribution ratio of iron(III) as a function of pH when the concentration of β-diketone is 0.10 *M*. (●) AA; (△) DPM; (○) DNVM; (□) DIVM.

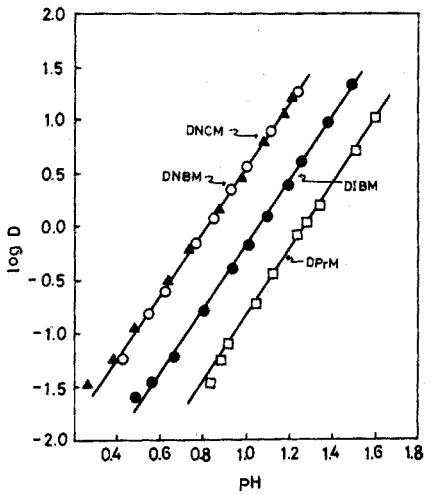

Fig. 4. Distribution ratio of iron(III) as a function of pH when the concentration of β-diketone is 0.10 *M*. (□) DPrM; (●) DIBM; (○) DNBM; (▲) DNCM.

3 for the copper and iron chelates, respectively.

In the case of acetylacetonate, the plots deviate from the straight lines with the theoretical slopes 2 and 3. The deviations were assumed to be due to the aqueous chelate formation. Because of these deviations, the extraction constants were obtained by the curve-fitting method[11].

For the distribution data of the metals investigated, the composition of the extractable complexes and the extraction constants, K_{ex}, were obtained. In addition, the two-phase stability constants, $K_f \cdot P_{MA_n}$, were calculated according to Starý's procedure[12,13] from the values of the acid dissociation constant, K_a, and of the distribution coefficient, P_{HA}, of the β-diketones used. The results obtained with the method described above are summarized in Table II.

TABLE II

EQUILIBRIUM CONSTANTS FOR COPPER(II) AND IRON(III) CHELATES OF ACETYLACETONE AND ALKYL-SUBSTITUTED β-DIKETONES

	pK_a	$\log P_{HA}$	$\log K_{ex}$		$pH_{\frac{1}{2}}$		$\log K_f \cdot P_{MA_n}$	
			Fe(III)	*Cu(II)*	*Fe(III)*	*Cu(II)*	*Fe(III)*	*Cu(II)*
AA	8.84±0.04	0.65±0.04	−0.98	−3.60	1.46	3.35	27.49	15.38
DPrM	9.55±0.03	1.61±0.04	−0.82±0.07	−4.34±0.04	1.28	3.17	32.66	17.98
DNBM	9.67±0.04	2.88±0.05	0.54±0.05	−3.94±0.04	0.82	2.98	38.19	21.16
DNVM	9.72±0.04	4.15±0.05	0.54±0.05	−3.96±0.04	0.82	2.98	42.15	23.78
DNCM	9.71±0.04	5.46±0.07	0.54±0.05	−3.92±0.04	0.82	2.96	46.05	26.42
DIBM	9.82±0.04	3.04±0.04	−0.17±0.05	−4.42±0.05	1.06	3.20	38.41	21.30
DIVM	9.88±0.03	4.05±0.04	1.05±0.06	−3.81±0.05	0.65	2.92	42.84	24.05
DPM	11.57±0.03	3.98±0.05	−1.18±0.03	−5.19±0.05	1.39	3.60	45.47	25.91

With regard to the extraction constants of the copper and iron acetylacetonate, some comparable studies give the following values: log K_{ex} −3.60 (present work), −3.93 (Starý and Haldky[12]), −4.32 (Newman and Klotz[14]) and −3.70 (Hasegawa[15]) for copper, and −0.98 (present work) and −1.32 (Starý and Haldky[12]) for iron. No explanation for the differences in the above values is offered. However, the formation constants for the copper and iron chelates in the aqueous phase obtained by the curve-fitting method agree with the experimental results of Izatt[16] (Table III).

TABLE III

THE FORMATION CONSTANT IN THE AQUEOUS PHASE OF COPPER(II) AND IRON(III) ACETYLACETONATES

Metal	*Method*	*AA inital concentration*	*log* β_1[a]	*log* β_2	*log* β_3
Cu(II)	Present work	0.10 *M*	8.41	14.82	
		1.00 *M*	8.28	14.56	
	Titration[16]		8.22	14.95	
Fe(III)	Present work	0.10 *M*	9.17	18.34	—
	Titration[16]		9.8	18.8	26.3

[a] $\beta_n = [MA_n^{m-n}]/[M^{m+}][A^-]^n$.

As can be seen from Table II, the acid dissociation constant, pK_a, and the distribution coefficient, log P_{HA}, of these β-diketones increase as the number of carbon atoms in the aliphatic chain increases. Their apparent pK_a values increase considerably with increased branching of the alkyl chain near the donating oxygen atom. The

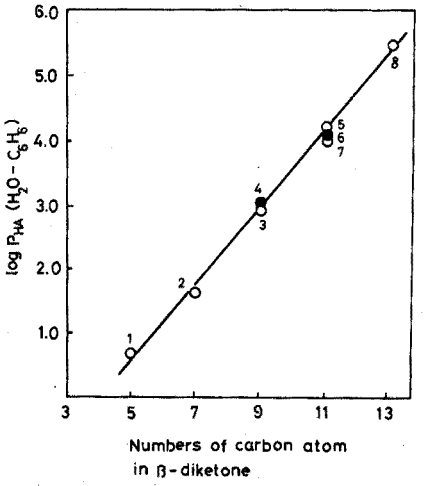

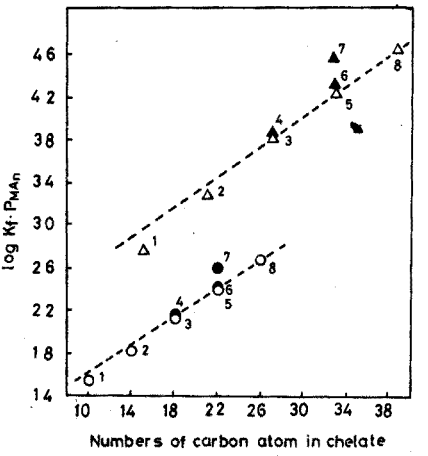

Fig. 5. Correlation between the distribution coefficient of a β-diketone and the number of carbon atoms in its molecule. (1) AA; (2) DPrM; (3) DNBM; (4) DIBM; (5) DNVM; (6) DIVM; (7) DPM; (8) DNCM.

Fig. 6. Correlation between the two-phase stability constants for copper(II) and iron(III) chelates of β-diketones and the number of carbon atoms in the chelate. (1) AA; (2) DPrM; (3) DNBM; (4) DIBM; (5) DNVM; (6) DIVM; (7) DPM; (8) DNCM. (△, ▲) Iron(III) chelate; (○, ●) copper(II) chelate.

pK_a values for the normal alkyl group rise, up to a certain limit, as the chain lengthens. The log P_{MA_n} values also increase regularly with the carbon number of the alkyl chain in the β-diketones, but the change in log P_{MA_n} is much less pronounced when normal groups are compared with branched ones with the same number of carbon atoms.

The correlation between log P_{HA} or log $K_f \cdot P_{MA_n}$ and the additional carbon atoms of the β-diketones and of their chelates is shown in Figs. 5 and 6. In Fig. 5, log P_{HA} values are plotted against the number of carbon atoms in normal alkyl groups. The points fall on a straight line with a slope of 0.61. This value is identical with that reported by Dyrssen *et al.*[8] and others[7], who state that log P_{HA} of a homologous series of organic reagents increases by a factor of 4 for each additional carbon atom.

Figure 6 also shows that log $K_f \cdot P_{MA_n}$ increases with increasing number of the carbon atoms in the alkyl chain in β-diketone chelates. Starý[13] has reported that the $K_f \cdot P_{MA_n}$ value for benzoylacetone and for dibenzoylmethane is approximately 2.4 and 4.6 units higher than that for acetylacetone. The distribution coefficients, P_{MA_n}, for β-diketone chelates were extremely large, as shown in Figs. 1–4, and could not be obtained experimentally. However, it is well known that the formation constants of metal chelates are related to the acid dissociation constants of the ligands. Calvin and Wilson[17] have pointed out that the formation constants of acetylacetone, trifluoroacetylacetone, furoylacetone and benzoylacetone chelates are directly proportional to the acid dissociation constants of these ligands. This fact can be applied to the β-diketones used here. Since the pK_a and log K_{ex} values for DNBM, DNVM and DNCM are the same (Table II), it would be expected that the log K_f values of these copper or iron chelates would also be the same. Consequently, the variation in log $K_f \cdot P_{MA_n}$ is caused by the difference in log P_{MA_n} only. The three points of log $K_f \cdot P_{MA_n}$ for each copper and iron chelate fall almost on a straight line of slope 0.65 as shown by the dotted line in Fig. 6. The deviation of the logarithmic plots from the slope is probably due to the difference in the acid dissociation constants of the β-diketones, or more precisely, to the difference in the formation constants of the chelates.

The logarithm of the distribution coefficient of the β-diketones and of their chelates is a linear function of the number of carbon atoms in the molecule, and hence P_{HA} and P_{MA_n} increase by a factor of 4 for each additional carbon atom. The extractability of metal chelates by β-diketones increases with increasing number of carbon atoms in the molecule.

On the assumption that K_f values are the same when K_a values are the same, one can consider that K_{ex} and $K_f \cdot K_a^n$ are constant for the DNBM, DNVM and DNCM chelates. Therefore, in the extraction equation[18], $K_{ex} = K_f \cdot K_a^n \cdot P_{MA_n} / P_{HA}^n$, the following correlation is expected between the P_{HA} and P_{MA_n}

$$\log P_{MA_n} = n \log P_{HA} + \text{const.}$$

where n designates the electric charge on the metal ion.

The authors wish to thank Dr. Totaro Goto for his helpful advice.

SUMMARY

A series of alkyl-substituted β-diketones consisting of acetylacetone, dipropionylmethane, diisobutyrylmethane, dipivaloylmethane, di-*n*-butyrylmethane, di-*n*-

valerylmethane, di-*n*-caproylmethane and diisovalerylmethane has been studied, in order to establish the effect of substituents on the extraction constants and the acid dissociation constants. The logarithm of the distribution coefficients of the β-diketones and of their copper(II) and iron(III) chelates was a linear function of the number of carbon atoms in the molecule. It was found that the distribution coefficient increased by a factor of 4 for each additional carbon atom.

RÉSUMÉ

Une étude est effectuée sur une série de β-dicétones substituées, afin d'examiner l'influence des substituants sur les constantes d'extraction et les constantes de dissociation acide. Le logarithme des coefficients de partage des β-dicétones et des chélates de cuivre(II) et de fer(III) est une fonction linéaire du nombre d'atomes de carbone dans la molécule. On constate que le coefficient de partage augmente avec un facteur de 4 pour chaque atome de carbone additionnel.

ZUSAMMENFASSUNG

An einer Reihe von alkylsubstituierten β-Diketonen und zwar an Acetylaceton, Dipropionylmethan, Diisobutyrylmethan, Dipivaloylmethan, Di-*n*-butyrylmethan, Di-*n*-valerylmethan, Di-*n*-caproylmethan und Diisovalerylmethan wurde der Einfluss der Substituenten auf die Extraktionskonstanten und Säuredissoziationskonstanten untersucht. Der Logarithmus der Verteilungskoeffizienten der β-Diketone und der Kupfer(II)- und Eisen(III)-chelate war eine lineare Funktion der Anzahl Kohlenstoffatome im Molekül. Es wurde festgestellt, dass der Verteilungskoeffizient mit jedem zusätzlichen Kohlenstoffatom um den Faktor 4 zunimmt.

REFERENCES

1 FA-CHUN CHOU AND H. FREISER, *Anal. Chem.*, 40 (1968) 34.
2 Y. MARCUS AND A. S. KERTES, *Ion Exchange and Solvent Extraction of Metal Complexes*, Wiley–Interscience, New York, 1969.
3 J. AGGETT AND M. H. TIMPERLEY, *Anal. Chim. Acta*, 47 (1969) 551.
4 Z. KOLARIK AND H. PANKOVA, *J. Inorg. Nucl. Chem.*, 28 (1966) 2325.
5 T. SEKINE AND M. ONO, *Bull. Chem. Soc. Japan*, 38 (1965) 2087.
6 A. S. KERTES AND Y. MARCUS (Editors), *Solvent Extr. Chem., Proc. Int. Conf. 1968*, 1969, p. 157.
7 J. FRESCO AND H. FREISER, *Anal. Chem.*, 36 (1964) 631.
8 D. DYRSSEN, S. EKBERG AND D. H. LIEM, *Acta Chem. Scand.*, 18 (1964) 135.
9 H. KOSHIMURA AND T. OKUBO, *Anal. Chim. Acta*, 49 (1970) 67.
10 C. R. HAUSER AND J. T. ADAMS, *J. Amer. Chem. Soc.*, 66 (1944) 1220.
11 T. SEKINE AND D. DYRSSEN, *J. Inorg. Nucl. Chem.*, 29 (1967) 1475.
12 J. STARÝ AND E. HALDKY, *Anal. Chim. Acta*, 28 (1963) 227.
13 J. STARÝ, *The Solvent Extraction of Metal Chelates*, Pergamon Press, Oxford, 1964.
14 L. NEWMAN AND P. KLOTZ, *Solvent Extr. Chem., Proc. Int. Conf. 1966*, 1967, p. 128.
15 Y. HASEGAWA, *Bull. Chem. Soc. Japan*, 42 (1969) 3425.
16 R. M. IZATT, *J. Phys. Chem.*, 59 (1955) 170; 59 (1955) 80.
17 M. CALVIN AND K. W. WILSON, *J. Amer. Chem. Soc.*, 67 (1945) 2008.
18 G. H. MORRISON AND H. FREISER, *Solvent Extraction in Analytical Chemistry*, John Wiley, London, 1957.

Analytica Chimica Acta
Elsevier Publishing Company, Amsterdam
Printed in The Netherlands

VISCOMETRIC TITRATIONS

A NEW TECHNIQUE APPLIED TO ACIDIMETRY AND ALKALIMETRY

R. B. SIMPSON, H. M. N. H. IRVING AND J. S. SMITH*
Department of Inorganic and Structural Chemistry, The University of Leeds, Leeds 2 (England)
(Received 15th January 1971)

In a classical paper on the fluidity of electrolytes, Bingham[1] showed that the fluidity of a solution of an electrolyte (fluidity $\phi = 1/\text{viscosity } \eta$) can be represented as the sum of the fluidity of the water alone, ϕ_w, and that due to the ions present. Thus

$$\phi = \phi_w + c(\Delta_a + \Delta_c) \quad (1)$$

where c is the molal concentration and Δ_a and Δ_c are the equivalent ionic elevations in the fluidity of water produced by one equivalent weight of anions (or cations respectively) in a normal solution at 25°.

On the basis of the observed additivity of ionic fluidities and the fact that hydrogen and hydroxyl ions both *lower* the mobility of water whereas many other cations and anions cause increases, Bingham calculated hypothetical titration curves for sodium or potassium hydroxide with nitric or hydrochloric acid in molal solutions at 25°. These all took the form of two straight lines intersecting acutely at the calculated end-point. These predictions do not seem to have been tested experimentally, although this is scarcely surprising in view of the labour that would have been involved using the equipment available at that time.

Although measurements of viscosity are of great importance in industrial analysis and control, notably in the fields of fuels, lubricants and polymers, there have been few cases where the phenomenon has been exploited in the analysis of aqueous solutions and, so far as we are aware, no successful attempt has been made to consider the feasibility of viscometric measurements in titrimetric analysis. When, however, an alkali BOH is added to a monobasic acid HA, the composition of the solution will gradually change from that of a mixture of the ions H^+ (solvated) and A^- (solvated) with undissociated (HA), as the cations B^+ (solvated) replace the solvated protons and the concentration of undissociated HA is reduced. As in conductivity titrations, where the total conductivity depends on the concentrations of all the ionic species present and on their respective mobilities, in a viscometric titration the total viscosity will depend upon the concentration of all the dissolved species (undissociated molecules as well as ions) and their individual effects on the flow-time of the solution as a whole. To take the simplest case provided by the titration of a strong acid HA by a strong base BOH, if the effects of H^+ (solvated) and B^+ (solvated) on the flow-times are

* Present address: Dept. of Chemical Sciences, The Hatfield Polytechnic, Hatfield, Hertfordshire.

different, there will be a net change in the viscosity during the neutralisation reaction After the end-point, the addition of excess B^+ (solvated) and OH^- (solvated) should again progressively influence the net viscosity but, intuitively, one would expect to a different extent. In short a "viscometric titration curve" in which viscosity is plotted against concentration of titrant added should show a well defined break-point. Should this occur at the stoicheiometric end-point, a new analytic procedure would become available. Even if the break-point did not coincide with the stoicheiometric end-point the determination could still be useful, provided that the break-point was strictly reproducible.

Instrumentation

The design and successful operation of a fully automatic suspended-level viscometer[2] has enabled us to measure and record flow-times of the order of 100–300 sec with a precision of 1 part in 10^6. More recently, this apparatus has been combined with a Radiometer Automatic Burette (ABU12b) and the use of the logic control units has been extended so that it became possible to determine the flow-time of a sample to the nearest millisecond, to repeat this determination as often as required and to print out the results. A known aliquot portion of titrant is then added and automatically mixed with the solution in the viscometer and the flow-time of the mixture is measured as before. Successive aliquots are added to provide data from which a graph of flow-time against volume of titrant can subsequently be plotted. The volume and number of aliquot portions of titrant can be preset or changed manually at any stage and the whole sequence of operations proceeds automatically[3].

TITRATION CURVES

To show the possibilities of this new analytical technique, a number of acid–base titrations have been examined, in the first instance, and examples of these are illustrated in the following graphs. It should be emphasised that these graphs are direct plots of measured flow-time against volume of titrant added. No attempt has been made to introduce a correction for the dilution of the sample by the titrant though this factor and changes in the density of mixtures would need to be considered if actual or relative viscosities were to be calculated from the experimental results. The really remarkable linearity of most of the plots and the sharpness of the end-point indications came as a surprise.

Figure 1 shows results for the titration of *ca.* 13 ml of 0.01 *M* sodium hydroxide by 0.1 *M* hydrochloric acid (curve A), and *ca.* 13 ml of 0.1 *M* pyridine (curve B) or 0.1 *M* sodium hydroxide (curve C) by *M* hydrochloric acid. In each case the titrant was added in aliquot portions of 0.050 ml, and the stoicheiometric end-point was reached when the equivalent amount of acid had been added. It is noteworthy that the slopes of the lines before the end-points are very much the same, since in each case hydroxyl ions are being replaced by chloride ions. After the end-point the slopes due to the increase in viscosity as aliquot portions of 0.1 *M* hydrochloric acid are added to *ca.* 14.3 ml of $9.09 \cdot 10^{-3}$ *M* pyridinium or sodium chloride are identical. That due to the addition of excess of hydrochloric acid to $9.09 \cdot 10^{-4}$ *M* sodium chloride (curve A) is less steep but the location of the end-point is still well defined.

At this point, it must be stressed that the experiments reported were not de-

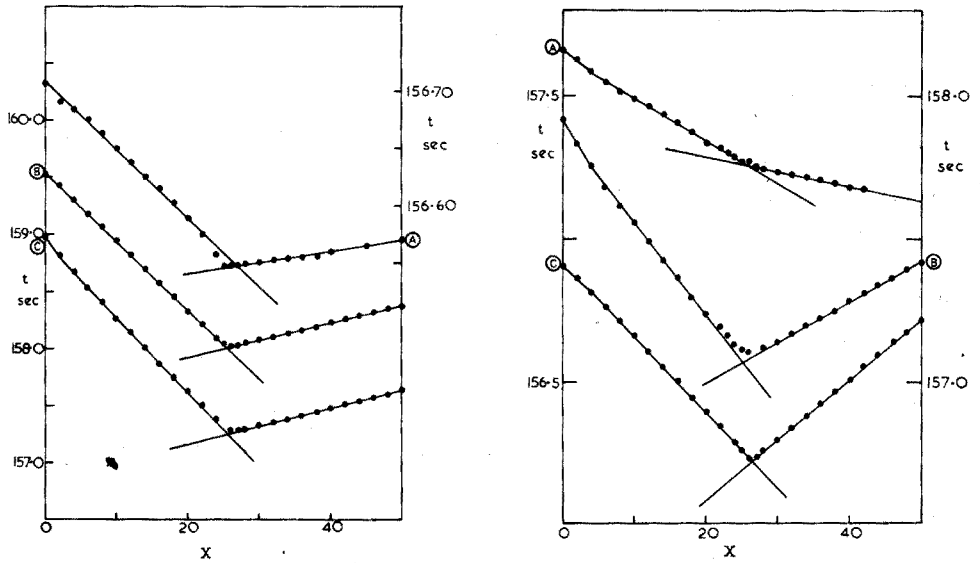

Fig. 1. (A) Titration of 0.01 *M* NaOH by 0.1 *M* HCl. Titration by 1 *M* HCl of 0.1 *M* pyridine (B) and 0.1 *M* NaOH (C). Approx. 13 ml of sample were used and here and elsewhere the titrant was always added in aliquot portions of 0.050 ml. Flow-times are given as ordinates and the number of aliquot portions of titrant as abscissae.

Fig. 2. The titration by 0.1 *M* HCl of *ca.* 13 ml of 0.01 *M* ammonia containing 1 *M* $NaNO_3$ (A). The titration by 1 *M* HCl of *ca.* 13 ml of 0.1 *M* ammonia (C) or 0.1 *M* ammonia containing 1 *M* $NaNO_3$ (B).

signed to establish the accuracy and precision of acid–alkali titrations at various concentration levels, but to establish the feasibility of end-point indication by the viscometric method.

Titration of bases

Figure 2 shows curves for the titration of the weak base ammonia under various conditions. As in the titration of pyridine (Fig. 1, curve B) the contrast with a pH-titration is well marked. Even with 0.01 *M* ammonia there is a well defined break at the stoicheiometric end-point even when this titration is performed in the presence of a substantial amount of neutral salt (*M* sodium nitrate). Comparison of curves C and B shows that the presence of neutral salt has caused a rounding of the end-point with no significant shift in its position.

Figure 3 shows the titration curve for a commercial sample of ethylenediamine (en). Two sharp end-points are obtained. That there is a small difference in the two titration values is probably due to the sample having absorbed some carbon dioxide.

When it had been shown that discrete end-points can be obtained corresponding to the protonation of the bases en and enH^+ respectively, an obvious extension was to study the titration of a mixture of bases. Two weak bases were chosen since their titration presents a problem sometimes difficult to resolve by pH-titration where extensive and possibly overlapping buffer regions would mitigate against the successful determination of individual components. However, as shown in Fig. 4 for the titration of a mixture of ammonia and pyridine, there is a sharp break-point when the ammonia alone has been titrated and a second to mark the titration of the pyridine.

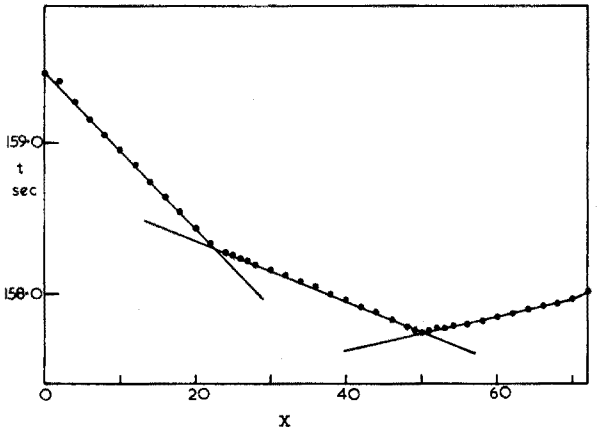

Fig. 3. The titration of *ca.* 13 ml of a commercial sample of ethylenediamine (0.1 *M*) by 1 *M* HCl.

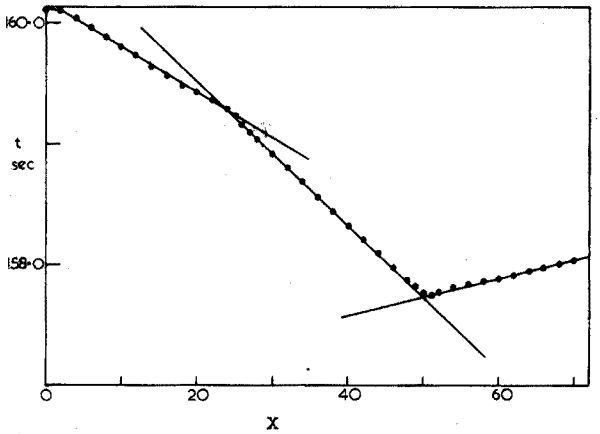

Fig. 4. The titration by 1 *M* HCl of *ca.* 13 ml of a mixture containing 0.1 *M* ammonia and 0.1 *M* pyridine.

Here again, the accuracy and precision attainable in the analysis of mixtures of different composition have not been explored in detail.

Titration of acids

In pH-titrations the curve for the titration of an alkali by an acid will normally retrace in the reverse sense the curve for the titration of this acid by the same alkali. Viscometric titrations resemble conductivity titrations in presenting a different picture, especially when weak acids or bases are involved. This is illustrated in Fig. 5 where curve C for the titration of 0.1 *M* hydrochloric acid by a *M* sodium hydroxide solution should be compared with Fig. 1, curve C for the reverse titration. Even when a weak acid such as acetic acid ($pK = 4.76$) is used a satisfactory end-point is found (Fig. 5, curve B), and in marked contrast to the situation with pH-titrations, the end-point for the very weak acid phenol ($pK = 10.0$) is even better.

Figure 6 displays the effect of titrating two dibasic acids. Sulphuric acid (curve A) is very strong ($pK_1 \sim 0$, $pK_2 = 1.92$) and oxalic acid (curve B) is much weaker ($pK_1 =$

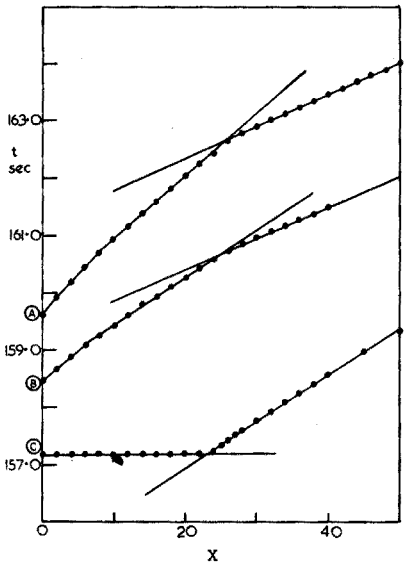

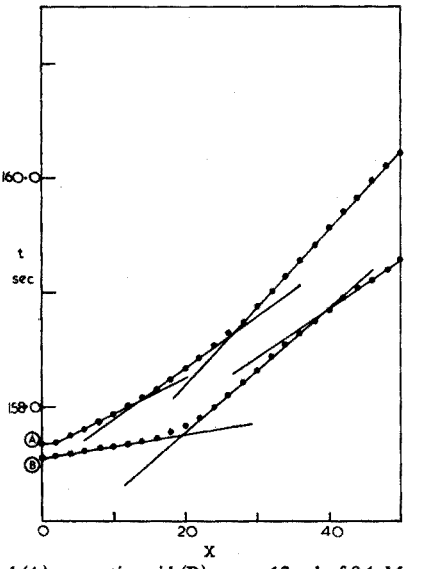

Fig. 5. The titration by 1 *M* NaOH of *ca.* 13 ml of 0.1 *M* phenol (A) or acetic acid (B) or *ca.* 12 ml of 0.1 *M* HCl (C).

Fig. 6. The titration by 1 *M* NaOH of *ca.* 13 ml of 0.05 *M* H_2SO_4 (A) or *ca.* 20 ml of 0.05 *M* oxalic acid (B).

1.27, $pK_2 = 4.27$). Only one end-point is detectable in the pH-titration of sulphuric acid.

The success in finding two fairly clear end-points in the titration of two such different dibasic acids was encouraging, and it seemed worthwhile to examine other typical polybasic acids. Results for citric acid (Fig. 7, curve A) show three discrete

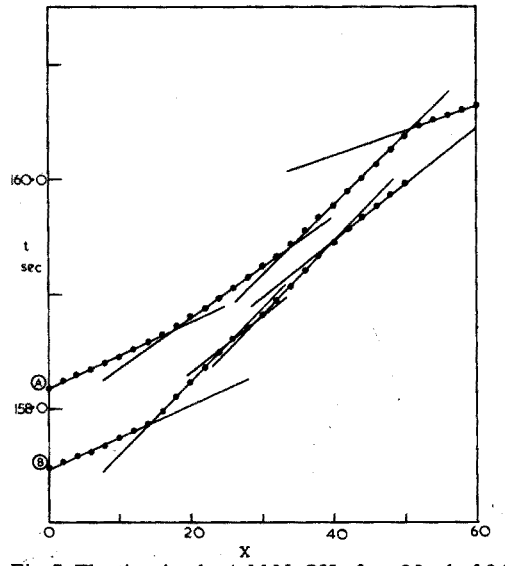

Fig. 7. The titration by 1 *M* NaOH of *ca.* 25 ml of 0.033 *M* citric acid (A) or phosphoric acid (B).

end-points corresponding to equal amounts of added alkali. For phosphoric acid (curve B) end-points corresponding to the protonation of PO_4^{3-} and $H_2PO_4^-$ occur in approximately the places expected but there are two illdefined breaks or a series of inflexions covering the region where the protonation of HPO_4^{2-} would be expected. It is noteworthy that Bingham's calculated fluidity titration curve for the neutralisation of phosphoric acid by potassium hydroxide predicted clear breaks only for the protonation of PO_4^{3-} and $H_2PO_4^-$ and he suggested that the absence of an intermediate break-point may have resulted from a compensation of opposing factors in the fluidities of the component ions. What is important to realise is that the absence of an expected break-point cannot be used to establish the non-existence of a particular species in solution. As a corollary the existence of a break-point may not be adequate proof of the existence of a particular species in solution unless its presence as the dominant species can be supported by independent evidence. This is because the viscosity of a mixture (and hence its flow time) is not simply a linear function of the concentration of each species present. In short, caution must be exercised in interpreting the viscometric titration curve of an unknown substance.

This point is further illustrated by the titration of ethylenediaminetetraacetic acid (EDTA; H_4Y) shown in Fig. 8, curve B. Here the break-points when 12, 25.8, 38.7 and 51.6 0.050-ml aliquot portions of alkali have been added are in the ratio 0.93:2:3:4 suggesting that they correspond with the protonation of the species Y^{4-}, HY^{3-}, H_2Y^{2-} and H_3Y^-. It is noteworthy that in pH-titrations of this acid the first end-point does not occur until two equivalents of alkali have been added since the respective pK values (2.0, 2.67, 6.16 and 10.26) lead to overlapping buffer regions in the pH range 1–5. On the other hand, it is reasonable to expect that the differently charged anions Y^{4-},

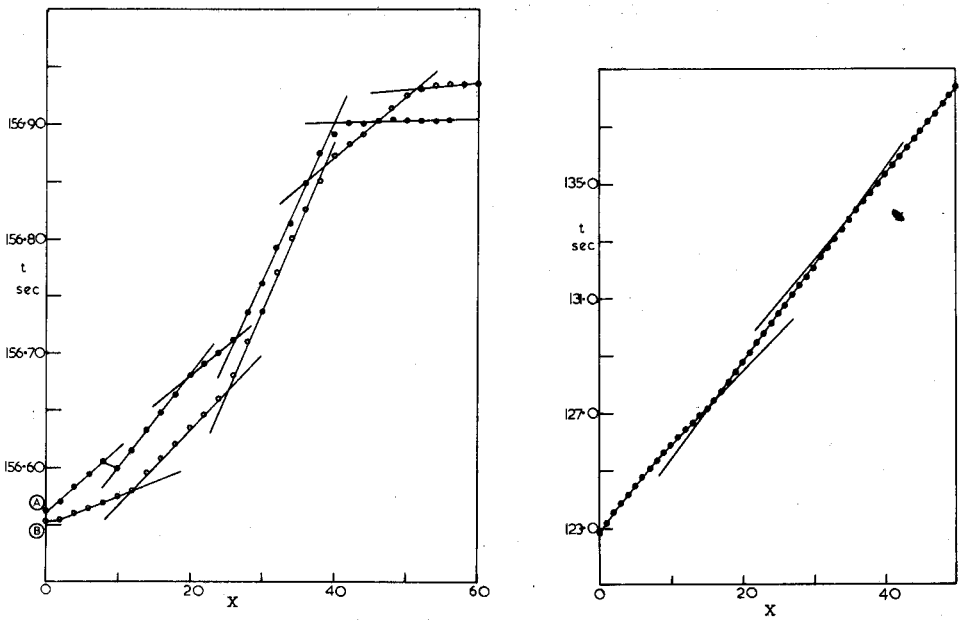

Fig. 8. The titration by 0.1 *M* NaOH of *ca.* 30 ml of 0.0025 *M* DCTA (A) or EDTA (B).

Fig. 9. The titration by 1 *M* NaOH in methanol of *ca.* 16 ml of 0.05 *M* salicylic acid in methanol.

HY^{3-} and H_2Y^{2-} would have sufficiently different effects on the viscosity of the solution to permit of their differentiation.

With the much bulkier anions derived from 1,2-diaminocyclohexanetetraacetic acid (DCTA) the position in the early stages of the neutralisation is clearly unusual. Furthermore, the breaks occurring after the addition of 20, 26.2 and 40 0.050-ml aliquot portions respectively are not in the expected ratio 2:3:4 leading to doubt about the homogeneity of the sample of complexone used.

The final graph (Fig. 9) shows the titration of the weak dibasic salicylic acid (H_2Sal) in methanolic 0.1 *M* solution by a methanolic solution of *M* sodium hydroxide. Here the changes in flow-time are very much larger than in previous measurements but at first sight the titration curve appears to be almost continuous. On closer examination it is clearly segmented and break-points at *ca.* 17 and 34 0.050-ml aliquot portions correspond fairly well to the neutralisation of the carboxylic acid ($pK_1 = 3.0$) and of the phenolic group ($pK_2 = 13.4$), respectively.

DISCUSSION

The above results are intended only as examples to illustrate a novel technique of potential interest to analysts. They report measurements (all by R.B.S.) in Leeds, but many of the results have been confirmed by titrations carried out with a substantially identical automatic viscometer constructed by one of us (J.S.S.) and operated independently in London whence further work will be reported in due course. However, attention should be drawn to certain general features. Whereas in pH-titrations the dissociation constants of the acids and bases involved are the essential factors that determine the form of titration curves—and hence the feasibility of determining very weak acids (or bases) and of analysing mixtures—in the present technique these factors are complemented by, and in some cases dominated by, differences in the effect of the components on the net viscosity of the solution. In this sense viscometric titrations have a closer affinity to conductimetric titrations; but again the new technique has special advantages in that titrations can be carried out equally well in the absence or presence of a high concentration of neutral salt.

Since changes in viscosity form the basis of viscosity titrations it will be clear that reasonable predictions of the course of possible titrations must depend on an extensive knowledge of the viscosity changes produced by particular ions and on the way in which mixtures of ions at different concentrations affect the net viscosity (and hence the flow rate) of a solution. Although there exists a good deal of information on the viscosity of various electrolytes in water, but much less on the viscosities of mixtures of electrolytes[4], no theory of viscometric titrations applicable even to acid–base systems has yet been published. In its absence only the most qualitative picture of a titration curve can be predicted and the effect of varying the concentration of reactants, or the presence or absence of a neutral salt background, and more particularly the influence of the strength of the acid and/or base used on the sharpness and accuracy of the end-point can as yet only be investigated experimentally.

Progress on the theoretical interpretation of viscometric titration curves can be envisaged on two lines. The Dole-Jones equation[4]

$$\eta = \eta_0(1 + Ac^{\frac{1}{2}} + Bc) \qquad (2)$$

can be used to present data on the viscosity of an electrolyte covering all analytically significant concentrations, c. Here A is a coefficient referring to interionic effects and the B coefficient can be separated into additive terms presenting the effects of individual ions. It may be possible to establish comparable equations for admixtures of electrolytes and to calculate the flow-times appropriate to various stages of a neutralisation titration after due allowance has been made for volume, concentration and density changes as the titration proceeds. A theory on these lines can probably be developed when further fundamental experimental work has been completed.

An alternative approach is to represent the flow-time, t, of the solution by an equation of the form

$$t = t_0(1 + \Sigma c_i T_i) \tag{3}$$

where t_0 is the flow-time for pure water and T_i an empirically determined coefficient for the i-th species, derived by a computer-programmed analysis of experimental titration curves.

One of us (R.B.S.) is grateful to the Science Research Council for a maintenance grant and J.S.S. wishes to thank the Royal Society and the Chemical Society for grants towards the construction of his apparatus.

SUMMARY

By using a recently designed fully automatic viscometer aliquot portions of one liquid (0.050 ml) can be added in succession from an automatic burette to a second liquid contained in a suspended level viscometer: after mixing, flow-times are measured with a precision of 1 part in 10^6 and the results printed out. When, *e.g.* an alkali (or acid) is added from the burette to an acid (or alkali) contained in the viscometer the plot of flow-times against the number of aliquots added constitutes a "viscosity titration curve". This novel technique is illustrated by curves for the titration by hydrochloric acid of sodium hydroxide, ammonia, pyridine, a mixture of ammonia and pyridine, and ethylenediamine. The titration of mono-, di-, tri- and tetra-basic acids of various strengths by sodium hydroxide is illustrated by graphs for hydrochloric and acetic acids, phenol, sulphuric and oxalic acids, citric and phosphoric acids, and EDTA and DCTA. Salicylic acid titrated as a dibasic acid in methanol. The graphs form a series of straight lines intersecting at the stoicheiometric end-points and it is noteworthy that the titration of ammonia is not adversely affected by a high concentration (1 M) of neutral salts.

RÉSUMÉ

On décrit un nouveau dispositif de titrage, combiné avec un viscosimètre et une burette automatiques. Après mélange, les vitesses d'écoulement sont mesurées avec une précision de 1 pour 10^6, et les résultats sont imprimés. Cette nouvelle technique est illustrée par des courbes de titrage d'hydroxyde de sodium, d'ammoniaque, de pyridine, d'un mélange ammoniaque–pyridine et d'éthylènediamine au moyen d'acide chlorhydrique. On donne également les courbes de titrage des acides acétique, sulfurique, oxalique, citrique et phosphorique ainsi que du phénol, de l'EDTA et du DGTA. L'acide salicylique est titré comme un acide dibasique, dans le méthanol.

ZUSAMMENFASSUNG

Durch Anwendung eines neu entworfenen vollautomatischen Viskosimeters können aliquote Anteile einer Flüssigkeit (0.050 ml) nacheinander aus einer automatischen Bürette einer zweiten Flüssigkeit zugefügt werden, die sich in dem Viskosimeter befindet. Nach dem Mischen werden die Fliesszeiten mit einer Reproduzierbarkeit von $1 \cdot 10^{-6}$ gemessen und die Ergebnisse ausgedruckt. Wenn aus der Bürette z.B. eine Alkalilösung (oder Säure) zu einer Säure (oder Alkalilösung) gegeben wird, die in dem Viskosimeter enthalten ist, ergibt die Auftragung der Fliesszeiten gegen die Anzahl der zugefügten Aliquote eine "Viskositätstitrationskurve". Dieses neuartige Verfahren wird an Hand der Kurven für die Titration von Natriumhydroxid, Ammoniak, Pyridin, einer Mischung von Ammoniak und Pyridin sowie Äthylendiamin mit Salzsäure erläutert. Die Titration von ein-, zwei-, drei- und vierbasigen Säuren verschiedener Stärke mit Natriumhydroxid wird durch die Diagramme für Salz- und Essigsäure, Phenol, Schwefel- und Oxalsäure, Citronen- und Phosphorsäure sowie EDTA und DCTA veranschaulicht. Salicylsäure in Methanol wurde als zweibasige Säure titriert. Die Auftragungen ergeben eine Reihe von Geraden, die sich an den stöchiometrischen Endpunkten schneiden. Es ist bemerkenswert, dass die Titration von Ammoniak durch hohe Neutralsalzkonzentrationen (1 *M*) nicht ungünstig beeinflusst wird.

REFERENCES

1 E. C. BINGHAM, *J. Phys. Chem.*, 45 (1941) 884.
2 J. S. SMITH, H. M. N. H. IRVING AND R. B. SIMPSON, *Analyst*, 95 (1970) 743.
3 R. B. SIMPSON, H. M. N. H. IRVING AND J. S. SMITH, *Analyst*, in press.
4 R. H. STOKES AND R. MILLS, *Viscosity of Electrolytes and Related Properties, The International Encyclopaedia of Physical Chemistry and Chemical Physics, Topic 16, Vol. 3*, Pergamon Press, London, 1965.

Analytica Chimica Acta
Elsevier Publishing Company, Amsterdam
Printed in The Netherlands

THE DETERMINATION OF SULFATE BY ATOMIC ABSORPTION INHIBITION TITRATION

R. W. LOOYENGA AND C. O. HUBER
Department of Chemistry, University of Wisconsin-Milwaukee, Milwaukee, Wisc. 53201 (U.S.A.)
(Received 19th January 1971)

The need for a rapid, sensitive method for the determination of sulfate at the trace level has prompted a number of investigations into flame spectrometric methods. Because sulfate (at trace levels) has not been amenable to direct determination by absorption or emission techniques, a number of indirect methods have been proposed. Precipitation of sulfate with excess barium chloride and subsequent determination of residual barium forms the basis for the indirect determination of sulfate by atomic emission[1] and atomic absorption[2-4]. A similar method with lead as the precipitant has also been proposed[5]. Recent work has been reported on the direct determination of sulfate by molecular flame emission[6] and molecular flame absorption[7]. Such methods ordinarily lack sensitivity and specificity. A new and sensitive atomic flame method using a microwave induced plasma for sampling and a microwave powered source was recently reported[8].

Sulfate and certain other anions tend to form refractory compounds with the alkaline earth metals, resulting in a depression or inhibition of the atomic absorption or emission signal. In our laboratory work has been conducted on the utilization of these inhibition effects for the determination of anions. Development of a new, semi-automatic titration technique[9], termed atomic absorption inhibition titration (a.a.i.t.) has led to a more complete understanding of chemical inhibition and its potential as an analytical tool. The a.a.i.t. technique has been successfully applied to phosphate[10] and silicate[9] determinations. Although sulfate inhibition is well documented[11-14], no reports on applications of the analytical usefulness of these effects have appeared.

This paper reports a method based on the sulfate inhibition of the sensitive magnesium atomic absorption. Interfering ions in the sample such as phosphate, silicate, magnesium and calcium are conveniently removed by ion exchange. A standard magnesium solution is titrated into the sample solution with simultaneous aspiration of the titration solution into a hydrogen–air flame while monitoring the magnesium signal. The titration end-point is indicated by a distinct increase in the magnesium absorption.

EXPERIMENTAL

Apparatus

The atomic absorption spectrometer was a Jarrell-Ash model 82–516 equipped with a "tri-flame" premix, laminar-flow burner of slot dimensions 0.5 ×100 mm. A 10-in. recorder was used for all atomic absorption measurements. Solutions were aspi-

rated directly from the titration vessel by means of a suitable length of fluorinated polyethylene tubing (0.027 in. i.d.). A constant delivery rate of titrant was attained using a constant-flow infusion pump, fitted with a 30-ml syringe and fluorinated polyethylene needle (0.044 in. i.d.). A suitable but slightly less convenient, alternative means of titrant delivery is a constant-flow device constructed from a reservoir buret with ground-glass tip fitted to a suitable length of 0.027 in. i.d. tubing. Aspirating and titrant delivery tubes were conveniently separated and supported by a commercial electrode holder originally designed for potentiometric electrodes which was fitted with two stoppers containing short lengths of glass tubing. Plastic beakers or wide-mouth bottles, 100–150 ml in volume, serve as suitable titration vessels. A magnetic stirrer was used for rapid mixing of the titration solutions.

Interfering cations (*e.g.* alkaline earth metals) were removed by passing the sample solution (pH 3–4) through an ion-exchange column containing sulfonated polystyrene type cation-exchange resin in the hydrogen form (Amberlite IR 120, Rohm and Haas). Similarly, where necessary, potentially interfering anions can be removed on a short column of a weakly basic anion-exchange resin.

Reagents

All solutions were prepared from reagent-grade chemicals, deionized distilled water, and acid-hardened (1 : 1 H_2SO_4–HNO_3, overnight) volumetric flasks. Solutions were stored in polyethylene containers.

Standard sulfate solution (1.00 mg SO_4 ml^{-1}) was prepared from dried reagent grade Na_2SO_4.

Standard magnesium solution (2.00 mg Mg^{2+} ml^{-1}) was prepared from $MgCl_2 \cdot 6\,H_2O$ which had been dried 4 h at 70°. This concentration was confirmed by titrating with a standard EDTA solution.

Procedure

Interfering ions are removed from the sample solution (pH 3–4) by ion exchange.

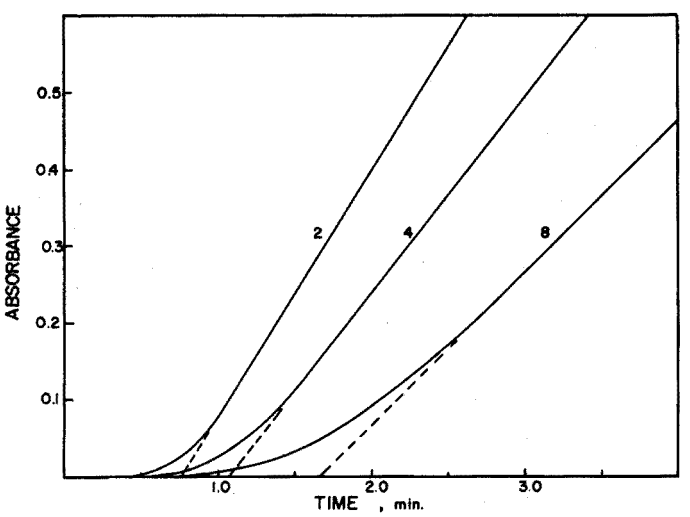

Fig. 1. Titration curves recorded for titrations of 2.0, 4.0 and 8.0 μg SO_4^{2-} ml^{-1} with 50 μg Mg ml^{-1} solution. Titrant flow rate, 1.49 ml min^{-1}. Chart speed, 2.0 in. min^{-1}. H_2:air, 30:10 (ft^3 h^{-1}).

An aliquot of sample solution, containing 0.05–1.0 mg SO_4^{2-}, is pipetted into the titration vessel and diluted to 50 ml. The titration vessel is placed on the magnetic stirrer and the aspirating and titrant delivery tubes inserted. After the solution has begun aspirating into the flame, titrant flow (1–3 ml min^{-1}) and recorder chart travel (2 in. min^{-1}) are initiated simultaneously from a common switch. The magnesium absorption is monitored at a position 8 mm above the burner head, using the 285.2 nm resonance line of magnesium and a hollow-cathode current of 4 mA. Hydrogen flow is maintained at 30 psi (30 $ft^3 h^{-1}$) and air at 30 psi (10 $ft^3 h^{-1}$). Total titration time is less than five min (see Fig. 1).

RESULTS AND DISCUSSION

Titration curves

Typical titration curves for standard sulfate solutions are shown in Fig. 1. Essentially complete inhibition of the magnesium atomic absorption is observed at magnesium to sulfate ratios less than unity. Addition of titrant in excess of this ratio results in the linear increase in magnesium absorption, thereby indicating the end-point of the titration. Extrapolation to the base line locates the end-point. Rate of titrant delivery was chosen to approximate aspiration rate.

Sulfate concentration

Data on end-point *vs.* sulfate determinations (Table I) show excellent agreement over the concentration range 1–20 p.p.m. sulfate. The titration blank (mainly mechanical) is indicated in the calibration graph by the intercept on the absorbance

TABLE I

DETERMINATIONS OF SULFATE BY THE A.A.I.T. METHOD

SO_4^{2-} added ($\mu g\ ml^{-1}$)	SO_4^{2-} found ($\mu g\ ml^{-1}$)	SO_4^{2-} added ($\mu g\ ml^{-1}$)	SO_4^{2-} found ($\mu g\ ml^{-1}$)
1.00	0.86	10.0	10.0
2.00	1.94	12.0	12.1
4.00	4.00	16.0	15.9
6.00	6.00	20.0	20.1
8.00	8.00		

axis. No concentrations greater than 20 p.p.m. were attempted. In the absence of traces of interfering ions, *e.g.* phosphate and silicate, the method should be applicable down to about 0.1 p.p.m. sulfate.

Loss of analyte by aspiration is accounted for when establishing the "titre", because the relative loss of sulfate by aspiration is constant.

Flame conditions

Methods based on inhibition effects require the use of relatively cool flames in which the compounds formed in the evaporating droplets are stable. The hydrogen–

air flame provides conditions at which sulfate inhibition is realized without significant interference from less stable compounds.

A number of experimental adjustments influence inhibition by anions[8]. Inhibition ordinarily increases with hydrogen : air flow ratio, but decreases as beam height or total gas flow rate increase. These variables help establish flame temperature in the light path. In general, inhibition is increased at lower flame temperatures.

In optimizing the fuel-to-oxidant ratio for maximum sulfate inhibition, it was found that although inhibition was somewhat greater in very fuel-rich flames, such conditions decreased the sensitivity of the magnesium signal beyond the end-point, thereby decreasing the sensitivity of the method. Hence, the ratio selected represents a compromise between high fuel-to-air ratio with higher inhibition on one hand, and lower fuel-to-air ratio for greater magnesium sensitivity on the other.

Acidity

A study of the effect of hydrogen ion concentration was conducted over a pH range of 1–9.5. No significant effect on the titration curve shape or end-point position was observed.

Specificity

Metal ions which precipitate or form refractory compounds with sulfate must be absent. These are conveniently removed by ion exchange. Alkali metals interfere at the 0.1 *M* level but are tolerated at lower concentrations. Chloride, acetate and nitrate do not interfere at 0.1 *M*. Phosphate and silicate do interfere and must be removed before titrating. Such anions are sufficiently basic so that separation from sulfate solution (*e.g.* by ion exchange) is usually straightforward. It should be noted here that interference of other ions is not necessarily predictable based on solution chemistry because the significant equilibrium and/or rate processes occur in the high-temperature dehydrating droplets.

Precision

The reproducibility of the method was estimated from determinations on six solutions, each containing 5.00 μg sulfate ml^{-1}. Using 100.0 μg Mg titrant ml^{-1}, these solutions required a mean titration time of 1.32 min. The estimated standard deviation was 0.01 μg SO_4^{2-} ml^{-1}.

Concluding observations

A.a.i.t. provides a suitable method for many sulfate samples. Although inhibition is used it is a direct titration and thus not dependent on difference measurements. Selectivity is comparable to most present methods while speed and sensitivity are somewhat better. Finally, the technique should provide a relatively easy general method for further investigations into sulfate reactions in flame sampling spectrophotometry.

The financial support of this work by the Federal Water Pollution Control Administration, Department of Interior through grant number 16020DHD is gratefully acknowledged.

SUMMARY

Sulfate can be rapidly and conveniently determined by titration with magnesium solution while the atomic absorption signal is monitored, *i.e.* atomic absorption inhibition titration (a.a.i.t.). Concentrations as low as 1 μg SO_4^{2-} ml^{-1} can be determined. Alkali metals and commonly occurring monovalent anions do not interefere at 0.1 *M* levels.

RÉSUMÉ

On décrit une méthode de dosage rapide des sulfates à l'aide de magnésium, par titrage inhibition par absorption atomique. On peut doser ainsi jusqu'à 1 μg SO_4^{2-} ml^{-1}. Les métaux alcalins et les anions courants monovalents ne gênent pas.

ZUSAMMENFASSUNG

Sulfat kann schnell und bequem durch Titration mit Magnesiumlösung bestimmt werden, wobei das Magnesium-Atomabsorptionssignal gemessen wird. Diese Atomabsorptions-Inhibitionstitration (a.a.i.t.) erlaubt die Bestimmung von Konzentrationen bis zu 1 μg SO_4^{2-} ml^{-1} herab. Alkalimetalle und die üblichen einwertigen Anionen stören nicht.

REFERENCES

1 W. M. Shaw, *Anal. Chem.*, 30 (1958) 1682.
2 D. A. Roe, P. S. Miller and L. Lutwak, *Anal. Biochem.*, 15 (1966) 313.
3 R. Dunk, R. A. Mostyn and H. C. Hoare, *At. Absorption Newslett.*, 8 (1969) 79.
4 F. F. Yates and L. H. McCormic, *Soil Sci. Soc. Amer. Proc.*, 34 (1970) 705.
5 S. Rose and D. F. Boltz, *Anal. Chim. Acta*, 44 (1969) 239.
6 R. M. Dagnall, K. C. Thompson and T. S. West, *Analyst*, 92 (1967) 506.
7 K. Fuwa and B. L. Vallee, *Anal. Chem.*, 41 (1969) 188.
8 H. E. Taylor, J. H. Gibson and R. K. Skogerboe, *Anal. Chem.*, 42 (1970) 1569.
9 R. W. Looyenga and C. O. Huber, *Abstr. 1970 Detroit Anachem Conf., Detroit, Mich., October 1970*, No. 59.
10 C. O. Huber and W. Crawford, *Anal. Chem.*, 43 (1971) 498.
11 G. L. Baker and L. H. Johnson, *Anal. Chem.*, 26 (1965) 465.
12 D. J. Halls and A. Townshend, *Anal. Chim. Acta*, 36 (1966) 278.
13 I. Rubeska and B. Moldan, *Anal. Chim. Acta*, 37 (1967) 421.
14 C. Rocchiccioli and A. Townshend, *Anal. Chim. Acta*, 41 (1968) 93.

Analytica Chimica Acta
Elsevier Publishing Company, Amsterdam
Printed in The Netherlands

COULOMETRIC INVESTIGATION ON THE USE OF SINGLE CRYSTALS OF SODIUM CHLORIDE AS A PRIMARY STANDARD

TAKAYOSHI YOSHIMORI AND TATSUHIKO TANAKA
Faculty of Engineering, Science University of Tokyo, Kagurazaka, Shinjuku-ku, Tokyo (Japan)
(Received 10th December 1970)

Sodium chloride is generally used as the primary standard substance for argentimetry or mercurimetry. Several methods for drying the reagent are, however, shown in the literature. Marinenko and Taylor[1] dried the reagent at 110° for 3 h in their excellent investigation on the determination of its purity by the precise coulometric titration. According to the Japanese Industrial Standard (JIS)[2], the reagent should be ignited in a platinum crucible at 500–650° for 40–50 min. Kolthoff and Sandell[3] recommend the same method as JIS.

These procedures indicate that the drying of the reagent is somewhat troublesome. In the experience of the present authors, each weighing bottle containing the aliquot of the hot salt should be cooled in its own desiccator. If a desiccator containing many weighing bottles is opened to remove the first aliquot, moisture is introduced into the desiccator and is adsorbed by the other samples in it.

Single crystals of sodium chloride synthesized from a melt of the salt are readily available as the cell or prism for infrared absorption spectroscopy. It seemed probable that the crystal has sufficient purity for use as a primary standard, and also little water is adsorbed on its surface. The crystal, however, has not been used for this purpose.

Taylor and Smith[4] showed that drying of the coarse crystal is unnecessary. Bates and Wichers[5] prepared single crystals of benzoic acid and compared their purity against primary-standard potassium hydrogen phthalate (NBS Standard Sample 84d) by differential titration. Comparison of their result with that obtained by Eckfeldt and Shaffer[6] (the same potassium hydrogen phthalate was analyzed by precise coulometric titration) indicates that the purity of the above crystal was somewhat less than 100%. Rokosz[7] has prepared single crystals of potassium hydrogenphthalate, but these crystals have not been analyzed and nor have their purities been compared with those of the other standard reagents. These facts indicate that single crystals cannot automatically be regarded as "pure" substances.

In this investigation, the purities of single crystals of sodium chloride were determined by precise coulometric titration, and the adsorbed water on their surfaces was also determined coulometrically.

EXPERIMENTAL

Apparatus and reagents

The instruments for the coulometric generation of the titrants were similar to those shown previously[8]. The assembly and the circuit for potentiometric end-point

location are shown in Fig. 1. The *IR* drop through a standard resistor (10 ohm) was measured with a precise potentiometer. From the certificated values of these measuring devices, it could be expected that the standard deviation of the error in the measurement of the generating current was less than 0.005%. As the Faraday constant, 96487.2 coulomb was used.

A 50-Hz oscillator based on the frequency of a quartz crystal and a cycle counter were used to measure the time interval of the electrolysis[9]. All samples were weighed with a microbalance. A weighing bottle of nearly the same weight as that containing the sample was used as a counterpoise. All weights were corrected for absolute weights, and all weighings were corrected for air buoyancy.

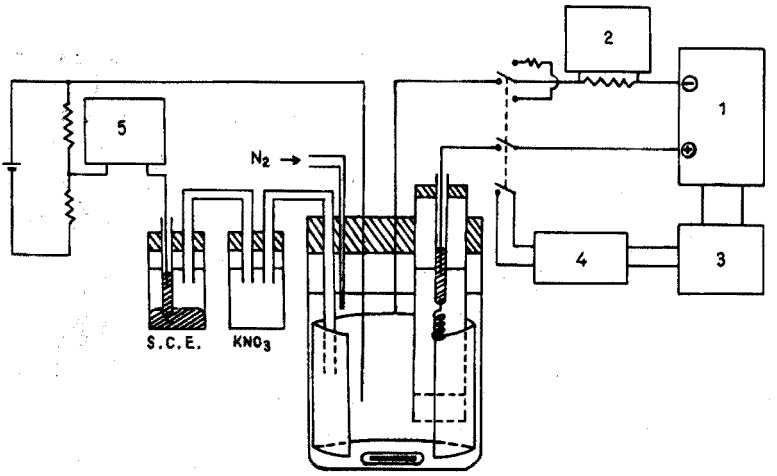

Fig. 1. Apparatus. (1) Constant current source; (2) potentiometer; (3) stabilizer; (4) timer; (5) potentiometer (mV).

The end-point of the titration was located potentiometrically with the circuit shown in Fig. 1. Because the measuring range of the potentiometer was not enough to measure the potential difference between a silver electrode and a saturated calomel electrode, the applied voltage device shown in Fig. 1 was inserted into this circuit.

A tall-form beaker (about 650 ml) was used as the electrolytic cell. Its outside was painted red in order to protect silver salts from light. The generator anode was a pure silver plate of large area (10 × 11 cm and about 0.1 mm thick), and the generator cathode was a platinum spiral (0.5 mm diameter and 50 mm length). The diaphragm under the cathode compartment was prepared as follows: the bottom of a polyethylene tube was closed with a polyethylene plate which had many fine holes. An agar–agar gel saturated with potassium nitrate was plugged on the bottom, the thickness of the layer being about 15 mm.

All reagents were of analytical grade, and were used without further purification. A 50% (v/v) methanol solution which was 1 *M* in sodium nitrate and 1 *M* in acetic acid was used as the anolyte.

Procedure

Preparation of sample. The sample was a synthetic optical crystal of sodium

chloride, which was manufactured by the Stockbarger method (Horiba Ltd., Japan). The single crystal was broken into pieces about 0.2 g in weight, and the surfaces of the pieces were polished with an ethanolic chromium(III) oxide emulsion. After being washed with ethanol, the crystals were wiped with chamois.

In order to test the purity, the sample prepared as above was stored, without heating, in a desiccator at room temperature for about 3 h. Magnesium perchlorate was used as a desiccant throughout this investigation.

Coulometric titration. Nitric acid (1 *M*) saturated with sodium nitrate were poured into the cathode compartment, and then about 0.5 μeq of silver nitrate solution was added to it in order to precipitate any traces of halides or other impurities which react with silver ion. About 600 ml of the anolyte specified above was placed into the cell. In order to remove dissolved oxygen from the anolyte, nitrogen was passed through the solution for about 1 h. Then the gas was allowed to flow over the anolyte throughout the titration.

As a pretitration, a solution containing about 3 mg of sodium chloride was added to the cell, and this was electrolyzed at a constant current of about 25 mA. Near the end-point of the titration, the generating current was cut off and the potential of the indicator electrode was measured with the potentiometer. Then the solution was further electrolyzed and the potential was measured again, the small increments of electrolysis being repeated until after the end-point; the titration was then continued for about 10 sec or more. The end-point of the titration was located from the differential titration curve. Figure 2 shows an example of the curve.

After the pretitration had been completed, about 95% of the silver ion required to react with the weighed sodium chloride was generated in the electrolyte at a constant current of about 129 mA. The weighed sample was then introduced into the cell and dissolved by stirring. After the complete dissolution of the sample, the residual chloride ion was titrated with the electrolytically generated silver ion. In

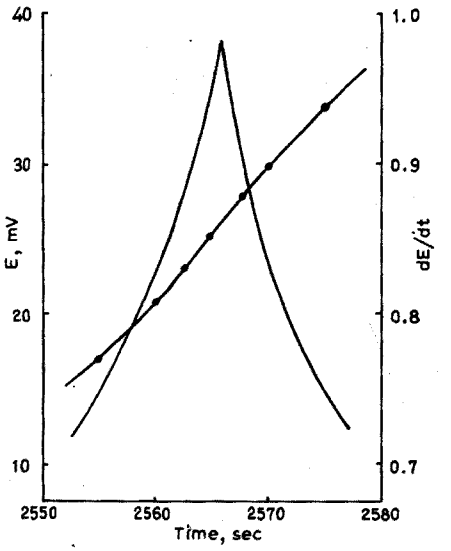

Fig. 2. Potentiometric titration curve and differential titration curve of single crystal.

TABLE I

VARIANCE OF WEIGHTS OF FOUR SINGLE CRYSTALS DRIED BY DIFFERENT METHODS (in mg)

Method of drying	1	2	3	4
Room temp., $Mg(ClO_4)_2$ desiccator	506.154	583.001	142.223	144.315
110°, 3.5 h	506.149	582.996	142.222	144.313
600°, 50 min	506.150	582.995	142.222	144.311

this case, a constant current of 25 mA was used to generate the titrant. The end-point was located by the same method as that used for the pretitration.

The time of electrolysis was measured graphically from the distance between the peak of this differential titration curve and that of the pretitration. The amount of electricity used throughout the main titration was calculated from the electrolytic time and the current.

RESULTS AND DISCUSSION

Water on the surfaces of single crystals

The loss in weight of single crystals was first measured under various drying conditions. The results obtained (Table I) indicate that the adsorbed water on the surface of the crystal could be removed simply by storage of the sample in a desiccator at room temperature for a few hours.

Next, the adsorbed water on the crystal was determined by carrier gas extraction followed by coulometric titration as described previously[10]. The sample crystal was stored in the desiccator at room temperature for about 3 h, and the heating temperature for generation of water from the sample was 600°. The results obtained are shown in Table II. The amounts of water obtained by this method were nearly consistent with those in Table I.

These results indicate that satisfactory dehydration of these single crystals can be obtained by storage in a desiccator containing magnesium perchlorate at room temperature for more than few hours.

Determination of the purity of the crystal

At the start of this investigation, the weighed sample was dissolved with water

TABLE II

DETERMINATION OF ADSORBED WATER ON SURFACES OF SINGLE CRYSTALS

Sample weight (mg)	*Surface area (cm^2)*	*H_2O found ($\mu g\ cm^{-2}$)*
148.216	1.0222	0.437
152.627	1.0272	0.547
127.979	0.9108	0.369
122.591	0.8850	0.570
	Mean	0.481

TABLE III

PURITY TESTS OF SINGLE CRYSTALS

Sample	*No. of detns.*	*Mean value of purity* (%)	$\hat{\sigma}$ (%)
1	6	99.9881	0.0143
2	6	99.9932	0.0138
3	14	99.9949	0.0124[a]

[a] V^{-1} value.

in a small beaker and then transferred to the cell; with this method the results obtained were always unfavorable. When the solid sample was introduced into the cell, it could be completely dissolved in the electrolyte by stirring for about 20 min. This technique prevented any errors from transference of the solution and from oxygen or other impurities in the washing water.

Three single crystals were divided into small portions (150–200 mg) and their surfaces were polished before storage in the desiccator at room temperature. The purities of the samples thus prepared were determined by the above-mentioned procedure. The results obtained are shown in Table III. It may be considered from the results that the original single crystals had somewhat different purities, but each original crystal was homogeneous enough. The deviations of the results are discussed below.

The purities of these single crystals were somewhat less than 100%. From the results in Tables I and II, less than 0.002 mg of adsorbed water was present on the surfaces of the crystals, which is not enough to balance the lower results in Table III.

Impurities in the crystals were next considered. Firstly, the acidic materials in a crystal were tested by the following method[2]. A part of the single crystal (2 g) was dissolved in 40 ml of water freed from carbon dioxide and ammonia. The pH value of this solution was 5.3. A solution of a crystal which had been heated at 600° for 50 min showed a pH value of 5.6. The pH value of a solution prepared by the same method from the primary-standard substance (certificated by the Industrial Inspection Institute, Japan) was 5.9. These results indicate that the crystal and the standard reagent contain some acidic impurities, of which the contents and the species are unknown, because the pH of the water used for dissolution was 6.3.

Secondly, the crystals were analyzed qualitatively by a spectroscopic method. These analyses showed that the crystals contained an appreciable amount of calcium and aluminum and also trace amounts of magnesium, silicon and silver. The amounts of these impurities may be enough to balance the results in Table III. When the accuracy of the ordinary titrimetric procedure is considered, the contents of the impurities are small enough for the crystals to be used as standard materials for argentimetry.

The standard deviations of the results were somewhat larger than those reported previously for potassium dichromate[11]. The detection of the end-point may be the main source of the deviation because of the slight potential break through the end-point of the titration. Comparing these standard deviations with the results obtained by Marinenko and Taylor[1], the authors consider that the main source of error is not the inhomogeneity of each crystal but the location of the end-point of the titration.

In order to determine the purity, crystals of about 3 meq were used as sample. When the crystal was smaller than 100 mg, the weighing error was increased. With larger crystals (more than 0.3 g), high results were sometimes obtained under these experimental conditions; silver-rich precipitates of non-stoichiometric composition were perhaps produced first, and then the precipitates gradually changed to stoichiometric composition. This resulted in an unstable potential of the indicator electrode, and an unreasonably long time was needed in order to obtain the equilibrium potential of the electrode.

The interference of the condenser current on the generating electrode was also considered and investigated by the following method. The purity of the crystal was determined by the above method, but the generating current was cut 50 or 100 times during the electrolysis. The results obtained were 100.006 or 100.016% respectively, which indicated that some influence should be considered. If the generating current was cut for too long a time in order to measure the potential of the indicator electrode, some part of it could be used to recharge the electric double layer on the generating electrode. Therefore the current efficiency may be somewhat decreased, when the area of generating electrode is extremely large and the current is cut too often. In ordinary experiments, however, about 10 measurements of the potential of the indicator electrode were enough to locate the end-point of the titration. Accordingly, the interference caused by the condenser current was negligibly small.

CONCLUSION

Single crystals of sodium chloride are of sufficient purity (99.99% or more) and homogeneity, for use as the primary standard substance in argentimetry or mercurimetry. The adsorbed water on the surfaces is negligible, when polished crystals are stored in a desiccator over magnesium perchlorate.

The authors are grateful to Mr. S. Ishiwari of Hitachi Co. Ltd., for his valuable support of this investigation and to Mr. T. Harada for technical assistance.

SUMMARY

The use of single crystals of sodium chloride as a primary standard substance for argentimetry is described. The water on the surface and the purity of the crystal are measured by coulometric titration methods. The adsorbed water amounts to 0.48 $\mu g\ cm^{-2}$ when the sample is dried in a desiccator containing magnesium perchlorate at room temperature for about 3 h. The loss in weight of the crystal is negligible when it is heated at about 600°. The purities of three crystals, by precise coulometric titrations, are 99.988, 99.993 and 99.995%, with standard deviations of 0.0143, 0.0138 and 0.0124%, respectively. It can be concluded that the crystal is useful as a primary standard.

RÉSUMÉ

On propose l'utilisation d'un cristal unique de chlorure de sodium comme étalon primaire en argentimétrie. L'eau en surface et la pureté du cristal sont déter-

minées par titrage coulométrique. La quantité d'eau adsorbée est de 0.48 μg cm^{-2} lorsque l'échantillon est séché dans un dessicateur contenant du perchlorate de magnésium, à la température ordinaire, pendant 3 h. La perte en poids du cristal est négligeable lorsqu'il est chauffé à 600° environ. Les puretés de trois cristaux, déterminées par titrage coulométrique, sont respectivement 99.988, 99.993 et 99.995%, avec une déviation standard de 0.0143, 0.0138 et 0.0124%. On peut conclure que le cristal est utilisable comme étalon primaire.

ZUSAMMENFASSUNG

Es wird die Verwendung von Natriumchlorid-Einkristallen als Urtitersubstanz für die Argentimetrie beschrieben. Das Wasser an der Oberfläche und die Reinheit des Kristalls werden durch coulometrische Titration bestimmt. Die adsorbierten Wassermengen betragen bis 0.48 μg cm^{-2}, wenn die Probe in einem Exsikkator über Magnesiumperchlorat bei Raumtemperatur etwa 3 h lang getrocknet wird. Der Gewichtsverlust des Kristalls ist vernachlässigbar, wenn er auf etwa 600° erhitzt wird. Die durch genaue coulometrische Titrationen bestimmten Reinheiten von drei Kristallen sind 99.988, 99.993 und 99.995% mit Standardabweichungen von 0.0143, 0.0138 und 0.0124%. Es kann gefolgert werden, dass sich der Kristall als Urtitersubstanz eignet.

REFERENCES

1 G. MARINENKO AND J. K. TAYLOR, *J. Res. Natl. Bur. Std.*, 67 A (1963) 31.
2 JIS (Japanese Industrial Standard), *K 8005*, 1966.
3 I. M. KOLTHOFF AND E. B. SANDELL, *Textbook of Quantitative Inorganic Analysis*, 3rd Edn., Macmillan, New York, 1952, p. 541.
4 J. K. TAYLOR AND S. W. SMITH, *Science*, 124 (1956) 940.
5 R. G. BATES AND E. WICHERS, *J. Res. Natl. Bur. Std.*, 59 (1957) 9.
6 E. L. ECKFELDT AND E. W. SHAFFER, JR., *Anal. Chem.*, 37 (1965) 1534.
7 A. ROKOSZ, Jagiellonian University, Krakow, private communication.
8 T. YOSHIMORI AND I. MATSUBARA, *Bull. Chem. Soc. Japan*, 43 (1970) 2800.
9 T. MIWA, T. YOSHIMORI AND T. TAKEUCHI, *J. Chem. Soc. Japan, Ind. Chem. Sect.*, 67 (1964) 2045.
10 T. YOSHIMORI AND S. ISHIWARI, *Bull. Chem. Soc. Japan*, 42 (1969) 1282.
11 T. YOSHIMORI, I. MATSUBARA, K. HIROSAWA AND T. TANAKA, *Japan Analyst*, 19 (1970) 681.

Analytica Chimica Acta
Elsevier Publishing Company, Amsterdam
Printed in The Netherlands

STROMLOSE ANREICHERUNGSMÖGLICHKEITEN VON SPUREN-METALLEN AN DER GRENZFLÄCHE QUECKSILBER/ELEKTROLYT

TEIL I. UNTERSUCHUNGEN AN EINIGEN ORGANISCHEN KOMPLEXBILDNERN AUF IHRE EIGNUNG ALS FILMBILDENDE SUBSTANZEN FÜR ANREICHERUNGSVERSUCHE ANORGANISCHER DEPOLARISATOREN

H. BERGE UND H. RINGSTORFF
Sektion Chemie, Universität Rostock, Rostock (D.D.R.)

(Eingegangen den 3. Januar 1971)

Obwohl es allgemein bekannt ist, dass der Reduktion von anorganischen Depolarisatoren gewöhnlich eine Adsorption vorausgeht, die in einzelnen Fällen die Oberflächenladung weit übertreffen kann, ist bisher noch nicht versucht worden, derartige Erscheinungen in der analytischen Praxis auszunutzen. Versuche zur Empfindlichkeitssteigerung bei der Bestimmung organischer Tenside liegen vor[1,2]. Einen 10- bis 50-fachen Empfindlichkeitsgewinn beobachteten Matysik[3] und Kalvoda[4] bei oszillopolarographischen Bestimmungen einiger Schwermetallionen in schwefelsaurer Grundlösung in Gegenwart von Phenol und Thioharnstoff. Als Ursache werden von Kalvoda Adsorptionserscheinungen genannt. Sohr und Liebetrau[5] berichten über eine starke Empfindlichkeitssteigerung bei der stromlosen Anreicherung von Zirkonium und Uran in der Adsorptionsschicht einer organischen Phosphorverbindung. In der vorliegenden Arbeit wurden organische Komplexbildner auf ihre Eignung als Filmbildner für Anreicherungszwecke getestet und adsorptive Anreicherungsmöglichkeiten einiger Ionen untersucht.

EXPERIMENTELLER TEIL

Geräte und Elektroden

Alle Messungen wurden bei $25 \pm 0.2°$ mit dem Gleich- und Wechselstrompolarographen "GWP 563" der Akademiewerkstätten für Forschungsbedarf Berlin durchgeführt. Für tensammetrische Messungen stand ein Tropfzeitgeber "TZG 1" des gleichen Herstellers zur Verfügung.

Die bei den Untersuchungen mit dem Tropfzeitgeber verwendete Elektrode hatte eine Ausflussgeschwindigkeit von 2.29 mg sec^{-1} in 0.1 *M* $NaClO_4$ bei geöffnetem Stromkreis und einer Niveauhöhe von 50 cm. Alle Potentialangaben beziehen sich auf die gesättigte Kalomelelektrode. Die für die Messungen am hängenden Quecksilbertropfen verwendete Anordnung, die in einem Luftthermostaten untergebracht war, wird in Abb. 1 gezeigt.

Ein runder Piacrylstopfen (1) mit 3 Schliffen NS 10 und einem Schliff NS 7.5 nimmt die Elektrolytbrücke mit der Referenzelektrode (2), die Messelektrode (3), einen Zweiwegehahn (4) und ein Gasableitungsrohr (5) auf. Das Messgefäss (6), wahlweise mit einem Thermostatenmantel ausgestattet, hat die Form eines Becher-

glases. Der Rand ist stark verbreitert und plangeschliffen. Ein Ring aus Silikongummi, der fest mit dem Piacrylstopfen verklebt ist, sorgt für eine gute Dichtung. Das Messgefäss wird durch 3 Federn, die sich leicht ein- und aushängen lassen, sehr fest gehalten. Der Zweiwegehahn ist so gebaut, dass nach dem Spülen während des Messvorganges ein leichter Schutzgasstrom (Argon) über die Oberfläche der Messlösung geleitet werden kann. Die Elektrolytbrücke lässt sich durch eine Schliffverbindung mit der Bezugselektrode schnell und leicht wechseln. Als Messelektrode diente eine umgebaute Radiometerelektrode mit sehr kleinem Quecksilberreservoir (0.13 cm^3) und silikonisierter Kapillare*. Silikonisiert wurde in einem Aluminiumblock[6] bei 300°. Vor dem Füllen der Elektrode wurde das Hg entgast. Die Oberfläche des verwendeten stationären Tropfens betrug jeweils $2.84 \cdot 10^{-2}$ cm^2.

Mit Hilfe der beschriebenen Messanordnung ist ein sehr rasches Wechseln der Probelösungen möglich. Die gesamte Anordnung wird lediglich um etwa 60° geschwenkt und dann lässt sich ohne Behinderung durch den Rührmagneten des Rührmotors das Messgefäss bequem auswechseln. Es wurde indirekt gerührt. Durch einen Anschlag beim Zurückschwenken nach erfolgten Probenwechsel nimmt das Messgefäss stets die gleiche reproduzierbare Stellung über dem Rührmagneten ein.

Lösungen und Chemikalien

Für die Messungen wurde tetradestilliertes Wasser verwendet. Beim zweiten Destillationsschritt erfolgte ein Zusatz von Kaliumpermanganat. Die aus p.a. Salzen

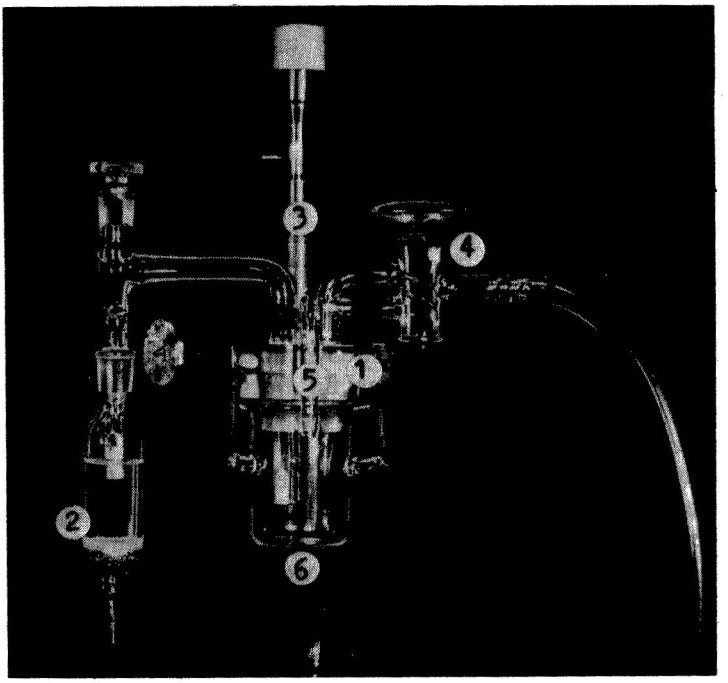

Abb. 1. Messapparatur für die Messungen mit der H.M.D.E.

* "H.D.M.E." = hanging mercury drop electrode. Die Bezeichnung soll auch weiterhin verwendet werden.

hergestellten Puffer und Grundelektrolyten wurden zur Reinigung an einer grossflächigen Quecksilberelektrode einer mehrstündigen Elektrolyse unterzogen.

ERGEBNISSE

Gleich- und wechselstrompolarographische Untersuchungen von Titangelb, Phenylarsonsäure, *o*-Aminophenylarsonsäure, *p*-Aminophenylarsonsäure, 8-Hydroxichinolin, Oxin-(5)-sulfonsäure, Thioxin, Tetraäthylammoniumdithiocarbamat, Rhodamin B, Magneson II, Tributylphosphat und Tripropylphosphat[7] zeigten, dass von diesen Verbindungen nur die erwähnten Phosphorsäureester Anforderungen genügen, die an organische Komplexbildner gestellt werden müssen, in deren Adsorptionsschicht Metallionenspuren angereichert werden sollen.
Sie sind.

1. Stark oberflächenaktiv, so dass schon bei sehr kleinen Konzentrationen der Bedeckungsgrad θ praktisch 1 wird. Die Konzentration des Komplexbildners an der Elektrodenoberfläche ist gegenüber der Konzentration im Lösungsinnern sehr gross.
2. Der Adsorptionsbereich ist ziemlich breit und das Desorptionspotential liegt negativer als die Reduktionspotentiale vieler polarographisch bestimmbarer Ionen.
3. Die Verbindungen selbst sind polarographisch inaktiv.
4. Die zur Komplexbildung befähigten Gruppen sind ins Lösungsinnere und nicht zur Hg-Oberfläche gerichtet[8].

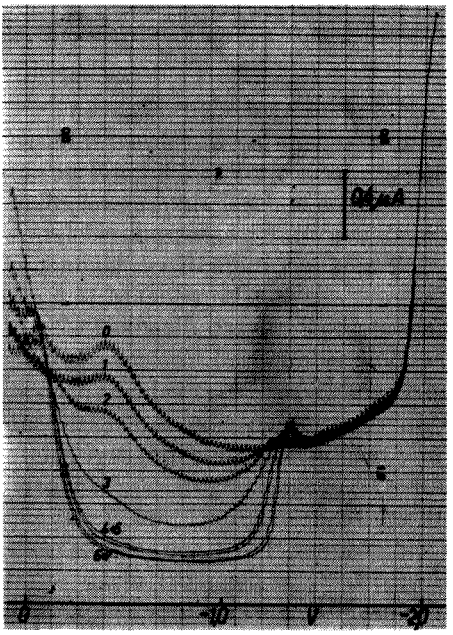

Abb. 2. Wechselstrompolarogramme von Tributylphosphat. (0) 0.1 *M* $NaClO_4$; + Tributylphosphat (*M*): (1) $2 \cdot 10^{-5}$; (2) $4 \cdot 10^{-5}$; (3) $8 \cdot 10^{-5}$; (4) $12 \cdot 10^{-5}$; (5) $14 \cdot 10^{-5}$; (6) $16 \cdot 10^{-5}$; (7) $18 \cdot 10^{-5}$. Amplitude 10 mV, Tropfzeit 1.5 sec.

Auf die Oberflächenaktivität organischer Phosphorverbindungen wurde schon mehrfach hingewiesen[8-13].

In Abb. 2 sind die tensammetrischen Kurven des Tributylphosphats (TBP) in Abhängigkeit von der Komplexbildnerionenkonzentration dargestellt. Bei TBP-Konzentrationen von 1.6–1.8·10^{-4} M wird die Sättigungserniedrigung erreicht, d.h. der Bedeckungsgrad θ ist 1. Der Potentialbereich der Adsorption erstreckt sich bei 2·10^{-4} M TBP von −0.05 V bis −1.3 V. Das Adsorptionsgleichgewicht an der Hg-Oberfläche stellt sich sofort ein.

Für Anreicherungsversuche ist es wichtig, den Einfluss des pH-Wertes auf die Oberflächenaktivität zu kennen. Beim TBP war in dem untersuchten Bereich pH 1.7 bis pH 12 keine merkbare Änderung der Oberflächenaktivität festzustellen. Bei pH Werten $\leqq$ 1.7 konnte der Desorptionspeak nicht mehr ausgewertet werden, denn es erfolgte ein fliessender Übergang in die Wasserstoffwelle. Andere Autoren erhielten bei der Untersuchung vieler oberflächenaktiver Substanzen ähnliche Ergebnisse[10,14].

Tripropylphosphat (TPP) ist auf Grund der geringeren Kettenlänge des Alkylrestes nicht mehr so stark oberflächenaktiv wie Tributylphosphat (Abb. 3). Der Bedeckungsgrad $\theta = 1$ wird erst bei etwa 4·10^{-4} M TPP erreicht, also mit mehr als verdoppelter Konzentration im Vergleich zum TBP. Der Adsorptionsbereich liegt zwischen −0.27 V und −1.25 V (TPP-Konzentration 4·10^{-4} M).

Sohr[15] fand bei oszillopolarographischen Untersuchungen, dass die Einstellung des Adsorptionsgleichgewichtes bei der Adsorption des TPP geschwindigkeitsbestimmend ist. Eine Abhängigkeit der Doppelschichtkapazität von der Hg-Ausflussgeschwindigkeit war aber bei tensammetrischen Aufnahmen nicht festzustellen. Das

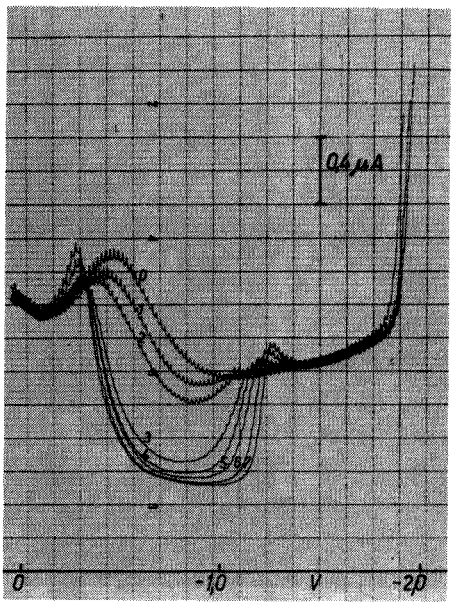

Abb. 3. Wechselstrompolarogramme von Tripropylphosphat. (0) 0.1 M $NaClO_4$; + Tripropylphosphat (M): (1) 4·10^{-5}; (2) 8·10^{-5}; (3) 1.2·10^{-4}; (4) 1.6·10^{-4}; (5) 2.0·10^{-4}; (6) 3.0·10^{-4}; (7) 4.0·10^{-4}. Amplitude 10 mV, Tropfzeit 1.5 sec.

Adsorptionsgleichgewicht stellt sich also sehr schnell ein. Läge unter den hier gegebenen Bedingungen eine Verzögerung der Gleichgewichtseinstellung vor, müsste sich bei veränderter Tropfzeit die Doppelschichtkapazität ändern. Bei niedriger Quecksilberausflussgeschwindigkeit (geringe Behälterhöhe, lange Tropfzeit) steht mehr Zeit zur Gleichgewichtseinstellung zur Verfügung als bei grossen Hg-Ausflussgeschwindigkeiten (grosse Behälterhöhe, kurze Tropfzeit). Stellt sich das Adsorptionsgleichgewicht langsam ein und wird bei kurzen Tropfzeiten kein Gleichgewichtszustand erreicht, müsste dann die Kapazitätserniedrigung geringer sein als bei langen Tropfzeiten. Die Mittelwerte des Kapazitätswechselstromes $i_c^{\sim}$ dürften dann im Wechselstrompolarogramm nicht übereinanderliegen, wie das beim TPP der Fall ist (Abb. 4).

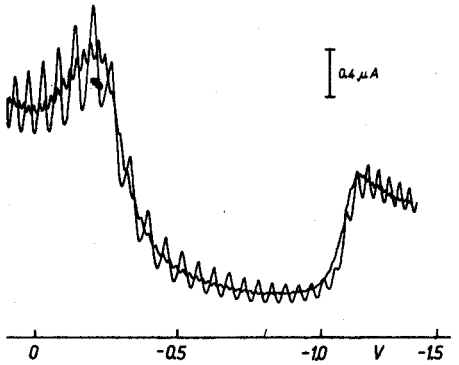

Abb. 4. Wechselstrompolarogramme von Tripropylphosphat bei verschiedenen Quecksilberausflussgeschwindigkeiten. $4 \cdot 10^{-4}$ *M* Tripropylphosphat. Tropfzeiten 2.0 und 7.0 sec.

Die Phenylarsonsäuren, 8-Hydroxichinolin, Oxin-(5)-sulfonsäure und Magneson II wurden zu schwach oder in einem zu schmalen Potentialbereich adsorbiert, um als Filmbildner Verwendung finden zu können. Magneson II wird ausserdem normalpolarographisch schon so früh reduziert, dass eine Nutzung der Verbindung für Anreicherungszwecke auch aus diesem Grunde nicht möglich ist. Die Halbstufenpotentiale der Reduktionsstufen liegen bei -0.65 V und -0.84 V (0.1 *M* KNO_3, 10^{-3} *M* Magneson II).

Titangelb, das u.a. Komplexe mit Ni, Co und Mn bildet, die alle inversvoltammetrisch schlecht bestimmbar sind, wird recht kräftig adsorbiert. Der Adsorptionsbereich liegt bei $1 \cdot 10^{-3}$ *M* Titangelb in 0.1 *M* $NaClO_4$ zwischen $+0.2$ V und -0.9 V. Im Gleichstrompolarogramm gibt die Verbindung in 0.1 *M* KNO_3 zwei Reduktionsstufen mit Halbstufenpotentialen von -0.29 V und -0.96 V (10^{-3} *M* Titangelb). Wegen der polarographischen Aktivität in diesem Potentialbereich wurden Anreicherungstests mit Titangelb nicht durchgeführt, zumal auch der Adsorptionsbereich nicht weit ins negative Potentialgebiet reicht.

Dem Titangelb vergleichbare Ergebnisse lieferte Rhodamin B. Dieser Komplexbildner wird bei einer Konzentration von $1 \cdot 10^{-3}$ *M* von etwa ± 0 V bis -1.2 V adsorbiert. Wie Titangelb wird Rhodamin B aber gleichstrompolarographisch schon früh reduziert. Die Halbstufenpotentiale liegen bei -0.59 V bzw. -1.13 V (0.1 *M* KNO_3, 10^{-3} *M* Rhodamin B).

Thioxin, ein universeller Komplexbildner, war wie erwartet stark oberflächenaktiv. Bei $4 \cdot 10^{-4}$ *M* Thioxin wird in Acetatpuffer pH 4.8 eine vollständige Oberflächenbedeckung der Elektrode erreicht ($\theta = 1$). Das Adsorptionsgleichgewicht stellt sich praktisch sofort ein. Normalpolarographische Untersuchungen zeigten aber, dass Thioxin als filmbildender Komplexbildner für Anreicherungszwecke ungeeignet ist. In einer 10^{-2} *M* NaOH Lösung erhält man bei $1 \cdot 10^{-4}$ *M* Thioxin eine weit negativ liegende Reduktionsstufe bei $E_{\frac{1}{2}} - 1.48$ V und eine Oxidationsstufe mit einem Halbstufenpotential von -0.77 V. Die Oxidationsstufe ist identisch mit der Oxidationsstufe der HgS-Bildung. Thioxin wird also gespalten und die zur Komplexbildung mit den anzureichernden Ionen benötigten $^{-}$SH Gruppen werden vom Quecksilber selbst blockiert. Ein Einsatz von Thioxin zur indirekten inversvoltammetrischen Bestimmung von Metallspuren[6] wäre möglich, denn es lässt sich an der stationären Hg-Elektrode gut anreichern. In Acetatpuffer pH 4.8 wurden 2 konzentrationsabhängige Peaks mit Spitzenpotentialen von -0.49 V und -1.53 V erhalten.

Ähnlich stark wie Thioxin wird Tetraäthylammoniumdithiocarbamat an der Quecksilberoberfläche adsorbiert. Im Gleichstrompolarogramm erhält man aber eine Oxidationsstufe bei $E_{\frac{1}{2}} - 0.54$ V (0.1 *M* NaOH, 10^{-4} *M* Tetraäthylammoniumdithiocarbamat), die sich nur durch Bildung eines schwerlöslichen Quecksilbersalzes dieser Verbindung erklären lässt. Ein Einsatz von Tetraäthylammoniumdithiocarbamat für indirekte Bestimmungsverfahren wäre daher denkbar, während die Verwendung für Anreicherungsversuche von Spurenmetallen in der Adsorptionsschicht aus den gleichen Gründen wie beim Thioxin nicht möglich ist.

Von den untersuchten Komplexbildnern kamen also wie schon erwähnt nur TBP und TPP für Anreicherungszwecke in Frage. Mit beiden Phosphorsäureestern wurden im pH-Bereich 2.7 bis 9.0 Anreicherungstests mit folgenden Ionen durchgeführt: MoO_4^{2-}, ZrO^{2+}, UO_2^{2+}, VO_3^{-}, WO_4^{2-}, Pb^{2+} und Tl^{+}.

Die Konzentration der Phosphorsäureester war jeweils hoch genug um den Bedeckungsgrad $\theta = 1$ zu gewährleisten. Angereichert wurde immer unter Rühren. Analytisch auswertbare Peaks ergaben UO_2^{2+} und WO_4^{2-}, wenn nach der Voranreicherung bei geöffnetem Stromkreis negativ polarisiert wurde. Der Stromkreis wurde bei Potentialen zwischen $+0.3$ V und -0.4 V geschlossen. Bei der Untersuchung der Abhängigkeit der Peakhöhen von der Phosphorsäureesterkonzentration verringerte sich mit abnehmender Komplexbildnerkonzentration überraschend die Peakhöhe nicht. Die Anreicherung von UO_2^{2+} und WO_4^{2-} erfolgte ebenso auch ohne TBP bzw. TPP. Auf nähere Einzelheiten der Anreicherungsversuche in Gegenwart filmbildender Phosphorsäureester soll daher nicht weiter eingegangen werden.

ZUSAMMENFASSUNG

Tributylphosphat (TBP), Tripropylphosphat (TPP), Titangelb, Phenylarsonsäure, *o*-Aminophenylarsonsäure, *p*-Aminophenylarsonsäure, 8-Hydroxichinolin, O-xin-(5)-sulfonsäure, Thioxin Tetraäthylammoniumdithiocarbamat, Rhodamin B und Magneson II wurden auf die Verwendbarkeit für Anreicherungsversuche von Spurenmetallen in der Adsorptionsschicht dieser Komplexbildner an der Quecksilberoberfläche untersucht. Nur Tributylphosphat und Tripropylphosphat erwiesen sich als geeignet. Anreicherungstests von MoO_4^{2-}, ZrO^{2+}, UO_2^{2+}, VO_3^{-}, WO_4^{2-}, Pb^{2+} und

Tl^+ in Gegenwart von Tributylphosphat und Tripropylphosphat waren beim UO_2^{2+} und WO_4^{2-} positiv.

SUMMARY

Tributylphosphate (TBP), tripropylphosphate (TPP), titan yellow, phenylarsonic acid, *o*- and *p*-aminophenylarsonic acid, 8-hydroxyquinoline, oxine-5-sulphonic acid, thioxine, tetraethylammoniumdithiocarbamate, rhodamine B and magneson II were studied for their suitability for the concentration of metal traces in the adsorption layer of these reagents on a mercury surface. Only TBP and TPP were suitable. Tests were made with MoO_4^{2-}, ZrO^{2+}, UO_2^{2+}, VO_3^-, WO_4^{2-}, Pb^{2+} and Tl^+; only uranyl and tungstate ions could be accumulated in the presence of TBP and TPP.

RÉSUMÉ

Tributylphosphate (TBP), tripropylphosphate (TPP), jaune titane, acide phénylarsonique, acide *o*- et *p*-aminophénylarsonique, l'hydroxy-8-quinoléine, l'acide oxinesulfonique-5, la thioxine, le tétraéthylammoniumdithiocarbamate, la rhodamine B et le magnéson II ont été examinés en vue de leur utilisation pour des enrichissements de métaux traceurs dans leur couche d'adsorption, à la surface du mercure. Seuls TBP et TPP conviennent. Les essais ont été effectués avec molybdate, zirconyle, uranyle, vanadate, tungstate, plomb et thallium(I). Seuls uranyle et tungstate ont donné des résultats positifs avec TBP et TPP.

LITERATUR

1 H. JEHRING, E. HORN, A. REKLAT UND W. STOLLE, *Collection Czech. Chem. Commun.*, 33 (1968) 1038.
2 H. JEHRING UND W. STOLLE, *Collection Czech. Chem. Commun.*, 33 (1968) 1670.
3 J. MATYSIK, *Chem. Zvesti*, 18 (1964) 407.
4 R. KALVODA, *J. Electroanal. Chem.*, 8 (1964) 378.
5 H. SOHR UND L. LIEBETRAU, *Z. Anal. Chem.*, 219 (1966) 409.
6 H. BERGE UND P. JEROSCHEWSKI, *Z. Anal. Chem.*, 230 (1967) 259.
7 H. RINGSTORFF, *Dissertation*, Universität Rostock, 1969.
8 H. SOHR UND K. H. LOHS, *J. Electroanal. Chem.*, 14 (1967) 227.
9 H. SOHR, *Chem. Zvesti*, 16 (1962) 316; *J. Electroanal. Chem.*, 11 (1966) 188.
10 H. SOHR UND K. H. LOHS, *J. Electroanal. Chem.*, 13 (1967) 107, 114.
11 H. SOHR, K. H. LOHS UND B. MOTHES, *Monatsber. Deut. Akad. Wiss. Berlin*, 8 (1966) 668.
12 P. NANGNIOT, *Anal. Chim. Acta*, 31 (1964) 313.
13 H. JEHRING, *Abhandl. Deut. Akad. Wiss. Berlin, Kl. Chem. Geol. Biol.*, 1 (1964) 472; *Chem. Zvesti*, 18 (1964) 313.
14 S. L. GUPTA UND S. K. SHARANA, *J. Indian Chem. Soc.*, 41 (1964) 384.
15 H. SOHR, *Dissertation*, TH Leuna-Merseburg, 1964.

Analytica Chimica Acta
Elsevier Publishing Company, Amsterdam
Printed in The Netherlands

STROMLOSE ANREICHERUNGSMÖGLICHKEITEN VON SPURENMETALLEN AN DER GRENZFLÄCHE QUECKSILBER/ELEKTROLYT

TEIL II. ADSORPTIVE ANREICHERUNGSVERSUCHE AN DER HÄNGENDEN QUECKSILBERTROPFENELEKTRODE OHNE VERWENDUNG OBERFLÄCHENAKTIVER KOMPLEXBILDNER. SPURENBESTIMMUNG VON URAN UND WOLFRAM

H. BERGE UND H. RINGSTORFF
Sektion Chemie, Universität Rostock, Rostock (D.D.R.)
(Eingegangen den 3. Januar 1971)

Im I. Teil[1] wurde darauf hingewiesen, dass eine Anreicherung von Uran und Wolfram an der "HMDE" möglich ist, ohne organische Komplexbildner zu verwenden, die eine Adsorptionsschicht an der Quecksilberoberfläche bilden. Eine Anreicherung des Urans und Wolframs erfolgte nicht in der Adsorptionsschicht von Tributylphosphat bzw. Tripropylphosphat, sondern auch trotz der Bedeckung der Quecksilberoberfläche mit diesen Substanzen. Daraufhin wurden weitere Ionen auf adsorptive Anreicherungsmöglichkeiten ohne Komplexbildner untersucht.

EXPERIMENTELLER TEIL

Für alle Messungen wurde die in der I. Mitteilung ausführlich beschriebene Apparatur verwendet. Als Leitelektrolyt fand bei den Anreicherungstests zunächst das ungepufferte System $NaOH/HClO_4$ Verwendung, um Komplexbildungsreaktionen des Grundelektrolyten mit den anzureichernden Ionen zu vermeiden. Die Polarisationsgeschwindigkeit betrug 800 mV min^{-1}. Alle angegebenen Potentiale beziehen sich auf die gesättigte Kalomelelektrode.

ERGEBNISSE UND DISKUSSION

Bei 3 verschiedenen pH Werten im Bereich von pH 2.7 bis pH 11 wurden Cd^{2+}, Zn^{2+}, Co^{2+}, Ni^{2+}, Mn^{2+}, Fe^{2+}, Fe^{3+}, Pb^{2+}, Tl^{+}, As^{3+}, Sb^{3+}, Cu^{2+}, CrO_4^{2-}, $Cr_2O_7^{2-}$, VO_3^{-} MoO_4^{2-}, ZrO^{2+} und UO_2^{2+} auf analytisch nutzbare Anreicherungseffekte an der "HMDE" untersucht. In den meisten Fallen konnte jedoch nur in sauren Lösungen gearbeitet werden, um eine Ausfällung der eingesetzten Ionen als Hydroxide zu vermeiden. Angereichert wurde wie bei den Anreicherungsversuchen mit oberflächenaktiven Komplexbildnern (vgl. Teil I)[1]. Konzentrationsproportionale und von der Anreicherungszeit abhängige Peaks wurden nur bei UO_2^{2+} und WO_4^{2-} erhalten. Das Spitzenpotential der Uranpeaks lag bei -0.66 V (0.1 *M* $NaClO_4$). Die Peakhöhe veränderte sich nicht, wenn der Stromkreis nach der Voranreicherung im Bereich von ± 0 V bis -0.3 V geschlossen wurde.

Der Wolframpeak hatte ein Spitzenpotential von -0.76 V in einer sauren 0.1 *M* $NaClO_4$-Lösung, pH 2.7.

Potentialabhängigkeit der Anreicherung

Wenn die Anreicherung durch Adsorption erfolgt, ist es zweckmässig bei geschlossenem Stromkreis zu konzentrieren, da Adsorptionsvorgänge stark potentialabhängig sind. Reichert man bei geöffnetem Stromkreis an, werden bei veränderter Lösungszusammensetzung sicher unterschiedliche Potentiale an der Elektrode zu erwarten sein. Die Potentialeinstellung kann ausserdem langsam erfolgen und zu schlecht reproduzierbaren Ergebnissen führen. In Abb. 1 ist der Spitzenstrom als Funktion des Anreicherungspotentials aufgetragen.

Sowohl beim Wolfram als auch beim Uran wächst die Peakhöhe zunächst linear wenn das Anreicherungspotential positiver wird. Ab +0.1 V beim Uran und +0.2 V beim Wolfram erreicht man dann keine wesentliche Empfindlichkeitssteigerung mehr und der Grundstrom wird schlechter.

Einfluss des pH-Wertes der Lösungen auf die Spitzenpotentiale und die Spitzenströme

Der pH-Wert der Probelösungen beeinflusst wie das Anreicherungspotential die Peakhöhe wesentlich. Uran lässt sich in Lösungen von pH 2.5 bis pH 7.3 anreichern.

In Britton–Robinson-Puffer beobachtet man ausgehend von pH 7.3 bis pH 3.8–4.0 ein fast lineares Ansteigen der Spitzenströme. Dann erfolgt ein rascher Abfall der Peakhöhe und ab pH 2.4 verschwindet der Peak völlig.

Sehr problematisch ist es, die pH-Abhängigkeit der Spitzenströme beim Wolfram zu messen. Im interessierenden pH Bereich steht kein brauchbarer Puffer zur Verfügung. Britton–Robinson-Puffer und McIlvain-Puffer lassen sich nicht verwenden, weil es zur Reaktion des Wolframats mit der Phosphorsäure des Puffers kommt.

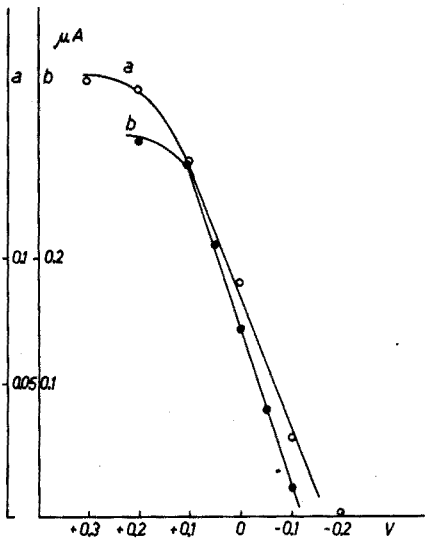

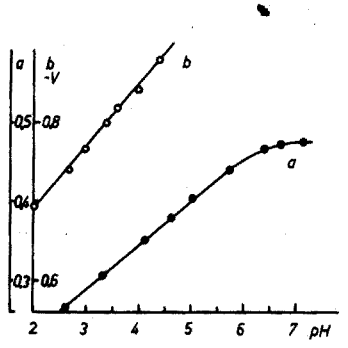

Abb. 1. Spitzenstrom als Funktion des Anreicherungspotentials. Anreicherungszeit 90 sec (a) $1 \cdot 10^{-6}$ *M* WO_4^{2} in Acetatpuffer pH 3.6; (b) $1 \cdot 10^{-6}$ *M* UO_2^{2} in Britton–Robinson-Puffer pH 5.02.

Abb. 2. Abhängigkeit der Spitzenpotentiale vom pH-Wert. (a) Uranpeak $1 \cdot 10^{-6}$ *M* UO_2^{2+}; (b) Wolframpeak $1 \cdot 10^{-6}$ *M* WO_4^{2-}. Anreicherungszeit jeweils 90 sec bei +0.1 V bzw. +0.2 V.

Es wurde deshalb in Perchloratlösungen gearbeitet und der pH-Wert mit $HClO_4$ eingestellt. Bei pH-Werten < pH 2 ist der Peak nicht mehr zu erkennen und es erfolgt ein fliessender Übergang in die Wasserstoffwelle. Zwischen pH 2 und pH 3 nimmt die Peakhöhe zu und fällt dann bis pH 4.4 wieder ab. In schwächer sauren Lösungen verschwindet der Peak. Wahrscheinlich wird auch dann noch eine Anreicherung stattfinden, aber eine Reduktion der Wolframate ist nur in stärker sauren Lösungen möglich.

Durch Änderungen des pH-Wertes der Grundlösungen werden auch die Spitzenpotentiale der Uran- und Wolframpeaks verschoben (Abb. 2). Die Spitzenpotentiale der sehr scharfen Uranpeaks sind sehr gut reproduzierbar. Bei den Wolframpeaks war die Reproduzierbarkeit der Spitzenpotentiale schlechter. Einzelmessungen differierten teilweise um 10 mV.

Uranbestimmung

Die Untersuchung der pH- und Potentialabhängigkeit der Anreicherung zeigten, dass beide Grössen massgeblichen Einfluss auf die Spitzenströme haben. Es wurde deshalb in gepufferter Lösung bei geschlossenem Stromkreis konzentriert. Als günstig erwies sich ein Anreicherungspotential von +0.1 V und die Verwendung von Britton–Robinson-Puffer als Grundelektrolyt. In Acetatpuffer gleichen pH-Wertes war die Empfindlichkeit 20fach verringert.

Abb. 3 zeigt die Abhängigkeit der Peakhöhe von der Konzentration bei pH 4.2 und pH 5.02. Bis zu Urankonzentrationen von $1 \cdot 10^{-6}$ *M* ist der Spitzenstrom praktisch linear von der Konzentration abhängig und strebt dann bei höheren Konzentrationen einen Grenzwert an. Der relative Fehler, ermittelt aus 15 Einzelmessungen, beträgt 1% bei $1 \cdot 10^{-7}$ *M* UO_2^{2+}, wenn die gleiche Messlösung verwendet wird. Wurden jeweils neue Lösungen angesetzt, vergrösserte sich der relative Fehler auf 5.5%.

Gute Linearität besteht zwischen Peakhöhe und Anreicherungszeit bis zu 3 Minuten. Auch bei sehr kleinen Urankonzentrationen wird dann ein Grenzwert angestrebt. Der Spitzenstrom lässt sich also nicht analog zur inversen Voltammetrie durch sehr lange Anreicherungszeiten vergrössern. Offensichtlich kommt es zur Ausbildung eines Adsorptionsgleichgewichts, dessen Lage von der Depolarisatorkonzentration abhängig ist, wenn nicht eine vollständige Bedeckung der Oberfläche erfolgt.

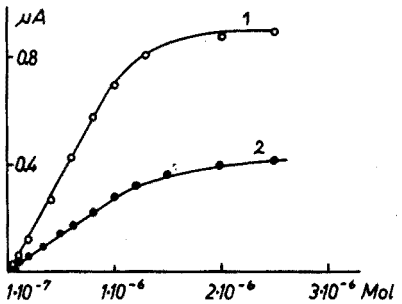

Abb. 3. Abhängigkeit des Spitzenstromes von der Urankonzentration. Anreicherungszeit 90 sec bei +0.1 V. (1) pH 5.02; (2) pH 4.2.

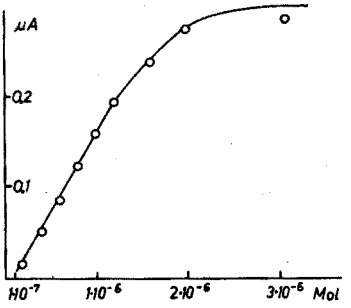

Abb. 4. Abhängigkeit des Spitzenstromes von der Wolframatkonzentration. Anreicherungszeit 90 sec bei +0.2 V. Acetatpuffer pH 3.6.

Wolframbestimmung

Wolfram wurde bei +0.2 V und in Acetatpuffer pH 3.6 angereichert. Acetatpuffer kann nicht mehr beim optimalen pH 3 eingesetzt werden und man muss einen Empfindlichkeitsverlust hinnehmen. Die Reproduzierbarkeit der Ergebnisse verbessert sich aber in gepufferter Lösung. Die Empfindlichkeit der Bestimmung ist nicht ganz so gross wie die Empfindlichkeit der Uranbestimmung. Die Peakhöhe ist von $1 \cdot 10^{-7}$ *M* bis fast $2 \cdot 10^{-6}$ *M* WO_4^{2-} der Konzentration direkt proportional (Abb. 4). Der relative Fehler, ermittelt aus 15 Einzelbestimmungen betrug bei $1 \cdot 10^{-6}$ *M* WO_4^{2-} 1.6%. Er vergrösserte sich auf 6.7%, wenn zur Berechnung Messergebnisse dienten, die im Laufe eines ganzen Jahres erhalten wurden. Bei Anreicherungszeiten bis zu 3 Minuten besteht strenge Linearität der Peakhöhe mit der Dauer der Voranreicherungszeit. Wie bei der Uranbestimmung strebt der Spitzenstrom bei längeren Anreicherungszeiten einem Grenzwert zu.

Bestimmung von Wolfram und Uran nebeneinander und in Gegenwart anderer Schwermetallionen

Eine gemeinsame Bestimmung von Uran und Wolfram in einer Grundlösung ist nur schlecht möglich. In Acetatpuffer, der sich gut für die Wolframbestimmung eignet, ist die Empfindlichkeit für die Uranbestimmung zu gering. Abb. 5 zeigt die Aufnahme einer Lösung, die gleichzeitig UO_2^{2+} und WO_4^{2-} enthält, in Acetatpuffer. Obwohl Uran, das sich unter geeigneten Bedingungen empfindlicher als WO_4^{2-} bestimmen lässt, im Überschuss zugegen ist, ist der Wolframpeak wesentlich höher. Er wird durch die Uranylionen nicht beeinflusst. In Britton–Robinson-Puffer, dem für die Uranbestimmung geeigneten Grundelektrolyten, wird bei gleichzeitiger Anwesenheit von UO_2^{2+} und WO_4^{2-} in der Probelösung nur der Uranpeak erhalten. Er wird auch bei 10-fachem Wolframüberschuss nicht gestört.

Kupfer, Blei, Vanadium und Molybdän sind bei der normalpolarographischen Bestimmung des Urans die wichtigsten Störelemente. Unter den hier gegebenen Bedingungen werden die Ionen aller 4 Elemente nicht angereichert und man sollte daher keine Beeinflussung des Uranpeaks erwarten. Das trifft bei Anwesenheit von Cu^{2+}, Pb^{2+} und VO_3^- auch tatsächlich zu, wenn die Konzentrationen der Ionen

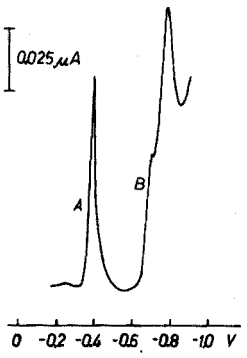

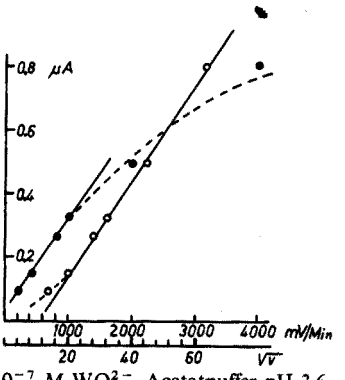

Abb. 5. Bestimmung von Wolfram und Uran in einer Lösung. $7.5 \cdot 10^{-7}$ *M* WO_4^{2-}, Acetatpuffer pH 3.6, $3 \cdot 10^{-6}$ *M* UO_2^{2+}. Angereichert 90 sec bei +0.2 V. (A) Uranpeak; (B) Wolframpeak.

Abb. 6. Abhängigkeit des Spitzenstromes von der Polarisationsgeschwindigkeit. $4 \cdot 10^{-7}$ *M* UO_2^{2+}, Britton–Robinson-Puffer pH 4.2. Anreicherungszeit 90 sec bei +0.1 V. (●) Aufgetragen gegen v; (○) gegen $v^{\frac{1}{2}}$.

nicht so hoch sind, dass auch ohne Anreicherung ein Peak erscheint. MoO_4^{2-} stört dagegen sehr. Schon bei $1 \cdot 10^{-6}$ *M* MoO_4^{2-} wird der Uranpeak wesentlich verkleinert. Die starke Beeinflussung des Spitzenstroms könnte eventuell auf die Bildung des schwerlöslichen Uranylmolybdats zurückzuführen sein.

Molybdat deformiert und erniedrigt auch den Wolframpeak. Von grösserem praktischen Interesse ist aber vor allem die Bestimmung des Wolframs in Gegenwart von Eisen. Fe^{3+} stört selbst bei 50-fachem Überschuss nicht.

Abhängigkeit der Spitzenströme von der Tropfenoberfläche und der Polarisationsgeschwindigkeit. Potential- und Kapazitätszeitkurven. Einfluss von Tensiden und Elektrolyten auf die Spitzenströme

Wie in der inversen Voltammetrie wächst der Spitzenstrom direkt proportional mit der Tropfenoberfläche. Die Quecksilberoberfläche wurde bei den Messungen in 5 Stufen zwischen $0.978 \cdot 10^{-2}$ und $2.847 \cdot 10^{-2}$ cm² variiert.

Die Abhängigkeit des Spitzenstroms von der Polarisationsgeschwindigkeit (v) ist in Abb. 6 dargestellt. Bei hohen Polarisationsgeschwindigkeiten besteht gute Linearität zwischen $v^{\frac{1}{2}}$ und dem Spitzenstrom, während bei langsamen Potentialänderungen ein fast lineares Wachstum mit v festzustellen ist. In der inversen Voltammetrie gilt für reversible diffusionsbedingte Reaktionen die Gleichung von Randles und Sevcik, die ein Wachstum der Spitzenströme mit $v^{\frac{1}{2}}$ fordert. Das fast lineare Wachstum der Peakhöhen mit v unter den hier vorliegenden Bedingungen bei langsamen Polarisationsgeschwindigkeiten deutet auf eine reine Oberflächenreaktion hin.

Eine Anreicherung des Urans und Wolframs durch spezifische Adsorption an der Grenzfläche Hg/Elektrolyt müsste Potentialänderungen an der Elektrode und Kapazitätsänderungen der Doppelschicht bewirken. Zum anderen müssten alle Faktoren, die in irgendeiner Weise den Aufbau der Doppelschicht wesentlich beeinflussen, Auswirkungen auf die Anreicherung haben. Potentialänderungen an der Elektrodenoberfläche waren nach Zusatz von Spuren UO_2^{2+} und WO_4^{2-} zum Leitelektrolyten auch nach Stunden nicht eindeutig zu messen. Die sich einstellenden Potentialendwerte differierten bis zu 11 mV. Grösser waren auch die beobachteten Potentialunterschiede zwischen reiner Grundlösung und Grundlösung mit Spurenmetall nicht.

Kapazitäts-Zeitkurven, die bei konstanten Potentialen von +0.1 V in Gegenwart von $1 \cdot 10^{-6}$ *M* UO_2^{2+} bzw. WO_4^{2-} aufgenommen wurden, zeigten keine Kapazitätsänderungen. Verändert man das Elektrodenpotential auf −0.2 bis −0.4 V, gibt es zunächst einen Kapazitätsabfall, bis nach etwa 60 sec ein konstanter Wert erreicht ist. Im Kapazitäts–Zeitdiagramm erhält man dann wieder eine parallel zur Zeitachse verlaufende Gerade. Die anfängliche Kapazitätserniedrigung bei Elektrodenpotentialen, die in der Nähe des elektrokapillaren Nullpunktes liegen, könnte durch Spurenverunreinigung des Leitelektrolyten mit adsorbierbaren Stoffen verursacht werden. Ähnliche Kapazitätserniedrigungen beim Lippmannpotential konnten auch Jehring und Stolle[2] trotz sorgfältiger Reinigungsarbeiten bei der Herstellung der Leitelektrolyten beobachten.

Die eingesetzten Tenside und die Veränderung der Elektrolytkonzentration zeigten den erwarteten Einfluss auf die Spitzenströme. Polyäthylenglykol und Triphenylbenzylphosphoniumchlorid verringerten die Spitzenströme um 20–60%. Die Tensidkonzentration war jeweils gerade so hoch, um an der Tropfenoberfläche

den Bedeckungsgrad $\theta = 1$ zu gewährleisten. Gelatine (wofatiert) unterdrückte noch stärker (Abb. 7), obwohl die eingesetzten Konzentrationen bei weitem nicht ausreichten, um eine maximale Kapazitätserniedrigung, d.h. die Sättigungserniedrigung ΔC_s zu erreichen.

Eine Erhöhung der Elektrolytkonzentration wirkt ähnlich wie der Zusatz von Tensiden und verringert die Spitzenströme (Abb. 8).

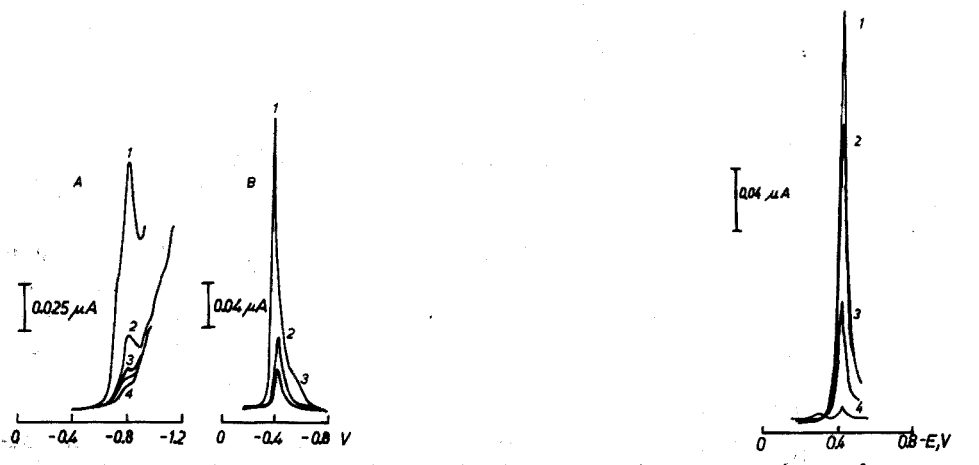

Abb. 7. Einfluss von Gelatine auf den Wolfram- und Uranpeak. *A. Wolframpeak.* $1 \cdot 10^{-6}$ *M* WO_4^{2-}, Acetatpuffer pH 3.6, angereichert 90 sec bei +0.2 V. (1) Ohne Gelatine; (2) mit 0.0008% Gelatine; (3) mit 0.0032% Gelatine; (4) mit 0.0080% Gelatine; (5) mit 0.0200% Gelatine. *B. Uranpeak.* $1 \cdot 10^{-6}$ *M* UO_2^{2+}, Britton–Robinson-Puffer pH 5.02, Anreicherungszeit 90 sec bei +0.1 V. (1) Ohne Gelatine; (2) mit 0.0008% Gelatine; (3) mit 0.0032% Gelatine.

Abb. 8. Einfluss der Leitsalzkonzentration auf den Uranpeak. $1 \cdot 10^{-6}$ *M* UO_2^{2+}, Britton–Robinson-Puffer, pH 5.02, Anreicherungszeit 90 sec bei +0.1 V. (1) Ohne $NaClO_4$; (2) mit 0.2 *M* $NaClO_4$; (3) mit 0.5 *M* $NaClO_4$; (4) mit 2.0 *M* $NaClO_4$.

Alle bisher vorliegenden Ergebnisse deuten darauf hin, dass eine Anreicherung durch spezifische Adsorption unmittelbar an der Quecksilberoberfläche nicht erfolgt. Der gesamte Potentialabfall von der Elektrodenoberfläche zum Innern der Lösung setzt sich aus dem Potentialabfall im helmholtzschen und im diffusen Teil der Doppelschicht zusammen. Für den Verlauf vieler chemischer Reaktionen spielt der Potentialabfall im diffusen Teil der Doppelschicht (ψ Potential) eine wichtige Rolle. Läge eine Adsorption im helmholtzschen Teil der Doppelschicht vor, müssten Potential- und Kapazitäts–Zeitkurven deutliche Potential- bzw. Kapazitätsänderungen infolge Adsorption erkennen lassen. Findet eine Anreicherung im diffusen Teil der Doppelschicht statt, lassen sich die nahezu konstanten Potentiale und auch die praktisch nicht veränderliche Doppelschichtkapazität eher erklären, denn der Einfluss der diffusen Doppelschicht auf die Gesamtkapazität ist sehr klein[3], besonders für Potentiale nicht zu nahe dem Lippmannpotential. Dass das ψ Potential und damit die diffuse Doppelschicht eine wesentliche Rolle bei den Anreicherungsvorgängen spielt, zeigt der bemerkenswert starke Einfluss der Leitelektrolytkonzentration auf die Spitzenströme. Erhöht man die Elektrolytkonzentration, nimmt die Ausdehnung der diffusen Doppelschicht stark ab und das ψ Potential wird sehr klein. Damit verkleinert

sich auch der Inhomogenitätsbereich an der Phasengrenze und elektrostatische Effekte können über die engste Grenzschicht hinaus kaum wirksam werden. Eine adsorptive Anreicherung im diffusen Teil der Doppelschicht durch elektrostatische oder chemische Wechselwirkungskräfte erklärt die bisherigen Ergebnisse am besten.

Der beim Zusatz von Tensiden festzustellende Abfall der Spitzenströme könnte verschiedene Ursachen haben:

1. eine Behinderung der Anreicherung durch die Anwesenheit der Tensidmoleküle in der Doppelschicht;
2. eine Behinderung der Durchtrittsreaktion durch die Tenside;
3. ein Zusammenwirken der unter 1. und 2. genannten Faktoren.

Wahrscheinlich wird die Behinderung der Durchtrittsreaktion bestimmend sein. Wäre die Anreicherung behindert, müssten auch die stark oberflächenaktiven Phosphorsäureester als Inhibitoren wirken (vgl. Teil I), was aber nicht zu beobachten war. Ohne Zweifel sind diese Tenside während des Anreicherungsvorganges an der Quecksilberoberfläche adsorbiert, nur wird wohl durch die Komplexbildungstendenz von Tributylphosphat und Tripropylphosphat[4] die Durchtrittsreaktion nicht entscheidend beeinflusst. Eine Anreicherung von UO_2^{2+} und ZrO^{2+} in der Adsorptionsschicht von Phosphorsäureestern, wie sie von Sohr und Liebetrau[5] beschrieben wird, dürfte allerdings nicht stattfinden. Die vor Sohr und Liebetrau erhaltenen Uranpeaks stimmen in Form und Potentiallage gut mit den Peaks überein, die von uns in ungepufferten Lösungen nach Anreichern an der HMDE bei geöffnetem Stromkreis erhalten wurden. Eine Anreicherung von ZrO^{2+} war mit und ohne phosphororganische Verbindung nicht zu bestätigen. Bei dem von den Autoren beschriebenen Zirkonpeak dürfte es sich um den reinen Desorptionspeak der zur Anreicherung verwendeten oberflächenaktiven Verbindung, Diisopropylmethylphosphonat handeln, denn das angegebene Spitzenpotential des Zirkonpeaks stimmt recht gut mit dem tensammetrisch ermittelten Desorptionspotential der Verbindung überein.

Eine völlige theoretische Erklärung der stromlosen Anreicherung von Uran und Wolfram ist noch offen und muss weiteren Untersuchungen vorbehalten bleiben.

ZUSAMMENFASSUNG

Uran- und Wolframspuren lassen sich stromlos an der stationären Quecksilberelektrode anreichen. Die Bestimmung von Uran und Wolfram nebeneinander und in Gegenwart anderer Schwermetallionen sowie der Einfluss des pH-Wertes, des Anreicherungspotentials, der Polarisationsgeschwindigkeit und der Einfluss von Tensiden und Elektrolyten auf die Spitzenströme werden untersucht.

SUMMARY

Traces of uranium and tungsten can be concentrated at a stationary mercury electrode at zero current. The determination of these metals in presence of each other, and in presence of other heavy metals is discussed. The effects of pH, concentration potential, speed of polarization and concentration of electrolytes and surfactants on peak currents are described.

RÉSUMÉ

Des traces d'uranium et de tungstène peuvent être enrichies à l'électrode de mercure stationnaire, à courant nul. On examine le dosage de ces metaux en présence les uns des autres, et en présence de métaux lourds. On décrit également l'influence du pH, du potentiel, de la vitesse de polarisation, de la concentration des électrolytes et des surfactants sur les pics de courant.

LITERATUR

1 H. BERGE UND H. RINGSTORFF, *Anal. Chim. Acta*, 55 (1971) 193.
2 H. JEHRING UND W. STOLLE, *Collection Czech. Chem. Commun.*, 33 (1968) 1038.
3 D. C. GRAHAME, *J. Amer. Chem. Soc.*, 76 (1954) 4819.
4 H. SOHR UND K. H. LOHS, *J. Electroanal. Chem.*, 14 (1967) 227.
5 H. SOHR UND L. LIEBETRAU, *Z. Anal. Chem.*, 219 (5) (1966) 409.

Analytica Chimica Acta
Elsevier Publishing Company, Amsterdam
Printed in The Netherlands

LE CUIVRE EN SOLUTION DANS L'EAU DE MER: FORME CHIMIQUE ET DOSAGE

ÉTUDE PAR POLAROGRAPHIE À TENSION SINUSOÏDALE SURIMPOSÉE

M. ODIER* ET V. PLICHON
Laboratoire de Chimie Analytique Générale associé au C.N.R.S., E.S.P.C.I., 10 rue Vauquelin, Paris (France)
(Reçu le 7 décembre 1970)

Parmi les micro-constituants du milieu marin, le cuivre est particulièrement important par son écologie[2]. Sillen et Sears[3] ont étudié théoriquement l'équilibre des espèces au sein de l'eau de mer: pour les cations de degré d'oxydation supérieur ou égal à 2, il peut y avoir compétition entre les complexes minéraux chlorure et hydroxyle. Ceci résulte de l'étude des constantes de formation des complexes en milieu chlorure et à pH 8. Nous avons trouvé une seule étude expérimentale électrochimique, portant sur le zinc et le cadmium[4].

Le cuivre en solution dans l'eau de mer est[5] au degré d'oxydation +2. Pour ce micro-constituant, il existe une autre possibilité de formation de complexe que par les ions chlorure et hydroxyle: en effet, le système "acide carbonique–bicarbonate–carbonate" constitue le principal tampon en pH de l'eau de mer (pH moyen: 8.2). La formation d'un complexe bicarbonate du cuivre peut donc être envisagée, car à pH 8, les ions bicarbonate prédominent à 98%[6]. Faucherre et Bonnaire[7] ont établi la formule et calculé la constante du complexe $[Cu(CO_3)_2^{2-}]$, produit de redissolution partielle du précipité $CuCO_3$ en présence d'un excès de carbonates alcalins. Meites[8] signale l'existence d'un précipité $K_2Cu(HCO_3)_4$ en milieu bicarbonate. Ce complexe est soluble dans un excès de bicarbonate sous la forme de $[Cu(HCO_3)_5]^{3-}$.

Ces résultats ne permettent pas de conclure à l'existence d'un complexe carbonate du cuivre dans les conditions de l'eau de mer. D'après une mise au point bibliographique récente[9], on ne possède pas d'autres données théoriques ou expérimentales.

Les autres complexes possibles, en particulier avec les ions fluorure et phosphate, ne sont pas envisagés ici. En effet, leur constante de formation est très petite, et la concentration de ces ions dans l'eau de mer est trop faible.

Pour la présente étude, la polarographie à tension sinusoïdale surimposée présente deux avantages principaux: d'une part, elle permet une étude expérimentale non destructive des solutions; d'autre part, par l'augmentation de la sensibilité d'un facteur 10 à 100 par rapport à la polarographie classique[10], elle permet de détecter des concentrations en cuivre aussi faibles que $5 \cdot 10^{-8}$ M, et ceci même en présence des macro-constituants de l'eau de mer.

---

* Ce mémoire recouvrira en partie la thèse de Doctorat de 3ème cycle de M. Odier[1].

PRINCIPE

La polarographie permet l'étude des complexes des cations métalliques, par mesure du déplacement des potentiels de demi-vague: la valeur du potentiel $E_{\frac{1}{2}}$, caractéristique d'un cation M^{n+}, est déplacée vers les potentiels négatifs en présence de l'agent complexant, et ceci d'autant plus que la concentration du complexant est plus élevée[11].

Dans le cas des systèmes électrochimiques réversibles, la différence des potentiels de demi-vague des ions libres ($E_{\frac{1}{2}}$) et des ions complexés ($E'_{\frac{1}{2}}$) a pour valeur, aux coefficients de diffusion près:

$$\Delta E_{\frac{1}{2}} = E_{\frac{1}{2}} - E'_{\frac{1}{2}} = (0.059/n)\,(\log \beta + m \log [X]) \qquad (1)$$

où n est le nombre d'électrons échangés, β la constante de formation du complexe, [X] la concentration en agent complexant, et m le nombre de coordination, selon les relations:

$$M^{n+} + m\,X^{p-} \rightarrow MX_m^{(mp-n)-} \qquad (2)$$

$$\beta = [MX_m]/[M^{n+}]\,[X^{p-}]^m \qquad (3)$$

Expérimentalement, la fonction $\Delta E_{\frac{1}{2}} = f(\log [X])$ se traduit graphiquement par une droite, dont la pente permet de déterminer la formule du complexe et dont l'ordonnée à l'origine permet de calculer la constante de formation β.

En polarographie à tension sinusoïdale surimposée[12], la courbe intensité–potentiel de réduction d'un cation est représentée par un pic. La valeur du potentiel au sommet de pic, E_p, est une valeur caractéristique du cation et du milieu, et est pratiquement identique à celle du potentiel de demi-vague $E_{\frac{1}{2}}$ de la polarographie classique: l'étude d'un complexe métallique est donc possible, par la même méthode, en mesurant le déplacement de E_p et en traçant les fonctions:

$$\Delta E_p = E_p - E'_p = f(\log [X]) \qquad (4)$$

et ceci en fonction des variations de concentration des divers agents complexants étudiés.

Nous ne rappelons pas ici le principe de la polarographie à tension sinusoïdale surimposée, que l'on peut trouver dans la bibliographie[10,12]. Nous indiquons simement ci-après les caractéristiques expérimentales que nous avons utilisées.

PARTIE EXPÉRIMENTALE

Les *solutions des divers agents complexants* ont été préparées avec les produits suivants: perchlorate de sodium (Merck, "P.A."); chlorure de sodium (Merck, Supra pur); bicarbonate de sodium (Prolabo "R.P.").

Le *tampon en pH*, dans les solutions contenant le bicarbonate, est assuré de la même façon que dans l'eau de mer naturelle, par maintien de la pression partielle de gaz carbonique au-dessus de la solution (CO_2 très pur à 99.99%, J.T. Baker Chemicals): après élimination de l'oxygène dissous par barbotage d'azote, on impose le pH convenable par adjonction de gaz carbonique à l'azote, dans des proportions déterminées.

Les valeurs des concentrations en bicarbonate données ci-dessous (*cf.* résultats

expérimentaux) sont calculées en fonction de la quantité totale en $NaHCO_3$ introduite en solution, du pH, et des constantes d'acidité apparentes K'_A de l'acide carbonique. Nous avons déterminé expérimentalement les valeurs de ces constantes dans chaque milieu envisagé: à force ionique nulle, les constantes réelles sont[13]:

$$K_1 = \frac{[CO_3^{2-}][H^+]}{[HCO_3^-]} = 10^{-10.2} \qquad K_2 = \frac{[HCO_3^-][H^+]}{[CO_{2\,diss}] + [H_2CO_3]} = 10^{-6.4}$$

Les constantes apparentes que nous avons déterminées ont pour valeurs:

Milieu	K'_1	K'_2
NaCl 0.5 *M*	$10^{-9.4}$	$10^{-6.0}$
$NaClO_4$ 0.5 *M*	$10^{-9.7}$	$10^{-5.9}$

Ces valeurs permettent de calculer la concentration en ions HCO_3^- libres, compte tenu de la relation:

$$[NaHCO_{3\,total}] = [CO_{2\,dissous}] + [H_2CO_3] + [HCO_3^-] + [CO_3^{2-}]$$

Toutes les mesures de potentiel sont faites par rapport à l'électrode au calomel saturé (E.C.S.), à $25.0 \pm 0.1°$.

Les courbes polarographiques sont réalisées avec l'ensemble polarographique Tacussel (Solea, Lyon), comprenant: un potentiostat PRT 30-01 à très faible bruit de fond; une unité d'adaptation UAP 2 délivrant le signal sinusoïdal et permettant la détection de phase; un enregistreur avec tiroir à haute sensibilité TEI. De plus, une cage de Faraday entoure la cellule et l'appareillage annexe; du phosphate disodique a été dissous dans l'eau de la jaquette thermostatique, pour blinder la cellule électriquement.

Les caractéristiques utilisées pour la plupart des solutions ont été les suivantes: tension sinusoïdale surimposée d'amplitude 10 mV, et de fréquence 27 Hz; angle de phase de détection d'environ $-3°$, réglé pour obtenir un courant de base minimum; diviseur de fréquence du marteau: 50 (d'où une fréquence de chute de gouttes de 0.54 Hz); déroulement des potentiels 15 ou 30 mV min^{-1}.

Un exemple des courbes obtenues est donné (Fig. 1).

RÉSULTATS

En milieu perchlorate de sodium, non complexant pour le cuivre, on détermine E_p, valeur de référence pour tous les résultats suivants dans la relation (4): $E_p = +25$ mV/E.C.S. dans $NaClO_4$ 0.5 *M*. La réduction est réversible avec échange de deux électrons.

En milieu chlorure de sodium, on n'observe qu'un seul pic de réduction: en effet, la réduction a lieu théoriquement de Cu^{2+} ou $CuCl^+$ à $CuCl_2^-$, puis de $CuCl_2^-$ à Cu^0, pour les milieux concentrés en chlorure, mais seul le pic correspondant à la deuxième étape de réduction — Cu(I) → Cu(0) — apparaît sur le polarogramme, le premier pic — Cu(II) → Cu(I) — étant masqué dans le mur d'oxydation du mercure[1].

La Fig. 2 donne les valeurs de E_p en milieu chlorure.En milieu chlorure dilué, ($[Cl^-] < 10^{-2}$ *M*), on n'observe aucune variation de E_p en fonction de la concentration en chlorure: dans ce cas, il n'y a pas de complexation du cuivre: le cuivre(II),

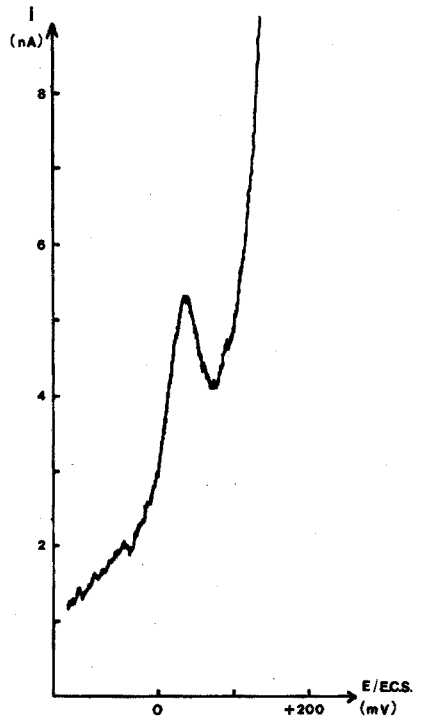

Fig. 1. Pic du cuivre en milieu chlorure. $[Cu] = 5 \cdot 10^{-7}\ M$; $[Cl^-] = 10^{-3}\ M$; $[NaClO_4] = 0.5\ M$.

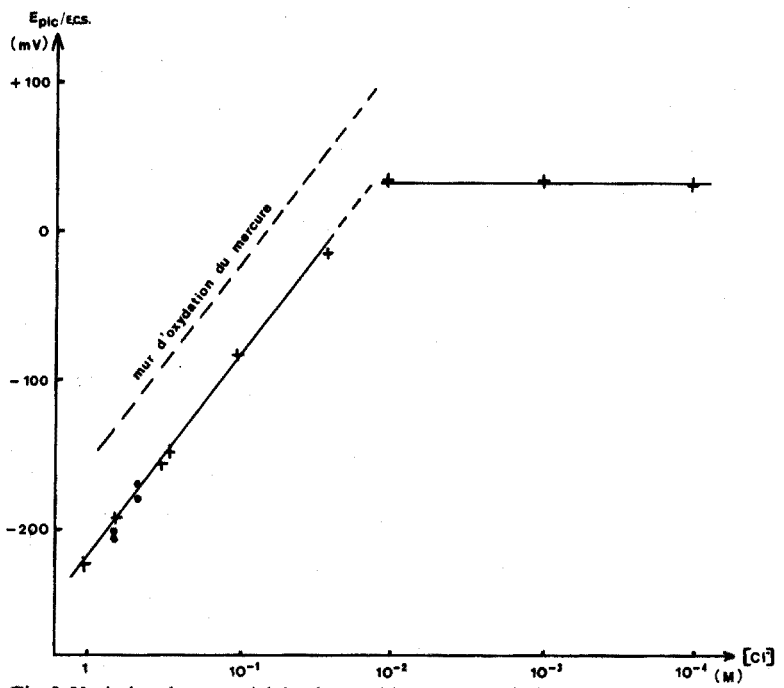

Fig. 2. Variation du potentiel de pic en milieu chlorure. (+) Milieu chlorure seul; (○) eau de mer naturelle.

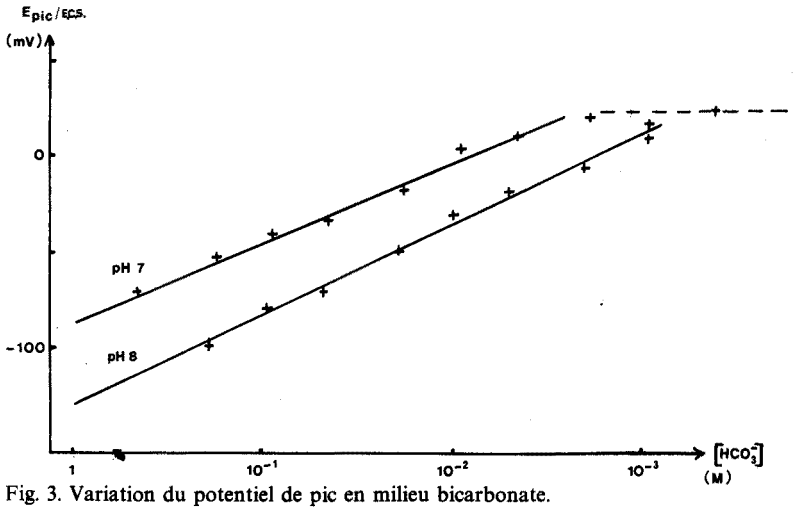

Fig. 3. Variation du potentiel de pic en milieu bicarbonate.

sous forme Cu^{2+}, est réduit directement en cuivre amalgamé. En milieu chlorure concentré (10^{-2} $M < [Cl^-] < 1$ M), la variation de E_p en fonction de la concentration en chlorure, correspond, en accord avec les données bibliographiques[13,14], à la réduction du complexe du cuivre(I): $CuCl_2^-$, dont la constante de formation est $\beta = 10^{+4.2}$.

En milieu bicarbonate de sodium, on observe un seul pic, qui correspond à la réduction du cuivre(II) en amalgame, en une seule étape réversible, avec échange de deux électrons. Le diagramme des variations de $E_p = f(\log[HCO_3^-])$ (Fig. 3) aux valeurs de pH 7 et 8, montre la complexation du cuivre par les ions bicarbonate et hydroxyle. Expérimentalement, la variation de concentration en ions HCO_3^- dépend de deux facteurs: d'une part, de la quantité totale de bicarbonate de sodium mise en solution; d'autre part, de la valeur du pH, qui influe sur la proportion d'ions HCO_3^- libres en solution. Dans l'intervalle de valeurs de pH de l'eau de mer (pH 7 à 8.5), nous avons vu que les ions bicarbonate prédominent à plus de 90%; nous étudions donc les variations de E_p en fonction de $\log[HCO_3^-]$, et nous écartons a priori la complexation par les ions carbonate.

Les valeurs des pentes des droites $E_p = f(pH)$ à $\log[HCO_3^-]$ constant et $E_p = f(\log[HCO_3^-])$ à pH 8 (Fig. 3) sont respectivement de 33 mV par unité de pH et de 48 mV par unité de $\log[HCO_3^-]$. Le complexe correspondant est de la forme:

$$[Cu(HCO_3)_m(OH)_p]^{(m+p-2)-}$$

et sa réduction aura lieu selon:

$$[Cu(HCO_3)_m(OH)_p] + 2e^- \rightleftharpoons Cu(Hg) + mHCO_3^- + pHO^-$$

Les calculs conduisent à $m \# 2$ et $p \# 1$, soit à la formule $[Cu(HCO_3)_2(OH)]^-$, que l'on peut aussi écrire $[Cu(HCO_3)(CO_3)]^-$. La polarographie ne permet pas de distinguer entre ces deux formules. Pour simplifier, nous n'écrirons que la première. La constante de formation, calculée à pH 8 et à $\log[HCO_3^-] = 0$, a pour valeur, à force ionique $I = 1$:

$$\beta = \frac{[Cu(HCO_3)_2(OH)^-]}{[Cu^{2+}][HCO_3^-]^2[OH^-]} = 10^{9.6}$$

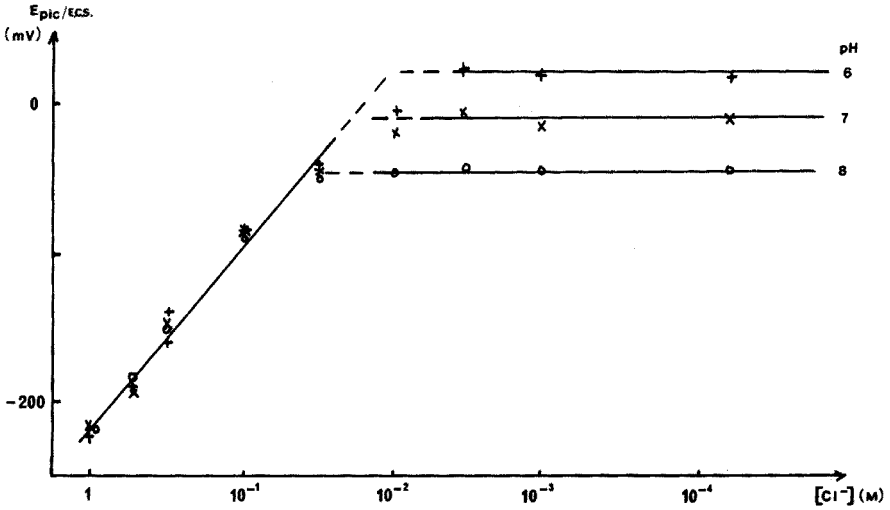

Fig. 4. Variation du potentiel de pic, en milieu chlorure, à concentration en bicarbonate constante (0.02 *M*).

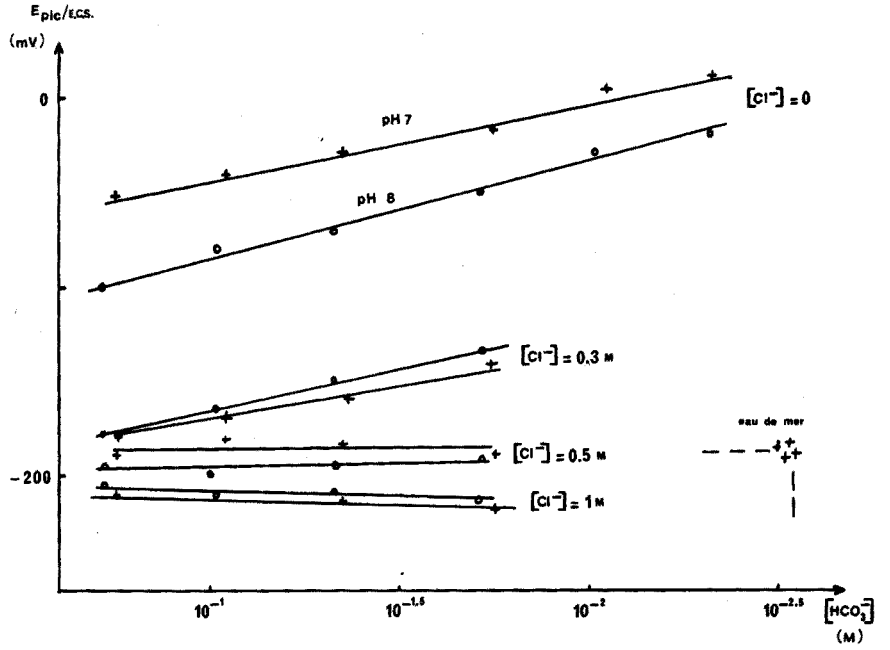

Fig. 5. Variation du potentiel de pic en fonction de la concentration en bicarbonate, à diverses valeurs de la concentration en chlorure.

Mélanges chlorure + bicarbonate, faisant fonction d'eau de mer artificielle

La Fig. 4 donne les variations de E_p en fonction de la concentration en chlorure, à diverses valeurs de pH et pour une quantité totale en espèces de l'acide carbonique égale à 0.02 mole par litre. La Fig. 5 donne les variations de E_p en fonction de la concentration en ions HCO_3^- à diverses valeurs de concentration en chlorure et respectivement à pH 7 et pH 8. Ces résultats expérimentaux ont les caractères suivants : on n'ob-

serve qu'un seul pic, comme dans les milieux précédents; dans les milieux concentrés en chlorure ($[Cl^-] > 0.5\ M$), la valeur du potentiel de pic est indépendante de la concentration en bicarbonate, à $[Cl^-]$ constante; par contre, la valeur de E_p varie avec la concentration en chlorure, et la fonction $E_p = f(\log [Cl^-])$ est une droite de pente 120 mV par unité de $\log [Cl^-]$; dans les milieux dilués en chlorure, il y a variation de E_p en fonction de $\log [HCO_3^-]$, avec des valeurs de pentes analogues à celles obtenues en milieu HCO_3^- seul (Fig. 2).

Eau de mer naturelle

Nous avons tracé les courbes de réduction du cuivre sur deux échantillons d'eau de mer provenant respectivement du large de Roscoff (Ile de Batz) et de la rade de Brest (Le Poulmic). Un exemple de courbe est donné (Fig. 6). Compte tenu des salinités de ces échantillons (respectivement $35.3^0/_{00}$ et inférieure à $27^0/_{00}$), les valeurs respectives des concentrations en chlorure sont 0.57 *M* et inférieure à 0.43 *M*. Les

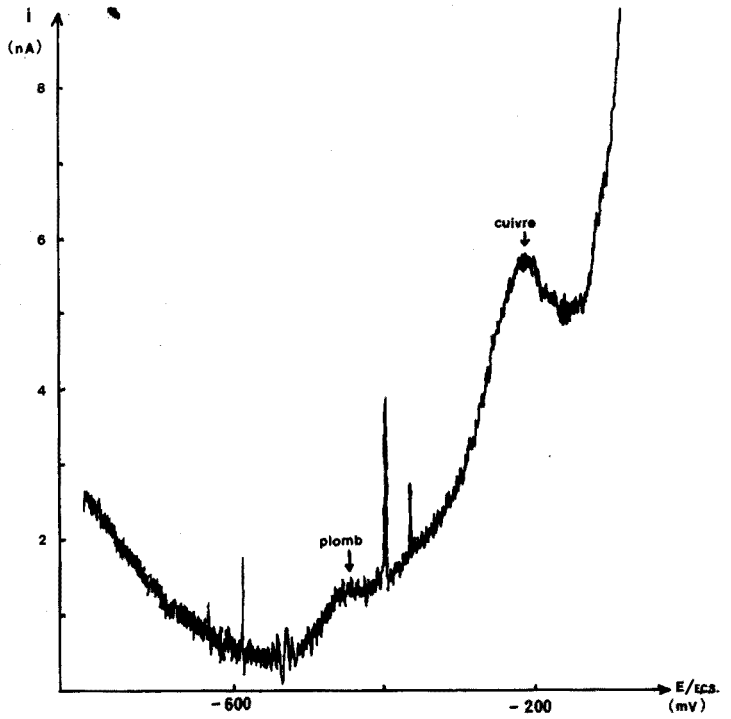

Fig. 6. Polarogramme d'une échantillon d'eau de mer naturelle de Roscoff. Cuivre ajouté $5 \cdot 10^{-7}$ *M*.

valeurs de E_p obtenues sont identiques aux valeurs obtenues en milieu $NaHCO_3 + NaCl$. Les lieux de prélèvement expliquent les teneurs élevées en cuivre.

DISCUSSION

Les deux questions qui se posent à partir de ces résultats expérimentaux sont les suivantes:

quelle est la nature de la réaction électrochimique à l'électrode?

quelle est la nature du complexe du cuivre en solution dans les milieux envisagés?

Dans les conditions de l'eau de mer, on observe un pic de réduction qui correspond, comme en milieu chlorure seul, à la réduction du complexe du cuivre(I) : $CuCl_2^-$. Mais ce n'est pas ce complexe qui existe en solution, car le cuivre est initialement au degré d'oxydation +2. D'autre part, compte tenu des constantes de formation du complexe chlorure et du complexe bicarbonate, le cuivre peut exister simultanément sous les trois formes Cu^{2+}, $CuCl^+$ et $[Cu(HCO_3)_2(OH)]^-$.

Nous proposons donc l'interprétation suivante: quelle que soit l'espèce qui prédomine, la réduction polarographique du cuivre(II) a lieu selon les deux étapes (1) et (2) suivantes, dont seule la seconde se traduit par un pic, la première étant masquée par le mur d'oxydation du mercure:

$$[Cu(HCO_3)_2(OH)]^- + 2Cl^- + e^- \rightleftharpoons CuCl_2^- + HCO_3^- + CO_3^{2-} + H_2O$$

(1) $$CuCl^+ + Cl^- + e^- \rightleftharpoons CuCl_2^-$$

$$Cu^{2+} + 2Cl^- + e^- \rightleftharpoons CuCl_2^-$$

(2) $$CuCl_2^- + e^- \rightleftharpoons Cu(Hg) + 2Cl^-$$

Les proportions relatives des trois espèces Cu^{2+}, $CuCl^+$ et $[Cu(HCO_3)_2(OH)]^-$ varient selon les concentrations en bicarbonate de l'eau de mer. Dans les conditions de l'eau de mer naturelle, à pH 8.0 et $[Cl^-] = 0.50\ M$, ces proportions sont comprises dans l'intervalle de valeurs suivantes:

Pour $[HCO_3^-] = 2.5 \cdot 10^{-3}\ M$: $Cu^{2+} = 60\%$
$CuCl^+ = 37\%$
$[Cu(HCO_3)_2(OH)]^- = 2\%$

Pour $[HCO_3^-] = 2.5 \cdot 10^{-2}\ M$: $[Cu(HCO_3)_2(OH)]^- = 60\%$
$Cu^{2+} = 24\%$
$CuCl^+ = 15\%$

Ce résultat est donné pour une concentration en cuivre $5 \cdot 10^{-7}\ M$ supérieure selon des études récentes[5,15] à celles des eaux de mer (1 à $5 \cdot 10^{-8}\ M$). L'application des lois d'action de masses indique que ces proportions ne sont pas modifiées si la concentration en cuivre est plus faible, sans toutefois éliminer la possibilité de formation d'autres espèces telles que complexes organique ou colloïdes.

Cette interprétation demande une confirmation, celle de l'existence de la première étape de réduction. C'est ce que nous examinons ci-dessous, par l'étude de la réduction du cuivre à une électrode de platine.

ÉTUDE COMPLÉMENTAIRE À UNE ÉLECTRODE DE PLATINE TOURNANTE

L'électrode de platine permet d'obtenir un domaine d'électroactivité plus grand que celui de l'électrode de mercure du côté des potentiels positifs. On peut alors observer les deux vagues de réduction du cuivre, quand elles existent. Nous avons tracé les courbes intensité–potentiel de réduction dans les mêmes milieux que précédemment, avec une concentration en cuivre égale à $10^{-4}\ M$. Un exemple des courbes est donné (Fig. 7). Les résultats expérimentaux sont groupés dans le Tableau I, qui

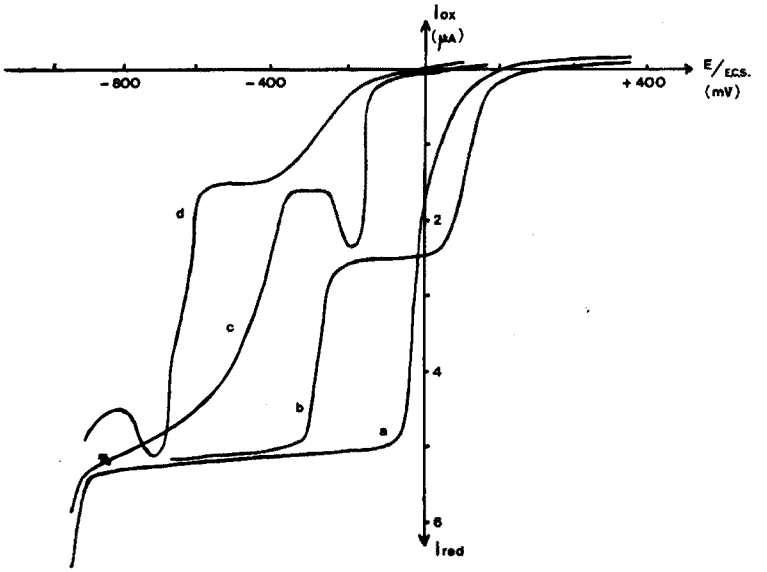

Fig. 7. Courbes de voltampérométric classique à une électrode tournante de platine poli. $[Cu] = 10^{-4}$ *M*. (a) En milieu perchlorate de sodium 0.5 *M*; (b) en milieu chlorure 0.5 *M*; (c) en milieu bicarbonate 0.5 *M*; (d) en milieu bicarbonate 0.5 *M* + chlorure 0.5 *M*.

TABLEAU I

RÉSULTATS EXPÉRIMENTAUX SUR ÉLECTRODE DE PLATINE TOURNANTE
(Concentration en cuivre 10^{-4} *M*; concentrations en bicarbonate: exprimées en quantités de sel totales mises en solution)

Courbe Fig. 7	*Milieu*	*pH*	*Nombre de vagues*	$E_{\frac{1}{2}}$/*E.C.S.* (*mV*)	*Observations*
a	$NaClO_4$ 0.5 *M*		1	−10	Bien définie
b	Cl^- 0.5 *M*	8	2	+155 −360	
		5	2	+135 −360	
c	HCO_3^- 0.5 *M*	8.5	2	−170 à partir de −350	Cuivrage de l'électrode dès la 1ère vague
d	Cl^- 0.5 *M* + HCO_3^- 10^{-3} *M*	6	2	+135 −370	
		7.7	1	−75	Présence d'un maximum et d'un précipité
	Cl^- 0.5 *M* + HCO_3^- 10^{-2} *M*	5.5	2	+135 −370	
		7.5	2	+10 −375	⟶ Avec maximum
	Cl^- 0.5 *M* + HCO_3^- 10^{-1} *M*	6.6 à 8.3	2	+10 −360	

donne les valeurs de potentiel de demi-vague en fonction des concentrations en chlorure et en bicarbonate dans chaque cas envisagé. ~

En milieu $NaClO_4$ 0.5 M, le cuivre(I) est dismuté. On n'observe qu'une seule vague, correspondant à la réduction directe de Cu^{2+} en Cu(0).

Dans les solutions contenant les ions chlorure, à pH inférieur à 6, on observe deux vagues. Le cuivre(I) apparait à l'électrode sous forme de précipité CuCl, à une valeur de potentiel de -100 mV/E.C.S. Aux valeurs de potentiel inférieures à -400 mV, l'électrode se recouvre d'un dépôt de cuivre métallique.

En milieu bicarbonate seul, on observe deux vagues. La première comporte un maximum et provient de la réduction de cuivre(II) en cuivre métallique: en effet, lorsque l'on impose le potentiel à une valeur du palier de la première vague, on observe un dépôt de cuivre sur l'électrode. La deuxième vague, mal définie, est due probablement à la réduction du cuivre(II) à l'électrode de platine recouverte de cuivre.

En milieu bicarbonate + chlorure, on observe encore deux vagues, mais elles ne correspondent pas aux précédentes. La première est déplacée vers les potentiels négatifs lorsque l'on fait croître la concentration totale en bicarbonate: ce déplacement confirme l'existence d'un complexe bicarbonate du cuivre. On ne peut en déterminer ni la formule, ni la constante par cette méthode, à cause de la lenteur des systèmes et de l'apparition d'un précipité. Néanmoins, ces résultats confirment qualitativement les résultats obtenus en polarographie à tension sinusoïdale surimposée.

DOSAGE DU CUIVRE DANS L'EAU DE MER

Le domaine des concentrations du cuivre dans l'eau de mer est compris, en moyenne, entre 1 et $5 \cdot 10^{-8}$ M[5,15]. On peut améliorer la limite de détection grâce au résultat expérimental suivant: la hauteur du pic du cuivre, en polarographie à tension sinusoïdale surimposée, est augmentée — de 80% à 300% selon les solutions — lorsque l'on acidifie les échantillons de pH 8 à pH 5, par barbotage de gaz carbonique pur. Cette augmentation de hauteur de pic a lieu aussi pour l'eau de mer, avec un facteur de multiplication de 1.5.

Nous avons utilisé les deux échantillons d'eau de mer précédents, de salinités respectives $35.3^0/_{00}$ et inférieure à $27^0/_{00}$. La teneur en cuivre d'un échantillon est mesurée par la méthode des étalons internes. Pour chacun des deux échantillons d'eau de mer précédents, une droite d'étalonnage des hauteurs de pic en fonction de la concentration est donnée (Fig. 8). Nous n'avons pas fait d'essais systématiques de précision ni de reproductibilité.

Limite de sensibilité

Les conditions de mesure de hauteur de pic (proximité du mur d'oxydation du mercure, courants parasites d'ordres de grandeur équivalents au courant mesuré) permettent de mesurer les concentrations en cuivre égales ou supérieures à $5 \cdot 10^{-8}$ mole par litre, soit 2.5 $\mu g\, l^{-1}$. Des mesures systématiques dans les eaux polluées peuvent être envisagées par cette méthode.

CONCLUSION

Nous nous sommes attachés ici à mettre en oeuvre la polarographie à tension sinusoïdale surimposée, pour déterminer l'espèce chimique sous laquelle se trouve

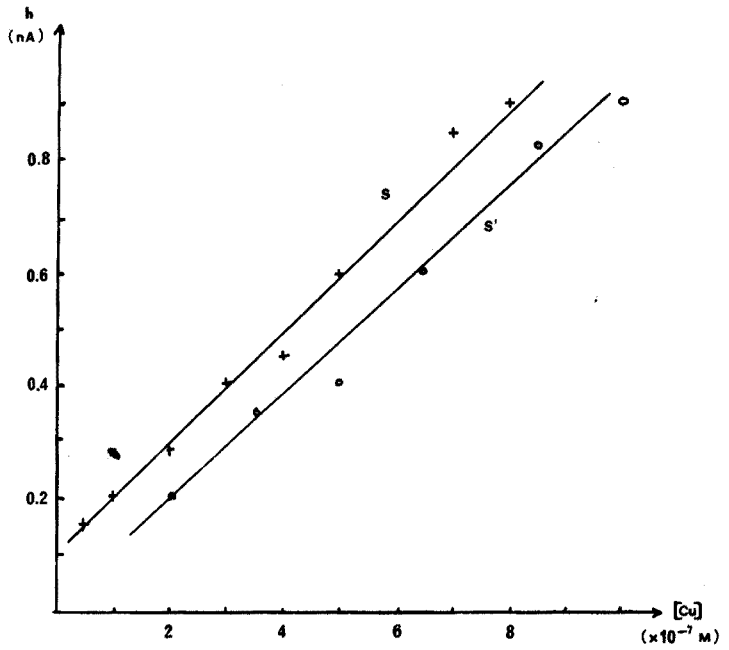

Fig. 8. Dosage du cuivre dans l'eau de mer ; droites d'étalonnage des hauteurs de pic en fonction de la concentration en cuivre. Salinité des échantillons : $S = 35.3^{0}/_{00}$; $S' < 27^{0}/_{00}$.

le cuivre en solution dans l'eau de mer. En plus des ions Cu^{2+} et $CuCl^{+}$, le cuivre existe aussi sous forme d'un complexe impliquant les ions bicarbonate et hydroxyle : la mesure des potentiels de pic de réduction du cuivre en solution dans des milieux perchlorate, chlorure et bicarbonate de sodium, à des valeurs de pH comprises entre 6 et 8.5, a permis de montrer l'existence du complexe $[Cu(HCO_3)_2(OH)]^{-}$ et de prévoir son existence dans l'eau de mer. Ce résultat n'élimine pas la possibilité pour le cuivre d'exister sous les autres formes prévisibles, en particulier, sous la forme de complexes organiques et de colloïdes, non envisagés dans cette étude.

Nous remercions Monsieur le Professeur G. Charlot, qui nous a accueilli dans son laboratoire, et Madame J. Badoz, Directeur de Recherche au C.N.R.S., pour l'intérêt qu'elle a bien voulu porter à cette étude. M. O. remercie le C.N.E.X.O. pour son aide matérielle.

RÉSUMÉ

La polarographie à tension sinusoïdale surimposée est utilisée pour déterminer la forme chimique du cuivre dans l'eau de mer. La variation du potentiel de demi-vague de réduction du cuivre(II) en fonction de la concentration de chacun des agents complexants et du pH, permet de déterminer la formule et la constante de formation de chaque complexe. D'après cette méthode, le cuivre en solution dans l'eau de mer est principalement sous les formes Cu^{2+}, $CuCl^{+}$ et $[Cu(HCO_3)_2(OH)]^{-}$. Une méthode de dosage est suggérée, après acidification des échantillons par CO_2

pur, à pH 5. La méthode permet d'atteindre la concentration de 2.5 $\mu g\, l^{-1}$ de cuivre dans l'eau de mer ($5 \cdot 10^{-8}$ *M*).

SUMMARY

A.c. polarography is used to determine the chemical forms of copper in sea water. The shift of the half-wave potential of reduction of copper(II) depending on the concentration of each ligand and on the pH, makes it possible to establish the formula and the formation constant of each complex. Copper in sea water is considered to be mainly present as Cu^{2+}, $CuCl^{+}$ and $[Cu(HCO_3)_2(OH)]^{-}$. An a.c.polarographic method for the determination of copper in some sea waters is proposed; samples are acidified to pH 5 by passing pure CO_2. Copper down to 2.5 $\mu g\, l^{-1}$ ($5 \cdot 10^{-8}$ *M*) can be determined.

ZUSAMMENFASSUNG

Die chemischen Formen von Kupfer in Meerwasser werden durch Wechselstrompolarographie ermittelt. Die Verschiebung des Halbwellenpotentials der Reduktion von Kupfer(II) in Abhängigkeit von der Ligandkonzentration und vom pH-Wert ermöglicht die Bestimmung der Formel und der Bildungskonstante eines jeden Komplexes. Hiernach liegt Kupfer in Meerwasser hauptsächlich als Cu^{2+}, $CuCl^{+}$ und $[Cu(HCO_3)_2(OH)]^{-}$ vor. Es wird eine Methode der Wechselstrompolarographie für die Bestimmung von Kupfer in Meerwasser vorgeschlagen; die Proben werden hierbei mit reinem CO_2 auf pH 5 gebracht. Kupfer bis zu 2.5 $\mu g\, l^{-1}$ ($5 \cdot 10^{-8}$ *M*) kann bestimmt werden.

BIBLIOGRAPHIE

1 M. ODIER, *Thèse 3° cycle*, Faculté des Sciences de Paris, 1970.
2 P. BOUGIS, *Publ. Staz. Napoli*, 32 (1962) Suppl. 497.
3 L. G. SILLÉN ET M. SEARS, *Oceanography*, Amer. Assoc. Adv. Science, Washington, 1961, pp. 549–582.
4 A. BARIC ET M. BRANICA, *J. Polarog. Soc.*, 13 (1967) 1.
5 R. P. BROOKS, B. J. PRESLEY ET I. R. KAPLAN, *Anal. Chim. Acta*, 38 (1967) 321.
6 K. SARUHASHI, *Papers Meteorol. Geophys. (Tokyo)*, 6 (1955) 38.
7 J. FAUCHERRE ET Y. BONNAIRE, *Compt. Rend.*, 248 (1959) 3, 3705–3707.
8 L. MEITES, *J. Amer. Chem. Soc.*, 72 (1950) 184.
9 K. V. KRISHNAMURTY, G. M. HARRIS ET V. S. SASTRY, *Chem. Rev.*, 70 (1970) 2, 171.
10 B. BREYER ET H. H. BAUER, *Alternating Current Polarography and Tensammetry*, Interscience, 1963.
11 I. M. KOLTHOFF ET J. J. LINGANE, *Polarography*, *Vol. 1*, Interscience, New York, 2e edn., 1952, Chap. 12.
12 H. SCHMIDT ET M. VON STACKELBERG, *Modern Polarographic Methods*, Academic Press, New York, 1963.
13 G. CHARLOT, *L'Analyse Qualitative et les Réactions en Solution*, Masson, Paris, 1963, pp. 127 et 275.
14 L. G. SILLÉN, *Stability Constants of Metal-Ion Complexes*, Section I, The Chemical Society, London, 1964, Special Publ. No. 17.
15 J. P. RILEY, in J. P. RILEY ET G. S. SKIRROW, *Chemical Oceanography*, Tome 2, Academic Press, Londres, 1966, pp. 323–384; et communication personnelle.

Analytica Chimica Acta
Elsevier Publishing Company, Amsterdam
Printed in The Netherlands

DIE FARBREAKTION DER KOHLENHYDRATE UND ALDEHYDE MIT CYSTEIN UND THIOGLYKOLSÄURE IN SCHWEFELSÄURE

G. KUNOVITS

Abteilung für Vitamin- und Ernährungsforschung, F. Hoffmann–La Roche & Co, AG, CH4002 Basel (Schweiz)

(Eingegangen den 15. März 1971)

Die Schwefelsäure–Cystein-Farbreaktion der Kohlenhydrate wurde von Dische[1] 1953 entdeckt. Seither wird sie für den Nachweis und die Bestimmung praktisch aller Zucker angewendet.

Der Mechanismus dieser Reaktion wurde bis heute nicht abgeklärt. Es gilt als erwiesen, dass die Kohlenhydrate bei der Schwefelsäurebehandlung nach Abspalten von Wasser in Furanderivate umgewandelt werden[2–4]. Aus Pentosen entsteht Furfurol, aus Hexosen Hydroxymethylfurfurol und aus Heptosen Dihydroxyäthylfurfurol. Das Cystein reagiert demnach nicht mit den Kohlenhydraten, sondern mit den Furfurolderivaten[5].

Nomura[6] hat festgestellt, dass durch die hydrolytische Spaltung des Furfurols 2-Oxo-Glutaraldehyd entsteht, der durch sein 2,4-Dinitrophenylhydrazon identifiziert wurde. Die enolische Form von 2-Oxo-Glutaraldehyd (I) ist aber der 2-Hydroxy-Glutaconaldehyd (II), einer der Vertreter der Polymethine[7].

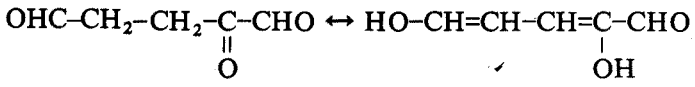

I II

Daraus ergibt sich die Möglichkeit der Entstehung von Polymethinfarbstoffen aus Furfurol und Cystein. Um dies nachzuprüfen, war es notwendig, die Reaktion zwischen 2-Hydroxyglutaconaldehyd und Cystein zu untersuchen. Die Herstellung von 2-Hydroxyglutaconaldehyd aus Furfurol ist äusserst umständlich. Andererseits wollten wir eine derartige Verbindung auf einem vom Furfurol unabhängigen Weg erhalten. Die beste Möglichkeit hierzu bietet der Glutaconaldehyd, der aus Pyridin verhältnismässig einfach herzustellen ist. Bei seiner Herstellung folgten wir den Angaben von Baumgarten[8,9].

REAKTION DES GLUTACONALDEHYDS MIT CYSTEIN IN SCHWEFELSÄURE

Der freie Glutaconaldehyd ist in wässrigen Lösungen unbeständig und kann deshalb in reiner Form nicht gewonnen werden. Sein enolisches Natriumsalz ist dagegen bei Zimmertemperatur beliebig haltbar. Falls man Glutaconaldehyd in Aethanol abs. löst und diese Lösung mit konz. Schwefelsäure vorsichtig ansäuert, wird sie bei einer bestimmten Schwefelsäure-Konzentration rotviolett. Es bildet sich hierbei ein rotes Oxonium-Ion (III), wie dies erstmals von Klages und Träger[10] festgestellt wurde.

Dieses Ion ist durch Mesomerie gegen Polymerisation stabilisiert.

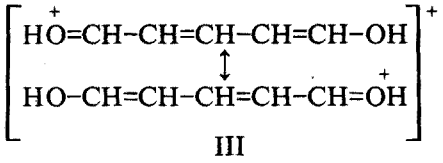

III

Der Glutaconaldehyd reagiert auch mit Cystein in Schwefelsäure bei Zimmertemperatur unter Bildung eines orangevioletten Farbstoffes. Das Absorptionsmaximum dieser Verbindung liegt bei 490 nm (Abb. 1).

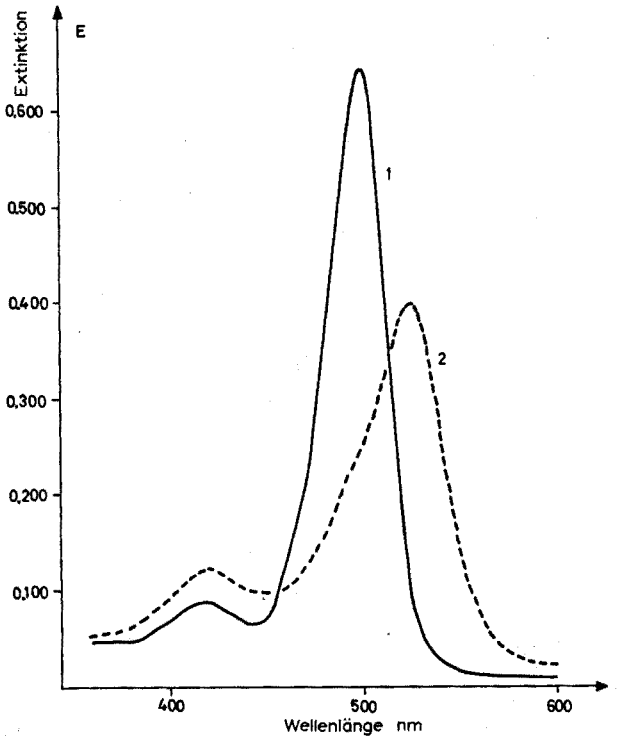

Abb. 1. Absorptionsspektren. (1) Glutaconaldehyd + Cystein in H_2SO_4 82 Gew. %; (2) isolierter Pentamethinfarbstoff (Verb. IV), gelöst in H_2O, pH = 1.6.

Wir haben versucht, diesen Farbstoff präparativ herzustellen. Nach zahlreichen Versuchen gelang es, eine Substanz von rotvioletter Farbe aus einem Reaktionsgemisch von Aethanol abs., Schwefelsäure, Glutaconaldehyd und Cystein verhältnismässig rein zu isolieren (Abb. 1). (Die Verschiebung des Absorptionsmaximums ist auf den Unterschied in der Säurekonzentration zurückzuführen.)

Die verschiedenen Analysen (Kernresonanz, Massenspektrum, i.r.- und u.v.-Spektren, Mikroanalyse) ergaben schliesslich für den Farbstoff die nachstehende Strukturformel (IV).

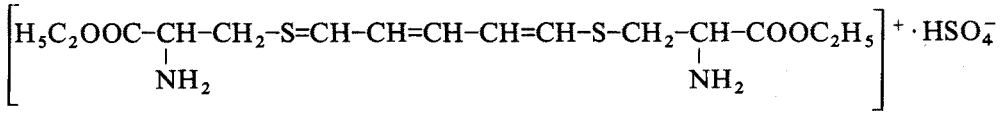

IV

Bei dieser Verbindung handelt es sich um einen Pentamethinfarbstoff von kationischem Typ. Das mesomere Kation wird durch Delokalisation der positiven Ladung zwischen den beiden S-Atomen am Kettenende stabilisiert. Der Substituent am S-Atom beeinflusst das Absorptionsmaximum des Farbstoffes nicht, solange er nicht befähigt ist, ein konjugiertes System zu bilden (wie z.B. Thiophenol). Der Reaktionsverlauf entspricht dem folgenden Schema:

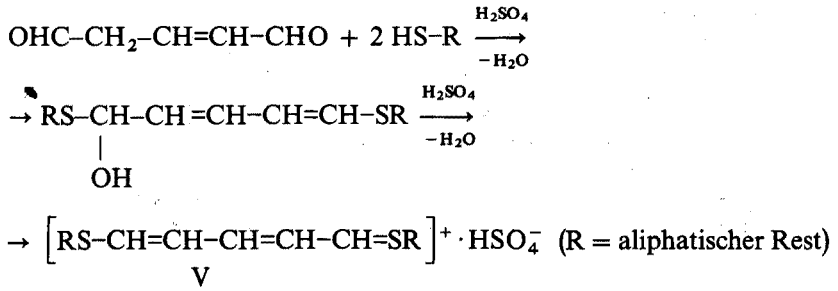

V

Diese Farbreaktion mit Glutaconaldehyd in Schwefelsäure gibt sämtliche aliphatische Merkaptoverbindungen, wie Thioglykolsäure, Thiomilchsäure, Thioglycerin, Homocystein, Glutathion etc. Das Ausmass dieser Reaktion hängt von der der SH-Gruppe benachbarten Methylengruppe ab. Ist sie zweifach substituiert, bleibt die Reaktion vollkommen aus (z.B. Penicyllamin).

REAKTION DER FURFUROLDERIVATE MIT CYSTEIN IN SCHWEFELSÄURE

Furfurol

Da das Furfurol mit Cystein in Schwefelsäure bei Zimmertemperatur unter Bildung eines rotvioletten Farbstoffes, dessen Absorptionsmaximum bei 535 nm liegt (Abb. 2), ebenfalls reagiert, ist die Analogie des Reaktionsverlaufes zu der Glutaconaldehyd–Cystein-Reaktion offensichtlich. Das dabei entstehende Polymethin-Kation muss nach dem hydrolytischen Aufspalten des Furanringes einen Hydroxy-Substituenten in der Polymethinkette enthalten (VI).

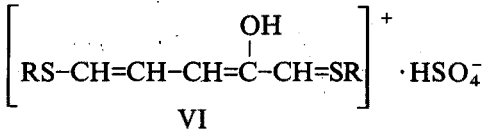

VI

Die Keto–Enol-Tautomerie erklärt das Vorhandensein zweier Maxima bei 505 und 535 nm (Abb. 2).

Hydroxymethylfurfurol (HMF)

Bei der Reaktion von HMF mit Cystein ist das Ausbleiben der Bildung des rot-

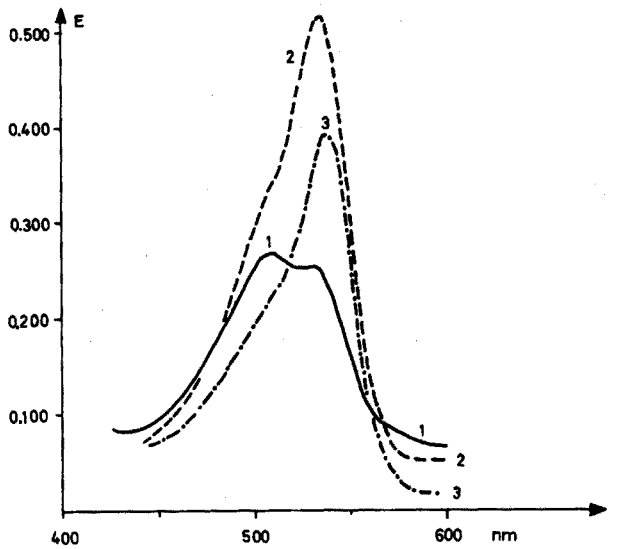

Abb. 2. Absorptionsspektren. Furfurol 1 μmol +5 ml H_2SO_4 82 Gew.% × 1 ml einer Cysteinlösung von: (1) 0.5, (2) 2.4, (3) 5.0%.

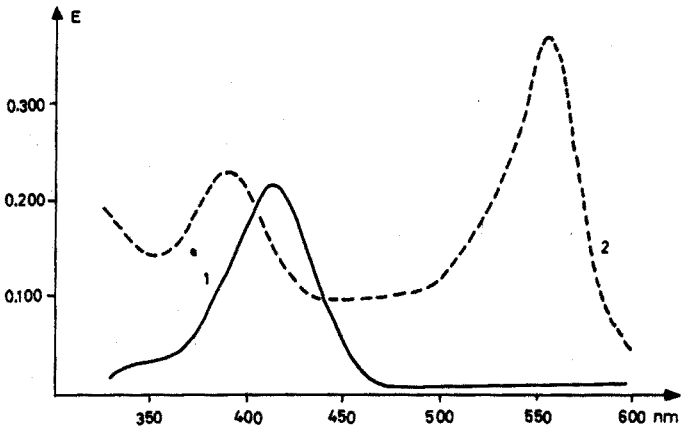

Abb. 3. Absorptionsspektren. (1) Hydroxymethylfurfurol +Cystein in H_2SO_4 82 Gew.%; (2) Hydroxymethylfurfurol +Thioglykolsäure in H_2SO_4 90 Gew.%. Erläuterungen im Text.

violetten Farbstoffes auffallend. Die hierbei entstehende grüngelbe Verbindung, deren Absorptionsmaximum bei 410 nm liegt (Abb. 3), ist wahrscheinlich durch Resonanz gemäss VII stabilisiert. Der Ring von HMF wird nicht aufgespalten.

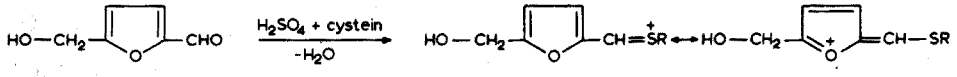

VII

Dihydroxyäthylfurfurol (DHAEF)

DHAEF reagiert mit Cystein in Schwefelsäure bei Zimmertemperatur unter Bildung eines rotvioletten Farbstoffes, dessen Absorptionsmaximum bei 505 nm liegt

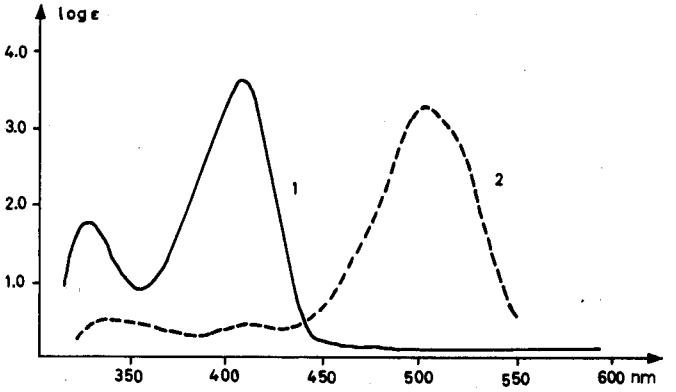

Abb. 4. Absorptionsspektren. (1) Sedoheptulosan in H_2SO_4 82 Gew. %, 5 min bei 100° erhitzt; (2) wie 1 + Cystein.

(Abb. 4). Es entsteht dabei bereits nach der Schwefelsäurebehandlung ein grüngelbes Zwischenprodukt (Abb. 4, Max. bei 405 nm). Der grösste Teil des DHAEF liegt in dieser Form vor. Neulich wurde von uns festgestellt, dass diese Reaktion des DHAEF mit Schwefelsäure wegen seiner Spezifität für die Bestimmung von Sedoheptulose in Mischungen von Pentosen und Hexosen geeignet ist. Wir führen diese Reaktion auf einen Wasserentzug im DHAEF-Molekül durch die Schwefelsäure unter Bildung von VIII zurück.

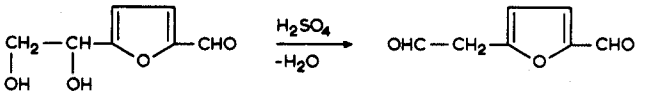

VIII

Das Cystein reagiert mit Verbindung VIII, wie dies aus Abb. 4 gut ersichtlich ist. Das Absorptionsmaximum bei 405 nm verschwand nach der Zugabe von Cystein fast vollständig. Die Seitenkette aus VIII wird wahrscheinlich als Essigsäure abgetrennt. Danach bildet sich hier ebenfalls das Kation V.

REAKTION DER THIOGLYKOLSÄURE MIT DEN KOHLENHYDRATEN IN SCHWEFELSÄURE

Wie bereits erwähnt (Seite 223), verhält sich Thioglykolsäure (TGS) gegenüber Glutaconaldehyd mit Schwefelsäure ähnlich wie Cystein und liefert die gleichen Reaktionen mit den Kohlenhydraten.

In einer Hinsicht, in ihrem Verhalten in Schwefelsäure (90–96%), unterscheiden sich die beiden Verbindungen wesentlich voneinander. Thioglykolsäure ist in der Lage, in konz. Schwefelsäure unter Verlust eines Mol H_2O teilweise in eine ringförmige Verbindung, ein Thioglykolid, überzugehen[11]. Die Anzahl der am Ring beteiligten TGS-Moleküle kann unterschiedlich sein. Diese strukturelle Änderung im TGS-Molekül ist optisch ebenfalls bemerkbar. Die Farbe der Schwefelsäure wird nach der Zugabe von TGS zitronengelb (Absorptionsmaximum bei 390 nm, Abb. 3).

Wir haben festgestellt, dass mit Hilfe des Thioglykolids der Ring von HMF auf-

zuspalten ist. Die Reaktion des TGS in konz. Schwefelsäure mit HMF unter bestimmten Bedingungen führt nämlich ebenfalls zum rotvioletten Polymethin-Kation (Abb. 3).

Diese Reaktion ist vor allem für den Nachweis von Fructose, die in Schwefelsäure schon bei Zimmertemperatur vollständig in HMF umgewandelt wird, geeignet.

Die nachstehende Methodik befasst sich mit dieser Nachweisreaktion als Modellfall.

Bestimmung von Fructose mit Thioglykolsäure in Schwefelsäure

Lösungen. TGS-Reagenz, 10 ml Wasser + 90 ml Schwefelsäure 96%. Die von der Verdünnungswärme noch heisse Mischung wird mit 0.5 ml Thioglykolsäure versetzt und auf Zimmertemperatur abgekühlt.
Fructoselösung (Fru), 1 μmol ml^{-1} (19.82 mg D-Fructose·H_2O ad 100 ml H_2O).
Glucoselösung (Glu 10), 10 μmol ml^{-1} (180.16 mg D-Glucose ad 100 ml H_2O).
Glucoselösung (Glu 1), 1 μmol ml^{-1} (Glu 10 1:10 verdünnen).
Xyloselösung (Xy), 1 μmol ml^{-1} (15.0 mg D-Xylose ad 100 ml H_2O).

TABELLE I

REPRODUZIERBARKEIT DER REAKTION VON FRUCTOSE MIT THIOGLYKOLSÄURE IN SCHWEFELSÄURE IN ABHÄNGIGKEIT VON DER KONZENTRATION

Konzentration (μmol Fructose)	0.01	0.02	0.03	0.04	0.05	0.10
Extinktion bei 550 nm	0.048	0.122	0.201	0.268	0.334	0.680
Abweichung vom Mittelwert (%)	−27	−7.6	+1.5	+1.5	+1.2	+3.0

TABELLE II

EINFLUSS VERSCHIEDENER ZUCKER AUF DIE REPRODUZIERBARKEIT DER FRUCTOSEBESTIMMUNG MIT THIOGLYKOLSÄURE IN SCHWEFELSÄURE

Konzentration (μmol)				*Extinktion bei 550 nm*	*Abweichung vom Mittelwert (%)*
Nr.	*Fru*	*Glu*	*Xy*		
1	—	0.05	—	0.021	—
2	—	0.10	—	0.027	—
3	—	0.50	—	0.157	—
4	—	—	0.05	0.004	—
5	0.03	0.03	—	0.221	+11.6
6	0.03	0.30	—	0.278	+40
7	0.03	—	0.03	0.201	+ 1.5
8	0.03	0.30	0.03	0.291	+47
9	0.05	0.05	0.05	0.313	+ 5.2

Ausführung der Reaktion. 4 ml TGS-Reagenz wird in einem starkwandigen Reagenzglas mit Schliff von 10 ml Inhalt vorgelegt. Man setzt dem Reagenz 0.02 ml Fru zu und vermischt es gut. Nach 5 Min wird die Mischung mit 2.0 ml Wasser versetzt und so lange vorsichtig geschwenkt, bis zwischen der Phasengrenze Säure-Wasser ein farbiger Ring entsteht. Nach dem Schütteln stellt man die Mischung ins Wasserbad mit einer Temperatur von 20°. Die Extinktion der Lösung wird nach einer Stunde bei 550 nm gegen eine Blindprobe ohne Fructose ermittelt.

Ergebnisse. Siehe Tabelle I und II. Die Messdaten sind Mittelwerte aus Parallelproben.

REAKTION DER THIOGLYKOLSÄURE MIT AROMATISCHEN ALDEHYDEN IN SCHWEFELSÄURE

Die Tatsache, dass sich der durch Resonanz stabilisierte Ring von HMF mit Hilfe von Thioglykolid öffnet, veranlasste uns, mit dieser Reaktion die Bestimmung aromatischer Aldehyde zu versuchen. Aufgrund der Analogie zu HMF prüften wir in erster Linie diejenigen Aldehyde, die eine Chinoid-Struktur zu bilden befähigt sind (Aldehyde mit Hydroxy- und Methoxysubstituenten).

Die ersten Versuche ergaben, dass diese Aldehyde in Schwefelsäure vollkommen analog zu HMF mit der Thioglykolsäure reagieren. Als Modellfall haben wir die *o*-, *m*- und *p*-Methoxybenzaldehyde (Anisaldehyde) untersucht.

Bestimmung der Anisaldehyde mit Thioglykolsäure in Schwefelsäure

Lösungen. TGS-Reagenz (siehe Bestimmung von Fructose).
2-Methoxybenzaldehyd-Lösung (*o*), 1 μmol ml^{-1} (13.6 mg ad 100 ml Aethanol).
3-Methoxybenzaldehyd-Lösung (*m*), 1 μmol ml^{-1} (wie beim *ortho*).
4-Methoxybenzaldehyd-Lösung (*p*), 1 μmol ml^{-1} (wie beim *ortho*).

Ausführung der Reaktion. Siehe Bestimmung von Fructose.

Ergebnisse. Siehe Tabelle III und IV.

DISKUSSION

Das aus der Reaktion von HMF bzw. *p*-Anisaldehyd mit Thioglykolsäure und Schwefelsäure resultierende Polymethin-Kation eignet sich für die photometrische Bestimmung dieser Substanzen in Konzentrationen von 0.03–0.1 μmol mit einer Genauigkeit von min. 95% (Tabellen I und III).

Mit dieser Methode kann ausserdem die Fructose mit anderen Zuckern in äquimolaren Mischungen, nicht höher als 0.05 μmol, selektiv bestimmt werden (Tabelle II).

Bei der Prüfung, inwieweit die Isomeren von *p*-Anisaldehyd in äquimolaren Mischungen dessen Bestimmung beeinflussen, zeigte sich, dass das *m*-Anisaldehyd nicht und das *o*-Anisaldehyd erst in höheren Konzentrationen störend wirkt (Tabelle IV).

Den Reaktionsverlauf zwischen dem Thioglykolid und den Aldehyden in Schwefelsäure können wir nicht restlos erklären. Wir nehmen an, dass die Ringspaltung beim HMF auf eine primäre Reaktion zwischen HMF und Thioglykolid zurückzuführen ist, aus der, im Gegensatz zu Cystein, keine Resonanzstabilisierung des Furanringes resultiert.

TABELLE III

REPRODUZIERBARKEIT DER REAKTION VON *p*-ANISALDEHYD IN SCHWEFELSÄURE IN ABHÄNGIGKEIT VON DER KONZENTRATION

Konzentration (μmol *p*-Anisaldehyd)	0.01	0.02	0.03	0.04	0.05	0.10
Extinktion bei 550 nm	0.065	0.156	0.252	0.356	0.442	0.916
Abweichung vom Mittelwert (%)	−26	−11	−4.2	+1.7	+0.9	+4.5

TABELLE IV

EINFLUSS DER ISOMEREN AUF DIE BESTIMMUNG VON *p*-ANISALDEHYD MIT THIOGLYKOLSÄURE IN SCHWEFELSÄURE

Konzentration von Anisaldehyd (μmol)				*Extinktion bei 550 nm*	*Abweichung vom Mittelwert* (%)	*Bemerkungen*
Nr.	*ortho*	*meta*	*para*			
1	0.03	—	—	0.042	—	Max. bei 532 nm
2	—	0.03	—	0.000	—	
3	—	—	0.03	0.252	−4.2	
4	0.03	0.03	—	0.041	—	Max. bei 532 nm
5	0.03	—	0.03	0.269	+2.3	
6	—	0.03	0.03	0.250	−4.9	
7	0.03	0.03	0.03	0.266	+1.1	

ZUSAMMENFASSUNG

Die Farbreaktion der Kohlenhydrate mit Schwefelsäure–Cystein wurde im Hinblick auf die Abklärung ihres Reaktionsverlaufes untersucht. An Hand eines isolierten, bisher unbekannten Farbstoffes aus Glutacondialdehyd und Cystein konnten die Reaktionsprodukte der H_2SO_4–Cystein-Reaktion der Kohlenhydrate als Pentamethinfarbstoffe vom kationischen Typ der allgemeinen Formel

$$\left[\overset{+}{\underset{}{\text{RS}}}\text{=CH–CH=CH–C(OH)=CH–SR}\right]^{+}\cdot X^{-}$$

$$(X^{-} = HSO_4^{-}, ClO_4^{-})$$

identifiziert werden. Diese Verbindungen sind als Hydroxy-Glutaconaldehyd-Abkömmlinge aufzufassen, die bei Reaktion von 1 Mol Furfurol mit 2 Mol Cystein nach hydrolytischer Aufspaltung des Furanringes und Bildung der oben aufgeführten Polymethin-Resonanzkette entstehen. Es wurde eine neue Nachweisreaktion für Kohlenhydrate und aromatische Aldehyde mit Thioglykolsäure gefunden, welche an Hand der Beispiele Fructose and Anisaldehyd beschrieben wird.

SUMMARY

The mechanism of the color reaction of carbohydrates with sulfuric acid–cysteine has been investigated. By means of a newly isolated dyestuff, formed by the

reaction of glutaconaldehyde with sulfuric acid and cysteine, the resulting colour has been characterized as a pentamethine dye of the cationic type with the general formula

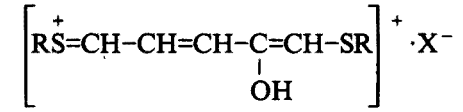

$(X^- = HSO_4^-, ClO_4^-)$

These compounds are derivatives of hydroxyglutaconaldehyde, formed by the reaction of 1 mol of furfurol with 2 mol of cysteine after hydrolytic cleavage of the furane ring, and formation of the resonance chain shown above. A new method for the identification of aldehydes with thioglycolic acid is described.

RÉSUMÉ

On examine le mécanisme de la réaction colorée des carbohydrates avec le mélange acide sulfurique–cystéine. Grâce à un colorant, nouvellement isolé, formé par la réaction glutaconaldéhyde, acide sulfurique et cystéine, on a pu caractériser la couleur résultante comme colorant pentaméthine de type cationique, de formule générale:

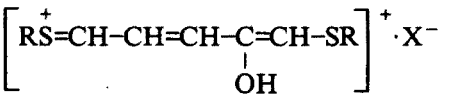

$(X^- = HSO_4^-, ClO_4^-)$

On décrit une nouvelle méthode d'identification des aldéhydes à l'aide d'acide thioglycolique.

LITERATUR

1 Z. DISCHE, *J. Biol. Chem.*, 204 (1953) 983.
2 F. BENDOW, *Biochem. Z.*, 294 (1937) 124.
3 G. HOLZMAN, R. V. MACALLISTER UND C. NIEMANN, *J. Biol. Chem.*, 171 (1947) 27.
4 M. IKAWA AND C. NIEMANN, *J. Biol. Chem.*, 180 (1949) 923.
5 *Methods in Carbohydrate Chemistry, Vol. I*, Academic Press, New York and London, 1962.
6 D. NOMURA, *J. Ferment. Technol. (Japan)*, 34 (1956) 466; *Chem. Abstr.*, 51 (1957) 5069c.
7 G. SCHWARZENBACH, K. LUTZ UND E. FELDER, *Helv. Chim. Acta*, 27 (1944) 576.
8 P. BAUMGARTEN, *Chem. Ber.*, 57 (1924) 1622.
9 P. BAUMGARTEN, *Chem. Ber.*, 59 (1926) 1166.
10 F. KLAGES UND H. TRÄGER, *Chem. Ber.*, 86 (1953) 1327.
11 P. KLASON UND T. KLASON, *Chem. Ber.*, 39 (1906) 734.

Analytica Chimica Acta
Elsevier Publishing Company, Amsterdam
Printed in The Netherlands

4-[(5-CHLORO-2-PYRIDYL)AZO]-1,3-DIAMINOBENZENE AS A NEW SENSITIVE AND SELECTIVE REAGENT FOR COBALT

SHOZO SHIBATA, MASAMICHI FURUKAWA, YOSHIO ISHIGURO AND SHOZO SASAKI
Government Industrial Research Institute Nagoya, Kita-ku, Nagoya (Japan)

(Received 11th January 1971)

Many reagents have been employed for the spectrophotometric determination of cobalt. Among the most important and the recent ones are thiocyanate[1], dithioxamide[2], 2,3-quinoxaline dithiol[3], nitroso R salt[1], 5-(ethylamino)-2-(2-pyridylazo)-*p*-cresol[4] and thiovioluric acid[5]. In a search for new sensitive and selective reagents, a thorough study of some azo compounds containing halogen-substituted pyridine has been made[6-8]. One of these compounds, 4-[(5-chloro-2-pyridyl)azo]-1,3-diaminobenzene (5-Cl-PADAB, formula I) was found to form a pink water-soluble complex with cobalt.

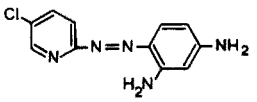

I

With 5-Cl-PADAB a highly sensitive and selective determination of microgram amounts of cobalt is possible under the optimal conditions established in this study. Sensitivities of this and other determinations of cobalt are shown in Table I.

EXPERIMENTAL

Reagents

5-Cl-PADAB solution. An ethanolic 0.1% (w/v) solution was prepared from

TABLE I

SENSITIVITIES OF DETERMINATIONS OF COBALT

Reagents	*Sensitivity (μg Co cm^{-2}) or molar absorptivity ($l\ mol^{-1}\ cm^{-1}$)*
Hydrochloric acid (conc.)[1]	0.200 (625 nm)
Thiocyanate[1]	0.055 (625 nm), 0.009 (310 nm)
Dithioxamide[9]	0.046 (400 nm), $1.295 \cdot 10^4$ (370 nm)
α-Nitroso-β-naphthol[9]	$2.65 \cdot 10^4$ (317 nm)
o-Nitrosoresorcinol[1]	0.0025 (430 nm)
Nitroso-R salt[1,9]	0.0019 (420 nm), 0.0042 (520 nm), $2.3 \cdot 10^4$ (420 nm)
Dithizone[9]	$5.92 \cdot 10^4$ (542 nm)
Thiovioluric acid[5]	0.0011 (425 nm)
5-(Ethylamino)-2-(2-pyridylazo)-*p*-cresol[4]	$7.4 \cdot 10^4$ (530 nm)
5-Cl-PADAB	0.00051 (570 nm), $1.13 \cdot 10^5$ (570 nm)

the pure material (see below). The solution is stable for several months if stored in an amber bottle.

Cobalt(II) solution. A stock solution was prepared from the 99.99% pure cobalt metal as chloride.

Buffer solution. Hydrochloric acid–potassium chloride, acetic acid–sodium acetate, boric acid–potassium chloride–sodium hydroxide and borax–sodium hydroxide and borax–sodium hydroxide mixtures were used for pH adjustment.

All the other reagents used, including the metal standard solution, were made from high-purity materials or purified reagents, and all solutions were prepared with redistilled water.

Apparatus

Absorbance curves were measured with a Model EPS-3T Hitachi recording spectrophotometer with 1-cm cells; absorbances were measured with a Model 124 Hitachi spectrophotometer with 1-cm cells. A Hitachi M5 type pH meter was used.

Preparation of reagent

The reagent was prepared by coupling *m*-phenylenediamine with 5-chloro-2-pyridyldiazotate in aqueous alcohol solution. The diazotate was prepared by adding a solution of isoamyl nitrite to a mixture of 5-chloro-2-aminopyridine and sodium amide under reflux.

Diazotation. Freshly prepared isoamyl nitrite (5.46 g) was added to a solution containing 6 g of 5-chloro-2-aminopyridine and 2.4 g of sodium amide in 80 ml of absolute ethanol. The mixture was refluxed for 2 h and cooled.

Coupling reaction. m-Phenylenediamine hydrochloride (8.4 g) was dissolved in 50 ml of water and added to the diazotate solution. The mixture was let cool overnight, and the precipitated red brown crystals were filtered and washed with water. Finally the precipitate was dissolved in hot ethanol and recrystallized from aqueous alcoholic solution (red brown, sublimed at about 200°). Purified material for physicochemical determinations can be obtained by sublimation *in vacuo*.

Colour reactions with metals

The coloured complexes were easily prepared by adding a few drops of a

TABLE II

COLOUR REACTIONS OF METALS WITH 5-Cl-PADAB

Ion	*Colour*			
	pH 5	H_2SO_4 *added*	*pH* 10	H_2SO_4 *added*
—	Yellow orange	Yellow	Yellow orange	Yellow
Ag^+	—	—	Pale red	—
Co^{2+}	Red purple	Bluish purple	Brown	Red purple
Cu^{2+}	Purplish red	—	Brown	—
Fe^{3+}	Dark orange	Grayish yellow brown	Yellowish brown	Dark orange
Hg^{2+}	Dark orange	—	Brown purple	—
Ni^{2+}	—	—	Dull red	—

solution of 5-Cl-PADAB in ethanol to a solution of heavy metals. The ions that gave a colour with the reagent are listed in Table II.

The following ions failed to give a detectable coloration at room temperature: silver, aluminum (at pH 5), bismuth, cadmium, calcium, manganese, magnesium, nickel (at pH 5), lead (at pH 5), praseodymium, terbium, thulium, thorium, uranium-(VI), tungsten, yttrium, zinc and zirconium. When mineral acid, *e.g.* sulfuric acid or hydrochloric acid, was added to the solution containing metal complexes, only cobalt and iron complexes were stable. The selectivity of 5-Cl-PADAB for cobalt is therefore excellent.

Absorbance curve

The absorbance curves of the reagent and its cobalt complex in aqueous solution at pH 5.0 (initial conditions of colour development) are shown in Fig. 1.

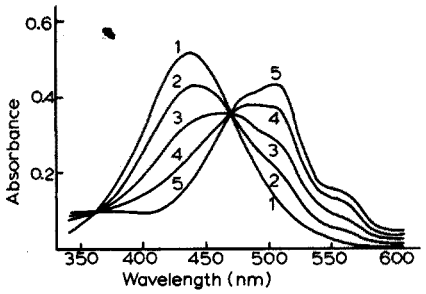

Fig. 1. Absorbance curves of 5-Cl-PADAB and its cobalt complex in aqueous solution at pH 5.0 with $1.6 \cdot 10^{-5}$ *M* 5-Cl-PADAB. Amount of Co present: (1) nil; (2) $2 \cdot 10^{-6}$ *M*; (3) $4 \cdot 10^{-6}$ *M*; (4) $6 \cdot 10^{-6}$ *M*; (5) $8 \cdot 10^{-6}$ *M*.

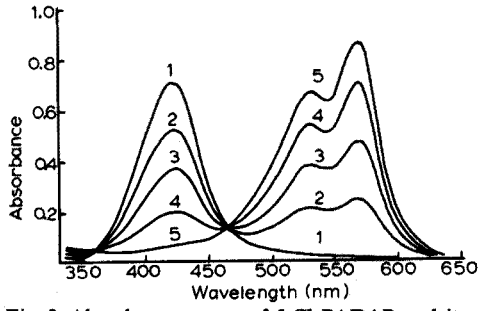

Fig. 2. Absorbance curves of 5-Cl-PADAB and its cobalt complex in 2.4 *M* hydrochloric acid solution. Concentrations of 5-Cl-PADAB and cobalt as in Fig. 1.

The curves show two absorption maxima at 506 and 560 nm, respectively. When hydrochloric acid is added to the sample solution, the cobalt complex may be changed to a different species (see below). The absorbance curves of the reagent and its complex in 2.4 *M* hydrochloric acid are shown in Fig. 2. The curve shows two absorption maxima at 530 and 570 nm, respectively.

Optimal pH

The effect of initial pH on colour development was studied by preparing a

series of solutions varying in pH region 2 to 12. The absorbance increased steeply in the pH range 2–3, but no change in absorbance was observed over the pH range 3.5–11.5. For these studies, the initial pH was as stated, but the absorbance was measured finally in 2.4 *M* hydrochloric acid media. Subsequent studies were carried out at an initial pH of 5.0 because nickel does not react with reagent at this pH.

Cobalt and 5-Cl-PADAB in an acid medium did not form any complexes; under these conditions, the ligand was clearly protonated on the heterocyclic nitrogen. However, the complex which was formed at pH 3.5–11.5 could be changed into another deeply coloured species which possessed increased absorptivity, by the addition of some mineral acid. The effects of acidity and the type of acid used on the colour development were studied by preparing a series of solution varying in final acidity but for which the colour had been developed initially at pH 5.0. The results obtained are shown in Fig. 3. No change in absorbance was observed over the acid range 6–12

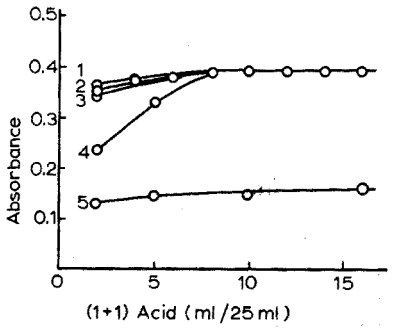

Fig. 3. Effect of final acid concentration on colour development of the cobalt–5-Cl-PADAB complex at 570 nm. 5 μg of cobalt per 25 ml. (1) H_2SO_4; (2) HCl; (3) HNO_3; (4) H_3PO_4; (5) CH_3COOH. Each (1 + 1) acid solution was made from the following analytical-grade reagent: H_2SO_4, 95%; HCl, 35%; HNO_3, 60–62%; H_3PO_4, $d = 1.8$; CH_3COOH, 99.0%.

ml of (1 + 1) hydrochloric acid, sulfuric acid, nitric acid or phosphoric acid. Subsequent studies were carried out with 10 ml of (1 + 1) hydrochloric acid (2.4 *M*).

Reagent concentration

The absorbances of a series of solutions containing 10 μg of cobalt and 0.1–1.0 ml of 0.1% dye solution were measured. It was found that 0.2 ml of this dye solution sufficed to complex 10 μg of cobalt; with higher reagent concentrations the absorbance was essentially constant.

Colour development, stability and effect of temperature

The minimum time for complete colour development of the complex was found to be 1–2 min at room temperature. The absorbance was then stable for at least 30 h.

Recommended procedure for the determination of cobalt

To a 25-ml volumetric flask, transfer a suitable aliquot of sample solution containing up to 0.5 p.p.m. of cobalt, and add 0.2 ml of ethanolic 0.1% (w/v) reagent solution. Adjust to pH 5.0 with buffer solution and mix. Then, add 10 ml of (1 + 1) hydrochloric acid, dilute to volume and mix. Measure the absorbance of the cobalt

complex produced at 570 nm against a reagent blank. Obtain the concentration of cobalt from a standard calibration curve obtained under identical conditions.

RESULTS AND DISCUSSION

Beer's law and sensitivity

The calibration graph proved to be linear over the range 0.02–0.5 p.p.m. of cobalt. The effective molar absorptivity for the cobalt complex was $1.13 \cdot 10^5$ l mol^{-1} cm^{-1} at 570 nm. The sensitivity of the reaction as calculated from Beer's law is 0.00051 μg Co cm^{-2} at 570 nm for log $I_0/I = 0.001$.

Effect of foreign ions

Numerous cations and anions were examined by applying the method to fixed amounts of cobalt in the presence of increasing quantities of the ion being studied (Table III). It is evident that many ions have no effect at the levels studied. Sulfate,

TABLE III

EFFECT OF FOREIGN IONS
(5.00 μg of cobalt taken)

Ion	*Amount added (mg)*	*Co found (μg)*	*Error (μg)*	*Ion*	*Amount added (mg)*	*Co found (μg)*	*Error (μg)*
Al^{3+}	5	4.93	−0.07	Ni^{2+}	0.1	5.00	±0.00
Be^{2+}	5	5.00	±0.00		1	5.13	+0.13
Bi^{3+}	5	4.82	−0.18	Pb^{2+}	5	5.00	±0.00
Cd^{2+}	5	5.00	±0.00	Th^{4+}	5	4.61	−0.39
Cr^{3+}	1	5.19	+0.19	Ti^{4+}	5	4.81	−0.19
Cr^{6+}	0.01	2.75	−2.25	U^{6+}	6	5.06	+0.06
Cu^{2+}	0.03	5.00	±0.00	V^{5}	3	4.87	−0.13
Fe^{3+}	0.05	5.77	+0.77	W^{6+}	5	3.52[a]	−1.48
	0.5	6.02	+1.02	Y^{3+}	5	4.81	−0.19
La^{3+}	5	4.93	−0.07	Zn^{2+}	5	4.93	−0.07
Mg^{2+}	5	4.82	−0.18	Zr^{4+}	5	4.55	−0.45
Mn^{2+}	5	4.93	−0.07				

[a] Precipitate formed.

chloride, bromide, nitrate, perchlorate, acetate, tartrate, citrate and phosphate did not interfere. Among the cations, interference was caused only by large amounts of iron(III) and chromium(VI). Chromium(III) did not interfere. Accordingly, 5-Cl-PADAB should be widely applicable as a colorimetric reagent for micro amounts of cobalt in many industrial and natural materials without separation.

Nature of the cobalt complex

The empirical formula of the complex was studied by the continuous variations and mole ratio methods. The Job curves obtained indicated the formation of a complex of cobalt in which the metal: ligand ratio is 1:2 (Fig. 4). The mole ratio method confirmed this conclusion. It is therefore probable that the complex contains divalent cobalt.

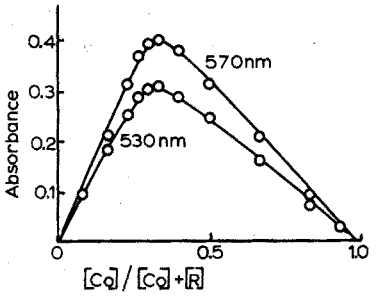

Fig. 4. Composition of cobalt–5-Cl-PADAB complex. [Co] + [5-Cl-PADAB] = $1.2 \cdot 10^{-5}$ *M*. 2.4 *M* hydrochloric acid solution.

The reaction of 5-Cl-PADAB with cobalt is very interesting, for it possesses high sensitivity and selectivity, and excellent stability in strongly acidic solution. The acid dissociation constants of the ligand, and further detail of the chelating reaction will be reported later.

SUMMARY

Cobalt(II) and 4-[(5-chloro-2-pyridyl)azo]-1,3-diaminobenzene (5-Cl-PADAB) in slightly acid, neutral or alkaline medium form a pink-coloured complex. This complex is very stable even in the presence of strong mineral acid. The complex has two absorption maxima at 530 and 570 nm in hydrochloric acid (2.4 *M*) solution. The colour is very stable and the system conforms to Beer's law; the optimal range for measurements in a 1-cm cell is 0.02–0.5 p.p.m. cobalt. Common anions and cations do not interfere; only chromium(VI) interferes seriously. The molar absorptivity is $1.13 \cdot 10^5$ l mol^{-1} cm^{-1} at 570 nm. The sensitivity is 0.00051 μg Co cm^{-2} at 570 nm for log $I_0/I = 0.001$.

RÉSUMÉ

Le cobalt(II) forme un complexe rose avec le 4-[(chloro-5-pyridyl-2)azo]-diamino-1,3-benzène (5-Cl-PADAB) en milieu légèrement acide, neutre ou alcalin. Ce complexe est très stable, même en présence d'acides minéraux forts. Il présente deux maxima d'absorption à 530 et 570 nm, en solution acide chlorhydrique 2.4 *M*. La couleur est très stable; le système obéit à la loi de Beer. Les mesures se font avec cuve de 1 cm, de 0.02 à 0.5 p.p.m. de cobalt. Les anions et cations communs ne gênent pas; seul chrome(VI) gêne. Coefficient d'extinction molaire: $1.13 \cdot 10^5$ mol^{-1} cm^{-1} à 570 nm. Sensibilité: 0.00051 μg Co cm^{-2} à 570 nm pour log $I_0/I = 0.001$.

ZUSAMMENFASSUNG

Kobalt(II) und 4-[(5-Chlor-2-pyridyl)azo]-1,3-diaminobenzol (5-Cl-PADAB) bilden in schwach saurem, neutralem oder alkalischem Medium einen rosagefärbten Komplex. Dieser Komplex ist sogar in Gegenwart starker Mineralsäure sehr beständig und hat in salzsaurer Lösung (2.4 *M*) zwei Absorptionsmaxima bei 530 und 570 nm. Die Färbung ist sehr beständig, und das System gehorcht dem Beerschen

Gesetz. Der optimale Bereich für Messungen in 1 cm-Küvetten ist 0.02–0.5 p.p.m. Kobalt. Die üblichen Anionen und Kationen stören nicht; nur Chrom(VI) stört erheblich. Der molare Extinktionskoeffizient ist $1.13 \cdot 10^5$ l mol^{-1} cm^{-1} bei 570 nm, die Empfindlichkeit bei 570 nm 0.00051 μg Co cm^{-2} für log $I_0/I = 0.001$.

REFERENCES

1 E. B. SANDELL, *Colorimetric Determination of Traces of Metals*, 3rd Edn., Interscience, New York, 1959, p. 408.
2 W. D. JACOBS AND J. H. YOE, *Anal. Chim. Acta*, 20 (1959) 332.
3 R. W. BURKE AND J. H. YOE, *Anal. Chem.*, 34 (1962) 1378.
4 S. I. GUSEV, N. N. KIRYUKHINA AND Z. A. BITOVT, *Zh. Analit. Khim.*, 23 (1968) 889.
5 R. S. CHAWLA AND R. P. SINGH, *Mikrochim. Acta*, 332 (1970).
6 S. SHIBATA, K. GOTO AND E. KAMATA, *Anal. Chim. Acta*, 45 (1969) 279.
7 S. SHIBATA, M. FURUKAWA, E. KAMATA AND K. GOTO, *Anal. Chim. Acta*, 50 (1970) 439.
8 S. SHIBATA, M. FURUKAWA AND S. SASAKI, *Anal. Chim. Acta*, 51 (1970) 271.
9 IUPAC, *Spectrophotometric Data for Colorimetric Analysis*, Butterworths, London, 1963, p. 98.

Analytica Chimica Acta
Elsevier Publishing Company, Amsterdam
Printed in The Netherlands

KINETIC DATA ON THE OXIDATION OF 1,1-DIPHENYL-2-PICRYLHYDRAZYL BY COPPER(II) AND IRON(III) PERCHLORATES, AND BY AMMONIUM HEXANITRATOCERATE(IV) IN ANHYDROUS ACETONITRILE

I. NĚMEC*, H. L. KIES AND I. NĚMCOVÁ*
Institute for Analytical Chemistry, University of Technology, Delft (The Netherlands)
(Received 20th December 1970)

The free radical, 1,1-diphenyl-2-picrylhydrazyl (DPPH), is of interest in the polymer industry, where it has been widely employed as an inhibitor and as a free radical trap. Solon and Bard[1] showed that a solution of this free radical in acetonitrile is capable of taking up one electron, forming a stable anion, or, on the other hand, repelling one electron, forming a stable cation. They found, using sodium perchlorate as supporting electrolyte and a rotating platinum electrode, two half-wave potentials at +0.70 and at +0.20 V, respectively, *vs.* aqueous S.C.E. These results were almost confirmed by Hall and Elving's experiments[2].

So far, the purely chemical oxidation of DPPH in a non-aqueous medium has been reported only once[3] in an article dealing with the action of lead(IV), cobalt(III), cerium(IV) and iron(III) acetates in anhydrous acetic acid. In all these cases a first-order reaction scheme with respect to each of the reactants was observed. The second-order rate constants were given.

The investigation reported here was planned in order to obtain kinetic data concerning the reactions between DPPH and the oxidizing agents, copper(II) perchlorate, iron(III) perchlorate and ammonium hexanitratocerate(IV) in acetonitrile.

EXPERIMENTAL

Reagents

DPPH (Fluka) and $(NH_4)_2Ce(NO_3)_6$ (Merck) were used without further purification. The cerium(IV) content was determined iodimetrically[4].

$Fe(II)(bipy)_3(ClO_4)_2$ was prepared as described by Burstall and Nyholm[5]. Its iron(II) content was determined in an aqueous 3 *N* solution of sulphuric acid by titration with a standardized aqueous solution of cerium(IV) sulphate.

For the other reagents, as well as for a description of the cell and the details of the procedure applied, the reader is referred to a former publication[6].

RESULTS

Voltammetric behaviour

The anodic wave of DPPH shows a reversible character and the slope of the

* On leave from Department of Analytical Chemistry, Charles University, Prague, Czechoslovakia.

plot $\log i/(i_d - i)$ *vs.* E amounts to $1/0.059\ V^{-1}$. The height of the wave is proportional to the concentration within the range 10^{-6}–$5 \cdot 10^{-3}$ *M*. The half-wave potential was found to be +0.46 V (*vs.* Ag/0.01 *M* $AgNO_3$ in acetonitrile); it did not depend on the concentration of DPPH.

No references were found on the voltammetric behaviour of cerium(IV) in acetonitrile. For this reason a voltammogram was recorded of a solution of ammonium hexanitratocerate in a 0.1 *M* solution of sodium perchlorate. An elongated wave was obtained with a half-wave potential of *ca.* +0.55 V. The calibration curve appeared to deviate from linearity.

After electrolysis of this solution at a rotating platinum spiral electrode, the electrode potential being kept at 0.1 V, the wave-height decreased while at the same time an anodic wave appeared that also showed an elongated shape. The anodic half-wave potential was +1.1 V, so that the redox system Ce(IV)/Ce(III) is highly irreversible in this medium.

The voltammetric behaviour of copper(II) and iron(III) in acetonitrile has been described previously[6].

Kinetic measurements

The stoichiometry of the reaction between DPPH and copper(II) perchlorate, iron(III) perchlorate, and ammonium hexanitratocerate(IV) was determined by potentiometric titration of a known amount of DPPH in 0.1 *M* sodium perchlorate with the oxidant, which was also dissolved in acetonitrile and standardized. A bright platinum electrode was used for indication while a silver sheet, dipping in a solution of 0.01 *M* silver nitrate in acetonitrile served as the reference electrode.

In all cases the stoichiometric ratio was proved to be 1:1.

On account of the course of the polarisation curves concerned, the voltage applied for amperometrically monitoring the concentration of DPPH can be best adjusted for the reactions with copper(II), iron(III), and cerium(IV) to 0.75, 0.80, and 0.88 V, respectively.

For the oxidation of DPPH by copper(II), expressed by the equation:

$$DPPH + Cu(II) \rightarrow DP^{+}PH + Cu(I)$$

a half-life time of about 0.8 sec was found for the initial concentrations: $[DPPH]_0 = 1.39 \cdot 10^{-5}$ *M* and $[Cu(II)]_0 = 2.00 \cdot 10^{-5}$ *M*.

The reaction was proved to be of the first order with respect to DPPH as well as to copper(II). The oxidation with iron(III) also followed the same pattern, but proceeded slightly faster.

The rate constants at 20° for the oxidation with copper(II) and iron(III), calculated in the same way as previously published[6], are listed in Tables I and II, respectively.

The reaction between DPPH and cerium(IV) proceeds much faster, which implies that exact measurement of the rate constant by the same technique is impossible. Only an approximate estimation of this constant was made, lower concentrations of the reactants being chosen ($\pm 5 \cdot 10^{-6}$ *M*). Provided that the overall order of the reaction is two and the stoichiometric ratio is 1:1, the rate constant is found to be $(1 \pm 0.6) \cdot 10^6$ $mole^{-1}$ 1 sec^{-1}.

In view of the potential application of the iron(II) bipyridyl complex as a redox

TABLE I

RATE CONSTANTS k FOR THE RATE LAW; $-d[DPPH]/dt = k[DPPH][Cu(II)]$

$[DPPH]_0 \cdot 10^5$ (*mol* l^{-1})	$[Cu(II)]_0 \cdot 10^5$ (*mol* l^{-1})	$k \cdot 10^{-4}$ (*mol* l^{-1} *sec*$^{-1}$)
0.94	1.51	2.60
0.94	1.51	2.35
1.39	2.00	2.46
1.39	2.00	2.25
1.39	2.49	2.32
1.45	2.00	2.56
1.45	2.00	2.40
1.41	2.49	2.18
1.85	2.48	2.38
1.88	2.48	2.39
1.88	2.48	2.20
		$k = (2.37 \pm 0.15) \cdot 10^4$

TABLE II

RATE CONSTANTS k FOR THE RATE LAW; $-d[DPPH]/dt = k[DPPH][Fe(III)]$

$[DPPH]_0 \cdot 10^5$ (*mol* l^{-1})	$[Fe(III)]_0 \cdot 10^5$ (*mol* l^{-1})	$k \cdot 10^{-4}$ (*mol* l^{-1} *sec*$^{-1}$)
0.96	1.22	4.68
0.95	1.82	4.20
1.42	1.58	4.33
1.43	1.81	4.15
1.43	1.81	4.62
1.41	1.97	4.09
1.42	2.41	4.27
1.88	1.97	4.80
1.89	2.40	5.02
1.89	2.40	4.85
		$k = (4.50 \pm 0.33) \cdot 10^4$

indicator in titrations with cerium(IV) in acetonitrile, it seemed worthwhile to study the reaction between this complex and cerium(IV). As is already mentioned in the literature[7], the redox system $Fe(III)(bipy)_3/Fe(II)(bipy)_3$ is reversible at the rotating platinum electrode in the absence of free bipyridyl. If the R.P.E. is kept at a potential of 0.9 V *vs.* $Ag/AgNO_3$ (0.01 *M* in acetonitrile), the anodic current observed during the reaction between cerium(IV) and $Fe(II)(bipy)_3$ exclusively corresponds to the oxidation of the iron(II) complex, as may be deduced from the position of the polarisation curves in the voltammogram. Because of the high reaction velocity, the rate constant could only be determined approximately, a 1 : 1 ratio and a second-order reaction path again being assumed (Table III).

Not only the knowledge of the reaction rate, but also information about the stability of the various oxidants is of paramount importance to the analyst.

The general procedure for the examination of the stability adopted in this

TABLE III

RATE CONSTANTS k FOR THE RATE LAW $-d[Fe(II)(bipy)_3]/dt = k[Fe(II)(bipy)_3][Ce(IV)]$

$[Fe(II)(bipy)_3]_0 \cdot 10^6$ (mol l^{-1})	$[Ce(IV)]_0 \cdot 10^6$ (mol l^{-1})	$k \cdot 10^{-5}$ (mol l^{-1} l sec^{-1})
6.9	7.9	5.8
6.9	7.9	5.2
8.8	9.8	4.8
8.8	9.8	5.3

TABLE IV

STABILITY OF SOME OXIDANTS DISSOLVED IN ACETONITRILE
(Relative percentage decrease in molarity during storage)

Days	*Cu(II)*		*Fe(III)*				*Ce(IV)*			
	0.01 *M*		0.01 *M*		0.05 *M*		0.01 *M*		0.05 *M*	
	a[a]	*b*[a]	*a*	*b*	*a*	*b*	*a*	*b*	*a*	*b*
1/4			5.7	1.5		0.3		4.2		2.0
1			8.2	7.2	1.4	0.9	72	9.6	39	
2			40	8.1	6.5	1.1	80	9.6	44	2.8
3			81	8.2	25.2	1.3	100		52	-2.8
4								9.6		2.8
5	0.2	0.2								
6			88		76	1.3				
7								10		4.0
8				13						
9						1.2				
10	0.4	0.3		39		1.3				
13								14		5.6
15	0.5	0.7								
17								21		8.0
22	0.6	0.6								

[a] a = Stored in daylight (summer season); b = stored in the dark.

work, involved taking samples after appropriate intervals, and titrating the lower valency state by a suitable method.

Copper(I). The sample was added to an acidified and de-aerated 0.5 *M* solution of iron(III) ammonium sulphate; the iron(II) formed by metathesis was then titrated with cerium(IV) sulphate[8] with biamperometric indication (applied tension 50 mV).

Iron(II). The sample was added to a 1 *M* sulphuric acid solution and biamperometrically titrated with cerium(IV)[9].

Cerium(III). The sample was added to a 40% potassium carbonate solution, previously de-aerated, and then titrated with potassium hexacyanoferrate(III)[10], again with a biamperometric end-point (applied tension 100 mV).

It was shown that the presence of acetonitrile does not interfere with these titrations; the possible presence of organic decomposition products was not investigated.

Table IV gives the results of this inquiry.

DISCUSSION

The simple procedure of amperometrically monitoring the concentration of one of the reactants, which was adopted during this investigation, proved to give satisfactory results. The rate constants found were even higher than those earlier reported in the literature[11].

It was found that the reaction in acetonitrile of DPPH with all the three oxidants in the presence of sodium perchlorate proceeds rapidly and according to a simple reaction rate equation. As is seen from Table V, there is no simple relation between the difference of the formal redox potentials of the two systems involved and the corresponding reaction rate constant. Thus far, cerium(IV) appears to be the most suitable of the three oxidants investigated, considered from the view-point of velocity; however, the number of reductants studied up to now is too small for generalisation.

The formal redox potentials from which the numerical values for ΔE were derived, originated from e.m.f. measurements as far as the DPP^+H/DPPH, Cu(II)/Cu(I), Fe(III)/Fe(II) and Ce(IV)/Ce(III) systems are concerned; for the $Co(III)(bipy)_3$/$Co(II)(bipy)_3$ and $Fe(III)(bipy)_3$/$Fe(II)(bipy)_3$ systems the corresponding voltammograms gave the information desired.

These data, together with information available from the literature are collected in Table VI.

The values for the formal redox potentials show large discrepancies between each other. Some of the reasons are the large influence exerted by the concentration and the nature[12,13,18,19] of the supporting electrolyte, the nature of the oxidized and reduced component of the redox couple, the presence of uncontrolled amounts of water[16], and sometimes, hydrolysis caused by traces of water still present in the solvent[15]. Experience has shown that a solution of an oxidant prepared electrolytically from the corresponding reductant behaves differently from a solution prepared by simply dissolving a salt of the higher valency state even after its (partial) dehydration[15]. Unfortunately, it happens rather often that literature does not contain enough information with respect to these points or that the experimental circumstances are not fully identical.

It was clearly shown that the more dilute the solution, the faster it decomposes.

TABLE V

DIFFERENCES OF FORMAL REDOX POTENTIALS, ΔE, AND CORRESPONDING RATE CONSTANTS, k

Reductant	*Oxidant*					
	Cu(II)		*Fe(III)*		*Ce(IV)*	
	ΔE (V)	k ($mol^{-1}\ l\ sec^{-1}$)	ΔE (V)	k ($mol^{-1}\ l\ sec^{-1}$)	ΔE (V)	k ($mol^{-1}\ l\ sec^{-1}$)
DPPH	0.26	$2.4 \cdot 10^4$	0.37	$4.5 \cdot 10^4$	0.39	$\sim 10^6$
$Co(II)(bipy)_3$	0.66	[a]	0.77	$3.4 \cdot 10^3$	0.79	$>10^7$
$Fe(II)(bipy)_3$	−0.03	[b]	0.07	[b]	0.09	$5.3 \cdot 10^5$

[a] Oxidation does not follow a simple second-order equation.
[b] Reaction does not proceed at all.

TABLE VI

COLLECTED VALUES FOR FORMAL AND HALF-WAVE POTENTIALS (*vs.* Ag/0.01 *M* Ag^+ in acetonitrile)

System	E_o		$(E_a)_{\frac{1}{2}}$		$(E_c)_{\frac{1}{2}}$	
	(V)	*Ref.*	*(V)*	*Ref.*	*(V)*	*Ref.*
DPPH	0.45	[a]	0.46	[a]	0.45	[f]
	0.41[b]	1				
Cu	0.660[b]	13	>0.8[e]	6	~0.4	6
	0.798	12				
	0.801	14				
	0.715	[a]				
Fe	1.57[d,e]	15	>1.0[c]	6	~0.5[c]	6
	1.1[d]	15	1.3[b]	16	0.8[b]	16
	0.82	[a]				
Ce	0.755[d]	14,17	1.1	[a]	0.55	[a]
	0.84	[a]				
$Co(bipy)_3$	0.050	[a]	0.075	6	0.025	6
$Fe(bipy)_3$	0.750	[a]	0.756	[f]	0.747	[f]

[a] Present investigation.
[b] Taking into account the value −0.290 V[18] for S.C.E. *vs.* Ag/0.01 *M* Ag^+ in acetonitrile.
[c] Anhydrous compounds.
[d] In the absence of inert electrolyte.
[e] Indistinct wave form.
[f] Unpublished results.

The striking detrimental influence of bright daylight on the stability makes it vital that solutions of the less stable reagents should be prepared in a room with diffuse light, and that the solutions must be stored in dark.

The excellent stability of copper(II) solutions has already been mentioned by Kratochvil *et al.*[20]. For this reason the present experiments were restricted to 0.01 *M* solutions.

A 0.1 *M* iron(III) perchlorate solution in acetonitrile shows a slightly inferior stability. The daily decrease in molarity was reported[15] to be only 0.1%.

Rao and Murthy's statement[4] concerning the stability of a cerium(IV) solution in acetonitrile could not be confirmed in detail; they claimed a higher stability for solutions stored in coloured bottles than was found here.

The authors thank Mr. den Os for performing the stability determinations. Two of us (I.N. and I.N.) wish to express their gratitude to the Chemistry Department of Delft University for assistantships, which made possible this investigation.

SUMMARY

A monoamperometric method with a rotating platinum electrode was used to acquire kinetic data for the oxidation of the free radical diphenylpicrylhydrazyl at 20°. The oxidants were copper(II) and iron(III) perchlorates and hexanitratocerate(IV); the medium was an anhydrous solution of sodium perchlorate in acetonitrile. The oxidations with copper(II) and iron(III) were shown to follow the second-order rate

law; the rate constants were $(2.37 \pm 0.15) \cdot 10^4$ and $(4.50 \pm 0.33) \cdot 10^4$ mol^{-1} l sec^{-1}, respectively. The oxidation by cerium(IV) is so fast that the result, $k = (1 \pm 0.6) \cdot 10^6$ has only approximate significance.

RÉSUMÉ

Une méthode monoampérique, avec électrode tournante de platine, est utilisée pour déterminer les valeurs cinétiques d'oxydation du radical libre diphénylpicrylhydrazyl à 20°. Les oxydants sont: perchlorates de cuivre(II) et de fer(III), et l'hexanitratocérate(IV); on travaille en milieu perchlorate de sodium anhydre dans l'acétonitrile. Les constantes de vitesse sont respectivement: $(2.37 \pm 0.15) \cdot 10^4$ et $(4.50 \pm 0.33) \cdot 10^4$ mol^{-1} l sec^{-1}. L'oxydation par le cérium(IV) est si rapide que le résultat: $k = (1 \pm 0.6) \cdot 10^6$ ne peut être qu'approximatif.

ZUSAMMENFASSUNG

Nach einer monoamperometrischen Methode mit einer rotierenden Platinelektrode wurden kinetische Daten für die Oxidation des freien Radikals Diphenylpicrylhydrazyl bei 20° erhalten. Als Oxidationsmittel wurden Kupfer(II)- und Eisen(III)-perchlorat sowie Hexanitratocerat(IV) verwendet; das Medium war eine wasserfreie Lösung von Natriumperchlorat in Acetonitril. Die Oxidationen mit Kupfer(II) und Eisen(III) folgten dem Geschwindigkeitsgesetz zweiter Ordnung; die Geschwindigkeitskonstanten waren $(2.37 \pm 0.15) \cdot 10^4$ bzw. $(4.50 \pm 0.33) \cdot 10^4$ mol^{-1} l sec^{-1}. Die Oxidation mit Cer(IV) verläuft so schnell, dass das Ergebnis $k = (1 \pm 0.6) \cdot 10^6$ nur als Näherungswert Bedeutung hat.

REFERENCES

1 E. Solon and A. J. Bard, *J. Amer. Chem. Soc.*, 86 (1964) 1926.
2 D. A. Hall and P. J. Elving, *Electrochim. Acta*, 12 (1967) 1363.
3 J. H. Sutcliffe and J. Walkley, *Nature*, 178 (1956) 999.
4 G. P. Rao and A. R. V. Murthy, *Z. Anal. Chem.*, 177 (1960) 86.
5 F. H. Burstall and R. S. Nyholm, *J. Chem. Soc.*, (1952) 3570.
6 I. Němec, H. L. Kies and I. Němcová, *Anal. Chim. Acta*, 49 (1970) 541.
7 N. Tanaka and Y. Sato, *Electrochim. Acta*, 13 (1968) 335.
8 I. M. Kolthoff and R. Belcher, *Volumetric Analysis*, Vol. III, Interscience, New York, 1957, p. 151.
9 Ref. 8, p. 147.
10 O. Tomíček, *Rec. Trav. Chim.*, 44 (1925) 410.
11 D. R. Rosseinsky and M. J. Nicol, *Electrochim. Acta*, 11 (1966) 1069; *Trans. Faraday Soc.*, 64 (1968) 2410.
12 B. Kratochvil, *Record Chem. Progr.*, 27 (1966) 253.
13 H. C. Mruthyunjaya and A. R. V. Murthy, *J. Electroanal. Chem.*, 18 (1967) 200.
14 B. Kratochvil, *Chem. Can.*, 20 (Dec. 1968) 19.
15 B. Kratochvil and R. Long, *Anal. Chem.*, 42 (1970) 43.
16 I. M. Kolthoff and J. F. Coetzee, *J. Amer. Chem. Soc.*, 79 (1967) 1852.
17 G. P. Rao and A. R. V. Murthy, *J. Phys. Chem.*, 86 (1964) 1573.
18 J. P. Billon, *J. Electroanal. Chem.*, 1 (1959/60) 486.
19 N. S. Moe, *Acta Chem. Scand.*, 19 (1965) 1023.
20 B. Kratochvil, D. A. Zatko and R. Markuszewski, *Anal. Chem.*, 38 (1966) 770.

Analytica Chimica Acta
Elsevier Publishing Company, Amsterdam
Printed in The Netherlands

DOSAGE DU MERCURE(II) EN PRESENCE D'ORGANOMERCURIELS

III. SÉPARATION SUR MICROBILLES DE VERRE ET DOSAGE PAR LA DITHIZONE

A. GORGIA ET D. MONNIER
Département de Chimie Minérale et Chimie Analytique, Université de Genève, Genève (Suisse)

(Reçu le 22 décembre 1970)

L'étude de divers complexants et réactifs du mercure(II), ainsi que celle du complexe NADH–Hg^{2+}, a montré que le dosage du mercure libre (ionique) en présence d'un grand excès d'organomercuriel ($[R–Hg–X] = 100\ [Hg^{2+}]$) exige une séparation préalable des deux constituants du mélange.

Pour réaliser cette séparation, nous avons fait appel à une technique d'adsorption de cations sur de la poudre ou des microbilles de verre[1] qui se comportent en l'occurrence comme une résine cationique.

Le but de cette étude était de rechercher les conditions permettant d'adsorber le mercure ionique sur le verre, sans adsorber, ni détruire les organomercuriels.

Le processus d'adsorption est discontinu, car il s'effectue par agitation d'une certaine quantité fixe de verre avec la solution aqueuse contenant le cation à séparer. Le dosage de l'élément ainsi séparé s'effectue après désorption au moyen d'un réactif approprié.

PARTIE EXPÉRIMENTALE

Matériel

Les microbilles de verre sodocalcique de 0.1 mm de diamètre (Centrale de Verreries, Aubervillier-Seine, France) sont lavées deux fois à l'eau bidistillée, puis traitées à la soude $5 \cdot 10^{-2}\ M$, rincées à l'eau bidistillée plusieurs fois et séchées dans une étuve.

La mesure de l'activité des solutions contenant le traceur (mercure-203) est effectuée au moyen de l'échelle Landis-Gyr. Les spectres-γ de ces solutions sont établis au moyen de l'analyseur Intertechnique-SA 40. La solution est mise en contact avec le verre au moyen d'un agitateur Hubsahl 275. La séparation des phases s'effectue avec la centrifugeuse Christ type V.J.1.

Pour la désorption du mercure(II), nous avons utilisé des tubes à centrifugation de 25 ml du type G.20 Jena Glass (Shott Mainz). La filtration des microbilles de verre est effectuée sur des filtres Millipores de 25 mm de diamètre (SMWP 025 0025 ea Sm 5μ white plain 25 mm).

Pour l'obtention des spectres u.v. des organomercuriels, la mesure de l'absorbance du dithizonate de mercure(II) et des dithizonates de R–Hg–X, nous avons utilisé le spectrophotomètre Beckman DB à double faisceau et balayage automatique et l'enregistreur Hitachi (cuves en quartz de 1 cm).

Les expériences ont été effectuées avec le mercure-203 et la Chlormérodrine marquée au mercure-203 (traceurs), soit avec du mercure non marqué et les organomercuriels habituellement utilisés lors des études précédantes[2].

Conditions d'adsorption sélective du mercure(II)

En pH acide (pH 4), la séparation des ions mercure(II) sur microbilles de verre en présence d'organomercuriels ne peut pas s'effectuer pour deux raisons:

1. par la compétition des protons et du mercure(II) en ce qui concerne l'échange sur le verre;

2. par le fait qu'en milieu acide, les organomercuriels se décomposent partiellement avec libération du mercure organique[2].

D'autre part, la solution doit être tamponnée avant l'agitation à cause des propriétés alcalines du verre[1].

Aux pH voisins de 7, milieu tampon (KH_2PO_4–Na_2HPO_4 10^{-1} M), le rendement d'extraction (adsorption) est de 50% pour du nitrate de mercure(II) $1.5 \cdot 10^{-6}$ M, ce qui peut s'expliquer par la présence dans la solution de $Hg(OH)_2$, non adsorbable par le verre.

Aux pH supérieurs à 8, le rendement diminue à 30% comme nous l'avons constaté avec un tampon acide–borique (pH 8) et borax–soude (pH 10), car le mercure(II) se trouve principalent sous forme $Hg(OH)_2$.

La charge des ions mercure(II) complexés devant être positive pour que cet ion soit échangé sur le verre, la condition sine qua non est de maintenir le mercure(II) sous forme cationique ce qui est possible en présence d'éthylènediamine car ce composé forme des complexes cationiques très stables avec le mercure(II). On observe en effet une forte augmentation du rendement d'adsorption du mercure sur le verre en présence de ce complexant. Nous avons d'autre part choisi l'éthylènediamine (EDA) de préférence à d'autres complexants car nous avons constaté que ce ligand ne libère pas le mercure organique des organomercuriels entre pH 5 et 7, condition nécessaire pour une séparation Hg^{2+}–organomercuriel.

L'emploi d'éthylènediamine en milieu tampon phosphate (pH 7.1) permet d'adsorber sur le verre en une seule opération, 85% du Hg^{2+} ($[Hg^{2+}]$ variant de 10^{-6} à $1.5 \cdot 10^{-5}$ M) sous forme de complexes chargés[1] $[Hg(EDA)OH]^+$ et $[Hg(EDA)_2]^{2+}$. Il a été donc possible dans ces conditions de mettre au point une méthode de séparation et de dosage du mercure(II) ionique en présence d'organomercuriels, en procédant à une seule extraction sur le verre grâce à la reproductibilité du rendement d'adsorption (85 ± 1.9%).

Mode opératoire

Adsorption du mercure(II) ionique sur le verre. Les solutions sont préparées dans des tubes en polystyrène de 20 ml. On introduit 1 ml d'éthylènediamine $2 \cdot 10^{-3}$ M, 1 ml de tampon phosphate pH 7.1 (10^{-1} M), et 8 ml de solution à analyser. Après adjonction de 2 g de microbilles de verre les solutions sont agitées pendant 30 min au moyen d'un agitateur Hubsahl 275[1]. Pour 10^{-6} $M \leqq [Hg^{2+}] \leqq 2 \cdot 10^{-5}$ M et $0 \leqq [R\text{–}Hg\text{–}X] \leqq 10^{-3}$ M, 85% du mercure(II) ionique sont adsorbes sur le verre.

Séparation des phases. Chaque solution est filtrée sous vide sur filtre Millipore. Le verre est lavé sur ce même filtre 4 fois avec 5 ml d'une solution $2 \cdot 10^{-4}$ M en éthylènediamine et 10^{-2} M en tampon phosphate (pH 7). Ces lavages sont nécessaires

pour éliminer toute trace d'organomercuriel resté dans les interstices du verre.

Désorption du mercure(II). Le filtre Millipore avec les microbilles de verre sont introduits dans des tubes à centrifugation de 25 ml. On ajoute 5 ml d'une solution d'acide sulphurique 2 *N*, 4 ml d'eau et 1 ml d'acide acétique 6 *N*, puis 5 ml d'une solution de dithizone 0.001% dans du CCl_4. Les tubes sont agités 1 min et centrifugés 3 min à 2500 r.p.m.

On prélève 4 ml de la phase organique et on effectue une deuxième désorption: 3 ml de la solution de dithizone sont ajoutés dans chaque tube à centrifugation contenant les microbilles de verre, la phase aqueuse et le millilitre de dithizone restant de la première extraction. Après agitation d'une minute et centrifugation de 3 min, on prélève 3 ml de la phase organique qu'on ajoute aux 4 ml de la première extraction. On répète cette opération une troisième fois.

Après cette troisième désorption, on prélève 3 ml de la phase organique qu'on additionne aux 7 ml des 2 premières désorptions. Ainsi, le volume final de la phase organique est de 10 ml. Cette triple désorption permet de récupérer les 70% de mercure(II) adsorbé.

Dosage du mercure par spectrophotométrie d'absorption. L'absorbance de la phase organique est lue à 490 nm et la concentration du mercure(II) est calculée par rapport à une courbe d'étalonnage selon la méthode habituelle[3], établie dans les mêmes conditions: adsorption–lavage de microbilles de verre–désorption.

RÉSULTATS EXPÉRIMENTAUX

Pour différents organomercuriels, il a été possible de doser des quantités de mercure(II) de l'ordre du $\mu g\ ml^{-1}$ à $\pm 10\%$ près, en présence de 100 fois plus d'organomercuriel, en tenant compte du mercure(II) non adsorbé lors de la première étape de l'analyse (extraction sur microbilles de verre) et des pertes lors du lavage.

Cependant malgré les lavages répétés des microbilles de verre, moins de 1% d'organomercuriel environ sont retenus (adsorbés) sur le verre et passent dans la phase organique lors de l'extraction. L'emploi d'organomercuriels marqués au mercure-203 lors des essais préliminaires (mesure de l'activité et enregistrement des spectres-γ des solutions à analyser avant et après agitation avec les microbilles de verre), ne permette pas une évaluation quantitative de cette adsorption, à cause de la faible activité spécifique de ces composés.

Ainsi les dithizonates d'organomercuriels présentent une absorbance à 490 nm semblable à celle de dithizonate de mercure(II)[4], interférant avec le dosage du mercure ionique et nécessitant donc la détermination d'un facteur correctif.

Cette correction se fait par l'emploi d'un standard d'organomercuriel pur traité en parallèle avec l'échantillon à analyser. L'influence des traces d'organomercuriels peut ainsi être déterminée lors du calcul de la concentration du mercure(II) ionique par référence à la droite d'étalonnage.

Ainsi malgré le nombre des étapes impliquées dans cette méthode, les opérations à effectuer sont simples et peuvent être realisées dans un temps relativement court, permettant ainsi l'analyse de séries d'échantillons en parallèle.

Un exemple typique de ce dosage est représenté sur la Fig. 1 et le Tableau I.

L'absorbance due à la présence d'organomercuriel (en traces), est transformée en "équivalents" de mercure. Ainsi pour la solution contenant initialement la Chlor-

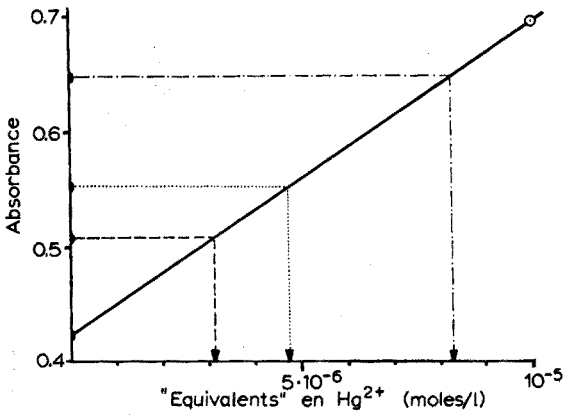

Fig. 1. "Droite de référence" pour le dosage du mercure(II) en présence de Chlormérodrine (CME), après séparation sur microbilles de verre. (-----) [CME] = $5 \cdot 10^{-4}$ M; (·····) [Hg^{2+}] = $5 \cdot 10^{-6}$ M; (-·-·-·-·-) [CME] = $5 \cdot 10^{-4}$ M + [Hg^{2+}] = $5 \cdot 10^{-6}$ M.

TABLEAU I

RÉSULTATS EXPÉRIMENTAUX DU DOSAGE DE MERCURE(II) EN PRÉSENCE DE CHLORMÉRODRINE (CME)

Solutions initiales (M)		*Après séparation*			
		$A_{490\ nm}$ *moyen*	*"Equivalents" de* Hg^{2+} *(M)*	*N*	*Ecart type rélatif (%)*
Hg^{2+}	$5 \cdot 10^{-6}$	0.552	$4.79 \cdot 10^{-6}$	5	±2.67
CME	$5 \cdot 10^{-4}$	0.508	$3.15 \cdot 10^{-6}$	5	±2.57
Hg^{2+} +CME	$5 \cdot 10^{-6}$ $5 \cdot 10^{-6}$	0.643	$8.17 \cdot 10^{-6}$	6	±2.35

mérodrine (CME), l'absorbance de 0.508, obtenue après extraction sur le verre, correspond à un "équivalent" de mercure(II) de $3.15 \cdot 10^{-6}$ M sur la droite d'étalonnage.

Pour calculer la concentration de mercure ionique dans mélange mercure(II)/organomercuriel, l'absorbance obtenue est transformée en "équivalent" de mercure ($A = 0.643 \rightarrow$ concentration "d'équivalent" de $Hg^{2+} = 8.17 \cdot 10^{-6}$ M). De la valeur ainsi obtenue on soustrait "l'équivalent" de mercure pour l'organomercuriel seul afin d'obtenir la concentration de mercure(II) ionique initialement présente dans le mélange:

$$8.17 \cdot 10^{-6}\ M - 3.15 \cdot 10^{-6}\ M = 5.02 \cdot 10^{-6}\ M$$

La reproductibilité est bonne puisque les écarts types rélatifs sont de l'ordre de ±2.5%.

CONCLUSION

Cette méthode permet donc de doser d'une manière satisfaisante $5 \cdot 10^{-6}$ mol l^{-1} de mercure(II) soit 1 μg ml^{-1}, en présence de $5 \cdot 10^{-4}$ mol l^{-1} d'organomercuriel, soit approximativement 2 mg ml^{-1}.

RÉSUMÉ

Une méthode pour le dosage du mercure ionique (de l'ordre de μg ml^{-1}) en présence d'un excès d'organomercuriel ([R–Hg–X] = 100[Hg^{2+}]) est décrite. Le mercure(II) est adsorbé sélectivement sur microbilles de verre sodocalcique dans un milieu tampon phosphate 0.1 *M* (pH 7.1)–éthylènediamine $2 \cdot 10^{-4}$ *M*. Les microbilles sont lavées avec le même tampon. Le mercure(II) est désorbé avec un système biphasique H_2SO_4–dithizone dans du CCl_4. Le mercure(II) est dosé par spectrophotométrie d'absorption à 490 nm et sa concentration initiale dans le mélange Hg^{2+}/organomercuriel est calculée par rapport à une droite d'étalonnage établie dans les mêmes conditions.

SUMMARY

A method is described for the determination of ionic mercury(II) (*ca.* 1 μg ml^{-1}) in the presence of excess organomercurial ([R–Hg–X] = 100[Hg^{2+}]). The mercury(II) is selectively adsorbed on microbeads of soda–calcium glass in 0.1 *M* phosphate buffer (pH 7.1) containing $2 \cdot 10^{-4}$ *M* ethylenediamine. The microbeads are washed with the same medium. Mercury(II) is desorbed with a two-phase sulfuric acid–dithizone–carbon tetrachloride system, and determined spectrophotometrically at 490 nm; the initial concentration in the organomercurial–mercury(II) solution is determined by reference to a calibration curve established under the same conditions.

ZUSAMMENFASSUNG

Es wird eine Methode für die Bestimmung von ionischem Quecksilber(II) (*ca.* 1 μg ml^{-1}) in Gegenwart überschüssiger Organoquecksilberverbindungen ([R–Hg–X] = 100[Hg^{2+}]) beschrieben. Das Quecksilber(II) wird in 0.1 *M* Phosphatpuffer (pH 7.1) mit einem Gehalt von $2 \cdot 10^{-4}$ *M* Äthylendiamin an Mikroperlen aus Natrium–Calcium-Glas selektiv adsorbiert. Die Mikroperlen werden mit demselben Medium gewaschen. Das Quecksilber(II) wird mit einem zweiphasigen Schwefelsäure–Dithizon–Tetrachlorkohlenstoff-Gemisch desorbiert und spektrophotometrisch bei 490 nm bestimmt. Die Ausgangskonzentration in der Organoquecksilber-Quecksilber(II)-Lösung wird durch Vergleich mit einer unter denselben Bedingungen erstellten Eichkurve bestimmt.

BIBLIOGRAPHIE

1 N. LAKHOUA, *Thèse No. 1514*, Université de Genève, 1970.
2 D. MONNIER ET A. GORGIA, *Anal. Chim. Acta*, 54 (1971) 497.
3 E. B. SANDELL, *Colorimetric Determination of Traces of Metals*, 1959.
4 H. M. N. H. IRVING ET A. M. KIWAN, *Anal. Chim. Acta*, 45 (1969) 255.

Analytica Chimica Acta
Elsevier Publishing Company, Amsterdam
Printed in The Netherlands

ETUDE ANALYTIQUE DE LA SEPARATION HAFNIUM–SCANDIUM SUR RESINE ANIONIQUE

LUCETTE BALSENC, R. BEELER, W. HAERDI ET D. MONNIER

Département de Chimie Analytique et Minérale et Département de Physique Nucléaire et Corpusculaire, Université de Genève, 1211-Genève-4 (Suisse)

(Reçu le 30 décembre 1970)

Bien que la fixation du hafnium et du scandium sur les résines anioniques ait été étudiée par un certain nombre d'auteurs[1-7], nous n'avons pas trouvé dans la littérature d'étude théorique concernant la fixation simultanée et la séparation de ces deux éléments l'un de l'autre. Nous avons donc consacré ce travail à ces problèmes.

Notre étude a porté sur la formation des sulfates complexes anioniques de hafnium et de scandium et sur le partage de ces derniers entre une résine chargée d'ions sulfate et une solution sulfurique.

Nous avons établi une relation donnant le coefficient de distribution de ces métaux sur la résine en fonction de différents facteurs (concentration du ligand, pH, etc.). Des équations sont proposées qui donnent la variation du coefficient de distribution conditionnel du hafnium et du scandium à pH et à force ionique constants, en fonction de la concentration du ligand.

Des courbes de distribution ont été calculées à partir des équations établies et comparées aux courbes expérimentales.

Des courbes expérimentales ont été établies donnant le coefficient de distribution conditionnel des deux métaux en fonction du pH.

ÉCHANGE DES COMPLEXES SUR UNE RÉSINE

Complexation

Soit un ion métallique M et un ligand L formant un complexe ML_n selon l'équilibre*:

$$M + nL \rightleftharpoons ML_n$$

dont la constante de stabilité globale apparente est β_n.

Les complexes mononucléaires se formant généralement par étapes, nous trouverons en solution non seulement ML_n mais encore tous les complexes successifs $ML, ML_2 \ldots ML_{n-1}$.

Equilibre d'échange sur la résine

Si la formation de complexe entre un ion central M et un ligand L conduit à un complexe chargé négativement ML_n, ce complexe peut se fixer sur une résine

* Dans la suite de ce travail, nous n'indiquerons pas le signe des ions.

anionique selon:

$$ML_n + X_R \rightleftharpoons ML_{nR} + X$$

Nous supposons que ML_n est le seul ion négatif en solution et que X a la même charge.

ML_n = ion complexe en solution à fixer sur la résine.
ML_{nR} = ion complexe fixé sur la résine
X_R = résine sous sa forme primitive.
X = ion mobile de la résine en solution.

En appliquant la loi d'action des masses à cet équilibre:

$$\frac{[ML_n]_R[X]}{[ML_n]\cdot[X]_R} = K_X^{ML_n} \tag{1}$$

$K_X^{ML_n}$ = constante d'équilibre de l'échange pour la résine considérée.

Dans l'expression des concentrations l'indice R indique que la particule est dans la phase résine (en meq g^{-1} de résine sèche); les concentrations des particules en solution (en meq ml^{-1} de solution) ne portent pas d'indice.

La répartition du complexe ML_n entre la résine et la solution est mesurée par le coefficient de distribution D_{ML_n}

$$D_{ML_n} = \frac{[ML_n]_R}{[ML_n]} = \frac{[X]_R}{[X]}\cdot K_X^{ML_n} \tag{2}$$

Si, comme nous l'avons admis, M ne forme qu'un complexe chargé négativement ML_n, et que $n=2$, seule cette particule est fixée sur la résine, alors qu'existent en solution tous les complexes successifs de ce métal. Le coefficient de distribution du métal D_M est donné par:

$$D_M = \frac{\text{concentration totale du métal sur la résine}}{\text{concentration totale du métal dans la solution}} = \frac{[M]_{TR}}{[M]_{TS}} \tag{3}$$

$$[M]_T = [M]_{TS} + [M]_{TR}$$

dans nos conditions: $[M]_{TR} = [ML_n]_R$

$$D_M = \frac{[ML_n]_R}{[M]\left(1 + \sum_{n=1}^{n=n}\beta_n[L]^n\right)} = \frac{D_{ML_n}\cdot\beta_n[L]^n}{[M]\left(1 + \sum_{n=1}^{n=n}\beta_n[L]^n\right)} \tag{4}$$

à condition que ML_n soit le dernier complexe.

L'équation (2) n'est valable que si le complexe ML_n n'est impliqué dans aucune réaction secondaire. Dans le cas contraire, si ML_n forme un autre complexe du type MAL_n (complexe mixte ne se fixant pas sur la résine) par exemple, nous définirons un nouveau coefficient de distribution dit "conditionnel" D'_{ML_n}

$$D'_{ML_n} = \frac{[ML_n]_R}{[ML'_n]} \quad \text{où} \quad [ML'_n] = \alpha_{ML_{n(A)}}\cdot[ML_n] \tag{5}$$

$[ML'_n]$ = concentration dans la solution du complexe sous toutes ses formes.
$\alpha_{ML_{n(A)}}$ = coefficient de réaction secondaire de Ringbom–Schwarzenbach.

Par souci de simplification, nous allons employer les symboles suivants dans les équations mathématiques:

$M_I = Hf^{4+}$, $M_{II} = Sc^{3+}$, et $L = SO_4^{2-}$.
$X = SO_4^{2-}$ en solution provenant de la résine
$X_R = SO_4^{2-}$ fixé sur la résine
k_1, k_2, k_3 = constantes apparentes successives de stabilité
$\beta_1, \beta_2, \beta_3$ = constantes apparentes globales de stabilité

Dans les équations chimiques, nous mettrons nommément les symboles des particules qui réagissent.

HAFNIUM

Fixation du hafnium en fonction de la concentration en sulfate

Nous admettons que le seul complexe négatif est $[Hf(SO_4)_3]^{2-}$, la fixation a lieu à pH constant, et le pH est tel qu'il ne se forme ni $[Hf(SO_4)_3]H^-$ ni $[Hf(SO_4)_3]H_2$.

Seul le complexe $Hf(SO_4)_3^{2-}$ chargé négativement se fixe sur la résine anionique selon l'équilibre d'échange:

$$Hf(SO_4)_3^{2-} + SO_{4\,R}^{2-} \rightleftharpoons Hf(SO_4)_{3\,R}^{2-} + SO_4^{2-} \quad (6)$$

Coefficient de distribution du hafnium

$$D'_{M_I} = ([X]_{R/[X]}) K_X^{M_I L_3} \cdot \beta_3 [L]^3 / \alpha_{M_{I(L)}} \quad (7)$$

Dans l'équilibre d'échange sur la résine, nous n'avons pas pris en considération le passage éventuel dans la résine, du complexe ML_2 par un équilibre de Donnan, suivi de la formation d'un complexe anionique dans la résine elle-même.

$$Hf(SO_4)_2 \rightleftharpoons Hf(SO_4)_{2\,R} \quad (8)$$

$$Hf(SO_4)_{2\,R} + SO_{4\,R} \rightleftharpoons [Hf(SO_4)_3]_R^{2-} \quad (9)$$

car nous avons constaté expérimentalement que, pour des concentrations de ligand correspondant à D'_M maximum (Fig. 1) la plus grande partie du hafnium se trouve déjà sous forme de complexe anionique: en effet, lors d'une électrolyse, le métal en solution migre vers l'anode.

Discussion

Des valeurs du coefficient de distribution apparent du hafnium (D'_{M_I}), calculées au moyen de l'éqn. (7) ont été portées sur un graphique logarithmique, en fonction de la concentration en sulfate. La courbe ainsi tracée ne correspond pas exactement à la courbe obtenue expérimentalement (Fig. 1a) et cette différence ne semble pas due à des erreurs de mesure. En reportant les mêmes courbes sur un graphique linéaire, nous constatons que la courbe expérimentale ne peut être approximée correctement par des termes s'étendant jusqu'au 3ème degré, mais bien par une équation de degré supérieur (Fig. 1b).

Nous formulons à ce propos l'hypothèse suivante : en présence d'un grand excès d'ions sulfate et en milieu relativement peu acide, il y aurait formation d'un second complexe anionique du hafnium, vraisemblablement du type $Hf(SO_4)_4^{4-}$. Celui-ci n'est pas décrit dans la littérature mais des complexes analogues ont été mis en évidence pour le zirconium et le thorium.

Par souci de simplification, nous désignerons, dans la suite de ce travail le complex hafnium : sulfate 1 : 4 par le symbole $[Hf(SO_4)_4]^{4-}$. Toutefois, il est probable que ce complexe ne revêt pas une telle forme, mais plutôt celle d'un sel basique, une partie des charges négatives étant portée par des oxygènes ou des hydroxyles. Il serait également vraisemblable que nous nous trouvions en présence de polymères.

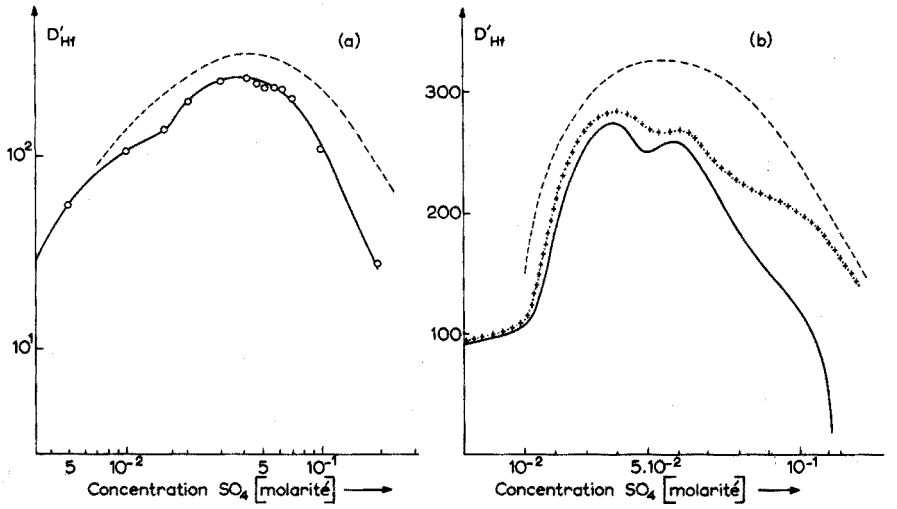

Fig. 1. Courbes expérimentales et calculées de $[SO_4]/D'_{Hf}$. (a) Courbe : (——) expérimentale, (------) calculée d'après éqn. (7). (b) Courbe : (——) expérimentale, (------) calculée d'après éqn. (7), (· + · + ·) calculée d'après éqn. (14).

Deux constatations expérimentales viennent appuyer cette hypothèse : en traçant la courbe de distribution du hafnium pour des concentrations élevées d'acide, on constate que :

1. Une augmentation de la concentration des protons par adjonction d'acide perchlorique ne modifie pas la forme de la courbe d'élution alors qu'une augmentation de la concentration des protons par adjonction d'acide sulfurique provoque une augmentation de la valeur du coefficient de distribution (Fig. 2).

Dans la première partie de la courbe (zone I), il y aurait formation successive des complexes $[Hf(SO_4)_3]H^-$ et $[Hf(SO_4)_3]H_2$; les deux courbes se superposent. Dans la zone II, nous nous trouverions en présence du complexe $[Hf(SO_4)_3]H_2$. On observe aussi la superposition des courbes. Finalement, dans la zone III, il y aurait, avec l'acide sulfurique, apparition d'un complexe du type $[Hf(SO_4)_4]H_n^{4-n}$, qui viendrait se fixer sur la résine, alors qu'en milieu perchlorique, la courbe est confondue avec les abscisses.

2. En procédant à une électrolyse, nous avons constaté que pour une même concentration de hafnium.

en milieu H_2SO_4 0.25 *M*, il y a migration du hafnium vers l'anode ($[Hf(SO_4)_3]^{2-}$ et $[Hf(SO_4)_3]H^-$),

en milieu H_2SO_4 1.5 *M*, il n'y a pour ainsi dire plus de migration ($[Hf\text{-}(SO_4)_3]H_2$),

en milieu H_2SO_4 *M*, il y a migration du hafnium vers l'anode ($[Hf(SO_4)_4]\text{-}H_n^{4-n}$).

En outre, il ne semble pas que dans nos conditions de travail, le hafnium complexé se trouve sous forme de sulfate de hafnyle; ce dernier, en milieu très acide, subissant une protolyse:

$$[HfO(SO_4)_2 \cdot 3H_2O]^{2-} + 2H^+ \rightarrow Hf(SO_4)_2 + 4H_2O \qquad (10)$$

Nous n'observerions pas d'augmentation de la valeur du coefficient D'_{M_I}, alors que la concentration de l'acide sulfurique augmente (Fig. 2).

En ce qui concerne l'élution, certains auteurs supposent qu'elle a lieu de la

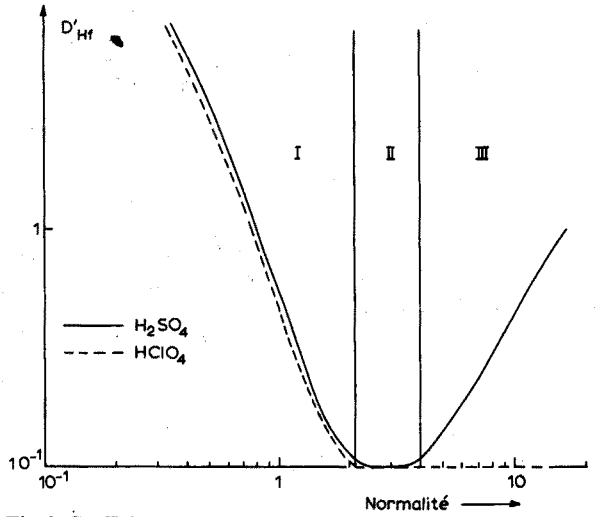

Fig. 2. Coefficient de distribution apparent du hafnium en fonction de la concentration en acide sulfurique ou perchlorique.

manière suivante:

$$[Hf(SO_4)_3]_R^{2-} + H^+ \rightleftharpoons Hf(SO_4)_2 + SO_4H_R^- \qquad (11)$$

$$Hf(SO_4)_{2\,R} + H^+ \rightleftharpoons HfSO_4^{2+} + SO_4H_R^- \qquad (12)$$

Cette hypothèse ne se confirme pas dans nos conditions car on devrait observer, lors de l'électrolyse en milieu très acide, une migration partielle du hafnium vers la cathode, ce qui n'est pas le cas.

Nous avons établi une nouvelle equation (14) reliant le coefficient de distribution apparent du hafnium à la concentration en sulfate de la solution. Cette relation tient compte de la présence des 4 complexes sulfate du hafnium.

Aux équilibres en solution (10), (11) et (12) vient s'ajouter:

$$Hf^{4+} + 4SO_4^{2-} \rightleftharpoons Hf(SO_4)_4^{4-} \qquad (13)$$

ce qui donne, pour le coefficient D'_{M_I}:

$$D'_{M_I} = \frac{[M_IL_3]_R + [M_IL_4]_R}{[M_I] + [M_IL] + [M_IL_2] + [M_IL_3] + [M_IL_4]}$$

$$D'_{M_I} = \left[\left(\frac{[X]_R}{[X]} \right) \cdot K_X^{ML_3} \frac{\beta_3}{\beta_4[L]} + \left(\frac{[X]_R}{[X]} \right)^2 \cdot K_{2X}^{ML_4} \right] \cdot \frac{\beta_4[L]^4}{\alpha_{M_IL}} \qquad (14)$$

Une courbe de distribution, tracée en portant sur un graphique des valeurs du coefficient de distribution conditionnel D'_{M_I} calculées au moyen de l'équation (14) en tenant compte des activités, en fonction de la concentration en sulfate de la solution, est donné dans la Fig. 1b. Elle est semblable à la courbe expérimentale sauf pour des concentrations élevées de sulfate. Cet écart provient probablement du fait que nous n'avons pas tenu compte dans nos calculs de l'action antagoniste des ions sulfate, venant se fixer compétitivement sur la résine.

Fixation du hafnium en fonction du pH

Nous avons constaté expérimentalement que le coefficient de distribution des complexes hafnium–sulfate varie comme l'inverse de la concentration des ions hydrogène dans la solution. Toutefois cette décroissance n'est pas linéaire car plusieurs facteurs tendent à abaisser la valeur de D'_{M_I} lorsque le pH diminue[9].

Conclusion

La fixation des sulfato-complexes du hafnium sur une résine anionique de forme sulfate, en milieu sulfurique est fonction à la fois de la concentration des ions sulfate et du pH de la solution. Le coefficient de distribution du métal varie entre certains limites en raison inverse de la concentration des ions sulfate et hydrogène.

Les conditions les plus favorables à la fixation et à l'élution de ces complexes ont été déterminées expérimentalement. Elles sont les suivantes:

Fixation: Concentration de sulfate comprise entre $2 \cdot 10^{-2}$ *M* et 10^{-1} *M*.
pH compris entre 3.5 et 4.5.

Elution: Concentration d'hydrogène comprise entre 2 *N* et 4 *N*.

SCANDIUM

Une étude analogue a été faite pour le scandium.

Nous avons établi des équations reliant le coefficient de distribution du métal à la concentration en sulfate de la solution.

Nous avons considéré trois complexes du scandium: $ScSO_4^+$, $Sc(SO_4)_2^-$ et $Sc(SO_4)_3^{3-}$. Nous n'avons pas tenu compte de la formation éventuelle du complexe polynucléaire $Sc[Sc(SO_4)_3]$. Dans nos conditions de travail, le métal en solution très diluée est mis en présence d'une solution concentrée de ligand; nous pouvons donc supposer que le "mur mononucléaire" est atteint.

Nous avons montré qu'en l'absence d'ions hydrogène libres le coefficient de distribution du scandium varie en raison inverse de la concentration des ions sulfate dans la solution. Cette diminution est probablement due à l'adsorption compétitive de l'ion SO_4^{2-} et du complexe $Sc(SO_4)_n^{p-}$ sur la résine.

Mais, en présence d'hydrogène libre dans la solution, une augmentation de la concentration du sulfate, en contribuant à abaisser la concentration de l'ion H^+ par

$$H^+ + SO_4^{2-} \rightleftharpoons SO_4H^-$$

favorise l'adsorption, ce qui a déjà été constaté expérimentalement par Hamaguchi *et al.*[6].

Fixation du scandium en fonction de la concentration en sulfate

La fixation a lieu à pH constant. Pour nos calculs (éqn. (18), fig. 3), nous admettons qu'il n'y a pas d'hydrogène libre en solution.

Equilibres d'échange sur la résine

$$[Sc(SO_4)_3]^{3-} + \tfrac{3}{2}SO^{2-}_{4R} \rightleftharpoons [Sc(SO_4)_3]^{3-}_R + \tfrac{3}{2}SO_4^{2-} \quad (14)$$

$$[Sc(SO_4)_2]^{-} + \tfrac{1}{2}SO^{2-}_{4R} \rightleftharpoons [Sc(SO_4)_2]^{-}_R + \tfrac{1}{2}SO_4^{2-} \quad (15)$$

Coefficient de distribution de $[Sc(SO_4)_3]^{3-}$

$$D_{M_{II}L_3} = ([X]_R/[X])^{\frac{3}{2}} \cdot K^{M_{II}L_3}_{\frac{3}{2}X} \quad (16)$$

Coefficient de distribution de $[Sc(SO_4)_2]^{-}$

$$D_{M_{II}L_2} = ([X]_R/[X])^{\frac{1}{2}} \cdot K^{M_{II}L_2}_{\frac{1}{2}X} \quad (17)$$

Coefficient de distribution du métal

$$D'_{M_{II}} = \frac{\beta_3[L]^3}{1+\beta_1[L]+\beta_2[L]^2+\beta_3[L]^3}\left[\left(\frac{[X]_R}{[X]}\right)^{\frac{3}{2}} \cdot K^{M_{II}L_3}_{\frac{3}{2}X} + \frac{1}{k_3[L]}\left(\frac{[X]_R}{[X]}\right)^{\frac{1}{2}} \cdot K^{M_{II}L_2}_{\frac{1}{2}X}\right] \quad (18)$$

Fixation du scandium en fonction du pH

Le coefficient de distribution total des complexes diminue avec le pH, chacun des coefficients de distribution partiels étant une fonction inverse de la concentration en hydrogène de la solution.

Nous n'avons pas calculé les valeurs de $D'_{M_{II}}$, faute de connaître les constantes $K^{M_{II}L_3H}$... etc.; en revanche nous avons tracé la courbe de distribution en portant les valeurs du coefficient de distribution $D'_{M_{II}}$ déterminées expérimentalement, en fonction du pH, la concentration du sulfate demeurant constante.

On remarque qu'un faible accroissement de la concentration des ions hydrogène libres en solution provoque une chute brutale du coefficient de distribution (Fig. 4).

Conclusions

Le coefficient de distribution apparent du scandium diminue lorsque la concentration des ions sulfate et hydrogène présents en solution, s'accroît.

Les conditions les plus favorables à la fixation et à l'élution du scandium sur une résine anionique de forme sulfate ont été déterminées expérimentalement:

Fixation: concentration de sulfate 10^{-1} M;
concentration d'hydrogène $\leqslant 10^{-3}$ N.

Elution: concentration d'hydrogène $\geqslant 0.4$ N.

CONCLUSIONS GÉNÉRALES

Les coefficients de distribution apparents du hafnium et du scandium sur une résine anionique de forme sulfate, sont fonction de la concentration en sulfate de la solution.

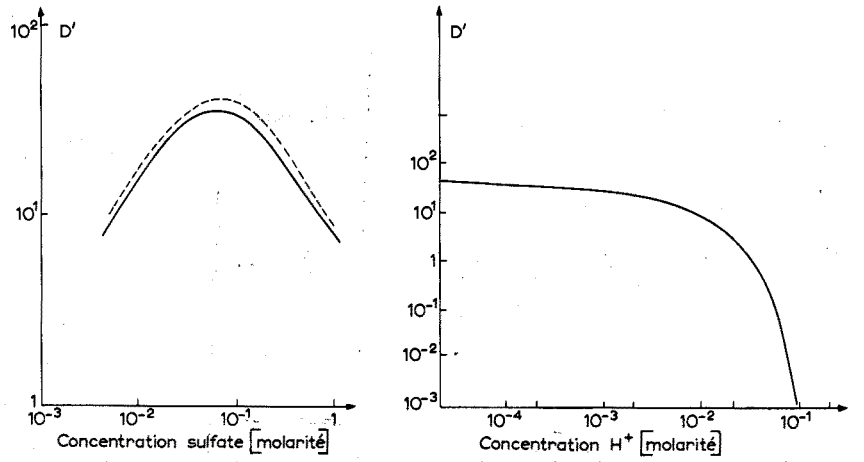

Fig. 3. Coefficient de distribution apparent du scandium en fonction de la concentration en sulfate (pH constant). (——) Courbe expérimentale, (------) courbe calculée.

Fig. 4. Idem en fonction de la concentration des ions hydrogène ($[SO_4]$ constante).

La concentration optimum en sulfate est plus faible pour le hafnium que pour le scandium. Une dilution de la solution favorise la fixation de l'hafnium aux dépens du scandium. Les coefficients de distribution du hafnium et du scandium diminuent tous deux avec le pH, mais D'_{Sc} diminue beaucoup plus rapidement que D'_{Hf}. Nous avons donc intérêt à effectuer la séparation à un pH suffisamment bas pour que le coefficient du scandium soit abaissé au maximum sans que celui du hafnium soit modifié.

Nous remercions le Fonds National Suisse qui nous a permis d'entreprendre ce travail.

RÉSUMÉ

Le partage des sulfo-complexes de hafnium(IV) et de scandium(III) entre une solution sulfurique et une résine anionique de forme sulfate a été étudié. Des équations liant la variation du coefficient de distribution à la concentration du ligand ont été établies pour les deux métaux; la nature des complexes formés en solution est discutée. Pour l'hafnium, les conditions les plus favorables de fixation sont les suivantes: concentrations du sulfate comprises entre $2 \cdot 10^{-2}$ et 10^{-1} M à pH 3.5–4.5. Pour l'élution, on utilise de préférence l'acide sulfurique $2N$–$4N$. Pour le scandium, on obtient l'adsorption avec une solution de sulfate 10^{-1} M à pH 3. Les concentrations d'acide sulfurique supérieures à 0.4 N sont recommandées pour l'élution.

SUMMARY

The distribution of hafnium(IV) and scandium(III) sulphate complexes between an anion-exchange resin in the sulphate form, and sulphuric acid solutions has been studied. Equations giving the variation of the distribution ratio with the ligand concentration have been established for both metals; the sulphate complexes

formed in solution are discussed. For hafnium, the optimal conditions for adsorption involve sulphate concentrations of $2 \cdot 10^{-2}$–10^{-1} *M* at pH 3.5–4.5; for elution 2–4 *N* sulphuric acid should be used. For scandium, optimal adsorption is obtained with 10^{-1} *M* sulphate at pH 3, and $\geqslant 0.4$ *N* sulphuric acid is best for elution.

ZUSAMMENFASSUNG

Die Verteilung von Hafnium(IV)- und Scandium(III)-Sulfat-Komplexen zwischen einem Anionenaustauscherharz in der Sulfatform und schwefelsauren Lösungen wurde untersucht. Für beide Metalle sind Gleichungen für die Änderung des Verteilungsverhältnisses mit der Ligandkonzentration aufgestellt worden; die in der Lösung gebildeten Sulfatkomplexe werden diskutiert. Für die Adsorption von Hafnium sind die optimalen Bedingungen: $2 \cdot 10^{-2}$–10^{-1} *M* Sulfat bei pH 3.5–4.5; für die Elution eignet sich 2–4 *N* Schwefelsäure. Für Scandium wird eine optimale Adsorption bei 10^{-1} *M* Sulfat und pH 3 erreicht; für die Elution wird $\geqslant 0.4$ *N* Schwefelsäure verwendet.

BIBLIOGRAPHIE

1 K. S. RAJAN ET J. GUPTA, *J. Sci. Ind. Res. India*, 14 B (1955) 453.
2 K. S. RAJAN ET J. GUPTA, *J. Sci. Ind. Res. India*, 16 B (1957) 459.
3 J. L. HAGUE ET L. A. MACHLAN, *J. Res. Natl. Bur. Std.*, 65 A (1961) 75; 66 A (1962) 517.
4 C. CORNET, M. THIBAULT, J. HUÉ ET B. TRÉMILLON, *Bull. Soc. Chim. France*, (1961) 286.
5 D. I. RYABCHIKOV, I. N. MAROV, A. N. ERMAKOV ET V. K. BELYAEVA, *J. Inorg. & Nucl. Chem.*, 26 (1964) 965.
6 H. HAMAGUCHI, A. OHUCHI, T. SHIMIZU, N. ONUMA ET R. KURODA, *Anal. Chem.*, 36 (1964) 2304.
7 F. W. E. STRELOW ET C. J. C. BOTHMA, *Anal. Chem.*, 39 (1967) 595.
8 B. NARÉN, *Acta Chem. Scand.*, 23 (2) (1969) 379.
9 L. BALSENC ET W. HAERDI, *Helv. Chim. Acta*, 52 (8) (1969) 2657.

Analytica Chimica Acta
Elsevier Publishing Company, Amsterdam
Printed in The Netherlands

SHORT COMMUNICATIONS

An improved ultraviolet spectrophotometric method for the determination of sulphur dioxide

Scoggins[1] recently described a very simple procedure for the determination of sulphite or sulphur dioxide. The sulphite solution is acidified with sulphuric acid, and the sulphur dioxide absorbance is measured at 276 nm. The method is not very sensitive, however; it cannot be applied to less than 0.01% by weight of sulphur dioxide in the measured solution. The present communication describes a similar method, in which the absorbance is measured at 198 nm. The molar absorptivity at this wavelength is more than four times greater than that at 276 nm, so that as little as 1 μg of sulphur dioxide per ml of measured solution can be determined. A comparison of interferences at the two wavelengths is also made.

Experimental

Sulphite and metabisulphite solutions, stabilized by EDTA, were prepared as described previously[2].

Procedure. Transfer to a series of 50-ml volumetric flasks, 0.5–10 ml aliquots of an 0.033% (w/v) sodium sulphite or 0.030% (w/v) sodium metabisulphite in 10^{-3} *M* EDTA solution. Add 30 ml of distilled water, followed by exactly 5 ml of 22.5% (v/v) sulphuric acid (M.A.R.). Dilute to the mark with distilled water, and measure the absorbance at 198 nm in stoppered, 1-cm quartz cells, against a blank composed of 5 ml of the sulphuric acid diluted to 50 ml. Prepare a calibration graph. Analyse unknown solutions, containing up to 30 μg of sulphur dioxide per ml, by the same procedure.

Results and discussion

Figure 1 shows the ultraviolet spectrum of sodium sulphite in 2.25% sulphuric acid. The molar absorptivities are 2,820 at 198 nm, and 610 at 276 nm. The latter value is appreciably larger than that of 500 found by Scoggins[1] and those of 440 and 360 measured by earlier workers[3]. Figure 2 is a comparison of the calibration graphs measured at the two wavelengths. Both are straight lines, and absorbance measurements at both wavelengths are reproducible to better than 0.01 absorbance units. Measurements at 198 nm, however, are more sensitive, and allow 1–30 μg of sulphur dioxide per ml of measured solution to be determined.

Scoggins[1] stabilized his sulphite solutions with tetrachloromercurate(II)[4], and claimed quantitative recoveries even when sulphite solutions in *N* sulphuric acid had been stored for several hours. Acidified tetramercurate(II)-stabilized solutions, however, do not give a peak at 198 nm. EDTA also stabilizes sulphite solutions[5], and such solutions, on acidification, give peaks both at 198 nm and 276 nm. Reproducible measurements were obtained at both wavelengths, with EDTA-stabilized solutions, whereas without a stabilizer, measurements were quite irreproducible.

Scoggins investigated the effect only of sulphate, thiosulphate, sulphide and an alkyl sulphonate on the determination of sulphite. The effect of a larger range of

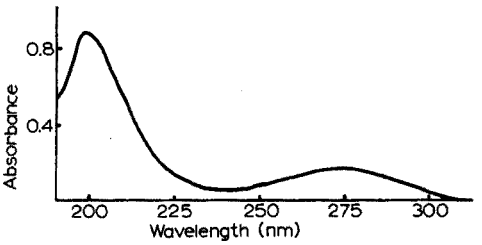

Fig. 1. Absorption spectrum (1-cm cell) of 15 μg of SO_2 per ml of 2.25% (v/v) H_2SO_4, stabilised by 10^{-4} *M* EDTA.

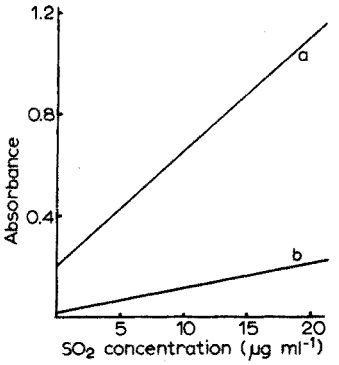

Fig. 2. Plot of absorbance *vs.* SO_2 concentration, measured at: (a) 198 nm, (b) 276 nm, by the recommended procedure.

anions on measurements at 198 and 276 nm is summarized in Table I. At 276 nm, the only interferences are sulphide (increased absorbance) and nitrite (decreased absorbance, owing to reaction with sulphite). The effect of thiosulphate is probably due to the presence of small amounts of sulphur dioxide. At 198 nm, fluoride, sulphate, phosphate, chloride and cyanide do not interfere, but sulphide, nitrite, thiosulphate, bromide, nitrate, thiocyanate and iodide also absorb at this wavelength, their molar absorptivities increasing in that order. Nevertheless, these effects can largely be overcome by sweeping the sulphur dioxide from the acidified solution with a stream of nitrogen[1], and absorbing in an alkaline EDTA solution.

TABLE I

EFFECT OF ANIONS ON THE DETERMINATION OF SULPHUR DIOXIDE

Anion[a]	*Absorbance at*		*Anion*[a]	*Absorbance at*	
	198 *nm*	276 *nm*		198 *nm*	276 *nm*
—	0.39	0.075	NO_2^-	1.34	0.025
F^-	0.40	0.075	$S_2O_3^{2-}$	1.46	0.09
SO_4^{2-}	0.39	0.075	Br^-	2.06	0.075
PO_4^{3-}	0.39	0.075	NO_3^-	$\gg$2.0	0.075
CN^-	0.39	0.075	SCN^-	$\gg$2.0	0.075
Cl^-	0.40	0.075	I^-	$\gg$2.0	0.075
S^{2-}	1.08	0.12			

[a] $8 \cdot 10^{-4}$ *M* in measured solution containing 4.25 μg of SO_2 per ml.

The authors thank Professor R. Belcher for his interest. M.K.B. thanks the Pakistan Government and the P.C.S.I.R. for leave of absence, and the Nuffield Foundation for the award of a fellowship.

Chemistry Department,
The University,
P.O. Box 363,
Birmingham B15 2TT (England)

M. K. Bhatty
A. Townshend

1 M. W. Scoggins, *Anal. Chem.*, 42 (1970) 1091.
2 M. K. Bhatty and A. Townshend, *Anal. Chim. Acta*, in press.
3 see V. Gold and F. L. Tye, *J. Chem. Soc.*, (1950) 2932.
4 P. W. West and G. C. Gaeke, *Anal. Chem.*, 28 (1956) 1816.
5 R. W. Humphrey, M. H. Ward and W. Hinze, *Anal. Chem.*, 42 (1970) 698.

(Received 5th March 1971)

Anal. Chim. Acta, 55 (1971) 263–265

Determination of zirconium in glasses, glass-ceramics and refractories with *p*-bromomandelic acid

Mandelic acid and its halosubstituted derivatives are very selective precipitants for zirconium and have been widely recommended for the gravimetric determination of zirconium[1,2]. *p*-Bromo- and *p*-chloromandelic acids are considerably more sensitive than mandelic acid and more convenient to use. For instance, because of the greater insolubility of the zirconium complex, the amount of *p*-bromomandelic acid required is about one-twentieth that of mandelic acid. This is especially advantageous when wet combustion of the excess of reagent is required before further analyses are done on the filtrate. The application of halomandelic acids to the determination of zirconium in steel[3] and aluminum alloys[4] has been reported.

The application of *p*-bromomandelic acid to the determination of zirconium in glasses, glass-ceramics, refractories, and minerals, presents some special problems owing to the complexity of matrices involved and the difficulties attending their decomposition. This present work describes a procedure that effectively circumvents most of the problems associated with the accurate determination of zirconium in these materials.

Reagent

Prepare a 0.1 *M* solution of *p*-bromomandelic acid by dissolving 5.8 g of reagent in 250 ml of warm water. Cool to room temperature and filter.

Procedure

Weigh sufficient ground sample to contain 5–50 mg of ZrO_2 into a platinum dish and decompose with hydrofluoric–sulfuric acid mixture by heating on a steam

bath. Fume to complete dryness on a hot plate; rinse the sides of the dish with 6 ml of 9 *M* sulfuric acid and repeat the fuming process. Ignite the decomposed sample in the full heat of an air-gas blast burner flame. For samples containing barium or lead, which form insoluble sulfates, their removal before the ignition of the residue is necessary. After the second fuming with sulfuric acid, add 8–10 ml of 9 *M* sulfuric acid and heat the sample on a hot plate for 5–10 min. Add *ca.* 100 ml of water, digest on a steam bath and remove the insoluble sulfates by filtration through Whatman No. 42 paper. Evaporate the filtrate to dryness and ignite in the original platinum dish used for decomposition.

Cover the ignited residue in the platinum dish with 10–15 times its weight of (2+1) Na_2CO_3–$Na_2B_4O_7$ flux and fuse. Dissolve the melt with 40–50 ml of 6 *M* hydrochloric acid on a hot plate. Transfer the solution to a 250-ml beaker and dilute to about 80 ml. Add 20 ml of the *p*-bromomandelic acid solution plus 4 ml of reagent for each 10 mg of ZrO_2 in excess of 50 mg. Heat the solution and digest at 85–95° for 20 min. Cool to room temperature, filter the precipitate on Whatman No. 40 paper and wash with cold water. Char the precipitate slowly, then ignite to constant weight in a pre-weighed platinum crucible at 1,000° and weigh as ZrO_2.

Results and discussion

Siliceous materials are most conveniently decomposed with either sulfuric–hydrofluoric acid or perchloric–hydrofluoric acid. Both acid mixtures were investigated in developing the present method. Sulfuric acid was found to be superior to perchloric acid for the subsequent elimination of fluoride by fuming and ignition;

TABLE I

SPECTROGRAPHIC EXAMINATION OF IGNITED ZIRCONIUM BROMOMANDELATES

Type of sample[a]	*Impurities found*[b]	
	Range (%)	*Element oxide*
B_2O_3–La_2O_3–CaO–SiO_2–BaO–ZrO_2(4.5%)–ZnO–MgO–As_2O_3	0.01–0.1	B_2O_3, SiO_2
	0.001–0.01	MgO
BaO–B_2O_3–SiO_2–La_2O_3–ZrO_2(0.9%)–Al_2O_3–As_2O_3	0.05–0.5	Al_2O_3, SiO_2
	0.01–0.1	BaO, MgO, La_2O_3
	0.005–0.05	Fe_2O_3, TiO_2
Al_2O_3–CaO–ZrO_2(10%)–MgO–BaO	0.01–0.1	SiO_2
	0.005–0.05	MgO, Fe_2O_3, CaO, Al_2O_3
SiO_2–Al_2O_3–Li_2O–ZrO_2(1.6%)–TiO_2–ZnO–Na_2O–Sb_2O_3	0.05–0.5	SiO_2
	0.01–0.1	BaO, Al_2O_3
	0.005–0.05	CaO, B_2O_3, Fe_2O_3, MgO
SiO_2–Al_2O_3–Li_2O–ZrO_2(2.2%)–P_2O_5[c]–TiO_2–K_2O–As_2O_3	0.05–0.5	P_2O_5
	0.005–0.05	SiO_2, Fe_2O_3
	0.001–0.01	B_2O_3

[a] Constituents given in decreasing order of weight percentages.

[b] The "range (%)" given was based on the ignited precipitates. For instance, 0.1% impurities means the ZrO_2 precipita obtained is 99.9% pure.

[c] Phosphate interference removed by extraction of the carbonate–borate fusion melt with hot water.

when perchloric–hydrofluoric acid was employed, incomplete elimination of fluoride occasionally resulted. This trace of residual fluoride caused low results, or prevented the precipitation of zirconium bromomandelate entirely. Ignition was necessary to remove the last traces of fluoride for samples containing lanthanum, aluminum, and calcium which form stable complexes with fluoride. The ignited residues were easily fused with carbonate–borate flux and dissolved in hydrochloric acid.

For phosphorus-containing samples, the phosphorus was removed by extraction of the carbonate–borate fusion melt with hot water and filtration. The filter paper was burned off, and the residue was fused with the flux again and dissolved in hydrochloric acid.

If little or no silica is present in the samples, they can be decomposed directly with a sodium carbonate–sodium borate fusion. A minor contamination of silica can be corrected by hydrofluoric–sulfuric acid treatment after ignition of the zirconium precipitate.

TABLE II

COMPARISON BETWEEN THE BROMOMANDELIC ACID AND OTHER METHODS FOR DETERMINING ZIRCONIUM IN GLASSES, GLASS-CERAMICS AND REFRACTORIES

Type of sample[a]	ZrO_2(%)		
	Br-mandelic acid	*Other method*	*Difference*
Si–Al–Li–Zr–Zn–As–Na	3.50, 3.49 Av. 3.50	3.45, 3.46 Av. 3.46[b]	+0.04
Si–Al–Li–Zr–Zn–As–Na	3.50	3.54[b]	−0.04
Si–Al–Mg–Ti–Zr–As–Na–Ca	3.54, 3.52 Av. 3.53	3.53[c]	0.00
Si–Al–Li–P–Zr–Ti–Na–K–As–Ca	2.52	2.52, 2.60 Av. 2.56[d]	−0.04
B–La–Ca–Si–Ba–Zr–Zn–Mg–As	4.45, 4.47 Av. 4.46	4.51, 4.54 Av. 4.52[e]	−0.06
Ba–B–Si–La–Zr–Al–As	0.92, 0.88 Av. 0.90	0.88[e]	+0.02
Ba–La–Si–B–Cd–Zr–Ti–Zn–Ta–Pb–W–As	3.25	3.29[d]	−0.04
Si–Al–Li–Zr–Ti–Zn–Na–Sb–K	1.55, 1.54, 1.56 1.55 Av. 1.55	1.52[f]	+0.03
Ba–Si–La–B–Cd–Zr–Zn–Ti–W–As–Al	2.36, 2.34 Av. 2.35	2.35[d]	0.00
Zr–Al–Si–Na	71.1	71.0[e]	+0.1
Zr–Al–Si–Na	62.1	62.0[e]	+0.1

[a] Constituents given in decreasing order of weight percentages.
[b] Gravimetric with cupferron[1].
[c] Zr + Ti separated as cupferrates from the sample, followed by determination of Zr by bromomandelic acid.
[d] Colorimetric with pyrocatechol violet[6].
[e] Titrimetric with EDTA in hot 1 *M* $HClO_4$ using xylenol orange as indicator[7].
[f] Colorimetric with alizarin red S[5].

Clean separation of zirconium from other elements in a wide range of compositions, comprised of such elements as Li, Na, K, Mg, Ca, Ba, Sr, La, Ti, B, Zn, Pb, Cd, Ta, Al, As and Sb, was demonstrated by spectrographic examination of the final ignited ZrO_2. Typical spectrographic results are shown in Table I. It is noteworthy that although sodium carbonate and borate were employed in the sample decomposition, the precipitate was found to be quite free of sodium and boron contamination. This is a definite advantage over other gravimetric methods (*e.g.* cupferron) where excessive amounts of sodium often lead to a high bias owing to severe coprecipitation.

The method has been applied for the determination of zirconium in a wide variety of glasses, glass-ceramics, and refractories. The completeness of the zirconium precipitation was checked by examining several of the filtrates spectrographically. Typical results are shown in Table II compared with values obtained by other accepted methods.

Mr. W. R. Strzegowski contributed important assistance in developing the method and analyzing the samples.

Research and Development Laboratories, Yao-Sin Su
Corning Glass Works, D. E. Campbell
Corning, N.Y. 14830 (U.S.A.)

1 I. M. KOLTHOFF AND P. J. ELVING, *Treatise on Analytical Chemistry*, Part II, Vol. 5, Interscience, New York, 1961, p. 95.
2 C. L. WILSON AND D. W. WILSON, *Comprehensive Analytical Chemistry*, Vol. 1c, Elsevier, New York, 1962, p. 507.
3 J. J. KLINGENBERG AND R. A. PAPUCCI, *Anal. Chem.*, 24 (1952) 1861.
4 R. A. PAPUCCI, D. M. FLEISHMAN AND J. J. KLINGENBERG, *Anal. Chem.*, 25 (1953) 1758.
5 I. M. KOLTHOFF AND P. J. ELVING, *Treatise on Analytical Chemistry*, Part II, Vol. 5, Interscience, New York, 1961, p. 101.
6 D. F. WOOD AND J. T. JONES, *Analyst*, 90 (1965) 125.
7 Y.-S. SU AND W. R. STRZEGOWSKI, unpublished work.

(Received 20th November 1970)

Anal. Chim. Acta, 55 (1971) 265–268

Analytica Chimica Acta
Elsevier Publishing Company, Amsterdam
Printed in The Netherlands

The crystal structure of primary zinc(II) dithizonate and its relevance to the stabilities of its *o*- and *p*-methyl derivatives

Despite the important role that dithizone (3-mercapto-1,5-diphenylformazan, PhNH·NH·CS·N:NPh, H_2Dz) plays in trace metal analysis the structure of its metal complexes—in particular that of the secondary dithizonates—is still a matter of controversy. Several authors have commented upon differences between the electronic absorption spectra of nickel, palladium and platinum complexes on the one hand and those of zinc dithizonate and other divalent metal dithizonates, $M(HDz)_2$, on the other[1,2]. Differences between the infrared spectra of various groups of dithizonates have also been noted[3,4].

These differences could arise from a number of causes but more direct evidence of differences in structure between zinc and nickel complexes is now available from quite a different source; for Math *et al.* have measured the stability constants in 50% aqueous dioxan of complexes of zinc and nickel with dithizone and several of its derivatives[4]. *o*-Methyl derivatives were found to decrease the stability of 1:1 complexes in the case of zinc but to increase the stability with nickel, whereas a *p*-methyl substituent enhanced the stability with both metals (Table I). The authors attribute

TABLE I

STABILITY CONSTANTS OF 1:1 ZINC AND NICKEL COMPLEXES OF SUBSTITUTED DITHIZONES ArNH·NH·CS·N:NAr (HL)

Ar	*Phenyl*	o-*Tolyl*	2,4-*Dimethyl phenyl*	p-*Tolyl*
$\log K_{ZnL^+}$	6.18	4.50	4.80	6.45
$\log K_{NiL^+}$	5.83	5.90	6.40	6.60

these differences to steric hindrance to chelation and comment that the observed relative stabilities can be explained if "the structures of the zinc and nickel dithizonates are postulated as (I), in which the zinc is tetrahedrally coordinated, and (II) in which

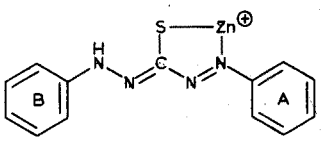

I

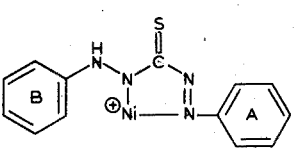

II

the nickel is octahedrally coordinated". They note in support the resemblance between the spectrum of nickel dithizonate and that of bis(3-methyl-1(or 5)-phenyl-5-(or 1)-*p*-tolylformazyl)nickel(II) which possesses two six-membered chelate rings each with two donor nitrogen atoms[5]. A recent X-ray structural determination shows the chelate groups to be non-planar[6]. The most noteworthy difference between the

infrared spectra of zinc and nickel dithizonates is the appearance of a band at 1210 cm^{-1} in the latter which Math *et al.*[4] tentatively assign to the thiocarbonyl group (>C:S). This band also appears strongly in the infrared spectra of 1,5-diphenyl-3-nitroformazan and 2-phenylazo-benzo-1,3,4(4H)-thiadiazine, neither of which contain thiocarbonyl groups and a lower frequency, *viz.* 712 cm^{-1}, now seems a more plausible assignment[7].

In view of the equivocable character of much of the physical evidence, it seems essential to rely on the unambiguous evidence provided by crystal structure determinations. A preliminary report[8] on the structure of nickel dithizonate, $Ni(HDz)_2$, shows that this molecule is centrosymmetric with coplanar chelate rings essentially similar to those reported in primary copper(II) dithizonate, $Cu(HDz)_2$[9]. The dithizone residue is definitely bonded through nitrogen and sulphur and not through two nitrogen atoms. From a full three-dimensional X-ray study[10] it is clear that the distance between adjacent molecules is too large to admit of any bonding and there is no question of octahedral coordination.

That bonding to nickel takes place through both nitrogen and sulphur is shown in the adduct of nickel dithizonate with 2,2'-bipyridyl, $Ni(HDz)_2 \cdot bipy$. Here four nitrogen atoms and two sulphur atoms lie in an essentially octahedral array round the central nickel atom[11] but the most interesting feature is that the two bonding sulphur atoms are in *cis*-positions. On the basis of this new evidence Math and Freiser predicted that nickel dithizonate itself would be square planar with dithizonate ligands bonded through sulphur and nitrogen in the *trans*-position[11]. This has now been verified experimentally[6,8].

To establish the hitherto undetermined structure of primary zinc(II) dithizonate, $Zn(HDz)_2$, we have undertaken a full three-dimensional X-ray crystallographic determination on the grey-green needles with a metallic reflex obtained by recrystallising a pure sample of the complex from chloroform. (Found: C, 54.0; H, 3.9; N, 19.4; S, 11.25; Zn, 11.3%. $C_{26}H_{22}N_8S_2Zn$ requires C, 54.2; H, 3.85; N, 19.45; S, 11.1; Zn, 11.4%.) The space group is $P2_1/a$ with $a = 15.21$ Å, $b = 22.25$ Å, $c = 7.84$ Å and $\beta = 91.4°$. There are four molecules in the unit cell.

Data were collected by the equi-inclination Weissenberg technique with copper Kα radiation. The structure based on 994 visually estimated intensities was solved by Patterson and Fourier techniques and refined by the block diagonal least squares method with anisotropic thermal parameters for the zinc and sulphur atoms to give an R factor of 12.2%.

The main structural features are shown in Fig. 1. The estimated standard deviations are Zn–S (0.009 Å), Zn–N (0.02 Å), $S\hat{Z}nN$ (0.7°), $Zn\hat{S}C$ (0.9°) and for the remainder of the bond-lengths and angles shown in the diagram they are equal to, or less than 0.03 Å and 2° respectively. The molecule consists of two bidentate dithizone residues tetrahedrally coordinated to zinc through two sulphur and two nitrogen atoms. One phenyl group (A) of each ligand is associated with a chelate ring whereas the other phenyl group (B) is extended as far as possible from the central atom with two intervening nitrogen atoms that hold it in the *trans*-configuration.

Distances of 1.47 Å are normal for single-bonded :N–N: and :C–N:, whereas for doubly bonded ·N=N· and :C=N· they are 1.25 and 1.27 Å, respectively. The values 1.30 Å for C(1)–N(3), 1.32 Å for N(3)–N(4) and 1.42 Å for N(4)–C(2) all correspond to partial double character, in fact to bond orders of 1.84, 1.60 and 1.10 on the Lofthus

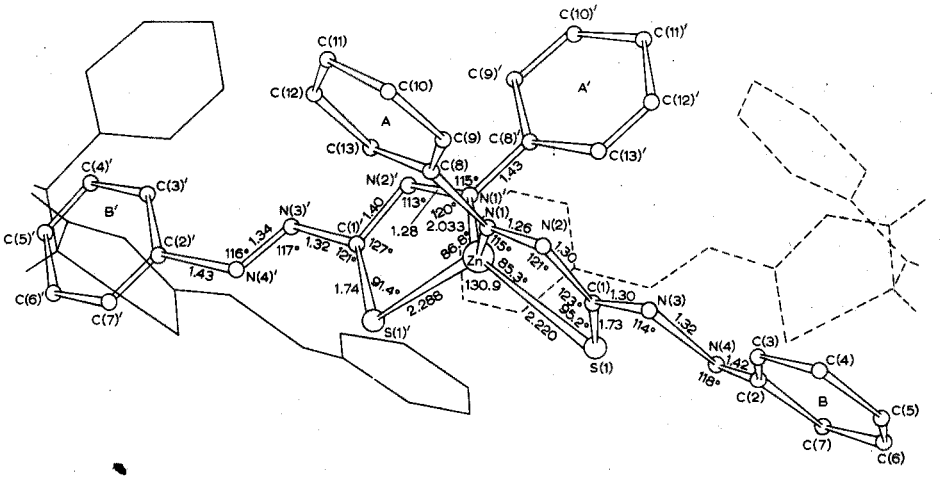

Fig. 1. The structure of primary zinc(II) dithizonate. Portions of adjacent molecules with the zinc atoms centred at $(x, y, -1+z)$ and $(x, y, 1+z)$ are shown by full lines and broken lines respectively. The distances Zn–N(1)=2.105 Å, N(1)–C(8)=1.40 Å, and the angle N(1)–Zn–N(1)′=110° have been omitted in the interests of clarity.

scale[12]. This effectively maintains the phenyl ring (B) coplanar with the planar chelate ring to which it is attached through N(3) and N(4). What is perhaps more surprising is that this coplanarity also extends to the phenyl group (A) attached through N(1) to the chelate ring so that the molecule as a whole can be envisaged as two planes through A–zinc–B and A′–zinc–B′ intersecting at about 85°, an angle which deviates little from the ideal of 90°. In general it may be said that the geometry of the dithizonate residues as determined here does not differ significantly from that found in other complexes, *viz.* mercury(II) dithizonate[13] and copper(II) dithizonate, or from that in dithizone itself or S-methyldithizone whose structures have recently been determined in this department[14].

Another feature of interest is the difference in bond lengths in the two chelate rings, for the distances Zn–S(1) of 2.220 and Zn–S(1)′ of 2.288 Å are significantly different. In the centrosymmetric nickel complex the two Ni–S distances are necessarily identical, *viz.* 2.19 Å. The distortion in the zinc complex can be explained in terms of the packing of individual molecules in the crystal lattice. With the coordinates of the central zinc atom at (x, y, z) Fig. 1 shows the positions of portions of the two adjacent molecules whose central zinc atoms have the coordinates $(x, y, -1+z)$ and $(x, y, 1+z)$. These are represented in Fig. 1 by full lines and broken lines respectively. An inspection of all the relevant intermolecular distances shows that the slight divergences from planarity of the dithizonate ligands are almost entirely due to changes in geometry effected to minimise repulsion between neighbouring atoms in the adjacent molecules referred to above. The chelate rings in particular are very restricted in position by the phenyl group B′ of the molecule (indicated by broken lines in Fig. 1) which forms part of the coplanar dithizonate moiety of the adjacent molecule. Any readjustment of these ring systems would further diminish some already short interatomic distances and this crowded situation has been relieved by S(1) moving

inwards towards the central zinc atom.

The position of the phenyl ring B′ in the molecule at $(x, y, 1+z)$ (Fig. 1 broken lines) relative to the two chelate rings is such that any twisting about its C(2)′–N(4)′ axis would reduce some already short intermolecular distances either between the ring incorporating S(1) or that incorporating S(1)′, depending on the direction of tilt. The angle of 85° between the two ring systems is obviously a compromise from the ideal angle of 90° induced by considerations of packing, for it can be shown that any attempt to increase it will again shorten a number of intermolecular distances.

There appear to be no considerations connected with packing alone which should determine the coplanarity of the phenyl rings A (or A′) and the chelate ring to which it is attached and there appears to be adequate freedom for out-of-plane rotation about C(8)–N(1) (or C(8)′–N(1)′). Here the situation is in complete contrast to that in the nickel complex where steric factors dictate that these phenyl rings cannot be coplanar with, and indeed are considerably out of the plane of, the chelate rings to which they are directly attached. As a direct consequence we can see why the presence of an *o*-methyl substituent must cause a distortion of the zinc dithizonate structure but need not do so for the nickel complex. Provided that the respective complexes retain the same structures in solution as they are now shown to have in the solid state (and assuming no major differences in the solvation energies of the relevant cations and anions by dioxan and water) the variations in formation constants reported by Math and Freiser are readily explicable.

Department of Inorganic and Structural Chemistry,
The University,
Leeds 2 (England)

Anne Mawby
H. M. N. H. Irving

1 G. Iwantscheff, *Das Dithizon und seine Anwendung in der Mikro- und Spurenanalyse*, GMBH, Darmstadt, 1958.
2 H. Irving and J. J. Cox, *Proc. Chem. Soc.*, (1959) 360.
3 A. Dyferman, *Acta Chem. Scand.*, 17 (1963) 1609.
4 K. S. Math, Q. Fernando and H. Freiser, *Anal. Chem.*, 36 (1964) 1762.
5 H. Irving, J. B. Gill and W. R. Cross, *J. Chem. Soc.*, (1960) 2087.
6 D. Dale, *J. Chem. Soc.*, (1967) 278.
7 H. M. N. H. Irving, A. M. M. Kiwan, D. C. Rupainwar and S. S. Sahota, *Anal. Chim. Acta*, submitted.
8 M. Laing and P. A. Alsop, *Talanta*, 17 (1970) 243.
9 R. F. Bryan and P. M. Knopf, *Proc. Chem. Soc.*, (1961) 203.
10 M. Laing and P. A. Alsop, *J. Chem. Soc.*, in press.
11 K. S. Math and H. Freiser, *Chem. Commun.*, (1970) 110.
12 A. Lofthus, *Mol. Phys.*, 2 (1959) 367.
13 M. Harding, *J. Chem. Soc.*, (1958) 4136.
14 P. A. Alsop, personal communication.

(Received 2nd March 1971)

Anal. Chim. Acta, 55 (1971) 269–272

Analytica Chimica Acta
Elsevier Publishing Company, Amsterdam
Printed in The Netherlands

Heterocyclic N,N'-disubstituted 1-amino-3-iminopropenes as analytical reagents

Tetradentate Schiff bases with strong chelating properties are formed by condensation of 8-aminoquinoline derivatives with malondialdehyde (I). Honeybourne and Webb[1] published a note briefly describing similar bidentate aromatic derivatives and formation of highly colored polymethine dyes of the same type with glutaconic aldehyde has been suggested as a selective test for an aromatic primary amino group[2,3].

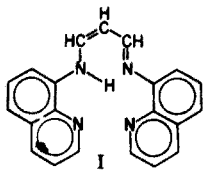

I

These azomethine compounds can be protonated in acid solution or deprotonated in basic solution as shown by the following:

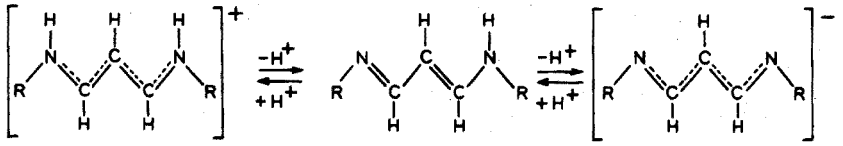

If the R substituents are nitrogen-containing heterocycles, two additional acid–base equilibria involving their protonation should be considered and schematically the overall picture is made clear by

$$H_4L^{3+} \overset{K_4}{\rightleftarrows} H_3L^{2+} \overset{K_3}{\rightleftarrows} H_2L^{+} \overset{K_2}{\rightleftarrows} HL \overset{K_1}{\rightleftarrows} L^{-} \qquad (1)$$

where K denotes the particular equilibrium dissociation constant.

Malonaldehyde-bis(3-methylanil), an aromatic bidentate Schiff base, reacts very slowly with metal ions; chelation occurs over a narrow pH range, and mixtures of reagent and cobalt(II) or nickel(II) produce a visible color change only after overnight standing at room temperature. The heterocyclic tetradentate ligands, however, react readily with copper, nickel, cobalt, zinc, cadmium and iron. The unusually slow chelation rate of the bidentate reagent suggests that its steric forms[4] are important in the chelation process; only structure II, of the three possible structures given below, is capable of forming metal chelates and only the free base, HL, exists in this favourable chelation form. Heterocyclic Schiff bases of this type having twice as many co-ordination sites in the molecule would be energetically more favorable to the rearrangement required for chelation.

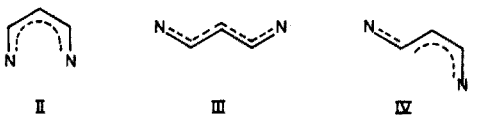

II III IV

This paper describes the results of an investigation of the tetradentate Schiff bases formed by reacting 8-aminoquinolines with 1,1,3,3-tetramethoxypropane.

Apparatus

A Bausch and Lomb Spectronic 505 recording spectrophotometer and a Unicam SP 500 spectrophotometer were used for absorptiometric measurements in matched 1.00-cm silica cells.

A Radiometer PHM4c meter, calibrated at $25 \pm 2°$ was used for pH measurements. Potentiometric acid–base titrations were made with a Metrohm Potentiograph E 436. The glass electrode response in 63% v/v ethanol was corrected for that in water by using the difference in titration curves obtained on titrating 5.0 ml of 0.1 *M* hydrochloric acid in 20 ml of each respective medium with sodium hydroxide.

A Perkin-Elmer 290 spectrophotometer was used for atomic absorption measurements.

Reagents

The Schiff bases were obtained by direct condensation of 1,1,3,3-tetramethoxypropane (Eastman Organic Chemicals) with the heterocyclic amine (Aldrich Chemical Co.) in an acidified solution; 8-aminoquinoline, 6-methoxy-8-aminoquinoline and 8-aminoquinaldine were the amines used.

The aldehyde diacetal and twice its molar amount of the amine were dissolved in a small volume of hot methanol and the solution was acidified with a 3.5 *M* amount of concentrated hydrochloric acid diluted 1 : 1 with methanol. A yellow crystalline solid of the trihydrochloride separated on cooling; the salt was washed with a methanol–ether mixture and dried in a desiccator under reduced pressure. It was necessary to add ether to the reaction mixture to precipitate the trihydrochloride of the quinaldine azomethine compound. The hydrochlorides were usually obtained as hydrates and a direct Fischer aquametric titration was used to determine the water content; the crude hydrochlorides were best purified by diethyl ether precipitation from their acidified methanol solutions.

Substitution of perchloric for hydrochloric acid in the preparation procedure or addition of perchloric acid to solutions of its hydrochloride, led to separation of the brown crystalline monoperchlorate; though pure and stable, its analytical value is decreased by its low solubility.

1-(8-*Quinolylamino*)-3-(8-*quinolylimino*)-*propene trihydrochloride hydrate* (QAQIP) was a bright yellow solid (m.p. 147°). Analysis: calculated for $C_{21}H_{16}N_4 \cdot 3HCl \cdot 2H_2O$ (mol.wt. 469.8), C 53.69, H 4.93, N 11.93, Cl 22.64, H_2O 7.67%; found C 53.40, H 5.02, N 12.25, Cl 21.92, H_2O 8.72%.

1-(8-*Quinolylamino*)-3-(8-*quinolylimino*)-*propene perchlorate* was obtained as dark brown crystals which were purified by crystallization from diluted dimethylformamide (m.p. 220°). Analysis: calculated for $C_{21}H_{16}N_4 \cdot HClO_4$ (mol.wt. 424.8), C 59.37, H 4.03, N 13.19, Cl 8.35%; found C 59.20, H 4.02, N 13.27, Cl 8.94%.

1-(6-*Methoxy*-8-*quinolylamino*)-3-(6-*methoxyquinolylimino*)-*propene trihydrochloride hydrate* formed as a cocoa-brown powder (m.p. 165°) easily soluble in water. The results of elemental analysis indicated that, like QAQIP, it was actually a hydrate containing slightly more than 3 moles of water of crystallization: calculated for $C_{23}H_{20}N_4O_2 \cdot 3HCl \cdot 3H_2O$ (mol. wt. 547.9), C 50.42, H 5.34, N 10.22, Cl 19.41%;

found C 50.06, H4.53, N 9.94, Cl 18.17%.

1-(8-*Quinaldylamino*)-3-(8-*quinaldylimino*)-*propene trihydrochloride hydrate* (2-*Me-QAQIP*) was obtained as a light brown powder (m.p. 163°). Analysis: calculated for $C_{23}H_{20}N_4 \cdot 3HCl \cdot 3H_2O$ (mol.wt. 515.9), C 53.55, H 5.67, N 10.86, Cl 20.62, H_2O 10.48%; found C 54.06, H 5.63, N 11.04, Cl 19.89, H_2O 11.34%.

Freshly prepared aqueous reagent hydrochloride solutions were used throughout this work; the chelate-forming ability decreased, on standing, as the result of hydrolytic –CH=N– bond cleavage (Fig. 1). Solutions in ethanol were more stable but not sufficiently so to be of any advantage.

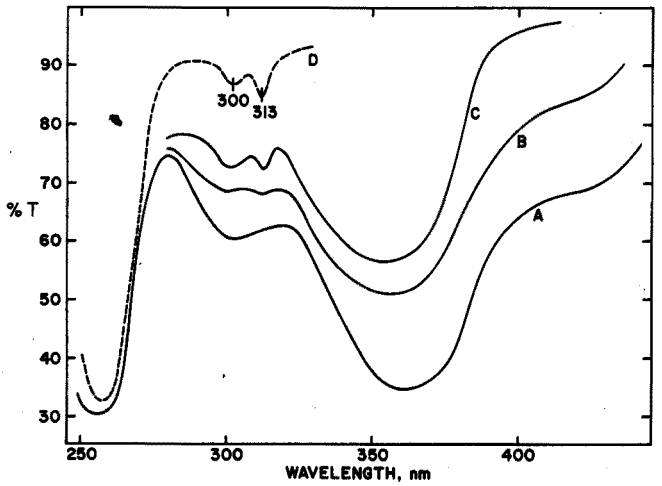

Fig. 1. Aging of an aqueous QAQIP solution. $c = 3 \cdot 10^{-5}$ mole l^{-1}. (A) Fresh solution; (B) 12 h old; (C) 36 h old; (D) 8-amino-quinoline-HCl.

Results and discussion

These heterocyclic trimethine compounds are triacidic bases having, in addition, a dissociable imino-hydrogen in the molecule and four equilibria, governed by dissociation constants K_1 through K_4, can be considered. The titration curves in Fig. 2 show that two moles of base are required for the first end-point which must correspond to deprotonation of both quinoline nitrogens (dissociation constants K_4 and K_3); the next step, requiring one equivalent of base, corresponds to the K_2 equilibrium (that of the singly-protonated reagent). In 63% (v/v) ethanol, the pK_2 calculated for QAQIP was 7.20 ± 0.01 and, for 2-Me-QAQIP, pK_2 was 7.50 ± 0.01; ethanol solutions were necessary at intermediate pH, in both potentiometric and spectrophotometric measurements, because of the limited solubility of the free Schiff bases. Estimated values of K_3 and K_4 are of the order of 10^{-2}; no attempt was made to determine K_1.

The existence of three possible isomers, of which only the *cis* form can have chelate-forming properties, could strongly influence the analytical applicability of these reagents. The uncharged base, HL, is the only species favoring the *cis* form and high polarity solvents could cause cleavage of the hydrogen-bridged *cis* form resulting in formation of a *trans* isomer. This has been verified by reagent n.m.r. spectra in

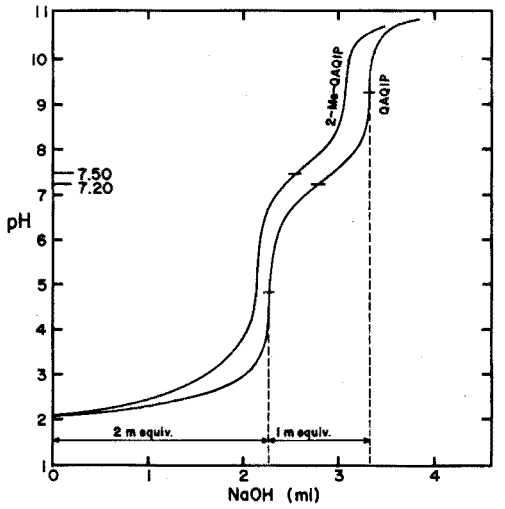

Fig. 2. Alkalimetric titration of QAQIP and 2-Me-QAQIP trihydrochlorides in 63% (v/v) ethanol ($t = 25.0 \pm 0.1°$, $I = 0.15$).

$CDCl_3$ and in DMSO (d_6) and by calculating the coupling constants of the adjacent methine protons; the low value (6.5 Hz) in $CDCl_3$ is typical for *cis* protons whilst that found in DMSO (11.0 Hz) is characteristic of a *trans* configuration. For extraction purposes, it follows that solvents of low polarity should be considered preferred.

Metal chelation. QAQIP and its methoxy derivative react readily, in acetate buffered or ammoniacal solution, with Cd^{2+}, Co^{2+}, Fe^{2+}, Mn^{2+}, Ni^{2+}, Pd^{2+}, and Zn^{2+}, to give pink to red complexes; other divalent and multivalent ions show no visible evidence of reaction. The chelates are easily extracted into chloroform. The methoxy chromophore is less sensitive in its reactions and the quinaldyl derivative (2-Me-QAQIP) reacts very slowly.

The absorption maximum in chloroform for the zinc and cadmium QAQIP chelates occurs at 536 nm with molar absorptivities of $4.2 \cdot 10^4$ and $2.7 \cdot 10^4$ l mole^{-1} cm^{-1} respectively. Both complexes are extracted over the pH range 6–10; distribution ratios for cadmium, determined from atomic absorption measurements, ranged from 0.04 at pH 3.62, to 3.1 at pH 6.77, and 76.0 at pH 9.17. Figure 3 shows that the reagent–metal mole ratio for the extracted cadmium species is 1 : 1 (Job's method in both one-phase[5] and two-phase[6] systems). The red crystalline cadmium salt, precipitated from solutions containing metal (as chloride) and reagent in 1 : 1 ratio, was readily soluble in chloroform, after drying, and its composition corresponded to $CdLCl_2$. For $Cd(C_{21}H_{16}N_4)Cl_2$ (mol.wt. 507.7) the calculated elemental results were C 49.68, H 3.17, N 11.04, Cl 13.97, Cd 22.14%; found C 50.58, H 3.22, N 11.03, Cl 13.14, Cd 22.75%.

Polar oxygen-containing solvents strongly affect the formation and extraction of the cadmium chelate. Table I shows absorbance readings obtained in the organic extracts of 10 ml of aqueous phase (containing $5 \cdot 10^{-4}$ mmole of Cd^{2+} or Zn^{2+}, $20 \cdot 10^{-4}$ mmole of QAQIP and 2 mmole of sodium acetate) by 25 ml of chloroform after addition of 2 ml of the particular polar solvent. Butyl cellosolve and symmetric diketones with unbranched alkyl groups were most effective in preventing cadmium

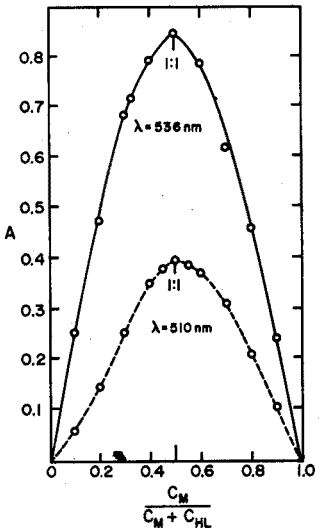

Fig. 3. Composition of the Cd-QAQIP chelate ($C_{Cd} = C_{HL} = 5 \cdot 10^{-4}$ mole l^{-1}, acetate buffered solution). (——) $CHCl_3$ extraction (2 min equilibration); (------) in diluted ethanol (1 : 3).

TABLE I

INFLUENCE OF POLAR SOLVENTS ON CHELATION OF CADMIUM AND ZINC

Solvent	*A 536,Cd*	*A 536,Zn*
—	0.51	0.70
Cyclohexanol	0.48	0.66
Tetrahydrofuryl alcohol	0.44	0.66
2-Butanone	0.41	—
Methyl isobutyl ketone	0.35	0.62
Diisobutyl ketone	0.34	—
Cyclohexanone	0.32	—
2-Pentanone	0.15	0.62
2-Heptanone	0.11	0.60
4-Heptanone	0.06	0.55
Butyl cellosolve	0.05	0.55
3-Pentanone	0.04	0.54
Reagent blank	0.03	

chelate formation. Studies of ultraviolet and visible spectra show no direct interaction between the ketone and QAQIP molecules; competitive solvation of cadmium ions is probably involved. Further studies of this phenomenon are warranted since such behaviour could permit the determination of zinc in the presence of cadmium.

Of the heterocyclic Schiff bases investigated, only the 8-aminoquinoline derivative (QAQIP) has analytical potential as a chelating agent. It reacts with a limited number of divalent transition metals to give extractable complexes with high molecular extinction coefficients. The sluggish reactions of the quinaldyl derivative are the result

of the steric hindrance caused by the methyl groups in the 2-positions; it is doubtful if analytical use could be made of this fact.

This work was supported by grants from the Defence Research Board and National Research Council of Canada. It is a pleasure to thank D. L. Hooper of this department for running and evaluating the n.m.r. spectra and L. Kabrt of the Department of Analytical Chemistry, Technical University of Prague, Czechoslovakia, for the data in Fig. 2.

Department of Chemistry, V. Zatka
Dalhousie University, J. Holzbecher
Halifax, Nova Scotia (Canada) D. E. Ryan

1 C. L. HONEYBOURNE AND G. A. WEBB, *Chem. Commun.*, (1968) 739.
2 F. FEIGL AND V. ANGER, *J. Prakt. Chem.*, 2, 139 (1934) 180.
3 F. FEIGL, *Spot Tests in Organic Analysis*, 6th Edn., Elsevier, Amsterdam, 1960, p. 281.
4 K. FELDMANN, E. DALTROZZO AND G. SCHEIBE, *Z. Naturforsch.*, 22b (1967) 722.
5 H. L. SCHLÄFER, *Komplexbildung in Lösung*, Springer-Verlag, Berlin, 1961.
6 T. B. PIERCE AND P. F. PECK, *U.K.A.E.R.E., R 4187*, Harwell, 1962.

(Received 10th December 1970)

Anal. Chim. Acta, 55 (1971) 273–278

Determination of zinc in uranium by differential linear sweep oscillographic polarography with a perchlorate–fluoride electrolyte*

The polarography of zinc has been well documented through 1967[1]. Zinc has been investigated polarographically in numerous substances, with numerous electrolytes.

Zinc has been determined in uranium and uranium-bearing materials polarographically. In all cases, however, the zinc was separated from the uranium before its determination[2–4]. Ball *et al.*[2] separated zinc from the uranium-bearing material by complexing the zinc with diethyldithiocarbamate, extracting the complex with chloroform and then back-extracting the zinc with dilute hydrochloric acid; the zinc was determined by derivative polarography. Ishii and Takeuchi[3] used a tributylphosphate extraction to separate the zinc from the uranium and a.c. polarography to determine the zinc. Goode and Campbell[4] separated the zinc from high-purity uranium metal by ion exchange on cellulose phosphate, and then determined the zinc by square-wave polarography with an orthophosphoric acid electrolyte. These separations were necessary because of the large excess of uranium present and because the uranium reduction precedes the zinc reduction, so that it is difficult to resolve the diffusion currents.

This communication reports on the use of differential linear sweep oscillographic polarography to determine zinc in the presence of uranium without prior separation.

* Work performed under U.S. Atomic Energy Commission contract AT(29-1)-1106.

Apparatus

A Davis Differential Cathode Ray Polarotrace, Type A-1660 (Southern Analytical, Ltd., Camberley, England) equipped with an electrode stand and a constant-temperature water bath, was used. All polarographic measurements were made at 30°. A polarographic cell with a mercury pool anode was used. Dual 15-cm long capillaries were used for all measurements. The $m^{\frac{2}{3}} t^{\frac{1}{6}}$ value of 1.01 was obtained at zero voltage in a solution which was 0.5 *M* in perchloric acid, 0.5 *M* in sodium perchlorate and 0.08 *M* in sodium fluoride.

Reagents

Stock solutions of zinc perchlorate were prepared by dissolving zinc metal (Baker Analyzed Reagent) in 20 ml of concentrated hydrochloric acid and 10 ml of concentrated nitric acid. This solution was taken to incipient dryness, and then 15 ml of concentrated perchloric acid were added. The salts were dissolved by cautiously warming on a hot plate, and this solution was then also taken to incipient dryness. The zinc salt was dissolved in 2.5 *M* perchloric acid, transferred to a volumetric flask, and diluted to volume with water. The final perchloric acid concentration was 0.5 *M*. The zinc solutions were standardized by the method of Körbl and Přibil[5,6].

The uranyl perchlorate solution was prepared from standard sample 950a U_3O_8 (U.S. National Bureau of Standards). The U_3O_8 was dissolved in concentrated nitric acid and taken to incipient dryness. The resulting uranium salts were dissolved in concentrated perchloric acid, and the solution was again taken to incipient dryness. The uranium salt was dissolved in concentrated perchloric acid, and the solution diluted to volume with water. The final perchloric acid concentration was 2.5 *M*.

All other chemicals were reagent grade, and the solutions were prepared in the normal manner.

Calibration procedure

Anodic calibration curves for zinc were prepared by pipetting aliquots of the standard stock solution into 10-ml volumetric flasks. Sufficient 2.5 W perchloric acid, 2.5 *M* sodium perchlorate and 0.8 *M* sodium fluoride were added to each volumetric flask to make the final concentrations 0.50 *M*, 0.50 *M* and 0.08 *M*, respectively. The solution was then diluted to volume with water. A portion of the solution was transferred to the electrolysis cell, and oxygen was removed by purging the solution with purified nitrogen for 5 min. Four each of ten different concentrations of zinc were polarographed.

The data are shown in Table I. It can be seen that the peak current was proportional to the zinc concentration. The relative standard deviation of the peak current quotient (μA mmol^{-1} l) for all 40 anodic traces was 3.01%.

Uranium sample preparation

The uranium sample (metal or oxide) was weighed directly into a tared 10-ml volumetric flask, and dissolved by cautiously adding 5 ml of 8 *M* nitric acid. The solution was evaporated to incipient dryness in a water bath and cooled, and 2 ml of 2.5 *M* perchloric acid was added. The solution was warmed in a water bath for 5 min to dissolve the salts and then cooled. Sodium perchlorate (2 ml of 2.5 *M* solution) and 1 ml of 0.8 *M* sodium fluoride were added and the solution was diluted to volume.

A portion of the solution was transferred to the electrolysis cell, and oxygen was removed by purging with purified nitrogen for 5 min. The solution was polarographed with an anodic polarization.

If the uranium: zinc ratio was less than 30:1, the reagent blank had only to be a solution which was 0.5 *M* in perchloric acid, 0.5 *M* in sodium perchlorate and 0.08 *M* in sodium fluoride. However, if the uranium: zinc ratio exceeded 30:1, the reagent blank should also contain approximately the same concentration of uranium as the sample. The uranium that was used in the reagent blank had to be free of zinc, otherwise low currents were obtained.

Analysis of standard zinc solutions

Eleven standard zinc solutions covering the range 0.50–200 μg Zn ml^{-1} were analyzed. The zinc aliquots were evaporated to incipient dryness in a water bath, cooled, dissolved in 2 ml of 2.5 *M* perchloric acid; analysis was then completed as described above. The average percent recovery for the eleven solutions was 99.5% with a recovery range of 91.3–110%.

Investigation of diverse ions

The effect of 32 diverse ions on the recovery of zinc was investigated in solutions which were $5.01 \cdot 10^{-4}$ *M* in zinc. The results are shown in Table II. They indicate that germanium, molybdenum, nickel, tin, vanadium, and tungsten would interfere if they were present in moderate concentrations. Germanium and tungsten are, however, not normally found in uranium metal or uranium salts, and the tin and vanadium concentrations are too low to cause interference. If nickel and/or molybdenum are present at interfering concentrations, the zinc can be separated from them by ion exchange. Zinc can be separated from nickel in 2 *M* hydrochloric acid on Dowex 1-X4 anion-exchange resin; zinc is retained on the column[7] and the nickel passes through. If molybdenum is present, it is retained with zinc. To separate the zinc and the molybdenum, the solution containing these elements must be made 9 *M* in perchloric acid and passed through a column containing Dowex 50W-X4 cation-exchange resin; molybdenum is retained, whereas the zinc is collected in the effluent[8].

TABLE I

PEAK CURRENT AS A FUNCTION OF THE ZINC CONCENTRATION
(0.50 *M* $HClO_4$, 0.50 *M* $NaClO_4$, 0.08 *M* NaF)

Zn^{2+} concn. (*C*) ($mol\ l^{-1}$)	$(i_p)_a$ (μA)	$(i_p)_a/C$ ($\mu A\ mmol^{-1}$)
$1.00 \cdot 10^{-5}$	0.19	19.2
$2.51 \cdot 10^{-5}$	0.50	19.9
$5.01 \cdot 10^{-5}$	0.96	19.2
$1.00 \cdot 10^{-4}$	2.01	20.1
$2.51 \cdot 10^{-4}$	4.94	19.7
$5.01 \cdot 10^{-4}$	9.75	19.5
$7.52 \cdot 10^{-4}$	15.3	20.3
$1.00 \cdot 10^{-3}$	20.5	20.5
$2.00 \cdot 10^{-3}$	39.6	19.8
$3.01 \cdot 10^{-3}$	59.5	19.8

Recovery of zinc in the presence of uranium

The effect of uranium on the polarographic determination of zinc was determined by spiking uranium solutions with standard zinc solutions. When the ratio of uranium to zinc was 30:1 or less, the sample solution composition was 0.5 *M* in perchloric acid, 0.5 *M* in sodium perchlorate, and the uranium sample. Attempts to increase this ratio failed because uranium was reduced to uranium(III) during the 5-sec delay period and then oxidized to uranium(IV) during the sweep period. The uranium(III)/(IV) potential is approximately -1.01 V *versus* the mercury pool, whereas the zinc peak is -1.16 V. As the uranium : zinc ratio was increased, the uranium peak increased proportionally. When the uranium to zinc ratio exceeded 30 : 1, the zinc peak merged with the uranium peak.

Attempts were made to eliminate the uranium interference by adding uranium to the blank solution in the same concentration as in the sample, so that the uranium(III) peak could be deducted. However, the resulting displays were ill-defined.

It has been reported that uranium(III) can be precipitated by fluoride in an acid solution[9], and that fluoride has no adverse affect on the zinc peak potential or peak current[10]. This was confirmed.

Sodium fluoride was then added to samples containing uranium and to uranium blanks. The zinc peaks were well-defined, and the interference caused by the uranium(III) was eliminated. However, as the concentration of the uranium was increased (uranium–zinc ratio greater than 150:1), it was observed that with each sub-

TABLE II

INVESTIGATION OF DIVERSE IONS

($5.01 \cdot 10^{-4}$ *M* zinc, 0.5 *M* $HClO_4$, 0.5 *M* $NaClO_4$, 0.08 *M* NaF)

Ion added	*μg ion per 10 ml*	*% Zn recovery*[a]	*Ion added*	*μg ion per 10 ml*	*% Zn recovery*[a]
Ag	1000	a	Mo(VI)	1000	c
Al	1000	a		50	a
Ba	1000	a,b	Ni(II)	1000	c
Ca	1000	a,b		10	a
Cd	1000	a	Pb(II)	1000	a
Ce(IV)	1000	a,b	Sb(V)	250	a
Ce(III)	1000	a,b	Si	1000	a
Co(II)	10000	a	Sn(IV)	1000	c
Cr(III)	1000	a,b		130	a
Cu(II)	1000	116	Sr	1000	a,b
	500	a	Th	1000	a,b
Fe(III)	1000	a	Ti(III)	1000	118
Fe(II)	1000	a		500	a
Ga(III)	1000	a,b	V(V)	1000	130
Ge	1000	81		200	a
	215	a	W(VI)	1000	c
Hg(II)	1000	a		< 10	c
K	1000	a,b	Y	1000	a,b
Li	1000	a,b	Zr	1000	a,b
Mg	1000	a,b			
Mn(II)	1000	a			

[a] a = ±5%; b = precipitate formed or solution became cloudy; c = ill-defined.

sequent display of the same solution, the peak current decreased, indicating that some of the zinc was being co-precipitated with the uranium trifluoride.

In order to minimize the effect of this co-precipitation, only the peak current of the first scan after the cell circuit had been closed was recorded. If, for some reason, the peak current of the first scan was not recorded, the cell circuit was opened for about 30 sec. The circuit was closed, and the peak current of this first scan was recorded. However, when the uranium–zinc ratio exceeded 300:1, the uranium interference became significant, even when the initial peak currents were measured as above.

Chemistry Research and Development, C. E. Plock
Dow Chemical Company, Rocky Flats Division, J. Vasquez*
Golden, Colo. 80401 (U.S.A.)

1 C. L. SCHMITZ, E. F. EWEN AND S. P. DODD (Editors), *Bibliography of Polarographic Literature 1922–1967*, Sargent-Welch Scientific Company, Chicago, 1969.
2 R. G. BALL, D. L. MANNING AND O. MENIS, *U.S. At. Energy Comm. Rept. ORNL-2717*, 1959.
3 D. ISHII AND T. TAKEUCHI, *Bunseki Kagaku*, 10 (1961) 272; *Chem. Abstr.*, 57 (1962) 26.
4 G. C. GOODE AND M. C. CAMPBELL, *Anal. Chim. Acta*, 27 (1962) 422.
5 J. KÖRBL AND R. PŘIBIL, *Chemist-Analyst*, 45 (1956) 102.
6 J. KÖRBL, R. PŘIBIL AND A. AMR, *Chem. Listy*, 50 (1956) 1440.
7 K. A. KRAUS AND F. NELSON, *Proc. Intern. Conf. Peaceful Uses At. Energy*, Vol. VII, United Nations, 1956, p. 113.
8 F. NELSON, T. MURASE AND K. A. KRAUS, *J. Chromatog.*, 13 (1964) 503.
9 G. L. BOOMAN AND J. E. REIN, in I. M. KOLTHOFF AND P. J. ELVING, *Treatise on Analytical Chemistry, Vol. 9, Part II*, Interscience, New York, 1962, p. 14.
10 F. J. MINER, *Ph.D. Thesis*, Oregon State University, 1955.

(Received 10th December 1970)

* Present address: Chemistry Department, Denver Center, University of Colorado, Denver, Colo. 80202.

Analytica Chimica Acta
Elsevier Publishing Company, Amsterdam
Printed in The Netherlands

ANNOUNCEMENT

VERANSTALTUNGEN DER GESELLSCHAFT DEUTSCHER CHEMIKER 1971

6.–9. Juli	4. *Europäisches Symposium "Lebensmittel—Fortschritte in der Verfahrenstechnik der Lebensmittelverarbeitung mit besonderer Berücksichtigung der Proteine, Enzyme und Aromen".* Veranstaltet von der Arbeitsgruppe "Lebensmittel" der Europäischen Föderation für Chemie-Ingenieur-Wesen in Prag (Tschechoslowakei).
10.–13. September	*Sektion Kristallkunde in der Deutschen Mineralogischen Gesellschaft.* Vortragstagung in Karlsruhe.
13.–18. September	*Hauptversammlung der Gesellschaft Deutscher Chemiker in Karlsruhe.* Folgende Fachgruppen werden sich an der GDCh-Hauptversammlung durch Veranstaltungen beteiligen: "*Analytische Chemie*" "*Angewandte Elektrochemie*" "*Anstrichstoffe und Pigmente*" "*Festkörperchemie*" "*Freiberufliche Chemiker*" "*Geschichte der Chemie*" "*Gewerblicher Rechtsschutz*" "*Kern-, Radio- und Strahlenchemie*" "*Lebensmittelchemie und gerichtliche Chemie*" "*Makromolekulare Chemie*" "*Wasserchemie*"
27. September–1. Oktober	*EUCHEM-Konferenz "Kinetik chemischer Elementarreaktionen" in Göttingen.* Die Teilnehmerzahl ist auf 100 begrenzt.
28.–29. September	*Tagung "Analytik organischer Spurenstoffe im Wasser".* Veranstaltet von den GDCh-Fachgruppen "Wasserchemie", "Analytische Chemie", "Lebensmittelchemie und gerichtliche Chemie" und dem Haus der Technik, Essen.
4.–9. Oktober	*Colloquium Spectroscopicum Internationale XVI in Heidelberg.*
13.–15. Oktober	*GDCh-Fachgruppe "Angewandte Elektrochemie".* Vortragstagung in Jülich.

Unterlagen über die genannten Veranstaltungen können nach Erscheinen auf Anforderung durch die GDCh-Geschäftsstelle, 6000 Frankfurt (M), Postfach 119075, zur Verfügung gestellt werden.

Analytica Chimica Acta
Elsevier Publishing Company, Amsterdam
Printed in The Netherlands

BOOK REVIEWS

Solvent Extraction Research, Edited by A. S. Kertes and Y. Marcus, Interscience–J. Wiley and Sons, Inc. New York, 1970, xvi+439 pp., price £ 14.—.

The main title of this book does not really indicate that this is a collection of 42 papers presented at the 5th International Conference on Solvent Extraction, which was held at Jerusalem in September, 1968. All the papers, apart from the two plenary lectures by Professors Marcus and Freiser and one other paper, are included. The papers are arranged in sections comprising acidic and chelating extractants, solvating extractants and aliphatic ammonium salt extractants, synergic extraction systems, kinetics of solvent extraction, and applications in process chemistry.

The papers are interesting, particularly Healy's review of synergic extraction, and many are of direct interest to analytical chemists. Yet it must be asked, again, why these papers could not have been published in the usual scientific journals. They would then have appeared more rapidly, at less expense, and with greater general accessibility. These arguments, and others against this type of publication, have been repeated so often that it is difficult to understand why symposium organizers should add to their burdens by inflicting upon themselves the laborious task of collecting and editing the papers for such a book.

A. Townshend (Birmingham)

R. Y. Eagers, *Toxic Properties of Inorganic Fluorine Compounds*, Elsevier Publishing Company, Amsterdam, 1969, x+152 pp., price £2.75.

As the industrial and everyday usage of fluorinated materials increases, it is vital that more information should be available on acute and chronic fluorine poisoning. The drastic effects of ionic fluoride in large doses are not always appreciated, and this book is very useful in drawing attention to the sources of such poisoning.

The text is mainly concerned with the effects of all types of inorganic fluorine compounds in humans; both massive doses, accidental or intentional, and chronic industrial poisoning are dealt with in detail, and many case histories are given. Endemic and allergic poisoning is also considered. The toxicity of inorganic fluorides for animals, plants, bacteria, etc. is discussed briefly.

The book is warmly recommended as a cautionary text for anyone concerned with fluorinated compounds.

A. M. G. Macdonald (Birmingham)

CONTENTS

(continued on page 4 of cover)

Continued from inside page of cover